

WHOLE-BODY POSTURES DURING STANDING HAND-FORCE EXERTIONS:
DEVELOPMENT OF A 3D BIOMECHANICAL POSTURE PREDICTION MODEL

by

Suzanne Groves Hoffman

A dissertation submitted in partial fulfillment
of the requirements for the degree of
Doctor of Philosophy
(Industrial and Operations Engineering)
in The University of Michigan
2008

Doctoral Committee:

Emeritus Professor Don B. Chaffin, Co-Chair
Research Associate Professor Matthew P. Reed, Co-Chair
Associate Professor Richard E. Hughes
Associate Professor Bernard J. Martin

© Suzanne Groves Hoffman

2008

In loving memory of my Grandmother, Annette Winburn

ACKNOWLEDGEMENTS

I would like to begin by thanking my co-chair Matthew Reed. I am forever indebted to Matt for all he has taught me and for the countless hours he spent patiently working side-by-side with me to make this dissertation happen. His positive attitude and genuine love for data, even in the wee hours of the morning, kept me going when progress was frustratingly slow. Working with him to analyze my data, while at times like drinking from a fire hose, gave me confidence and showed me it can be fun to get lost in the data. Matt also taught me how to effectively present information graphically and provided me with the tools and know-how to create great figures. His experience and high standards in writing, graphics, modeling, and data analysis challenged me, pushing me to my limits and teaching me a great deal about myself.

I feel honored to have had the opportunity to get to know Don Chaffin, co-chair of my committee, through my dissertation work and as a student in his occupational biomechanics course. His breadth of knowledge and impact on the fields of ergonomics and biomechanics are inspiring. It has been a privilege to have him as an advisor. I would also like to thank the other two members of my committee, Bernard Martin and Richard Hughes for their unique perspectives on my work. Also, a special thank you to Richard for his enthusiasm and kindness, and for not forgetting what it's like to be a Ph.D. Candidate.

I am fortunate to have shared an office with David Wagner, who always was incredibly generous with his time. Without his help on everything from data collection, to creating a GUI in Matlab, to combining the chapters of my dissertation, it surely would have taken me at least another year to graduate. Having a graduate student, and better yet a friend, to share the ups and downs of the PhD journey with was invaluable.

A special thanks to my family and friends who have been an incredible source of support. Especially my husband, Rob, who always believed in me and stood by my side through it all. Words cannot express how grateful I am and how blessed I feel to have him for a husband. To my father who thinks being an engineer means you can do anything and to my mother - the tireless cheerleader, thank you for the opportunities you provided me and for always telling me I could do anything I put my mind to. And to the countless other people who have supported me along the way, especially Awoo, Ginger, Becky and Ava (thanks for the laughs), Catherine and John, Billy and Amanda, Big Julia, The Murrays, T, Monica, and our Holy Faith family – thank you!

I would also like to thank my manager, Bob Tilove, and co-worker, Diana Wegner, for their support during my transition from graduate student to an employee of General Motors. Lastly, I am grateful to the many people within the Center for Ergonomics who have helped me along the way and the HUMOSIM Partners for their financial support and genuine interest in my research. Their outward enthusiasm towards my research was a great motivator.

Table of Contents

Dedication	ii
Acknowledgements	iii
List of Figures.....	xi
List of Tables	xxi
Abstract	xxiii
CHAPTER 1	1
INTRODUCTION	1
1.1. Thesis Statement.....	1
1.2. Applied Problem.....	1
1.3. Theoretical Problem	5
<i>Hypothetical Basis for Forceful Posture-Prediction Method.....</i>	<i>10</i>
1.4. Research Objectives	11
1.5. Dissertation Organization	12
1.6. References.....	14
CHAPTER 2	18
EXPERIMENTAL DESIGN AND METHODS	18
2.1. Overview of Methods for Plant and Laboratory Studies.....	18
2.2. General Objectives	18
2.3. Plant Methods	19
2.4. Laboratory Study Methods.....	19
<i>Participants</i>	<i>19</i>
<i>Facilities</i>	<i>20</i>
<i>Test Conditions</i>	<i>23</i>
<i>Procedures</i>	<i>25</i>
1st Session: Anthropometry, Body Segment Mass Estimation and Strength Testing	25
2nd Session: Maximal and Submaximal Standing Exertions	27
2.5. Analysis Methods.....	29
2.6. Appendix: Body Segment Mass Estimation	30

2.7. References.....	36
CHAPTER 3.....	37
PREDICTING ACTUAL HAND FORCES FROM REQUESTED FORCE VECTOR DURING STANDING HAND-FORCE EXERTIONS.....	37
3.1. Abstract.....	37
3.2. Introduction	38
3.3. Methods.....	40
<i>Participants and Test Conditions</i>	40
<i>Data Analysis</i>	41
3.4. Results	42
<i>Mean Strengths for One- and Two-Handed Exertions Across Handle Heights</i>	42
<i>Differences Between Actual and Requested Hand Force Vectors</i>	44
<i>Off-Axis Forces During Two-Handed Push/Pull Exertions</i>	46
<i>Off-Axis Forces During Two-Handed Up/Down Exertions</i>	48
<i>Off-Axis Forces During One-Handed Push/Pull Exertions</i>	50
<i>Off-Axis Forces During One-Handed Up/Down Exertions</i>	54
3.5. Summary and Discussion	55
3.6. References.....	60
CHAPTER 4.....	61
PREDICTING TWO-HAND FORCE EXERTION POSTURES	61
4.1. Abstract.....	61
4.2. Introduction	62
<i>High-Level Hypotheses</i>	62
<i>Governing Constraints and Assumptions</i>	63
<i>Hypothesized Biomechanical Principles</i>	63
<i>Hypothesized Behaviors</i>	64
4.3. Methods.....	65
<i>Participants</i>	65
<i>Test Conditions</i>	66
<i>Data Analysis</i>	68
Definition of Hand-Force Plane	68
Postural Metrics	69
Statistical Analysis Approach	72
4.4. Results: Posture Selection Trends	73
<i>Elbow Posture</i>	73
<i>Effect of Shoulder Moment on Posture</i>	76

Shoulder Location with Respect to Point of Force Application	76
Relationship Between Off-Axis Forces and Posture	81
Interaction Between Shoulder Location and Off-Axis Forces.....	83
Level of Acceptable Shoulder Moment	86
<i>Foot Placements during Two-Handed Force Exertions</i>	92
Effect of Hand Force on BOS Length during Push Exertions.....	92
Effect of Hand Force on BOS Length during Pull Exertions	94
4.5. Results: Regression Models	97
<i>Shoulder Moment Target Value</i>	98
<i>Torso Inclination in the Hand-Force Plane</i>	101
Torso Inclination Angle Regression Model for Up/Down Exertions.....	102
Torso Inclination Angle Regression Model for Pull Exertions.....	102
Torso Inclination Angle Regression Model for Push Exertions	103
<i>Pelvis Pitch with Respect to Torso Inclination</i>	105
<i>Lateral Pelvis Displacement</i>	106
<i>Base-of-Support (BOS) Length</i>	106
BOS Length Regression Model for Push Exertions	107
BOS Length Regression Model for Pull Exertions.....	108
4.6. Discussion	108
<i>Sensitivity to Shoulder Moment</i>	109
<i>Preference Towards Neutral Posture</i>	112
<i>Predicting Foot Placements from Balance Requirements</i>	113
<i>Limitations and Future Work</i>	114
4.7. References.....	115
CHAPTER 5.....	116
PREDICTING ONE-HAND FORCE EXERTION TASK POSTURES.....	116
5.1. Abstract.....	116
5.2. Introduction	117
<i>High-Level Hypotheses</i>	117
<i>Governing Constraints and Assumptions</i>	118
<i>Hypothesized Biomechanical Principles</i>	118
<i>Hypothesized Behaviors</i>	119
5.3. Methods.....	119
<i>Participants</i>	119
<i>Test Conditions</i>	119
<i>Data Analysis</i>	120
Postural Metrics.....	121
Statistical Analysis Approach	121

5.4. Results: Postural Strategies Observed	122
Push Versus Pull Exertions	122
Open Versus Closed Orientation.....	123
5.5. Results: Posture Selection Trends	124
<i>Elbow Posture.....</i>	<i>124</i>
<i>Effect of Shoulder Moment on Posture</i>	<i>126</i>
Shoulder Location with Respect to Point of Force Application	127
Relationship Between Off-Axis Forces and Posture	129
Interaction Between Shoulder Location and Off-Axis Forces.....	131
Level of Acceptable Shoulder Moment	132
<i>Pelvis Location and Orientation with Respect to Hand-Force Plane.....</i>	<i>136</i>
Lateral Pelvis Displacement.....	136
Out-of-Plane Rotation Angle	137
<i>Foot Placements during One-Hand Force Exertions.....</i>	<i>141</i>
Effect of Hand Force on BOS Length during Push Exertions.....	141
Effect of Hand Force on BOS Length during Pull Exertions	141
5.6. Results: Regression Models	142
<i>Shoulder Moment Target Value.....</i>	<i>143</i>
<i>Torso Inclination in the Hand-Force Plane.....</i>	<i>145</i>
Torso Inclination Angle Regression Model for Up/Down Exertions.....	146
Torso Inclination Angle Regression Model for Pull Exertions.....	146
Torso Inclination Angle Regression Model for Push Exertions	147
<i>Pelvis Pitch with Respect to Torso Inclination.....</i>	<i>148</i>
<i>Base-of-Support (BOS) Length</i>	<i>149</i>
BOS Length Regression Model for Push Exertions	150
BOS Length Regression Model for Pull Exertions.....	151
5.7. Discussion	151
5.8. References.....	153
CHAPTER 6.....	154
DEVELOPMENT AND VALIDATION OF A THREE-DIMENSIONAL BIOMECHANICAL POSTURE PREDICTION MODEL FOR STANDING HAND FORCE EXERTIONS.....	154
6.1. Abstract.....	154
6.2. Introduction	155
<i>Requirements for Posture Prediction Models used for Ergonomics</i>	<i>155</i>
<i>Previous Approaches to Posture Prediction for Standing Tasks</i>	<i>155</i>
<i>Biomechanical Posture Prediction: Overview of Approach.....</i>	<i>157</i>
<i>Support for Biomechanical Approach.....</i>	<i>157</i>
Postural Behaviors Observed in Laboratory and Industry	157

Explanations of Hand Force and Posture from Literature.....	158
6.3. Model Development	158
<i>Underlying Biomechanical Principles</i>	<i>160</i>
<i>Overview of Model Structure and Posture Prediction Sequence</i>	<i>160</i>
<i>Model Formulation.....</i>	<i>162</i>
1. Compute Actual Hand Force Vector and Define Hand-Force Plane	163
2. Predict Included Elbow Angle	164
3. Position Shoulder with Respect to Point of Force Application.....	165
4. Set Torso Inclination in the Hand-Force Plane.....	165
5. Compute Foot Placements in the Hand-Force Plane	166
6. Set Out-of-Plane Shoulder Rotation Angle.....	168
7. Lateral Displacement of Pelvis out of Hand-Force Plane.....	169
8. Compute Pelvis and Torso Orientations	170
9. Kinematic Constraints and Adjustments	172
6.4. Matlab Implementation.....	172
<i>Three-Dimensional Human Body Linkage Definition.....</i>	<i>173</i>
<i>Graphical User Interface.....</i>	<i>178</i>
6.5. Model Performance.....	179
<i>Qualitative Model Performance</i>	<i>180</i>
<i>Quantitative Performance: Validation Against Withheld Data.....</i>	<i>184</i>
<i>Sensitivity Analysis</i>	<i>188</i>
6.6. Discussion	189
<i>Summary.....</i>	<i>189</i>
<i>Model Structure</i>	<i>190</i>
<i>Model Performance.....</i>	<i>190</i>
<i>Limitations and Future Work.....</i>	<i>192</i>
Model Linkage.....	192
<i>Model Structure</i>	<i>194</i>
6.7. References.....	196
CHAPTER 7.....	198
DISCUSSION	198
7.1. Overview	198
<i>Summary of Principal Empirical Findings</i>	<i>198</i>
<i>Unexpected Findings.....</i>	<i>200</i>
<i>Summary of Principal Contributions</i>	<i>200</i>
7.2. Principal Contributions.....	200
<i>Shoulder Location with Respect to Point of Force Application & Shoulder Moment</i>	<i>204</i>

<i>Torso Inclination</i>	208
<i>Pelvis Location and Orientation</i>	209
<i>Base-of-Support</i>	209
<i>Current Approaches to Posture Prediction</i>	212
Optimization-Based Posture Prediction	212
Statistical Modeling and Data-Based Inverse Kinematics	213
Artificial Neural Networks	213
Motion Modification	214
<i>Current Biomechanics-Based Posture-Prediction Model Formulation</i>	214
<i>Opportunities to Improve Model Performance</i>	215
7.3. Limitations	217
<i>Laboratory Study</i>	217
<i>Posture Prediction Model</i>	219
7.4. Future Research	220
7.5. References	224

List of Figures

Figure 1.1. Factors hypothesized to affect posture selection for standing hand-force exertion tasks.....	7
Figure 1.2. Organization of determinants of posture into posture-prediction algorithm.	11
Figure 2.1. Laboratory configuration with visual force feedback display, 6-DOF load cell and moveable force platforms for measuring forces and moments at the hands and feet respectively.	20
Figure 2.2. Force handle adjustability.	21
Figure 2.3. Visual force-feedback display with goal (blue diamond) shown for required level of force in requested direction and maximal allowable off-axis forces indicated by grey limit bars.....	21
Figure 2.4. Retro-reflective marker set used to track whole-body motion.	22
Figure 2.5. (a) Optical marker and (b) digitized landmark locations.....	23
Figure 2.6. Principal (forward, back, left, right, up, down) and non-principal (forward-up, forward-down, back-up, back-down, forward-right, forward-left, back-right, back-left) hand force directions.	24
Figure 2.7. Participant in the experimental setup performing an exertion on the fixed force handle while receiving visual feedback on hand force via an LCD screen.....	24
Figure 2.8. Illustration of standardized strength tests (Stobbe, 1982).....	26
Figure 2.9. Functional strength tests (University of Michigan, 2000).	27
Figure 2.10. Experimental design: Block I performed by all subjects, blocks 2a and 2b performed by subjects assigned to Design I and Design II respectively.	28
Figure 2.11. Metrics used to quantify whole-body postures during standing hand force exertions.....	30
Figure 2.12. Illustration of segment parameters.	31
Figure 2.13. Body segment mass estimation apparatus & tasks used to quantify: (a) upper arm mass, (b) mass of (forearm + hand), (c) thigh mass, and (d) mass of the (shank + foot).....	33
Figure 2.14. Illustration of center-of-mass displacements during (a) <i>fhv</i> task and (b) <i>wav</i> task for estimation of (forearm + hand) mass and mass of upper arm, respectively.....	34
Figure 2.15. Illustration of center-of-mass displacements during (a) <i>sfv</i> task and (b) <i>wlv</i> task for estimation of (shank + foot) mass and mass of thigh, respectively.	35
Figure 3.1. Mean one and two-handed strengths at thigh, elbow, and overhead handle heights expressed as a percent of body weight (H denotes stature).	43
Figure 3.2. Cumulative distribution function for two-handed push/pull lateral off-axis force.	46
Figure 3.3. Vertical off-axis force during two-handed elbow-height push/pull exertions expressed as a percent of the magnitude of the requested horizontal force. Linear fits are highly significant ($p <$ 0.01).....	47

Figure 3.4. Vertical off-axis force during two-handed thigh-height push/pull exertions expressed as a percent of the magnitude of the requested horizontal force.....	47
Figure 3.5. Vertical off-axis force during two-handed overhead push/pull exertions expressed as a percent of the magnitude of the requested horizontal force.	48
Figure 3.6. Cumulative distribution function for lateral off-axis forces during two-handed downward exertions at elbow-height.	48
Figure 3.7. Lateral off-axis forces during upward exertions, when expressed as a fraction of the magnitude of the requested vertical force, are not significantly different across handle heights ($\alpha=0.05$).....	49
Figure 3.8. Fore-aft off-axis forces during two-handed up/down exertions. Linear fit is highly significant ($p < 0.01$) for two-hand downward exertions and significant ($p < 0.05$) for upward exertions at thigh-height.	50
Figure 3.9. Cumulative distribution functions for lateral off-axis force magnitude during one-handed forward/back exertions and one-handed left/right exertions.	51
Figure 3.10. Lateral off-axis forces across handle heights during one-handed exertions to the left performed using a push or pull strategy. Within strategy, lateral off-axis forces are not significantly different across handle heights.....	51
Figure 3.11. Lateral-off axis forces across handle heights during one-handed pulls to the right. Differences in lateral off-axis forces across handle heights are highly significant ($p < 0.01$). At the overhead handle height lateral off-axis forces are negligible, 3.13 N (0.7 lbs) on average.	52
Figure 3.12. Vertical off-axis forces during forward and back exertions at elbow height. Differences in vertical off-axis forces are highly significant ($p < 0.01$) when pushing with flexed versus extended elbows.....	53
Figure 3.13. Vertical off-axis forces during forward and back exertions at thigh height. Differences in vertical off-axis forces are highly significant ($p < 0.01$) when pushing with flexed versus extended elbows.....	53
Figure 3.14. Vertical off-axis force during overhead forward and back exertions.	53
Figure 3.15. Cumulative distribution function for lateral off-axis forces during one-handed downward exertions at elbow-height.	54
Figure 3.16. Lateral off-axis forces during one-handed upward exertions. Linear fit for elbow-height upward exertion is highly significant ($p < 0.01$).	54
Figure 3.17. Fore-aft off-axis forces during one-handed up/down exertions. Linear fit is highly significant ($p < 0.01$) for one-hand downward exertions at elbow height.....	55
Figure 4.1. Hand force directions and force direction constraint conditions for two-handed thigh, elbow, and overhead height exertions. Forces levels were 25%, 50%, and 75% of maximum for all directions as well as maximal exertion for unconstrained force directions.	65
Figure 4.2. Examples of risky two-handed thigh-height, elbow-height, and overhead pulling strategies excluded from the analysis.....	67

Figure 4.3. Examples of two-handed thigh-height up exertions excluded from the analysis.....	67
Figure 4.4. Top and side-view of hand-force plane defined as the vertical plane in which the actual hand-force vector lies. Transformation between the global and hand-force plane coordinate frames is performed by the rotation matrix, R , a pure rotation of θ_z about the global z-axis. As defined, the z-axis of the global and hand-force coordinate frame is coincident.....	69
Figure 4.5. Definition of base-of-support and metrics used to quantify foot placements.....	71
Figure 4.6. Postural metrics used to quantify whole-body postures with respect to the hand-force plane....	72
Figure 4.7. Two-handed pushing strategies: (a) elbows flexed; (b) elbows extended.....	74
Figure 4.8. Distribution of included right elbow angle during two-handed push exertions at (a) overhead, (b) elbow, and (c) thigh-height.....	74
Figure 4.9. Prevalence of flexed (Flex.) and extended (Ext.) elbow pushing strategies across handle heights. A flexed elbow posture was used for 73%, 97% and 75% of push exertions at elbow, overhead, and mid-thigh handle heights.....	75
Figure 4.10. Distribution and cumulative distribution function for included right elbow angle during two-handed pulls at thigh, elbow, and overhead heights.....	75
Figure 4.11. Prevalence of flexed (Flex.) and extended (Ext.) elbow postures during two-handed pulls at mid-thigh, elbow, and overhead handle height.....	76
Figure 4.12. Differences in shoulder height adjustment with change in actual force (AF) magnitude when pushing at elbow-height with elbows extended (“E”) versus flexed-elbow (“F”) posture.....	77
Figure 4.13. Change in included elbow angle and fore/aft distance from shoulder to point of force application with force magnitude when pushing with extended versus flexed-elbow posture.....	78
Figure 4.14. Change in shoulder height with increasing hand force magnitude during two-handed push exertions at mid-thigh, elbow, and overhead handle heights.....	78
Figure 4.15. Change in shoulder height with increasing hand force magnitude during two-handed pulls at mid-thigh, elbow, and overhead handle heights.....	79
Figure 4.16. Change in fore/aft shoulder location with increasing hand force magnitude during up/down exertions at thigh, elbow, and overhead handle heights.....	80
Figure 4.17. Torso pitch during thigh-height upward exertions.....	80
Figure 4.18. Relationship between change in shoulder height from neutral and hand force magnitude during elbow-height vertical up/down exertions (left) and thigh-height and overhead up exertions (right)...	81
Figure 4.19. Relationship between magnitude and direction of resultant hand force vector and vertical force component during directionally unconstrained two-handed elbow-height push exertions performed with flexed versus extended elbow strategy.....	82
Figure 4.20. Vertical off-axis forces generated during directionally unconstrained two-handed push exertions performed at thigh, elbow, and overhead handle heights.....	82
Figure 4.21. Vertical off-axis forces generated during directionally unconstrained two-handed pulls performed at thigh, elbow, and overhead handle heights.....	83

Figure 4.22. Comparison of change in shoulder height from neutral with actual hand force (AF) magnitude across directionally constrained (✕) versus unconstrained (▲) thigh-height pulls.	84
Figure 4.23. Actual vertical off-axis forces (F_z AF) expressed as a fraction of body weight generated during directionally constrained (✕) versus unconstrained (▲) thigh-height pulls. An increase in vertical off-axis force with increasing actual hand force (AF) magnitude is observed for unconstrained trials. ...	85
Figure 4.24. Comparison of shoulder flexion/extension moments across actual hand force (AF) magnitude during directionally constrained (✕) versus unconstrained (▲) thigh-height pulls.	85
Figure 4.25. Change in actual hand force (AF) direction with change in shoulder height from neutral during two-handed pulls performed at mid-thigh (blue), elbow (red), and overhead (green) handle heights. ...	86
Figure 4.26. Actual horizontal off-axis forces (F_x AF) normalized to body weight generated during overhead upward exertions. An increase in horizontal off-axis force with increasing actual hand force (AF) magnitude is observed.	86
Figure 4.27. Change in shoulder flexion/extension moment with actual vertical hand force (F_z AF) and magnitude of resultant hand force vector, both normalized by body weight, for two-handed elbow-height pushes performed with a flexed-elbow strategy.	87
Figure 4.28. Change in shoulder flexion/extension moment with actual hand force (AF) magnitude for two-handed push exertions performed at mid-thigh (blue), elbow (red), and overhead (green) heights. ...	88
Figure 4.29. Cumulative distribution function for two-handed elbow-height pushes showing shoulder flexion moments are less than 30 Nm for 90% of trials.	88
Figure 4.30. Relationship between shoulder flexion/extension moment and change in shoulder height from neutral standing height during two-handed thigh (blue), elbow (red), and overhead (green) push exertions.	89
Figure 4.31. Cumulative distribution of magnitude of shoulder flexion/extension moments during two-handed push exertions at thigh, elbow, and overhead handle height.	90
Figure 4.32. Change in shoulder flexion/extension moment with increase in actual magnitude of two-hand pull force (AF) for trials performed at mid-thigh (blue), elbow (red), and overhead (green) handle heights.	90
Figure 4.33. Cumulative distribution function for magnitude of shoulder flexion/extension moments during elbow-height (leftmost) and thigh-height (rightmost) pull exertions.	91
Figure 4.34. Cumulative distribution function of magnitude of shoulder moment during two-handed up down exertions showing shoulder moment is less than or equal to 33 Nm in 90% of all trials.	91
Figure 4.35. Relationship between shoulder moment and fore-aft shoulder location during pull-up (leftmost), push-up, and push-down (rightmost) vertical exertions.	92
Figure 4.36. Lengthening of base-of-support with increasing push force. Linear relationship between horizontal push force and length of base-of-support is highly significant ($p < 0.01$) for two-handed push exertions at mid-thigh and elbow height. Relationship is not significant for overhead exertions.	93

Figure 4.37. Length of base-of-support versus fore-aft distance from rear boundary of base-of-support to pelvis, both normalized by stature, for two-handed push exertions. For each handle height, linear relationship is highly significant ($p < 0.01$).	93
Figure 4.38. Fore-aft distance from rear boundary of base-of-support to pelvis, normalized by stature, for two-handed push exertions. Average offset for thigh-height push exertions is significantly different from mean offsets at elbow and overhead heights for $\alpha = 0.05$.	94
Figure 4.39. Mean torso inclination angle at each handle height during two-handed push exertions. On average, torso inclination angle is significantly different at each handle height for $\alpha = 0.05$ with large forward flexion during thigh-height exertions and more upright torso posture during overhead trials.	94
Figure 4.40. Lengthening of base-of-support with increasing hand force during two-handed pulls at mid-thigh, elbow, and overhead handle heights. Linear relationships are highly significant ($p < 0.01$). Grey markers denote high-force exertions performed with parallel stance identified as outliers and excluded from analysis.	95
Figure 4.41. Length of base-of-support versus fore-aft distance from front boundary of base-of-support to pelvis, both normalized by stature, for two-handed pull exertions. For each handle height, linear relationship is highly significant ($p < 0.01$).	96
Figure 4.42. Mean fore-aft distance from front boundary of base-of-support to pelvis for two-hand pulls performed at mid-thigh, elbow, and overhead heights. On average, the fore-aft offset during thigh-height trials is significantly different from offsets during elbow and overhead exertions ($p < 0.01$).	96
Figure 4.43. Mean torso inclination angle during two-hand pulls at mid-thigh, elbow, and overhead handle heights. Torso inclination angle is significantly different for thigh-height exertions, as compared to elbow and overhead exertions, for $\alpha = 0.05$.	97
Figure 4.44. Definition of hand force components and postural metrics used to predict shoulder flexion/extension moment. Shoulder extension moments are defined positive where extension of the shoulder corresponds to raising the arm, in the sagittal plane, from a resting posture along side the torso to overhead.	99
Figure 4.45. Actual versus predicted shoulder flexion/extension moment for two-handed push, pull, up, and down exertions at mid-thigh, elbow, and overhead handle heights ($p < 0.001$).	100
Figure 4.46. Hand force and postural metrics used to predict torso inclination in the hand-force plane. Torso inclination angle is with respect to the vertical and defined positive rearward.	101
Figure 4.47. Actual versus predicted torso inclination angle for two-handed exertions in the vertical up/down direction spanning mid-thigh to overhead handle heights ($p < 0.001$).	102
Figure 4.48. Actual versus predicted torso inclination angle for two-handed pulls spanning mid-thigh to overhead handle heights ($p < 0.001$).	103
Figure 4.49. Actual versus predicted torso inclination angle for two-handed push exertions performed at mid-thigh, elbow, and overhead handle heights ($p < 0.001$).	104

Figure 4.50. Residual torso inclination angle across handle heights for two-handed push exertions. Mean residuals at overhead and mid-thigh handle heights are significantly different from mean residual at elbow height for $\alpha = 0.05$.	105
Figure 4.51. Actual versus predicted pelvis pitch with respect to torso inclination for two-handed exertions ($p < 0.001$).	106
Figure 4.52. Definition of metrics used to predict base-of-support length for two-hand push exertions. The active boundary of the base-of-support is the rear boundary when pushing and front boundary when pulling.	107
Figure 4.53. Actual versus predicted base-of-support length normalized by stature for two-handed push exertions performed at mid-thigh, elbow, and overhead handle heights ($p < 0.01$).	107
Figure 4.54. Actual versus predicted base-of-support length for two-handed pull exertions ($p < 0.01$).	108
Figure 4.55. Unusual flexed-elbow forward overhead exertion.	110
Figure 5.1. Participant in the laboratory performing an upward exertion on a fixed force handle while receiving visual feedback on hand force via an LCD screen. The force handle is shown in a horizontal orientation. Minimal constraints were imposed on foot placements by requiring subjects to keep their feet within the gridded area of the platform.	120
Figure 5.2. One-hand force exertions performed using push versus pull strategy. All participants chose to pull back and to the right thus a picture of a push back and to the right is not shown.	122
Figure 5.3. Prevalence of push and pull strategies across hand force directions.	122
Figure 5.4. Open, neutral, and closed torso strategies used across different hand force directions. All downward exertions were performed using a neutral or open strategy thus a picture of closed downward exertion is not shown.	123
Figure 5.5. Prevalence of torso orientation strategies within push, pull, up and down exertions.	124
Figure 5.6. Distribution of included right elbow angle during one-handed push exertions at (a) overhead, (b) elbow, and (c) thigh-height.	125
Figure 5.7. Prevalence of flexed (Flex.) and extended (Ext.) elbow pushing strategies across handle heights.	125
Figure 5.8. Distribution and cumulative distribution function for included right elbow angle during one-handed pulls at thigh, elbow, and overhead heights.	126
Figure 5.9. Prevalence of flexed (Flex.) and extended (Ext.) elbow postures during one-handed pulls at mid-thigh, elbow, and overhead handle height.	126
Figure 5.10. Change in shoulder height, relative to point of force application, with increasing hand force during one-handed push exertions at mid-thigh, elbow, and overhead handle heights.	128
Figure 5.11. Change in shoulder height, relative to point of force application, with increasing hand force during one-hand pulls at mid-thigh, elbow, and overhead handle heights.	128
Figure 5.12. Change in fore/aft shoulder location with increasing hand force magnitude during up/down exertions at thigh, elbow, and overhead handle heights.	129

Figure 5.13. Torso inclination angle during thigh-height upward exertions.	129
Figure 5.14. Vertical off-axis forces generated during one-handed push exertions performed at thigh, elbow, and overhead handle heights.....	130
Figure 5.15. Vertical off-axis forces generated during one-hand pulls at thigh, elbow, and overhead handle heights.	130
Figure 5.16. Horizontal off-axis forces generated during elbow-height down exertions and upward exertions at mid-thigh, elbow, and overhead handle heights.....	131
Figure 5.17. Shoulder height, relative to point of force application, and vertical off-axis forces generated during directionally constrained and unconstrained thigh-height pull exertions.....	131
Figure 5.18. Shoulder height, relative to point of force application, and vertical off-axis forces generated during directionally constrained and unconstrained elbow-height pull exertions.....	132
Figure 5.19. Shoulder flexion/extension moments during directionally constrained and unconstrained thigh (leftmost plot) and elbow-height (rightmost plot) pulls.....	132
Figure 5.20. Utilization of internal bracing during (a) elbow-height upward exertions and (b) thigh-height forward exertions.....	133
Figure 5.21. Relationship between shoulder flexion/extension moment and drop in shoulder height for one-hand push exertions at mid-thigh, elbow and overhead handle heights. Black and grey data points correspond to trials in which bracing was or may have been used and were excluded from the analysis.....	133
Figure 5.22. Cumulative distribution function for absolute value of shoulder flexion/extension moments during forward exertions. 90% of unbraced trials had moments less than or equal to ~37 Nm as compared to 75 Nm for braced trials and 47 Nm for both braced and unbraced trials combined.....	134
Figure 5.23. Change in shoulder flexion/extension moment with horizontal pull force for one-handed back exertions at mid-thigh, elbow and overhead handle heights.....	135
Figure 5.24. Relationship between shoulder flexion/extension moment and drop in shoulder height during one-handed pulls at thigh, elbow, and overhead handle heights.....	135
Figure 5.25. Cumulative distribution function for one-hand pulls showing magnitude of shoulder flexion/extension moment is less than or equal to 35 Nm for 90% of trials.....	136
Figure 5.26. Variation in lateral displacement of the pelvis out of the hand-force plane across handle heights and with horizontal hand force during one-hand pulls.....	137
Figure 5.27. Change in lateral displacement of the pelvis with horizontal hand force for push exertions at mid-thigh (mean = -43 mm), elbow (R2 Adj = 0.06), and overhead (R2 Adj = 0.19) heights.....	137
Figure 5.28. Distribution of axial rotation moments [Nm] about the lumbar spine during one-hand exertions (mean = 2.3 Nm, Std.Dev. = 14.9 Nm).....	138
Figure 5.29. Distribution of out-of-plane rotation angle during one-hand push, pull, up, and down exertions performed at mid-thigh, elbow, and overhead handle heights.....	139

Figure 5.30. Relationship between out-of-plane rotation angle and horizontal hand force during one-hand pulls at thigh (R^2 Adj = 0.36), elbow (R^2 Adj = 0.13), and overhead (mean = 17 degrees) handle heights.	139
Figure 5.31. Change in shoulder fore-aft location with vertical hand force and associated change in out-of-plane rotation angle during elbow-height downward exertions.	140
Figure 5.32. Relationship between out-of-plane rotation angle and shoulder fore-aft location during upward exertions performed at thigh (mean = 34 degrees), elbow (R^2 Adj = 0.37), and overhead (mean = 10.6 degrees) handle heights.	140
Figure 5.33. Relationship between horizontal hand force and BOS length and fore-aft distance from rear boundary and BOS length during one-hand push exertions.	141
Figure 5.34. Change in length of BOS with pull force and relationship between BOS length and offset from front edge of BOS and pelvis during one-hand pulls. Grey data points correspond to 75% and maximal exertions performed with a parallel stance (BOS length \leq 1.5 foot lengths), and were excluded from the analysis.	142
Figure 5.35. Definition of hand force components and postural metrics used to predict shoulder flexion/extension moment. Shoulder extension moments are defined positive where extension of the shoulder corresponds to raising the arm, in the sagittal plane, from a resting posture along side the torso to overhead.	144
Figure 5.36. Actual versus predicted shoulder flexion/extension moment (Eqn 1) for one-handed push, pull, up, and down exertions at mid-thigh, elbow, and overhead handle heights ($p < 0.001$).	144
Figure 5.37. Hand force and postural metrics used to predict torso inclination in the hand-force plane. Torso inclination angle is with respect to the vertical and defined positive rearward.	145
Figure 5.38. Actual versus predicted torso inclination angle (Eqn 2) for one-handed exertions in the vertical up/down direction spanning mid-thigh to overhead handle heights (R^2 Adj = 0.37, RMSE = 6.98, $p < 0.001$).	146
Figure 5.39. Actual versus predicted torso inclination angle (Eqn 3) for one-handed pulls spanning mid-thigh to overhead handle heights (R^2 Adj = 0.54, RMSE = 12.9. $p < 0.0001$).	147
Figure 5.40. Actual versus predicted torso inclination angle (Eqn 4) for one-handed push exertions performed at mid-thigh, elbow, and overhead handle heights (R^2 Adj = 0.72, RMSE = 9.78 deg, $p < 0.001$).	148
Figure 5.41. Actual versus predicted pelvis pitch with respect to torso inclination (Eqn 5) for one-handed exertions (R^2 Adj = 0.47, RMSE = 8.02, $p < 0.001$).	149
Figure 5.42. Definition of metrics used to predict base-of-support length for two-hand push exertions. The active boundary of the base-of-support is the rear boundary when pushing and front boundary when pulling.	150

Figure 5.43. Actual versus predicted base-of-support length normalized by stature for one-handed push exertions performed at mid-thigh, elbow, and overhead handle heights (R^2 Adj = 0.72, RMSE = 0.066, $p < 0.001$).	150
Figure 5.44. Actual versus predicted length of base-of-support for one-handed pulls (R^2 Adj = 0.27, RMSE = 0.087, $p < 0.001$).	151
Figure 6.1. Laboratory and industry postures consistent with hypothesized biomechanical principles.	158
Figure 6.2. High-level model development process: postural behaviors (sensitivity to joint loads, standing balance requirements and aversion to slips and falls) and empirical models from data are used to predict key postural metrics, which coupled with kinematics, define task postures.	159
Figure 6.3. Definition of postural metrics used to define standing hand-force postures.	161
Figure 6.4. Main components and overall flow of the model.	162
Figure 6.5. Top and side-view of hand-force plane defined as the vertical plane in which the actual hand-force vector lies. Transformation between the global and hand-force plane coordinate frames is performed by the rotation matrix, R , a pure rotation of θ_z about the global z-axis. As defined, the z-axis of the global and hand-force coordinate frame is coincident.	163
Figure 6.6. Use kinematics of upper-extremity (1) and shoulder moment threshold (2) to set two-dimensional shoulder location in the hand-force plane.	165
Figure 6.7. Set torso inclination angle to obtain pelvis location in the hand-force plane.	166
Figure 6.8. Use target COP location computed from static equilibrium condition to position “active” foot (4). Set “passive” foot with respect to “active” foot to achieve desired BOS (5).	168
Figure 6.9. Orientation of shoulder vector with respect to hand-force plane used to define pelvis and torso orientations with respect to the hand-force plane.	169
Figure 6.10. Lateral displacement of the pelvis out of the hand-force plane to define 3D pelvis location.	170
Figure 6.11. Definition of pelvis pitch angle (θ_{pelvis}) relative to the torso.	171
Figure 6.12. Anatomical landmarks and measures used to define linkage representation of human body.	173
Figure 6.13. Linkage representation of the human body exploded to show DH frames.	175
Figure 6.14. Linkage structure and update linkage function used to generate three-dimensional representation of posture. Linkage is rooted at pelvis and recursion is used to traverse each branch of the linkage computing forward kinematics and continuously updating joint and segment properties needed to display linkage.	178
Figure 6.15. Graphical user interface (GUI) developed in Matlab.	179
Figure 6.16. Comparison of select, actual (light lines, ■) and predicted (dark lines, ●) two-hand postures across handle heights for a subset of directionally unconstrained trial conditions. Actual task postures correspond to individual data trials (i.e. data points) selected from dataset reserved for model validation.	180
Figure 6.17. Comparison of select, actual (light lines, ■) and predicted (dark lines, ●) one-hand postures across handle heights for a subset of directionally unconstrained trial conditions. Actual task postures	

correspond to individual data trials (i.e. data points) selected from dataset reserved for model validation.....	181
Figure 6.18. Actual (■) and predicted (●) two-hand elbow-height pushing postures showing drop in shoulder height and lengthening of base-of-support with increasing hand force magnitude. Forces are relative with low force corresponding to 25% of a subject’s maximum and high force corresponding to 75% of their maximum. Actual task postures correspond to individual data trials (i.e. data points) selected from dataset reserved for model validation.	182
Figure 6.19. Changes in actual (■) and predicted (●) two-hand pulling postures with change in handle height and hand force magnitude. Forces are relative with low force corresponding to 25% of a subject’s maximum and high force corresponding to 75% of their maximum. Actual task postures correspond to individual data trials (i.e. data points) selected from dataset reserved for model validation.....	183
Figure 6.20. Observed versus predicted torso flexion/extension angle across all trials grouped on task hand (one-hand = blue, two-hand = red). Marker style denotes force direction: ▲ = up, ✖ = push, + = pull, O = down.....	185
Figure 6.21. Observed versus predicted shoulder fore/aft location across all trials grouped on task hand (one-hand = blue, two-hand = red). Marker style denotes force direction: ▲ = up, ✖ = push, + = pull, O = down.....	186
Figure 6.22. Observed versus predicted shoulder height with respect to the point of force application across all trials grouped on task hand (one-hand = blue, two-hand = red). Marker style denotes force direction: ▲ = up, ✖ = push, + = pull, O = down.	187
Figure 6.23. Observed versus predicted fore-aft offset from pelvis to active boundary of BOS across all trials grouped on task hand (one-hand = blue, two-hand = red). Marker style denotes force direction: ▲ = up, ✖ = push, + = pull, O = down.	188
Figure 6.24. The effects of body weight and hand force magnitude on two-hand push / pull model predictions. Body weight spans from 445 N (100 lbs) to 890 N (200 lbs) and hand force magnitude from 44.5 N (10 lbs) to 223 N (50 lbs).....	189
Figure 6.25. Sensitivity of model predictions for two-hand push/pull exertions to shoulder moment criterion. The shoulder moment criterion spans from 10 Nm to 40 Nm and body weight spans from 445 N (100 lbs) to 890 N (200 lbs).....	189
Figure 6.26. Hyperextension of the lumbar spine used by a subset of subjects during high-force exertions.	193
Figure 6.27. Discrepancies between actual and predicted postures associated with internal bracing.	193

List of Tables

Table 2.1. Subject summary statistics. Subject 23 was identified as an outlier and excluded from analysis.	20
Table 2.2. Summary of optical marker and digitized landmark locations (L = left, R = right).	22
Table 2.3. Anthropometric measures.	26
Table 2.4. Summary statistics for male and female subjects showing anthropometric equivalency of subjects across designs.	29
Table 2.5. Summary statistics for male and female subjects showing equivalency in subject strengths across designs.	29
Table 2.6. Summary statistics on isolated, functional elbow and shoulder strength test measures for male and female subjects grouped by experimental design; strengths for 50%tile male and female from Kumar (2004) are provided for comparison; mean (stdev) given in Nm.	29
Table 2.7. Segment parameters; masses as a percent of total body mass; COM locations given as the distance, expressed as a percent of segment length, along the segment from the origin to the COM of the segment; WJC = wrist joint center, EJC = elbow joint center, SJC = shoulder joint center, HJC = hip joint center, KJC = knee joint center (de Leva, 1996).	31
Table 3.1. Direction of right (RH) and two-handed (2H) force exertions performed at each handle height.	41
Table 3.2. Mean strengths for one- and two-handed exertions at each handle height [N].	44
Table 3.3. Mean difference in actual and requested hand force magnitude and direction for all two-handed exertions. Force direction is quantified by vertical / fore-aft and lateral off-axis force components. (mean difference = actual force – requested force, * denotes highly significant with $p < 0.001$, gray shading denotes not significant, # / # denotes push / pull mean differences.	44
Table 3.4. Mean difference in actual and requested hand force magnitude and direction for one-handed exertions. Force direction is quantified by vertical / fore-aft and lateral off-axis force components. (mean difference = actual force – requested force, * denotes highly significant with $p < 0.001$, gray shading denotes not significant, # / # denotes push / pull mean differences.	46
Table 3.5. Models for predicting two-hand off-axis forces from the requested hand force magnitude.	58
Table 3.6. Models for predicting one-hand off-axis forces from the requested hand force magnitude.	58
Table 4.1. Test conditions and number of directionally unconstrained trials analyzed (women / men).	67
Table 4.2. Test conditions and number of directionally constrained trials analyzed (women / men) with all hand force directions grouped as push, pull, up, or down exertions. Directionally constrained trials were not performed at the overhead handle height and all maximum exertions were directionally unconstrained.	68
Table 6.1. Empirical parameters used in the posture-prediction model.	161

Table 6.2. Mean included elbow angles [degrees] specified for different task conditions.....	164
Table 6.3. Regression equations for predicting torso inclination in the hand-force plane.	166
Table 6.4. Regression equations used to compute base-of-support length as a fraction of stature.	167
Table 6.5. Regression equations developed to predict out-of-plane rotation angle during one-hand exertions.	168
Table 6.6. Predictive equations and mean values used to define lateral displacement of the pelvis during one-hand exertions.....	170
Table 6.7. Regression equations for pelvis pitch angle [deg] relative to the torso.....	171
Table 6.8. Segment lengths as a percent of stature, mass as a percent of total body mass, and COM location with respect to proximal end as a percent of segment length (male / female) from de Leva (1996), *subject data, and **UGS Jack Human figure model.....	174
Table 6.9. Denavit-Hartenberg parameters and zero-posture joint angles (θ_i^0) for the upper-body (RU=right upper-body, LU=left upper-body).	176
Table 6.10. Denavit-Hartenberg parameters and zero-posture joint angles (θ_i^0) for the lower-body (RL=right lower-body, LL=left lower-body, Bof = ball-of-foot).....	177
Table 6.11. Model performance for torso flexion/extension angle [deg] measured by correlation coefficient (r) and standard deviation of model residuals (RMSE).....	185
Table 6.12. Model performance for fore/aft shoulder location [cm] (x_{shoulder}).	186
Table 6.13. Model performance for shoulder height relative to point of force application [cm] (h_{shoulder})..	187
Table 6.14. Model performance for (x active edge of BOS – x pelvis) [cm].	188

ABSTRACT

Hand force and posture are key determinants of body loads during standing hand-force exertions. Current digital human modeling tools lack validated posture prediction for these common tasks and assume the nominal force requested is representative of the actual hand force applied by the worker. Furthermore, a change in hand force is not reflected in the simulated task posture. To address this need, a three-dimensional model to predict whole-body postures for a wide range of standing hand-force exertions was developed based on the following general biomechanical hypothesis: People choose postures that maintain shoulder moments below a threshold, and to minimize lower-back torsion, while attempting to maintain their torso orientation near vertical. To tune and validate the model, posture data were gathered from nineteen men and women in a laboratory study of force exertions with one and two hands. Participants exerted maximum forces and 25%, 50%, and 75% of maximum at three handle heights. The exertions included pushes, pulls, and vertical up/down exertions against a stationary handle. Posture and force data were analyzed for use in a hybrid biomechanical/empirical model formulation. The off-axis forces that were observed were consistent with participants reducing shoulder moment and increasing ground reaction force to improve foot traction. Shoulder flexion/extension moments were less than or equal to 37 Nm in 90% of trials, regardless of hand force magnitude and direction. Pelvis location and orientation during one-hand exertions support the hypothesis that postures are selected to reduce rotational moments about the lumbar spine. A tradeoff between torso inclination and change in shoulder position with increasing hand force was observed for exertions performed at a mid-thigh handle-height. Across both one- and two-handed exertions, shoulder flexion/extension moment was found to be well predicted by task conditions and posture variables, with an adjusted R^2 value of 0.82 and 0.92, and root mean square error (RMSE) of 10.7 Nm and 5.48 Nm for one- and two-handed trials, respectively. The

resulting posture-prediction model showed good performance for push/pull exertions. For up/down exertions, the wide range of tactics demonstrated by the study participants limited the model performance. Agreement between observed and predicted postural metrics was good when validated against 20% of trials withheld from the original dataset, with correlation coefficients ranging from 0.847 to 0.531 for all exertions.

CHAPTER 1

INTRODUCTION

1.1. Thesis Statement

Accurate representation of working postures is critical for ergonomic assessments with digital human models because posture has a dominant effect on analysis outcomes. Most current digital human modeling tools require manual manipulation of the digital human to simulate force-exertion postures or rely on optimization procedures that have not been well validated. Automated posture prediction based on human data would improve the accuracy and repeatability of analyses. This thesis asserts that posture and force data from the laboratory, coupled with basic mechanics can be used to develop an algorithm that accurately predicts standing hand-force exertion postures. More specifically, a model that uses the biomechanics of balance and joint loading to predict three-dimensional whole-body postures can produce realistic working postures for a variety of task conditions, and provide insight into the posture selection process when forceful exertions are required.

1.2. Applied Problem

Work cell environments are being designed virtually in an effort to decrease design time and eliminate the cost associated with physical prototypes; however, worker safety and quality of life remain a priority. In 2006 the Bureau of Labor Statistics (BLS) reported manufacturing as having one of the highest nonfatal occupational injury and illness incidence rates among goods-producing private industry sectors with six incidents occurring per 100 full-time employees annually. Of these cases, over 200,000 resulted in days away from work and approximately 270,000 cases required job transfer or restriction (BLS, 2006). In total, more than half the cases in manufacturing resulted in days away from work, job transfer, or restriction. A review of BLS and the National

Safety Council (NSC) databases by Mital et al. (1999) found overexertion injuries to be the leading type of exposure and one of the most costly injuries to treat with 25.9% of overexertion involving disability in the manufacturing sector in 1995. In total, it is estimated that on-the-job injuries cost the U.S. \$142.2 billion in 2004 (NSC, 2006). If product development time and cost prohibit or reduce the use of physical mock-ups of work cells, companies must practice reactive ergonomics and incur injury-related costs. An alternative is to provide ergonomists and job designers with tools to assess jobs virtually, early in the development.

Digital human figure models (DHM), virtual representations of a human, allow human-product and human-process interactions to be assessed virtually by bringing the human, product, and work cell geometry together in a computer-aided design (CAD) environment. Historically DHMs have been used to statically assess reach capability, line-of-sight, and clearance for people of various size and shape (Chaffin, 2001). Existing tools work well for these types of analyses, but manual manipulation of the human figure makes even simple analyses time consuming, and can result in postural inconsistencies within and across analysts. Task postures have a strong effect on the outcome of many ergonomic analyses using DHMs; thus, postural differences result in poor repeatability and reproducibility of analysis outcomes. Posture is especially critical when assessing jobs involving forceful exertions since joint loads are dependent on the location and orientation of body segments with respect to hand loads. Improved posture and motion simulation capabilities would increase the utility of DHMs by decreasing simulation time and eliminating the need for analysts to make assumptions about working postures.

There are several challenges associated with developing DHM tools for use in industry. Existing ergonomic analysis tools are used to guide design decisions and, when proven, can be used to justify potentially costly changes in product design, tooling, and job layout. To be seen as credible, however, posture-prediction models intended for ergonomic evaluation of industry jobs must produce accurate postures for the range of task conditions observed in industry. The model must be capable of replicating the different postural strategies prevalent in industry, and ergonomic evaluation of predicted postures must yield outcome measures consistent with analysis of actual working postures. Posture-prediction for standing tasks has been accomplished using a variety of

approaches but none of the previous methods have resulted in a model that satisfies all of the above-mentioned criteria.

The University of Michigan's 3D Static Strength Prediction Program (3DSSPP), a manikin-based task-analysis tool, uses a statistical model, combined with inverse kinematics, to predict force-exertion postures. Regression equations based on data from Kilpatrick (1970) and Snyder et al. (1972) were integrated into a behavioral inverse kinematics algorithm (Beck, 1992). This algorithm defines whole-body postures by predicting body segment positions based on hand location and orientation (supine, semi-prone, or prone), and worker height and weight. Predictive equations are based on postural data collected under no-load conditions, thus the effects of hand force on posture are not reflected in model predictions.

Reed et al. (2002) and others have presented predominantly statistical approaches to posture and motion prediction. Data from human volunteers performing tasks similar to those that are to be simulated are analyzed to express postural variables as a function of task and operator characteristics. Seidl (1994), in work to develop posturing models for the RAMSIS manikin, created a posture-prediction algorithm that maximizes the likelihood of joint angles relative to a database of human postures for similar tasks. Faraway (2003) has developed statistical methods for motion prediction that can also be used to predict static task postures. These methods provide validated accuracy for tasks similar to those in the underlying dataset, including the effects of task variables. However, all of the statistical approaches are limited in a manner similar to the motion-capture approaches, which is that the prediction accuracy degrades substantially for task conditions outside of the range of the underlying database.

Several strength-based posture-prediction models have recently been developed. The general proposition of these models is that workers will choose postures in which their joints can exert the largest torque. Seitz et al. (2005), building on earlier work by Rothaug (2000), developed an optimization-based approach for posture prediction that is based on human posture and strength data. The algorithm favors postures with low joint torques as well as high joint strength, and includes the effects of passive joint stiffness. The latter improves the ability to predict resting or low-force postures. The Seitz et al. model differs from other optimization approaches in being based on extensive human posture and

strength data. Strength functions have been used as a “naturalness” constraint to improve the visual realism of predicted postures (Liu, 2003, Zhao et al., 2005). “Naturalness,” a subjective criterion, is necessary but not sufficient validation for ergonomic analysis. More generally, joint-specific human functions have their peaks near the centers of the joint ranges of motion, so a joint-angle-based strength-optimization algorithm is largely equivalent to minimizing joint deviations from “neutral” positions. No validation has been found in the literature that supports the possibility that subject-specific differences in joint strength correspond to differences in task postures.

Seitz et al. (2005) acknowledge that while computed postures are “plausible,” a comparison between predicted and actual postures was not presented. Similarly, the work by Liu (2003) and Zhao et al. (2005) has proven capable of predicting “natural” as opposed to “awkward” postures but, naturalness is not a quantitative measure, and again, predicted postures have not been compared against postures actually used by workers.

Many researchers have proposed that work postures can be predicted by optimization of such factors as potential energy, deviation from neutral joint angles, discomfort, and strength. The general approach is to select, from among the set of postures that are kinematically consistent with the task constraints, the posture that minimizes (or maximizes) an objective function. The recognition that human postures are not, even on casual inspection, consistent with any single optimization criterion, has led to the use of multi-objective optimization. For example, Marler et al. (2005) propose three “key” considerations (tendency to move different body segments sequentially, preference towards comfortable neutral position, discomfort of movement near joint range-of-motion limits) that they hypothesize are related to human posture selection behavior. Multi-objective optimization for posture prediction relies on the user to change the relative weights or priorities assigned to each objective to produce accurate postures. In effect, this approach substitutes the potentially more tractable problem of choosing a vector of objective weights, for the basic problem of choosing joint angles, but does not itself provide a validated solution to the posture-prediction problem.

Posture and motion prediction can also be accomplished by modifying motion-capture data to conform to the requirements of the task (Park et al. 2004). For this approach to be accurate, the underlying dataset must include tasks that are substantially

similar to those being simulated, including with respect to the directions and magnitudes of forces. Recent progress in this area (e.g., Dufour et al., 2001) suggests that the method can be effective for tasks, such as vehicle ingress/egress, in which span of the variables affecting the motions is relatively small. However, this approach does not provide a general solution to the prediction of postures in a variety of novel tasks.

We propose a new approach to the prediction of standing postures with high hand forces that combines many of the advantages of previous approaches with several innovations. One major principle underlying the new method is the recognition that some aspects of posture are much more critical for biomechanical ergonomic analyses than are others. For instance, for standing tasks with hand-force exertions, an ergonomist is focused most frequently on low-back and shoulder loading, because injuries to these areas are common and costly. These outcome measures are influenced most strongly by torso inclination relative to gravity, and by the position of the hands with respect to the shoulders and low-back. The accuracy of an algorithm for posture prediction that is intended for use in ergonomics should be judged on the basis of its ability to predict important outcome measures, such as task-specific joint loading, rather than on global measures of joint angle correspondence.

1.3. Theoretical Problem

Standing tasks involving forceful exertions are prevalent and potentially costly. Looking only at push/pull exertions, a subset of standing hand-force exertions, Kumar et al. (1995) found that approximately half of manual materials handling tasks consist of pushing and pulling. The association of heavy lifting with low-back pain has made mechanical lifting aids an increasingly popular way of attempting to decrease low-back stresses when manually handling loads (Chaffin *et al.*, 1999). The introduction of high inertia materials handling devices (MHDs) into the workplace has reduced the amount of heavy lifting performed by workers at the expense of increasing the prevalence of high-force push/pull exertions (Nussbaum *et al.*, 2000).

As with lifting, low-back pain is associated with pushing and pulling, and a study regarding push/pull risk factors indicates that shoulder and upper-extremity complaints are also likely related to pushing and pulling (Hoozemans *et al.*, 1998). In general, manual materials handling and jobs involving hand force application through tool use are

responsible for approximately 45% of all industrial over-exertion injuries, resulting in \$110 billion in annual compensation in the U.S. alone (Mital & Das, 1987).

Accurate assessment of jobs involving hand forces is critical since risk of injury is greatly increased when job strength requirements exceed worker capabilities (Chaffin *et al.*, 1978). Ergonomic evaluation of worker capabilities requires accurate representation of task postures since it has been shown that a 10-degree error in the limiting joint angle can result in +/- 30% variations in percent capable predictions (Chaffin & Erig, 1991). This research is focused on three-dimensional whole-body posture prediction for standing hand force exertions. A model, which accurately predicts task postures, would eliminate the need for analysts to make assumptions about working postures, and improve the accuracy and repeatability of ergonomic analyses.

An understanding of the posture selection process, including factors affecting posture and the tradeoffs workers make when selecting task postures, is essential to development of a robust posture-prediction algorithm. Several different worker characteristics and job descriptors are hypothesized to influence posture selection for standing hand-force exertions, and are summarized in Figure 1.1. In addition to kinematic constraints resulting from task requirements, along with worker anthropometrics and capabilities, it is hypothesized that standing balance, sensitivity to joint moment loads (specifically at the shoulder), and our aversion to slips and falls impose biomechanical constraints that influence the posture selection process. These areas of biomechanics have been researched extensively with a significant number of studies focusing on mechanical joint loading, balance, and frictional requirements in the context of push/pull exertions. For a defined posture, balance, strength, and available friction at the feet also have been used to provide insight into hand force capability under different task conditions.

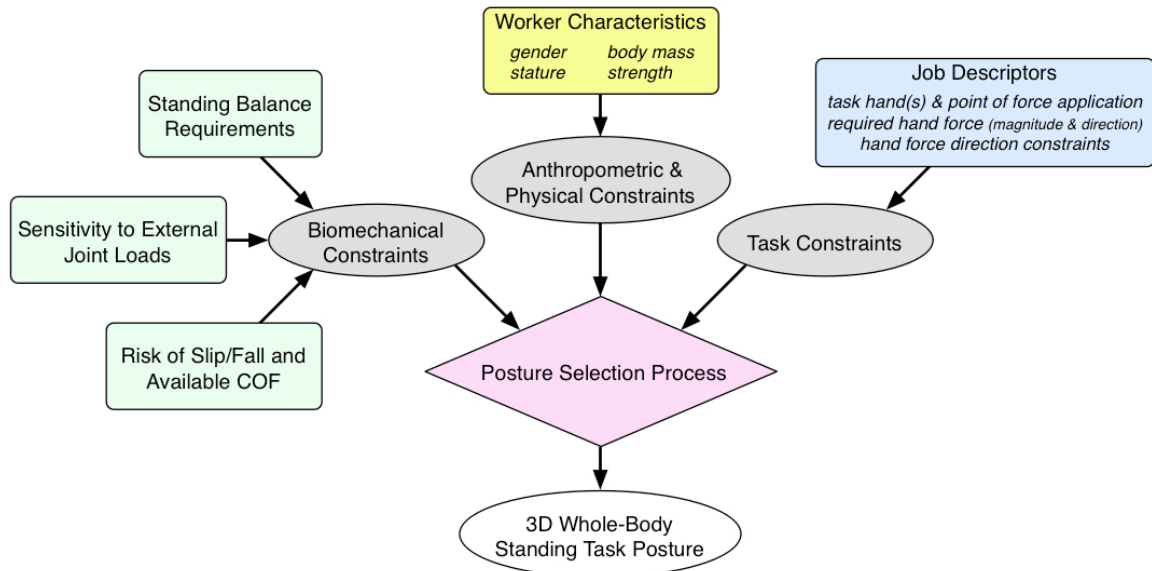


Figure 1.1. Factors hypothesized to affect posture selection for standing hand-force exertion tasks.

Several studies have quantified the effects of posture on mechanical loading of the low back and shoulders during pushing and pulling. de Looze et al. (2000) examined the effects of handle height and hand force magnitude on hand force direction, and the effect of these changes on low-back and shoulder loads. Subjects pushed or pulled on either a stationary bar or moveable cart at various handle heights and horizontal force levels. Changes in force exertion were reflected in changes in both shoulder and low-back torques, indicating that an accurate assessment of musculoskeletal loading during pushing and pulling tasks requires knowledge of both the force magnitude and direction. The effect of handle height and thus posture on low-back and shoulder loads was also examined by Hoozemans *et al.* (2004), as was the effect of cart weight. Both factors were found to have a significant effect on mechanical loading, which was lowest when pushing or pulling low weight carts at shoulder height.

The resultant hand force during nominally horizontal pushing has been quantified by several researchers and found to contain a significant vertical component. de Looze et al. (2000) and Granata et al. (2005) both observed a downward component during low-force exertions at low handle heights (e.g. waist height) and upward components with increasing force level and handle height. Both studies found this trend to be significant and highly reproducible. Kerk (1994) addressed the importance of force direction in the

context of ergonomics by illustrating how the assumption of a pure horizontal force results in an underestimation of the worker's horizontal push capability.

Force exertion capability models predict the maximal hand force possible under a given set of task conditions. Typical constraints include stability (or whole-body balance requirements), joint muscle strength, and friction requirements at the floor (Kerk, C. J., 1998). The model developed by Kerk (1998) is a two-dimensional model restricting it to the analysis of symmetric sagittal plane exertions. Despite this limitation, a benefit of this type of model is its ability to simultaneously consider the multiple factors governing hand force exertion capability.

Postural stability diagrams (PSDs) are similar to force exertion capability models in that they provide a graphical representation of the feasible hand force solution space for a given posture (Grieve, D. W., 1979). Locations of the center of pressure, body's center of gravity, and centroid of force exertion at the hands define the condition for static equilibrium, allowing it to be represented as a straight line on the PSD. Feasible hand forces are those combinations of vertical and horizontal force components that satisfy the static equilibrium condition (Wilkinson, A. T., 1995). As with force exertion capability models, the solution space of feasible hand forces afforded by the PSD is specific to the posture used in the equations for static equilibrium.

Basic mechanics have been used to explain postural strategies commonly observed during pushing and pulling exertions. Early work by Gaughran and Dempster (1956) measured maximal push and pull exertions in various seated postures, and performed a mechanical analysis of the force system (subject, seat, and force handle) to explain differences in push/pull strengths across postures. Dempster (1958) conducted a similar analysis of two-handed standing, seated, and braced pulls using free body diagrams. Both analyses show that the magnitude of the push/pull force one can exert is related to the relative magnitudes of the gravitational and horizontal force couples acting on the system (subject, seat/ground, force handle). These analyses illustrate how the condition of static equilibrium might be used to identify preferred pushing and pulling postures, along with appropriate muscle and body balance limits.

Balance maintenance is an essential part of any type of task performance but is critical in push and pull exertions. For certain tasks, stability constraints have been shown

to be more limiting than floor traction or joint muscle strength constraints with regards to force exertion capability (Holbein & Chaffin, 1997). Functional stability limits are dependent on load and foot position conditions as shown by Holbein and Chaffin (1997), Holbein and Redfern (1997), and Lee T-H and Lee Y-H (2003). In each of these studies the effect of foot placements on stability limits while holding a load was investigated. Holbein and Chaffin (1997) also showed that in general, increased separation of the feet in a given direction allows for greater displacement of the center of gravity in that direction without loss of balance. This finding is relevant to high-force pushing and pulling tasks in that it suggests that a fore-aft split-stance may allow for greater body weight utilization, i.e. larger displacement of the COM in the anterior/posterior direction, during high-force exertions.

The effect of foot positions on push/pull exertions has been examined to determine how pushing and pulling strengths differ between trials with constrained versus unconstrained foot placements. MacKinnon (2002) studied the effect of standardized foot positions on the execution of a submaximal pulling task and found that pull forces and velocities did not differ significantly between trials performed with standardized as opposed to freely chosen foot positions. Maximal pushing and pulling strengths have however been shown to depend on foot placements. Chaffin *et al.* (1983) found pushing strengths to be significantly greater when subjects were allowed to adopt a fore-aft split-stance as compared to pushing strength values measured while constrained to a symmetrical or parallel-stance.

The potential for slipping is often a factor during horizontal push/pull exertions since the frictional force available at the feet limits the horizontal force one can exert. An early study by Dempster (1958) found that when standing on a high-friction rubber mat subjects were able to generate upward forces equal to approximately twice their body weight and horizontal pull forces equal to 75% of body weight, but when the friction at their feet was reduced their vertical pull force was unaffected while the horizontal pull force dropped significantly. Boocock *et al.* (2006) found floor surface did not have a significant effect on resultant hand forces but had a significant effect on the vertical components. When pushing the cart on the standard floor (versus the high-friction safety

floor) subjects exerted a larger downward force component thereby decreasing the required coefficient of friction.

Hypothetical Basis for Forceful Posture-Prediction Method

Review of the literature and observations made in the laboratory and automotive assembly plants suggest that balance, joint loads, and our aversion to slips and falls are key determinants of posture. Traditionally, people have focused on assessing balance, external joint torques, and strength capabilities in a given posture, or have studied the effects of posture on mechanical joint loading. This dissertation addresses the inverse problem of using balance requirements, sensitivity to joint loads, and aversion to slips and falls to predict whole-body postures. Hypothesized biomechanical principles are combined with kinematic constraints, conditions for static equilibrium, and empirical relationships in a posture-prediction algorithm to predict three-dimensional, whole-body postures for standing hand-force exertions (Figure 1.2). For a given postural strategy the hypothesized posture selection process uses standing balance requirements and a preference towards reduced shoulder loads to select a task posture from the set of kinematically feasible postures. The primary hypotheses regarding posture selection are:

1. Standing balance requirements and an aversion towards slips and falls can be used to set foot placements with respect to whole-body center of mass (COM).
2. People choose postures consistent with reducing the shoulder load moment, within the limitations imposed by balance and kinematic constraints. External loads are reduced by directing the hand force vector towards the shoulder joint center or decreasing the shoulder moment arm.
3. People incline their torsos from vertical the minimal amount necessary to generate the needed hand forces within the constraints of kinematics, except as necessary to reduce shoulder loading.
4. One-hand force application postures are consistent with reducing the rotational moment around the inferior-superior axis in the lower back.

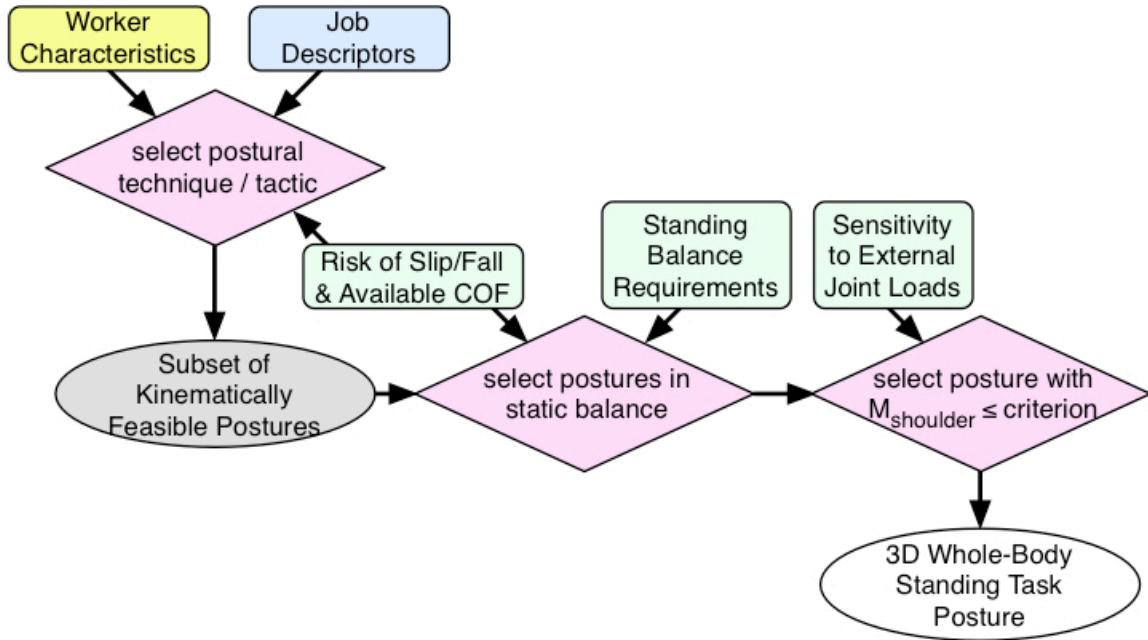


Figure 1.2. Organization of determinants of posture into posture-prediction algorithm.

1.4. Research Objectives

The work presented in this dissertation has five principal objectives:

1. Classify standing hand-force exertion postures by gross postural technique and investigate the effects of worker and task characteristics on tactic selection.
2. Quantify the relationship between actual and requested hand force and develop a model that predicts actual hand force vector from worker characteristics and task parameters.
3. Identify and analyze biomechanically critical aspects of postures to determine if task postures are consistent with hypothesized biomechanical principles.
4. Develop models from laboratory data to predict key postural metrics not explained by hypothesized biomechanical principles.
5. Develop and validate a three-dimensional posture prediction algorithm that combines kinematics, basic mechanics, and biomechanical principles in a hierarchical structure to predict whole-body postures for standing hand-force exertions.

1.5. Dissertation Organization

The body of this dissertation consists of six chapters, each of which supports one or more of the objectives of this research.

Chapter 2 provides an overview of the methods for a plant study and laboratory experiment. Observations from 30 jobs across three automotive assembly plants were used to design a laboratory based motion-capture study whereby 20 men and women performed standing hand-force exertions. The laboratory experiment was designed to quantify the effects of hand force location, magnitude, and direction on whole-body posture.

Chapter 3 examines the relationship between actual and requested hand force. Measured hand force data were analyzed to determine the effects of worker characteristics and task parameters on hand force magnitude and direction. Empirical models were developed to predict actual hand force magnitude and direction for tasks in which force direction is unconstrained. Postural data was used to group trials according to gross postural technique (push, pull, etc.) and all subsequent analyses conducted using these subsets of data.

Chapters 4 and 5 present statistical analyses one and two-handed standing hand force exertion postures. Biomechanically critical aspects of posture are identified and quantified with respect to the hand-force plane. Hypotheses regarding sensitivity to shoulder loads, selection of torso postures, and foot placements are tested in Chapter 4 for two-handed exertions. Analysis of postural metrics in Chapter 4 yields predictive models for (1) shoulder moment, (2) torso inclination, (3) pelvis orientation and (4) base-of-support length. A similar analysis is conducted in Chapter 5 for one-handed tasks. Postural features unique to one-hand exertions include (1) lateral displacement of the pelvis and (2) rotation of the torso and pelvis out of the force plane.

Chapter 6 presents the development and validation of the posture-prediction model that combines kinematics with biomechanical principles to predict whole-body standing hand-force postures from worker characteristics and task parameters. The posture-prediction algorithm used to predict key postural metrics with respect to the hand-force plane is outlined and integration of the algorithm into the larger model

structure discussed. Model performance is assessed and predicted postures compared against actual task postures for a subset of trials reserved for model validation.

1.6. References

- Beck, D. (1992). Human factors of posture entry into ergonomics analysis systems. PhD thesis, The University of Michigan, Ann Arbor, MI.
- BLS (2006). Workplace injuries and illnesses in 2006. Technical Report USDL 07-1562, United States Department of Labor, Washington, D.C.
- Boocock, M. G., Haslam, R. A., Lemon, P., and Thorpe, S. (2006). Initial force and postural adaptations when pushing and pulling on floor surfaces with good and reduced resistance to slipping. *Ergonomics*, 49(9):801–821.
- Chaffin, D., Freivalds, A., and Evans, S. (1987). On the validity of an isometric biomechanical model of worker strengths. *IIE Transactions*, 19:280–288.
- Chaffin, D., Stump, B., Nussbaum, M., and Baker, G. (1999). Low-back stresses when learning to use a materials handling device. *Ergonomics*, 42:94–110.
- Chaffin, D. B. (2001). Digital human modeling for vehicle and workplace design. Society of Automotive Engineers, Warrendale, Pa.
- Chaffin, D. B., Andres, R. O., and Garg, A. (1983). Volitional postures during maximal push/pull exertions in the sagittal plane. *Hum Factors*, 25(5):541–50.
- Chaffin, D. B. and Erig, M. (1991). Three-dimensional biomechanical static strength prediction model sensitivity to postural and anthropometric inaccuracies. *Iie Transactions*, 23(3):215–227.
- de Looze, M. P., van Greuningen, K., Rebel, J., Kingma, I., and Kuijer, P. P. (2000). Force direction and physical load in dynamic pushing and pulling. *Ergonomics*, 43(3):377–390.
- Dempster, W. (1958). Analysis of two-handed pulls using free body diagrams. *J Applied Physiology*, 13(3):469–480.
- Dufour, F., Lino, F., and Le Coz, J.-Y. (2001). Vehicle accessibility. Technical Report 2001-01-3431, SAE International, Warrendale, PA.
- Faraway, J. (2003). Data-based motion prediction. Technical Report 2003-01-2229, SAE International, Warrendale, PA.
- Center for Ergonomics. (2005). Three dimensional static strength prediction program (3DSSPP). The University of Michigan, Ann Arbor, MI, v 5.0.3 edition.
- Gaughran, G. and Dempster, W. (1956). Force analysis of horizontal two-handed pushes and pulls in the sagittal plane. *Human Biology*, 28(1):67–92.
- Granata, K. R. and Bennett, B. C. (2005). Low-back biomechanics and static stability during isometric pushing. *Hum Factors*, 47(3):536–549.

- Grieve, D. W. (1979). Environmental constraints on the static exertion of force: Psd analysis in task-design. *Ergonomics*, 22(10):1165–75.
- Holbein, M. and Redfern, M. (1997). Functional stability limits while holding loads in various positions. *International Journal of Industrial Ergonomics*, 19(5):387–395.
- Holbein, M. A. and Chaffin, D. B. (1997). Stability limits in extreme postures: effects of load positioning, foot placement, and strength. *Hum Factors*, 39(3):456–68.
- Hoozemans, M. J., van der Beek, A. J., Frings-Dresen, M. H., van Dijk, F. J., and van der Woude, L. H. (1998). Pushing and pulling in relation to musculoskeletal disorders: a review of risk factors. *Ergonomics*, 41(6):757–781.
- Hoozemans, M. J. M., Kuijper, P. P. F. M., Kingma, I., van Dieen, J. H., de Vries, W. H. K., van der Woude, L. H. V., Veeger, D. J. H. E. J., van der Beek, A. J., and Frings-Dresen, M. H. W. (2004). Mechanical loading of the low back and shoulders during pushing and pulling activities. *Ergonomics*, 47(1):1–18.
- Kerk, C., Chaffin, D., and et al (1994). A comprehensive biomechanical model using strength, stability, and cof constraints to predict hand force exertion capability under sagittally symmetric static conditions. *IIE Transactions*, 26(3):57–67.
- Kerk, C., Chaffin, D., and Keyserling, W. (1998). Stability as a constraint in sagittal plane human force exertion modeling. *Occupational Ergonomics*, 1(1):23–39.
- Kilpatrick, K. (1970). A Model for the design of manual workstations. PhD thesis, The University of Michigan, Ann Arbor, MI.
- Kumar, S., Narayan, Y., and Bacchus, C. (1995). Symmetric and asymmetric two-handed pull push strength of young adults. *Human Factors*, 37:854–865.
- Lee, T. H. and Lee, Y. H. (2003). An investigation of stability limits while holding a load. *Ergonomics*, 46(5):446–54.
- Liu, Y. (2003). Interactive reach planning for animated characters using hardware acceleration. PhD thesis, The University of Pennsylvania, Philadelphia, PA.
- MacKinnon, S. N. (2002). Effects of standardized foot positions during the execution of a submaximal pulling task. *Ergonomics*, 45(4):253–66.
- Marler, R., Rahmatalla, S., Shanahan, M., and Abdel-Malek, K. (2005). A new discomfort function for optimization-based posture prediction. Technical Report 2005-01-2680, SAE International, Warrendale, PA.
- Mital, A. and Das, B. (1987). Human strengths and occupational safety. *Clinical Biomechanics*, 2:97–106.

- Mital, A., Pennathur, A., and Kansal, A. (1999). Nonfatal occupational injuries in the united states part I - overall trends and data summaries. *International Journal of Industrial Ergonomics*, 25:109–129.
- NSC (2006). *Injury Facts*. National Safety Council, 2005-2006 edition.
- Nussbaum, M., Chaffin, D., Stump, B., Baker, G., and Foulke, J. (2000). Motion times, hand forces, and trunk kinematics when using material handling manipulators in short-distance transfers of moderate mass objects. *Applied Ergonomics*, 31:227–237.
- Park, W., Chaffin, D., and Martin, B. (2004). Toward memory-based human motion simulation: Development and validation of a motion modification algorithm. *IEEE Transactions on systems man and cybernetics, Part A: systems and humans*, 34(3):376–386.
- Reed, M., Manary, M., Flannagan, C., and Schneider, L. (2002). A statistical method for predicting automobile driving posture. *Human Factors*, 44:557–568.
- Reed, M., Manary, M., and Schneider, L. (1999). Methods for measuring and representing automobile occupant posture. In *SAE Transactions: Journal of Passenger Cars*, volume 108, SAE Technical Paper 990959.
- Rothaug, H. (2000). Combined force-posture model for predicting human posture and motion by using the ramsis human model. Technical Report 2000-01-2170, SAE International, Warrendale, PA.
- Seidl, A. (1994). *Das Menschmodell I Ramsis: Analyse, Synthese, und Simulation dreidimensionaler Körperhaltungen des Menschen [The man-model RAMSIS: Analysis, Synthesis, and simulation of three-dimensional human body postures.]*. PhD thesis, Technical University of Munich.
- Seitz, T., Recluta, D., Zimmermann, D., and Wirsching, H.-J. (2005). Focopp - an approach for a human posture prediction model using internal / external forces and discomfort. Technical Report 2005-01-2694, SAE International, Warrendale, PA.
- Snyder, R., Chaffin, D., and Schultz, R. (1972). Link system of the human torso. HSRI Report 71-112, Highway Safety Research Institute, and The University of Michigan, Ann Arbor, MI. and AMRL-TR-71-88, Aerospace Medical Research Laboratories, Ohio.
- Wilkinson, A., Pinder, A., and Grieve, D. (1995). Relationships between one-handed force exertions in all directions and their associated postures. *Clin Biomech (Bristol, Avon)*, 10(1):21–28.

Zhao, L., Liu, Y., and Badler, N. (2005). Applying empirical data on upper torso movement to real-time collision-free reach tasks. Technical Report 2005-01-2685, SAE International, Warrendale, PA.

CHAPTER 2

EXPERIMENTAL DESIGN AND METHODS

2.1. Overview of Methods for Plant and Laboratory Studies

Biomechanical analysis of standing tasks can provide insight into the postures selected and forces exerted at the hands. Analyses by Gaughran & Dempster (1956) and Kerk et al (1994) show how basic mechanics and task constraints, coupled with knowledge of strength and balance limits may be used to identify preferred postures.

Behaviors exhibited during a pilot study and observed in industry also suggest posture selection is driven by biomechanics. Through observation and qualitative assessment of foot placements and whole-body postures adopted during standing exertions a set of biomechanical principles were proposed. It is hypothesized that biomechanical principles can be used to predict postures employed during one- and two-handed standing exertions.

Based on the preceding, experimental methods were developed and a laboratory study conducted to obtain data required for detailed biomechanical analysis of high exertion standing tasks and to test the above hypotheses.

2.2. General Objectives

1. Develop and conduct a laboratory study to elicit the range of postural behaviors used in industry when performing standing hand-force exertions.
2. Investigate the effects of task parameters and worker characteristics on whole-body postures and quantify postural changes in response to changes in hand force magnitude and/or direction.
3. Compare actual and requested hand forces (magnitude and direction) during standing hand-force exertions.

4. Obtain postural and force data to test hypothesized biomechanical principles regarding posture selection.

2.3. Plant Methods

A plant study was conducted to gain insight into the types of postures selected when performing standing hand-force exertions in industry. Thirty jobs were studied across three automotive assembly plants for analysis. Jobs were selected based on hand force requirements (magnitude and direction) and work zone with a preference towards jobs with minimal postural constraints. Postures chosen for low, medium, and high-force hand exertions performed at a range of working heights were assessed qualitatively via video. Two operators were videoed for each job and for a subset of jobs estimates of hand forces were obtained using a Chatillon MSC-500 force gauge (Ametek, Inc., Largo, FL). The objectives of this study were to (1) qualitatively assess the effects of job requirements on posture and observe the types of postural strategies used over a range of different task conditions, (2) determine if postures observed in industry are consistent with the hypotheses outlined in Chapter 1 and observations from the laboratory, and (3) identify relevant task parameters (e.g. hand force, working height, etc) to study in the laboratory.

2.4. Laboratory Study Methods

Participants

Twenty paid participants, ten males and ten females, were recruited from a student population. Participants were required to be right-hand dominant and have no previous history of musculoskeletal disorders, low-back pain, shoulder pain, or reduced mobility. Table 2.1 lists summary attributes for the participants. All participants were young (median age 21 years) and relatively thin (median body mass index 23 kg/m²). An attempt was made to recruit men and women with widely varying body size and strength capabilities. Male participants ranged from 6th %tile to 94th %tile by stature and female participants ranged from 11th %tile to 93rd %tile by stature (Roebuck, 1995). Participant whole-body strength capabilities were characterized by standardized arm, torso, and leg lift strength tests (Stobbe, 1982) and expressed as population strength percentiles using data from Chaffin et al, 2006.

Table 2.1. Subject summary statistics. Subject 23 was identified as an outlier and excluded from analysis.

Subject Number	Experimental Design	Gender	Age [yrs]	Stature		Body Mass [kg]	Body Mass Index [kg/m ²]	%tile Strength		
				[cm]	%tile			Arm Lift	Torso Lift	Leg Lift
005	II	M	19	179.1	80	76.2	23.8	91	28	72
006	I	F	21	157.9	36	47.8	19.2	5	10	22
007	I	M	24	171.8	41	70.7	24.0	29	17	52
009	II	M	27	173.5	51	87.1	28.9	97	27	97
010	I	F	24	163.7	70	68.0	25.4	42	38	72
012	II	M	31	165.6	13	58.3	21.3	2	7	3
013	I	F	18	152.4	11	60.6	26.1	37	32	80
014	II	M	20	184.1	94	67.6	19.9	18	15	13
016	II	F	20	164.6	74	59.4	21.9	59	36	69
017	I	M	21	183.0	92	75.7	22.6	29	32	28
018	I	M	20	162.6	6	66.7	25.2	55	25	80
019	I	F	20	170.1	93	65.8	22.7	19	43	60
020	II	F	19	155.7	24	81.8	33.7	50	64	69
021	II	M	27	170.5	34	63.5	21.8	32	21	18
022	II	F	20	170.1	93	68.9	23.8	67	52	98
023	I	M	20	165.5	13	59.0	21.5	56	13	25
024	II	F	25	156.0	26	48.0	19.7	48	37	48
025	II	F	19	158.8	41	53.5	21.2	59	35	65
026	I	F	19	157.6	34	58.0	23.3	66	63	91
027	I	M	21	177.2	72	73.2	23.3	71	37	85

Facilities

The study was conducted in the Human Motion Simulation (HUMOSIM) laboratory at the University of Michigan. Data were obtained using a laboratory setup comprised of four systems: (1) force platforms, (2) force handle, (3) force feedback display, and (4) motion tracking system (Figure 2.1). Since it has been shown that preferred foot placements vary with task parameters (Holbein & Chaffin, 1997) reconfigurable force plates were utilized to capture ground reaction forces for various stances.

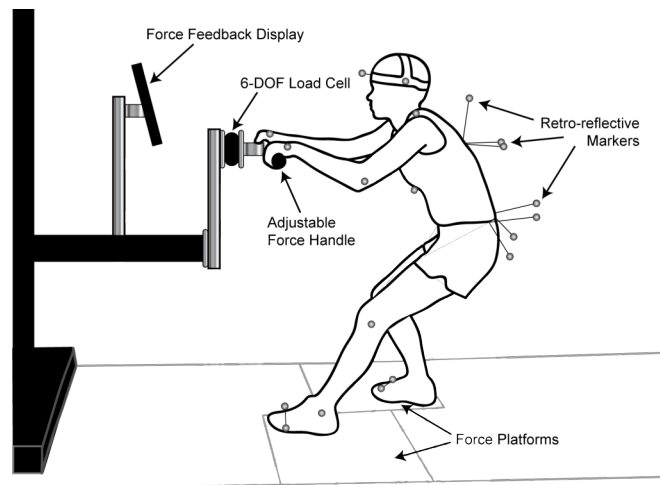


Figure 2.1. Laboratory configuration with visual force feedback display, 6-DOF load cell and moveable force platforms for measuring forces and moments at the hands and feet respectively.

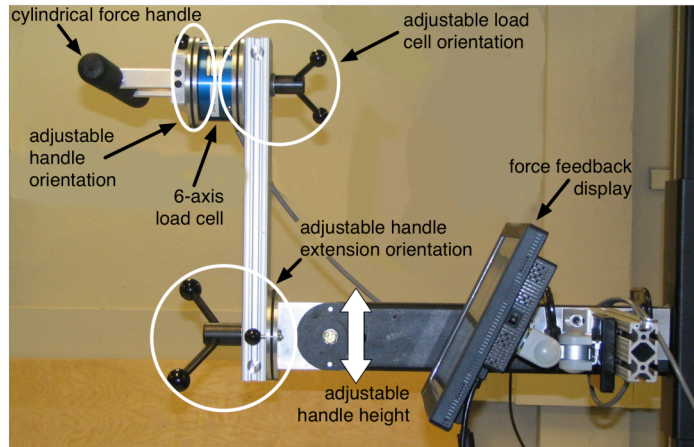


Figure 2.2. Force handle adjustability.

Forces and moments at the hands were measured via an adjustable force handle affixed to a 6-DOF load cell (JR3, Woodland, CA) (Figure 2.2). The handle was a cylindrical, rigid bar 470 mm long and 35 mm in diameter. The handle was covered with 5-mm-thick foam rubber that provided a high-friction grip.

Hand force feedback was presented visually to the subject allowing subjects to achieve and maintain requested hand forces. It has been reported that without feedback on hand forces, the measured hand force vector differs from that requested (Kerk, 1992). A force feedback display that provides the subject with real-time feedback on hand forces was developed in LabVIEW 7.1 to assist the subject in controlling variations in force magnitude and direction. The display indicates the desired force magnitude and direction, the subject's current force magnitude on the desired axis, and the magnitudes on axes orthogonal to the desired axis.

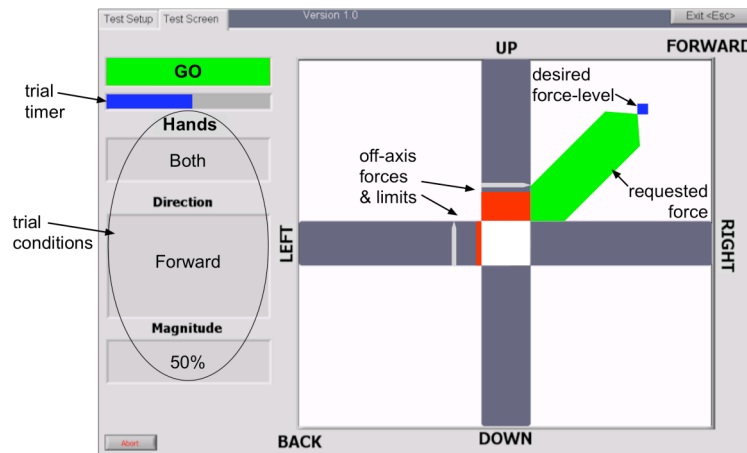


Figure 2.3. Visual force-feedback display with goal (blue diamond) shown for required level of force in requested direction and maximal allowable off-axis forces indicated by grey limit bars.

An eight-camera Qualysis Proreflex 240-MCU optical based motion tracking system was used to quantify whole-body motions and postures. Twenty-nine retro-reflective markers were placed on the subject at pre-defined body landmarks (Figure 2.4) and a digitization procedure followed. Optical marker locations are used in conjunction with twenty-six digitized points (twenty-five body landmarks plus 1 point on the floor) to capture whole-body postures. The set of optical markers and digitized points used is summarized in Table 2.2 and the locations illustrated in Figure 2.5. Digitization is used to define the location of additional body landmarks on the head, torso, pelvis, and feet with respect to the optical markers. Digitized points are later combined with three-dimensional marker data to create a linkage representation of the human body (Reed et al, 1999). Kinematic data were sampled at 50 Hz and all analog signals sampled at 500 Hz. Video was taken of each trial and synchronized with the kinematic data and analog data from the two AMTI force plates and a JR3 load cell.



Figure 2.4. Retro-reflective marker set used to track whole-body motion.

Table 2.2. Summary of optical marker and digitized landmark locations (L = left, R = right).

Optical Marker Locations		Digitized Landmark Locations	
L. & R. side of head	L. & R. foot – lateral	L. & R. Tragon	T10
Front of the head	Sternum top	L. & R. Infraorbital	T12
L. & R. Acromion	Sternum bottom	L. & R. Acromion	L3 (approximate)
L. & R. Lateral Epicondyle of Humerus	T8 – top	Vertex	L5
L. & R. hand – thumb side	T8 – left	Suprasternale	Sacrum
L. & R. hand – pinky side	T8 – right	Substernale	L. & R. PSIS
L. & R. Lateral Epicondyle of Femur	T1	C7	L. & R. ASIS
L. & R. Lateral Malleolus	L. & R. hip	T4	L. & R. foot – bigtoe
L. & R. foot – medial	L. & R. PSIS	T8	L. & R. foot – 5 th
			Metatarsalphalangeal

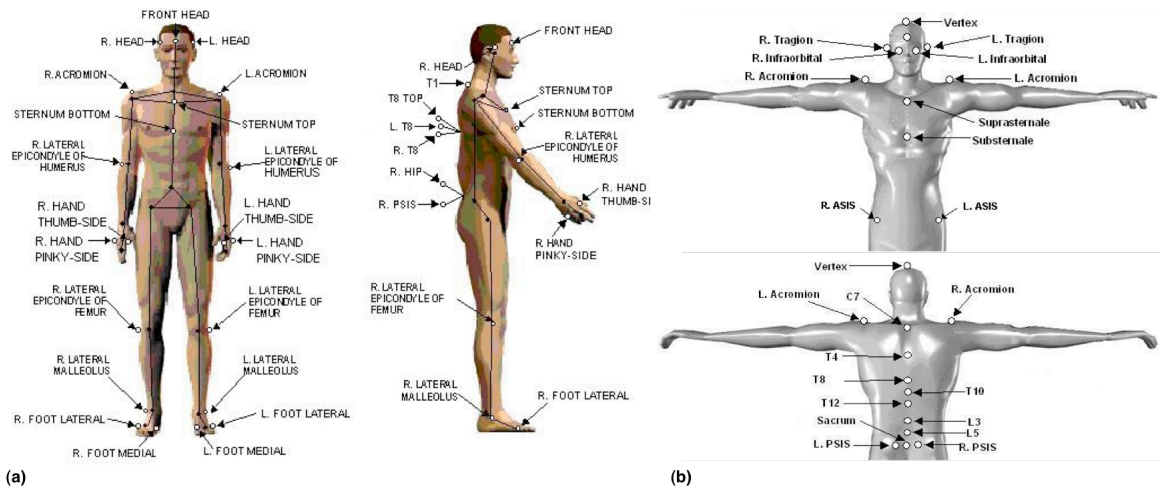


Figure 2.5. (a) Optical marker and (b) digitized landmark locations.

Test Conditions

A laboratory experiment was designed to quantify the effect of task parameters on whole-body standing postures. Task parameters investigated include hand force magnitude and direction, hand force directional constraint, handle height, and the number of hands used to perform the task. Three handle heights were chosen to span the range of working heights common in industry and observed in the plant study. Handle height was scaled for each subject to standing elbow height (63% of stature), mid-thigh height (41% of stature), and 0.1 m overhead. A total of fourteen different force directions were studied, 6 principal and 8 non-principal directions, in order to capture force exertion postures under various symmetric (i.e. sagittal) and asymmetric (i.e. cross-body) loading conditions (Figure 2.6). Exertions were performed on a raised platform with the requirement that subjects remain on the gridded region of the platform during all exertions (Figure 2.7). This constraint on foot placement was imposed in an effort to prevent subjects from aligning themselves with the direction of force and thus converting all asymmetric (i.e. cross-body) loading conditions into sagittal plane exertions.

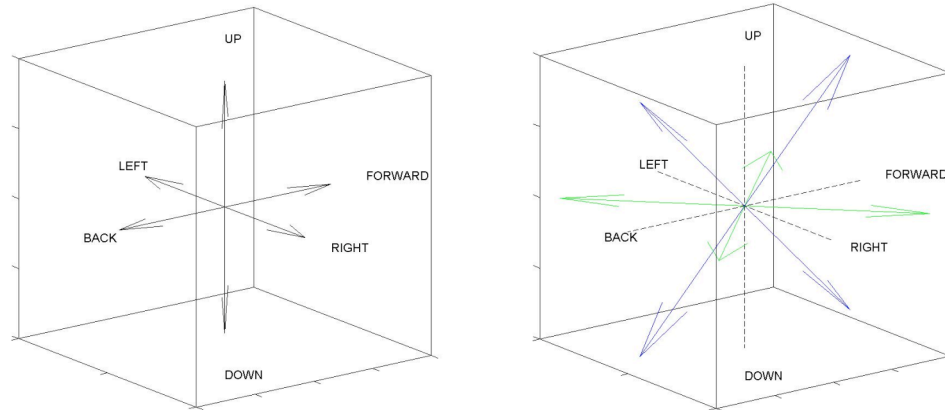


Figure 2.6. Principal (forward, back, left, right, up, down) and non-principal (forward-up, forward-down, back-up, back-down, forward-right, forward-left, back-right, back-left) hand force directions.

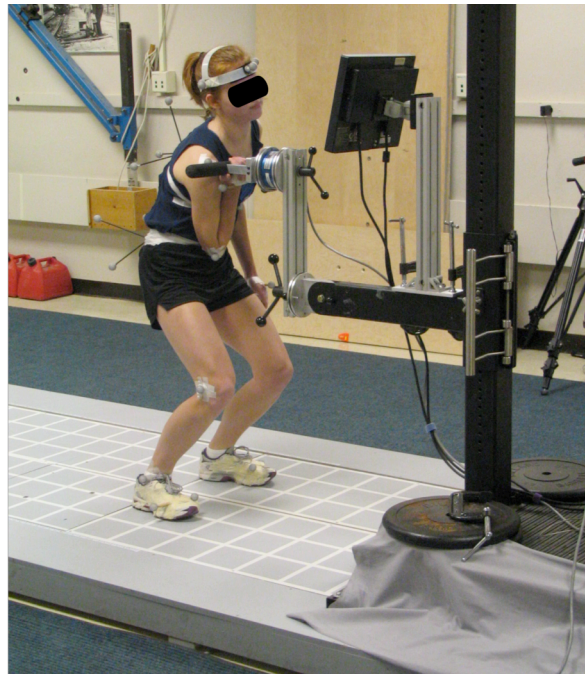


Figure 2.7. Participant in the experimental setup performing an exertion on the fixed force handle while receiving visual feedback on hand force via an LCD screen.

Constraints were imposed on hand force direction for a subset of the trials. Both directionally constrained and unconstrained exertions were performed in the principal directions. All exertions in non-principal directions directionally constrained. During unconstrained trials participants were told to exert a force in the requested direction but off-axis forces (i.e. forces in directions other than that requested) were not constrained and only the on-axis force magnitude was presented to the subjects. In constrained trials participants were provided with feedback on both the on-axis and off-axis force

magnitudes. For all trials, participants were required to achieve a desired force level in the requested direction. When force direction was constrained participants were also required to maintain off-axis forces below 20% of the requested force magnitude. All exertions were performed at 25, 50, 75, and 100% of each subject's maximum capability. During the exertions subjects were allowed to brace off their own body but were not permitted to brace externally off the testing apparatus.

Procedures

The scope of the experiment required the study be divided into two sessions. The first session was used to introduce each subject to the experiment, conduct anthropometric and strength measures, quantify body segment masses, and obtain data on their physical activity level. The institutional review board at the University of Michigan approved the protocol and all subjects provided written, informed consent. During the first session each participant was scheduled to return to the laboratory for a second session. Maximal and submaximal standing exertions were performed during the second session.

1st Session: Anthropometry, Body Segment Mass Estimation and Strength Testing

Subject anthropometry was characterized by thirty-six anthropometric measures (Table 2.3). Body mass distributions vary across populations (Pataky et al., 2003) and whole-body center-of-mass (COM) estimation has been shown to be sensitive to inaccuracies in body segment parameters (Lenzi et al., 2003). Discrepancies between top-down analysis based on body segment masses and posture, and force-plate data are expected when actual and estimated segment masses differ. One way of resolving these discrepancies is to better characterize mass distributions for each subject. Based on the work of Pataky and Zatsiorsky (2003) an apparatus and procedure for determining subject-specific body segment masses were developed. Body segment masses were estimated using a subset of the anthropometrics in combination with the change in total body center-of-pressure measured during a series of four tasks. The body segment mass estimation procedure is outlined in detail in the Appendix (Section 2.5).

Table 2.3. Anthropometric measures.

Body weight	Hand length & width
Stature (with & w/out shoes)	Wrist depth & width
Seated height	Elbow width
Head width & depth	Floor to L5 standing
Nasion to top of head	C7 to L5
Nasion height from floor	Pelvis depth (ASIS-to-PSIS)
C1 to C7	Hip center-to-knee length
Floor to C7 standing	Femoral epicondyle width
Floor to suprasternal notch	Knee height
C7 to suprasternal notch (vert & horiz)	Knee-to-ankle length
Suprasternal notch to acromion processes	Lateral malleolus to 1st metatarsalphalangeal (horiz)
Inter-acromion processes	Malleolus height & width
Shoulder-to-elbow length	Ankle-to-heel distance
Elbow-to-wrist length	Foot length

A series of strength tests were conducted to quantify participant strength capabilities. Three standardized strength tests provided measures of whole-body strengths and allow for comparison with strength values published for a large population (Figure 2.8). Whole-body strengths were measured by having the subject exert their maximum capable force against a fixed handle while in various postures. The exerted force was measured via a one-degree-of-freedom load cell.

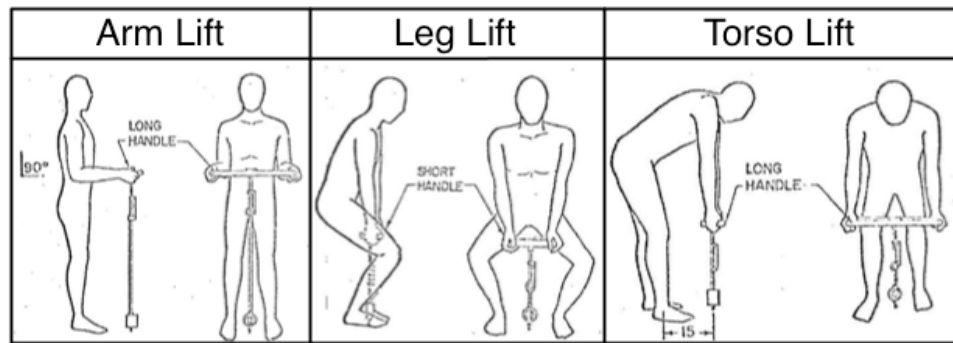


Figure 2.8. Illustration of standardized strength tests (Stobbe, 1982).

Functional strength tests were used to quantify specific elbow and shoulder strengths (Figure 2.9). The University of Michigan static strength test chair (version MFE4) was used for these tests. For each test the subject was seated and instructed to exert their maximum capable force against the chair or a strap depending on the particular strength being measured. During each, test deflections in the chair are measured via strain gauges and converted to strength measures (i.e. moments) using a calibration file.

Restraints were employed during the functional strength tests to prevent undesired movements and isolate the muscle or group of muscles being tested.

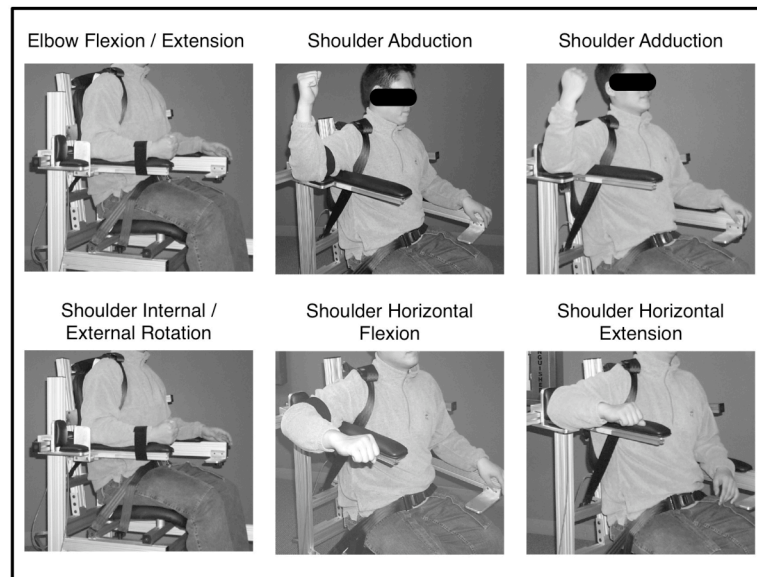


Figure 2.9. Functional strength tests (University of Michigan, 2000).

All strength tests were performed a minimum of two times and additional tests conducted when the difference in strength measures for a given test exceeded 15%. Subjects were given at least 1 to 2 minutes of rest between tests, depending on the sequencing of tests and muscles recruited during each test. Anthropometric measures were collected between strength tests to provide the subject with additional rest.

2nd Session: Maximal and Submaximal Standing Exertions

At the onset of the second session the subject performed each of the three standardized strength tests once. These strength tests were repeated at the end of the session as a measure of fatigue. Following strength testing the visual force feedback display was explained to the subject. A group of representative trials were used to illustrate how information is presented on the display for various trial conditions.

Subjects performed right-handed and two-handed exertions on a fixed force handle at prescribed handle heights. Each trial began with the subject at the end of a raised platform requiring them to take a few steps to approach the force handle. This decision was made in an attempt to ensure the postures captured were natural. Real-time visual feedback on the magnitude and direction of force exerted on the fixed handle was provided to the subject during each trial. Given the large number of conditions to be

tested a split-design was employed (Figure 2.10). Subjects were distributed between experimental designs I and II in a manner that yielded anthropometrically and strength equivalent groups (Table 2.4 and Table 2.5). All subjects performed elbow height exertions (Block 1). In addition, subjects assigned to Design I performed overhead exertions (Block 2a) and those assigned to Design II performed exertions at a mid-thigh handle height (Block 2b).

Prior to conducting the submaximal trials subjects completed a series of maximal exertions at the two assigned handle heights. Trials were blocked on handle height and maximum values were obtained for the principal force directions only. Maximal trials were 6 seconds in duration and were preceded by a practice trial. During the practice trials subjects were encouraged to explore different postural strategies. A minimum of one practice trial was conducted for each test condition and practice trials were repeated until the participant indicated they were comfortable with their posture. Practice trials served as an opportunity for subjects to identify their preferred posture and gain familiarity with the force feedback display. Maximum values were recorded and used to define submaximal force levels.

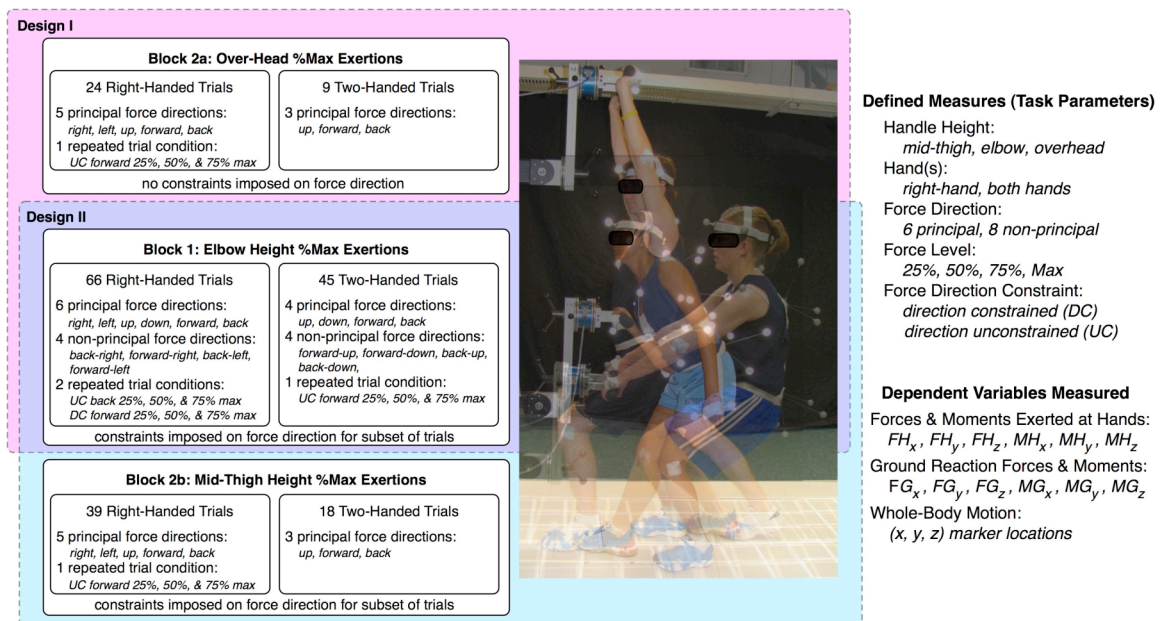


Figure 2.10. Experimental design: Block I performed by all subjects, blocks 2a and 2b performed by subjects assigned to Design I and Design II respectively.

Table 2.4. Summary statistics for male and female subjects showing anthropometric equivalency of subjects across designs.

Design	Males ($n_I = n_{II} = 5$)			Females ($n_I = n_{II} = 5$)		
	Age [years]	Stature [cm]	BMI [kg/m ²]	Age [years]	Stature [cm]	BMI [kg/m ²]
I	21.2 (1.6)	172.0 (8.4)	23.2 (1.6)	20.4 (2.3)	160.3 (6.8)	23.4 (2.7)
II	24.8 (5.1)	174.6 (7.2)	22.9 (3.7)	20.6 (2.5)	161.0 (6.2)	24.2 (5.6)

Table 2.5. Summary statistics for male and female subjects showing equivalency in subject strengths across designs.

Design	Males ($n_I = n_{II} = 5$)			Females ($n_I = n_{II} = 5$)		
	Arm Lift [N]	Torso Lift [N]	Leg Lift [N]	Arm Lift [N]	Torso Lift [N]	Leg Lift [N]
I	353.5 (175)	339.9 (100)	956.4 (483)	195.2 (68.5)	220.5 (85.1)	516.0 (208)
II	399.8 (113)	356.8 (78.5)	870.1 (327)	176.9 (27.2)	240.6 (43.4)	499.5 (66.3)

Table 2.6. Summary statistics on isolated, functional elbow and shoulder strength test measures for male and female subjects grouped by experimental design; strengths for 50%tile male and female from Kumar (2004) are provided for comparison; mean (stdev) given in Nm.

Functional Strength Test	Males ($n_I = n_{II} = 5, n_{Kumar} = 25$)			Females ($n_I = n_{II} = 5, n_{Kumar} = 22$)		
	Design I	Design II	Kumar, 2004	Design I	Design II	Kumar, 2004
Elbow flexion	56 (31.3)	57 (18.5)	77 (21.0)	32 (7.02)	30 (5.91)	41 (11.9)
Elbow extension	41 (21.9)	43 (14.4)	46 (10.9)	30 (11.6)	26 (3.63)	27 (9.12)
Shoulder medial rotation	41 (16.0)	38 (11.2)	52 (16.7)	21 (3.63)	21 (1.32)	21 (7.30)
Shoulder lateral rotation	25 (7.92)	23 (3.84)	33 (8.51)	15 (3.90)	16 (2.43)	19 (4.56)
Shoulder horizontal backward	17 (4.03)	15 (4.05)	67 (18.2)	10 (0.61)	12 (2.16)	33 (11.6)
Shoulder horizontal forward	35 (22.5)	32 (19.6)	92 (22.8)	15 (3.36)	18 (4.39)	40 (14.6)
Shoulder Abduction	22 (9.08)	20 (8.38)	71 (17.9)	12 (3.49)	14 (2.26)	37 (12.8)
Shoulder Adduction	24 (9.90)	20 (9.22)	67 (24.3)	11 (1.91)	11 (2.45)	30 (12.5)

Upon completion of the maximal trials, each subject then performed a series of submaximal exertions at the two assigned handle heights. Trials were again blocked on handle height. For each trial condition, exertions were performed in order of increasing force level. Within a block, trials without force direction constraints were competed before trials with directional constraints. Submaximal trial durations ranged from 6 to 12 seconds depending on the time required for a subject to achieve the hand force criteria and maintain the criteria for 3 seconds.

2.5. Analysis Methods

To quantify the observed postural differences and study the effects of hand force on posture, a set of biomechanical variables were calculated for each trial (Figure 2.11). The origin is defined as a point on the floor directly below the center of the handle. Forces on the handle are positive upward and rearward. These metrics were used to quantify elbow posture, shoulder location with respect to the point of force application,

torso inclination, the location and orientation of the pelvis with respect to the hand-force plane, and foot placements.

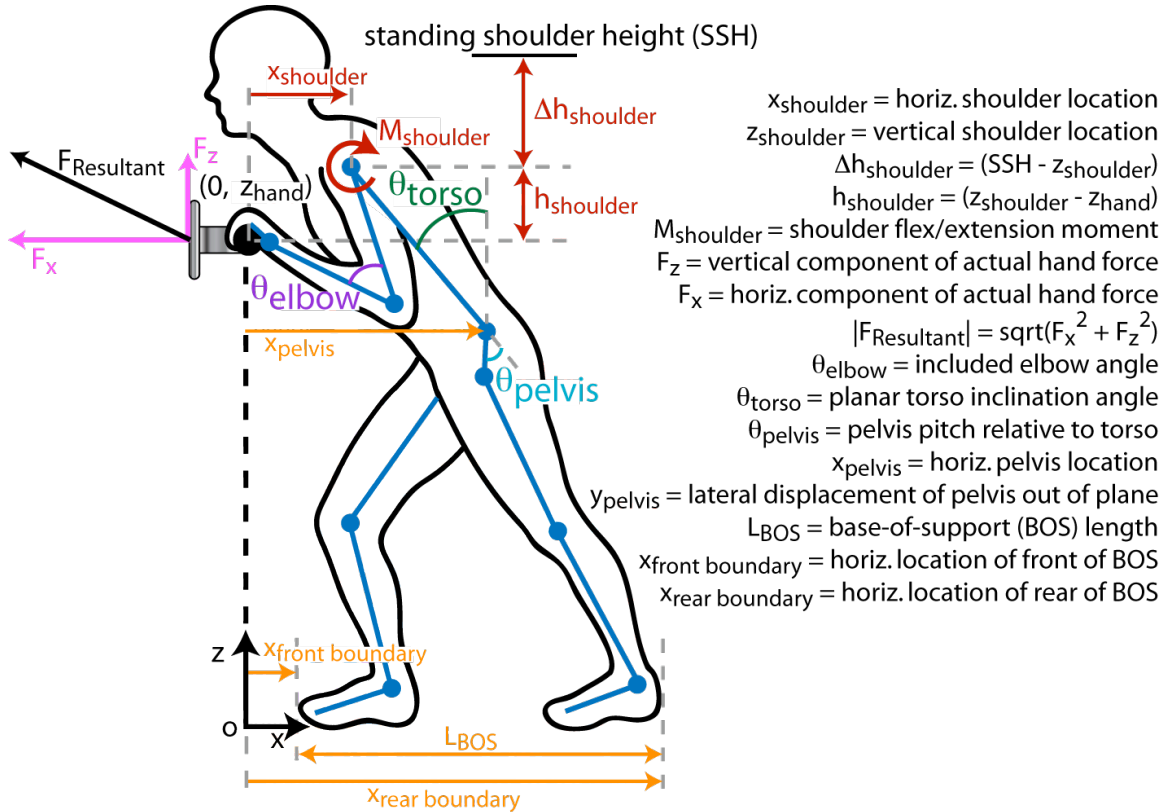


Figure 2.11. Metrics used to quantify whole-body postures during standing hand force exertions.

Analysis of variance (ANOVA) and linear regression were used to determine if hand force magnitude and/or direction are significant predictors of pushing postures. The effects of anthropometrics and additional task parameters (e.g. handle height) on posture were also examined. Factors identified as significant determinants were then used to build regression models to predict key postural metrics from task, worker, and other parameters.

2.6. Appendix: Body Segment Mass Estimation

Body mass distributions vary across populations (Pataky et al., 2003) and whole-body center-of-mass (COM) estimation has been shown to be sensitive to inaccuracies in body segment parameters (Lenzi et al., 2003). Discrepancies between top-down analysis based on body segment masses and posture, and force-plate data are expected when actual and estimated segment masses differ. One way of resolving these discrepancies is to better characterize mass distributions for each subject. Based on the work Pataky and

Zatsiorsky (2003) an apparatus and procedure for determining subject-specific body segment masses were developed.

Select anthropometric measures are taken to characterize subject anthropometry (Table 2.3). These measures combined with published segment parameters (Table 2.7) allow subject-specific COM distances, d_{COM} , to be determined (Eqns 1-7). Optical markers are placed on the shoulder, elbow, wrist, hip, knee, and ankle to track joint locations in three-dimensional space (Figure 2.12).

Table 2.7. Segment parameters; masses as a percent of total body mass; COM locations given as the distance, expressed as a percent of segment length, along the segment from the origin to the COM of the segment; WJC = wrist joint center, EJC = elbow joint center, SJC = shoulder joint center, HJC = hip joint center, KJC = knee joint center (de Leva, 1996).

Segment	Origin	Mass [%]		COM Location [%]	
		Female	Male	Female	Male
Hand	WJC	0.56	0.61	32.27	36.24
Forearm	EJC	1.38	1.62	45.59	45.74
Upper arm	SJC	2.55	2.71	57.54	57.72
Thigh	HJC	14.78	14.16	36.12	40.95
Shank	KJC	4.81	4.33	44.16	44.59
Foot	HEEL	1.29	1.37	-	-

$$d_{forearm}^{COM} = (COM\ Position)_{forearm} \cdot L_{forearm} \quad (1)$$

$$d_{hand}^{COM} = (COM\ Position)_{hand} \cdot L_{hand} \quad (2)$$

$$d_{forearm+hand}^{COM} = \left(\frac{m_{forearm}}{m_{lower-arm}} \right) \cdot d_{forearm}^{COM} + \left(\frac{m_{hand}}{m_{lower-arm}} \right) \cdot (L_{forearm} + d_{hand}^{COM}) \quad (3)$$

$$d_{shank}^{COM} = (COM\ Position)_{shank} \cdot L_{shank} \quad (4)$$

$$d_{shank+foot}^{COM} = \left(\frac{m_{shank}}{m_{lower-leg}} \right) \cdot d_{shank}^{COM} + \left(\frac{m_{foot}}{m_{lower-leg}} \right) \cdot (L_{shank} + \frac{1}{2} \cdot H_{ankle}) \quad (5)$$

$$d_{upper\ arm}^{COM} = (COM\ Position)_{upper\ arm} \cdot L_{upper\ arm} \quad (6)$$

$$d_{thigh}^{COM} = (COM\ Position)_{thigh} \cdot L_{thigh} \quad (7)$$

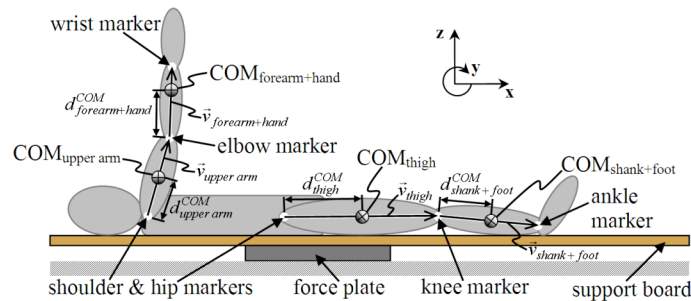


Figure 2.12. Illustration of segment parameters.

Marker locations are used to define vectors along the upper arm, (forearm + hand), thigh, and (shank + foot) segments (Eqns 8-11). Marker locations, segment unit vectors (Eqns 12-15), and segment COM distances together yield segment COM locations (Eqns 16-19). This series of calculations allows three-dimensional marker data to be used to track segment COM locations.

$$\vec{v}_{upper\ arm} = \langle x_{elbow} - x_{shoulder}, y_{elbow} - y_{shoulder}, z_{elbow} - z_{shoulder} \rangle \quad (8)$$

$$\vec{v}_{forearm + hand} = \langle x_{wrist} - x_{elbow}, y_{wrist} - y_{elbow}, z_{wrist} - z_{elbow} \rangle \quad (9)$$

$$\vec{v}_{thigh} = \langle x_{knee} - x_{hip}, y_{knee} - y_{hip}, z_{knee} - z_{hip} \rangle \quad (10)$$

$$\vec{v}_{shank + foot} = \langle x_{ankle} - x_{knee}, y_{ankle} - y_{knee}, z_{ankle} - z_{knee} \rangle \quad (11)$$

Unit vectors defined by normalizing the above segment vectors:

$$\vec{u}_{upper\ arm} = \left(\frac{\vec{v}_{upper\ arm}}{\|\vec{v}_{upper\ arm}\|} \right) \text{ and } \vec{u}_{forearm + hand} = \left(\frac{\vec{v}_{forearm + hand}}{\|\vec{v}_{forearm + hand}\|} \right) \quad (12) \& (13)$$

$$\vec{u}_{thigh} = \left(\frac{\vec{v}_{thigh}}{\|\vec{v}_{thigh}\|} \right) \text{ and } \vec{u}_{shank + foot} = \left(\frac{\vec{v}_{shank + foot}}{\|\vec{v}_{shank + foot}\|} \right) \quad (14) \& (15)$$

$$COM_{upper\ arm} = \langle x_{shoulder}, y_{shoulder}, z_{shoulder} \rangle + d_{upper\ arm}^{COM} \cdot \vec{u}_{upper\ arm} \quad (16)$$

$$COM_{forearm + hand} = \langle x_{elbow}, y_{elbow}, z_{elbow} \rangle + d_{forearm + hand}^{COM} \cdot \vec{u}_{forearm + hand} \quad (17)$$

$$COM_{thigh} = \langle x_{hip}, y_{hip}, z_{hip} \rangle + d_{thigh}^{COM} \cdot \vec{u}_{thigh} \quad (18)$$

$$COM_{shank + foot} = \langle x_{knee}, y_{knee}, z_{knee} \rangle + d_{shank + foot}^{COM} \cdot \vec{u}_{shank + foot} \quad (19)$$

Body segment mass estimations are obtained by having the subject perform a series of four tasks while lying on a support board (Figure 2.13). For each task the subject begins in a prescribed initial position, which they maintain for approximately 5 seconds before assuming the final position. When transitioning to the final position, the subject is instructed to restrict their motion to the x-z or sagittal plane and to hold the final position for 5 seconds. A force plate under the support board measures the forces and moments generated in both the initial and final positions. Total body center-of-pressure (COP) is calculated from the measured forces and moments and the change in COP between the initial and final positions is used to determine the mass of the displaced segment.









Task	Initial Position	Final Position
(a) whole-arm vertical raise (<i>wav</i>)		
(b) forearm + hand vertical raise (<i>fhv</i>)		
(c) whole-leg vertical raise (<i>wlv</i>)		
(d) shank + foot vertical raise (<i>sfv</i>)		

Figure 2.13. Body segment mass estimation apparatus & tasks used to quantify: (a) upper arm mass, (b) mass of (forearm + hand), (c) thigh mass, and (d) mass of the (shank + foot).

The mass of the upper arm and mass of the combined (forearm + hand) segment are determined from the *wav* and *fhv* tasks, respectively (Figure 2.14). Initial (i) and final (f) segment COM positions along the x-axis are given by equations 20 thru 23. From these positions, upper arm and (forearm + hand) COM displacements in the x-direction during each task are computed (Eqns 24-25). The mass of the (forearm + hand) is determined first by computing the change in whole-body COP resulting from the change in the COM location of the (forearm + hand) segment during the *fhv* task (Eqn 26). Using the resulting (forearm + hand) mass the above methodology is then repeated for the *wav* task to estimate the mass of the upper arm (Eqn 27).

$$\left(COM_{upper\ arm}^i \right)_x = \left(x_{shoulder}^i + d_{upper\ arm}^{COM} \cdot \bar{u}_{upper\ arm}^i \cdot \hat{i} \right) \quad (20)$$

$$\left(COM_{upper\ arm}^f \right)_x = \left(x_{shoulder}^f + d_{upper\ arm}^{COM} \cdot \bar{u}_{upper\ arm}^f \cdot \hat{i} \right) \quad (21)$$

$$\left(COM_{forearm\ +\ hand}^i \right)_x = \left(x_{elbow}^i + d_{forearm\ +\ hand}^{COM} \cdot \bar{u}_{forearm\ +\ hand}^i \cdot \hat{i} \right) \quad (22)$$

$$\left(COM_{forearm\ +\ hand}^f \right)_x = \left(x_{elbow}^f + d_{forearm\ +\ hand}^{COM} \cdot \bar{u}_{forearm\ +\ hand}^f \cdot \hat{i} \right) \quad (23)$$

$$\left(\Delta COM_{upper\ arm} \right)_x = \left(COM_{upper\ arm}^f \right)_x - \left(COM_{upper\ arm}^i \right)_x \quad (24)$$

$$\left(\Delta COM_{forearm\ +\ hand} \right)_x = \left(COM_{forearm\ +\ hand}^f \right)_x - \left(COM_{forearm\ +\ hand}^i \right)_x \quad (25)$$

$$m_{forearm + hand} = m_{WB} \cdot \left\{ \frac{(\Delta COP)_x^{flv}}{(\Delta COM_{forearm + hand})_x^{flv}} \right\} \quad (26)$$

$$m_{upper arm} = \frac{\left[m_{WB} \cdot (\Delta COP)_x^{wav} - m_{forearm + hand} \cdot (\Delta COM_{forearm + hand})_x^{wav} \right]}{(\Delta COM_{upper arm})_x^{wav}} \quad (27)$$

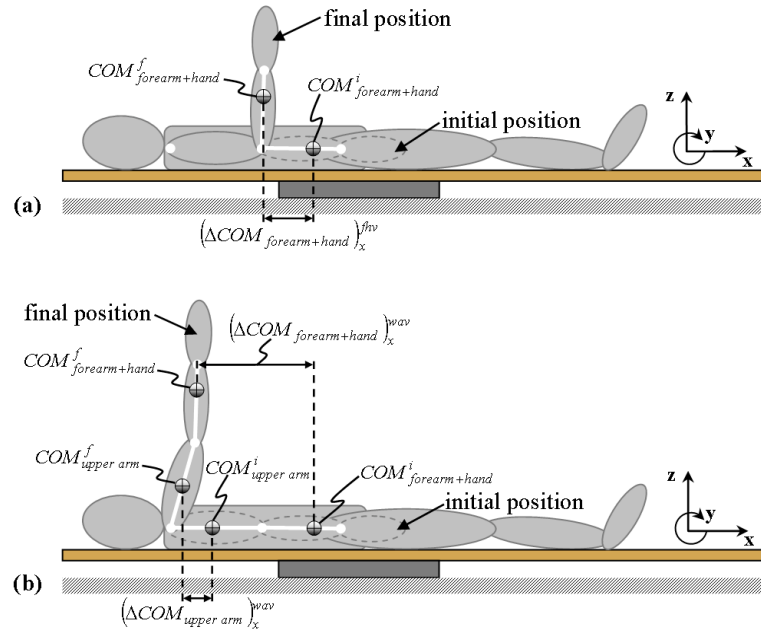


Figure 2.14. Illustration of center-of-mass displacements during (a) *flv* task and (b) *wav* task for estimation of (forearm + hand) mass and mass of upper arm, respectively.

For all tasks the change in COP in the x-direction is given by equation 28 where M_y , F_x , and F_z are the average forces and moments recorded by the force plate during the initial and final task positions.

$$(\Delta COP)_x = \left(\frac{-M_y^f + F_x^f \cdot z_o}{F_z^f} \right) - \left(\frac{-M_y^i + F_x^i \cdot z_o}{F_z^i} \right) \quad (28)$$

The mass of the combined (shank + foot) segment and thigh mass are determined from the *sfv* and *wlv* tasks, respectively (Figure 2.15). Initial and final segment COM positions along the x-axis are given by equations 29 thru 32. From these positions, thigh and (shank + foot) COM displacements in the x-direction during each task are computed (Eqns 33-34). The mass of the (shank + foot) is determined by computing the change in whole-body COP resulting from the change in the COM location of the (shank + foot)

segment during the *sfv* task (Eqn 35). With an estimate of the (shank + foot) mass, the above methodology is repeated for the *wlv* task to estimate the mass of the thigh (Eqn 36).

$$\left(COM_{thigh}^i \right)_x = \left(x_{hip}^i + d_{thigh}^{COM} \cdot \bar{u}_{thigh}^i \cdot \hat{i} \right) \quad (29)$$

$$\left(COM_{thigh}^f \right)_x = \left(x_{hip}^f + d_{thigh}^{COM} \cdot \bar{u}_{thigh}^f \cdot \hat{i} \right) \quad (30)$$

$$\left(COM_{shank+foot}^i \right)_x = \left(x_{knee}^i + d_{shank+foot}^{COM} \cdot \bar{u}_{shank+foot}^i \cdot \hat{i} \right) \quad (31)$$

$$\left(COM_{shank+foot}^f \right)_x = \left(x_{knee}^f + d_{shank+foot}^{COM} \cdot \bar{u}_{shank+foot}^f \cdot \hat{i} \right) \quad (32)$$

$$\left(\Delta COM_{thigh} \right)_x = \left(COM_{thigh}^f \right)_x - \left(COM_{thigh}^i \right)_x \quad (33)$$

$$\left(\Delta COM_{shank+foot} \right)_x = \left(COM_{shank+foot}^f \right)_x - \left(COM_{shank+foot}^i \right)_x \quad (34)$$

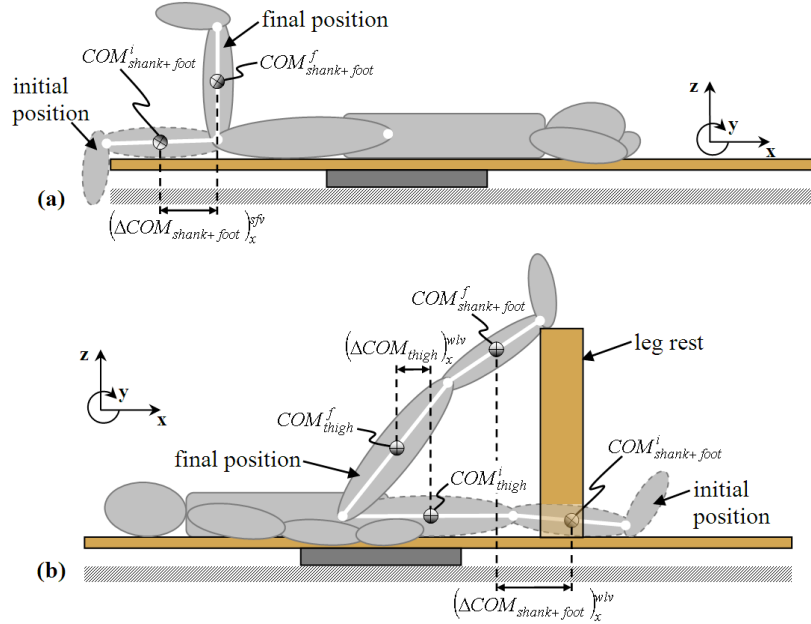


Figure 2.15. Illustration of center-of-mass displacements during (a) *sfv* task and (b) *wlv* task for estimation of (shank + foot) mass and mass of thigh, respectively.

$$m_{shank+foot} = m_{WB} \cdot \left\{ \frac{\left(\Delta COP \right)_x^{sfv}}{\left(\Delta COM_{shank+foot} \right)_x^{sfv}} \right\} \quad (35)$$

$$m_{thigh} = \frac{\left[m_{WB} \cdot \left(\Delta COP \right)_x^{wlv} - m_{shank+foot} \cdot \left(\Delta COM_{shank+foot} \right)_x^{wlv} \right]}{\left(\Delta COM_{thigh} \right)_x^{wlv}} \quad (36)$$

2.7. References

- Chaffin, D. B., Andersson, G. B. J., and Martin, B. J. (2006). Occupational biomechanics. John Wiley & Sons, New York, NY, 4th edition.
- de Leva, P. (1996). Adjustments to zatsiorsky-seluyanov's segment inertia parameters. *J Biomech*, 29(9):1223–1230.
- Gaughran, G. and Dempster, W. (1956). Force analysis of horizontal two-handed pushes and pulls in the sagittal plane. *Human Biology*, 28(1):67–92.
- Holbein, M. A. and Chaffin, D. B. (1997). Stability limits in extreme postures: effects of load positioning, foot placement, and strength. *Hum Factors*, 39(3):456–68.
- Kerk, C., Chaffin, D., and et al (1994). A comprehensive biomechanical model using strength, stability, and cof constraints to predict hand force exertion capability under sagittally symmetric static conditions. *IIE Transactions*, 26(3):57–67.
- Kerk, C. (1992). Development and evaluation of a static hand force exertion capability model using strength, stability, and coefficient of friction. PhD thesis, The University of Michigan, Ann Arbor, MI.
- Kumar, S., editor (2004). *Muscle Strength*. CRC Press, Boca Raton, FL.
- Lenzi, D., Cappello, A., and Chiari, L. (2003). Influence of body segment parameters and modeling assumptions on the estimate of center of mass trajectory. *Journal of Biomechanics*, 36:1335–1341.
- Pataky, T. C., Zatsiorsky, V. M., and Challis, J. H. (2003). A simple method to determine body segment masses in vivo: reliability, accuracy and sensitivity analysis. *Clin Biomech (Bristol, Avon)*, 18(4):364–368.
- Reed, M., Manary, M., and Schneider, L. (1999). Methods for measuring and representing automobile occupant posture. In *SAE Transactions: Journal of Passenger Cars*, volume 108, SAE Technical Paper 990959.
- Roebuck, J. A. (1995). *Anthropometric methods : designing to fit the human body*. Human Factors and Ergonomics Society, CA.
- Stobbe, T. J. (1982). The development of a practical strength testing program for industry. PhD thesis, The University of Michigan, Ann Arbor, MI.
- Woolley, C. B., Natalini, T., and Cascos, R. (2000). *HUMOSIM 1999 Summer Data Collection: Anthropometric Measurements*. Center for Ergonomics, The University of Michigan, Ann Arbor, MI.

CHAPTER 3

PREDICTING ACTUAL HAND FORCES FROM REQUESTED FORCE VECTOR DURING STANDING HAND-FORCE EXERTIONS

3.1. Abstract

Both the magnitude and direction of hand force are significant determinants of biomechanical outcome measures used for ergonomic job analyses. Given a task posture, changes in hand force magnitude and the direction of force with respect to joint locations result in variations in joint loads. Inaccuracies in hand forces affect our ability to accurately assess strength capability and the assumption of purely horizontal hand forces in pushing and pulling tasks can result in underestimation of hand force capability. Knowledge of how actual hand forces differ from the requested force vector could be used to enhance existing ergonomic analysis tools. Work regarding the relationship between hand force and posture suggests actual hand force is also a determinant of posture and can provide insight into posture selection. Previous work has quantified significant vertical force components during requested horizontal push/pull exertions. Studies also have shown that actual and requested hand forces differ significantly when feedback on hand force is not provided. The objective of this work was to quantify the actual hand force vector for a range of requested hand force magnitudes and directions and to develop predictive equations to compute actual hand force from the requested hand force vector. A study was conducted in which people were provided with feedback on force magnitude in the requested force direction. Off-axis forces (i.e. forces in directions other than requested) were quantified. Analysis of data indicates that off-axis forces are significant and well predicted by the magnitude of requested force for a subset of task conditions. For requested horizontal pushes, people push downward as well as forward at low forces, and push upward when the requested force exceeds about 50% of

capability. During two-handed exertions, lateral off-axis forces are negligible but vertical force components are large, exceeding the requested force magnitude when pushing and pulling overhead. For two-hand exertions in the vertical plane (up/down) significant fore-aft forces were measured. In addition to vertical forces, lateral off-axis forces were also significant during one-hand exertions. A set of regression equations with adjusted R^2 values ranging from 0.10 to 0.66 were developed to predict significant off-axis forces from the requested hand force magnitude.

3.2. Introduction

Ergonomic assessment of worker capability requires accurate representation of task postures and knowledge of hand forces. Joint loads are dependent on force magnitude and the location of joint centers relative to the line-of-action of the hand force vector. Hand force, specifically the vertical force component, also affects the available friction at the feet by acting to increase or decrease the normal force. Given a task posture, the hand force vector is critical to the assessment of strength and balance capabilities. Alternatively, when the posture is unknown, knowledge of the forces exerted at the hands can provide insight into the posture selected for the task.

Several studies have quantified the variations in joint loads associated with changes in both hand force magnitude and direction during push/pull exertions. de Looze et al. (2000) examined the effects of handle height on hand force direction and quantified the changes in low back and shoulder loads resulting from changes in force direction. In this study, participants pushed or pulled with different levels of horizontal force on either a stationary bar or moveable cart at various handle heights. Changes in the hand force vector were reflected in changes in shoulder and low back torques. Hoozemans et al. (2004) also found handle height, as well as cart weight, to have a significant effect on mechanical loading at the shoulders and low back. Object weight was also investigated by Nussbaum et al. (1999) and found to have similar effects for object transfers using materials handling manipulators. Transfer height and object mass had a significant effect on low-back compression and torso strength capability. The effect of object mass on shoulder strength capability was also significant. Variations in joints loads quantified in these studies indicate that an accurate assessment of musculoskeletal loading during pushing and pulling tasks requires knowledge of both the force magnitude and direction.

To stress the importance of hand force direction in the context of ergonomics Kerk (1994) used the relationship between hand force and shoe-floor friction to show how the assumption of a pure horizontal force results in an underestimation of the worker's push capability. Several have studied this relationship between hand force and shoe-floor friction and the relevance to slips and falls in the context of horizontal push/pull exertions. Dempster (1958) quantified the effect of friction on hand force capability and found that when standing on a high-friction rubber mat subjects were able to generate upward forces equal to approximately twice their body weight and horizontal pull forces equal to 75% of body weight. When the friction at their feet was reduced the horizontal pull force decreased significantly while the vertical pull force was unaffected. Boocock et al. (2006) found floor surface did not have a significant effect on resultant hand forces but had a significant effect on the vertical components when pushing a cart on a standard versus high-friction safety floor. These findings illustrate the importance of vertical hand force to the assessment of frictional requirements and hand force capability during push/pull exertions and suggest that actual push/pull forces are not purely horizontal.

Several researchers have quantified significant vertical hand forces during nominally horizontal pushing and pulling. de Looze et al. (2000) and Granata et al. (2005) both observed a downward component during low-force exertions at waist-high handle heights and upward components with increasing force levels with higher handle heights. In both studies, this trend was found to be significant and highly reproducible. Kerk (1992), while investigating how stability, strength and frictional requirements at the floor affect hand force capability, found that people do not exert only the required or requested hand force. Kerk reported that without feedback on hand force, the measured hand force vector differs significantly from that requested.

While previous studies have quantified the resultant hand force during push/pull exertions, this study is believed to be the first to predict actual hand forces from the requested hand force vector and task parameters. Furthermore, postural analyses presented later in chapters 4 and 5 show that hand force is a significant determinant of posture, and suggest that knowledge of actual hand forces is essential for prediction of task postures. The specific objective of the work reported in this chapter is to quantify the

relationship between actual and requested hand force, and develop models that predict the actual hand force vector from task parameters.

The following hypotheses were formulated through review of the literature, and were used to guide the work:

1. Differences between actual and requested hand force magnitude and direction are statistically significant.
2. Horizontal push/pull forces will have a significant vertical component. The vertical force will be directed downward when pushing on a fixed handle below shoulder height and upward when pushing on a fixed handle overhead. When pulling, the force will be directed upward for handles below shoulder height and downward for handles overhead.
3. Actual hand force can be predicted from task parameters (point of force application, number of hands, requested/required hand force) and characteristics of the worker (gender, stature, body mass).

3.3. Methods

Participants and Test Conditions

Nineteen participants performed right-handed and two-handed exertions in various force directions with required force levels spanning from twenty-five percent to one hundred percent of their maximum capability, in twenty-five percent increments. Each participant exerted force on a fixed handle at approximately elbow height (63% of stature), and mid-thigh height (41% of stature) or overhead (10 cm above stature). Forces at the hands were measured via an adjustable force handle affixed to a six-degree-of-freedom load cell (JR3, Woodland, CA).

Force directions exerted at each handle height are summarized in Table 3.1. Feedback was provided on the magnitude of force in the requested direction via a visual force feedback display. Participants were required to achieve the desired force level in the specified direction and maintain that level of force for 3 seconds. For all trials hand force direction was not constrained, in that feedback was not provided on off-axis forces. One of the original twenty participants, Subject 023, was excluded from this analysis. All nineteen participants analyzed were young (median age 21 years) and relatively thin

(median body mass index 23 kg/m²). Additional details regarding the experimental design and laboratory study are presented in Chapter 2.

Table 3.1. Direction of right (RH) and two-handed (2H) force exertions performed at each handle height.

Handle Height	Forward	Back	Left	Right	Up	Down
Overhead	RH / 2H	RH / 2H	RH	RH	RH / 2H	-
Elbow-Height	RH / 2H	RH / 2H	RH	RH	RH / 2H	RH / 2H
Thigh-Height	RH / 2H	RH / 2H	RH	RH	RH / 2H	-

Data Analysis

Mean and variances for both one- and two-handed strengths, normalized to body weight, were computed for each force direction at the three handle heights. A mean strength was computed for each test condition by averaging across all subjects the magnitude of force exerted in the requested direction during maximal efforts for the given test condition. Mean strengths were compared within and across trial conditions using the Tukey-Kramer HSD test with a significance of $p < 0.05$.

Actual and requested hand force vectors were compared using a paired t-test to determine if actual and requested mean hand force magnitudes and/or directions were significantly different. Actual force magnitude was defined by the resultant of the measured x, y, and z force components and were then compared to the magnitude of force requested in the x, y, or z direction. Off-axis forces measured in the lateral and vertical (for push/pull exertions) or fore-aft (for up/down exertions) directions were used to quantify differences in actual versus requested force direction. Actual and requested mean hand force directions differed when off-axis forces were found to be significantly non-zero. Differences in the means were considered highly significant for $p < 0.01$.

Prior to analyzing the relationships between actual and requested hand forces, trials were blocked on handle height and number of hands used. Within blocks, trials were grouped across force direction by exertion type (push, pull, up, or down). Off-axis forces were defined with respect to the plane defined by the requested hand force vector. For push/pull exertions, off-axis forces act in the lateral plane or cross-body direction, and in the vertical direction. Off-axis forces are in the lateral and fore-aft directions for up/down exertions.

Off-axis forces were expressed as a fraction of the magnitude of the requested hand force and the relative magnitude of off-axis forces analyzed for each test condition, using cumulative distribution functions. These comparisons served as a measure of the

significance of off-axis forces and associated external loads relative to the requested force vector. ANOVA was conducted to investigate the relationship between actual and requested mean hand force components, and to determine differences in hand forces across test conditions. Regression equations were developed for one and two-handed exertions at each handle height to model significant relationships between actual and requested hand force components.

Effects of worker characteristics on hand forces were assessed using ANOVA. Potential predictors included gender, stature, and body-mass-index (BMI). Effects were considered significant for $p < 0.01$ and were included in the final regression models if inclusion increased the adjusted R^2 by 0.02.

3.4. Results

Mean Strengths for One- and Two-Handed Exertions Across Handle Heights

Mean strength values were found to be greater for two-handed exertions than for one-handed exertions with the greatest value corresponding to two-handed upward exertions at thigh height. Variation in mean hand forces, for one- and two-handed tasks, across trial conditions is presented in Figure 3.1. One-handed overhead exertions to the left were associated with the lowest mean strength value. Comparison of mean strengths within and across trial conditions found no significant difference in push/pull strengths, except for one-handed exertions at thigh height. When expressed as a fraction of body weight, thigh-height pull strengths were, on average, greater than push strengths at approximately 33% versus 27% of body weight respectively. Mean values for each condition expressed in Newtons are presented in Table 3.2.

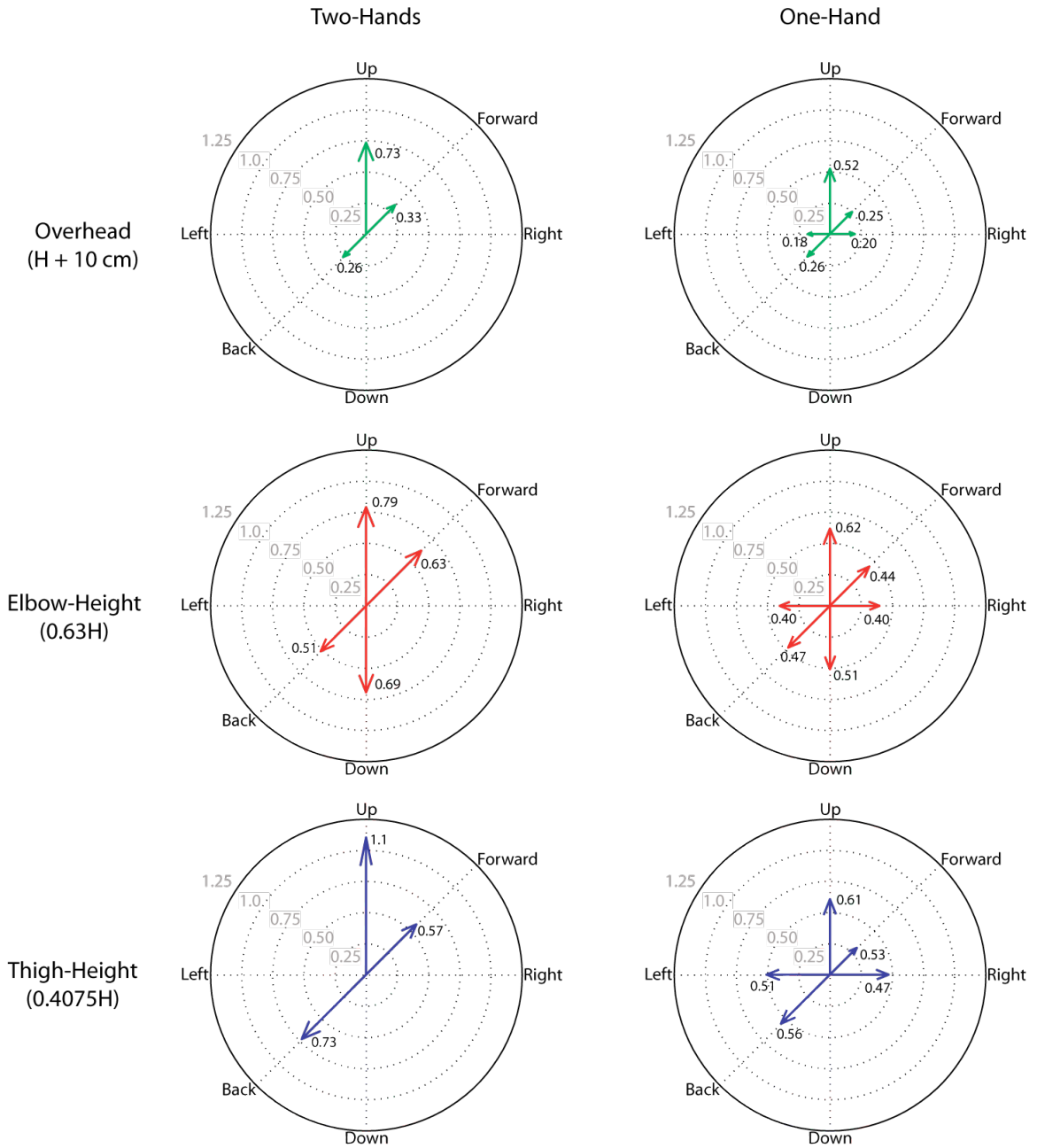


Figure 3.1. Mean one and two-handed strengths at thigh, elbow, and overhead handle heights expressed as a percent of body weight (H denotes stature).

Table 3.2. Mean strengths for one- and two-handed exertions at each handle height [N].

Handle Height	Strategy	One-Handed	Two-Handed	Absolute % Difference (Two-Hand minus One-Hand)
Thigh-Height	Push	-323	-382	15.4
	Pull	180	483	62.7
	Up	406	729	44.3
Elbow-Height	Push	-237	-421	43.7
	Pull	180	345	47.8
	Up	413	523	21.0
	Down	-341	-452	24.6
Overhead	Push	-130	-237	45.1
	Pull	123	159	22.6
	Up	340	435	21.8

Differences Between Actual and Requested Hand Force Vectors

Deviations in the actual hand force vector from that requested are presented as mean differences in hand force magnitude and direction during two- and one-handed exertions in Table 3.3 and Table 3.4, respectively. Across all test conditions, actual force magnitudes (vector sum of the on- and off-axis components) exceeded the requested force magnitude in 21 of 26 conditions ($p < 0.01$). Off-axis forces were significantly different from zero in all conditions.

Table 3.3. Mean difference in actual and requested hand force magnitude and direction for all two-handed exertions. Force direction is quantified by vertical / fore-aft and lateral off-axis force components. (mean difference = actual force – requested force, * denotes highly significant with $p < 0.001$, gray shading denotes not significant, # / # denotes push / pull mean differences.

Force Direction	Hand Force Magnitude			Hand Force Direction					
	Thigh	Elbow	Overhead	Vertical/Fore-Aft Off-Axis Force			Lateral Off-Axis Force		
				Thigh	Elbow	Overhead	Thigh	Elbow	Overhead
Back	23.0*	6.98*	81.9*	107*	39.4*	-148*	-12.6*	-8.13*	4.03
Forward	12.2*	13.1*	73.6*	-19.9	46.5*	139*	10.6*	0.51	-11.2*
Up	1.99	9.68*	6.98	16.4	-24.8	-76.5*	-48.0*	-23.7*	-22.6*
Down	-	-0.10	-	-	20.4*	-	-	18.1*	-

For two-handed exertions, actual hand force magnitude exceeded requested in fourteen of the sixteen conditions tested with the largest mean difference occurring for overhead-back exertions. Vertical off-axis forces relatively large for all two-handed back exertions and for forward exertions at the elbow and overhead handle heights. Fore-aft off-axis forces were not significantly different from zero during thigh- or elbow-height upward exertions, but significant forward forces were observed for overhead up exertions and for down exertions performed at elbow-height. Lateral or cross-body off-axis forces

were highly significant ($p < 0.01$) for all two-handed exertions with the exception of overhead back exertions that were significant ($p < 0.05$) and elbow-height forward exertions, which were not significant. Lateral off-axis forces were smaller than off-axis forces in the vertical or fore-aft direction during all conditions except upward thigh-height exertions.

Comparison of actual and requested hand force magnitudes for one-handed exertions yielded highly significant ($p < 0.01$) differences in fourteen of the sixteen conditions. The largest difference in hand force magnitude was observed for forward exertions performed overhead. During force exertions to the left, some participants pushed to the left while others pulled. Off-axis forces are presented separately for each strategy as mean difference when pushing / mean difference when pulling. Highly significant ($p < 0.01$) vertical off-axis forces were measured during all one-handed back, forward, and right exertions. Vertical off-axis forces were not significant during left exertions at elbow-height, but were highly significant for left exertions performed overhead. When pushing to the left at the thigh-height handle vertical off-axis forces were significant ($p < 0.05$); vertical forces were highly significant ($p < 0.01$) when pulling. Significant off-axis forces in the fore-aft direction were measured during all up/down exertions with fore-aft off-axis forces being highly significant ($p < 0.01$) for upward exertions and downward exertions at the elbow-height and overhead handle location. Lateral off-axis forces were significant ($p < 0.05$) during twelve of the sixteen test conditions and highly significant ($p < 0.01$) for forward, left (push only), right and up exertions at thigh height, elbow-height exertions in the left, right, up and down directions, and forward and left (push only) exertions performed overhead. During push exertions to the left, lateral off-axis forces were greater than or equal to vertical off-axis forces across all handle heights.

Table 3.4. Mean difference in actual and requested hand force magnitude and direction for one-handed exertions. Force direction is quantified by vertical / fore-aft and lateral off-axis force components. (mean difference = actual force – requested force, * denotes highly significant with $p < 0.001$, gray shading denotes not significant, # / # denotes push / pull mean differences.

Force Direction	Hand Force Magnitude			Hand Force Direction					
	Thigh	Elbow	Overhead	Vertical/Fore-Aft Off-Axis Force			Lateral Off-Axis Force		
				Thigh	Elbow	Overhead	Thigh	Elbow	Overhead
Back	24.1*	3.19*	36.0*	103*	29.2*	-87.4*	-5.61	-1.97	4.0
Forward	6.5*	12.1*	45.5*	-13.5*	34.6*	87.9*	8.84*	1.42	-4.56*
Left	8.0*	5.7*	20.6*	-13.8 / 33.2*	3.25 / -8.91	34.9* / -104*	-13.8* / 71.5	-25.2* / 25.0*	-22.8* / 30.1
Right	19.7*	7.9*	9.94*	74.6*	38.7*	-35.5*	46.1*	22.7*	0.26
Up	-0.74	23.6*	9.43*	10.5	-78.4*	-63.4*	-20.6*	-41.3*	-9.78
Down	-	1.21	-	-	24.0*	-	-	-8.05*	-

Off-Axis Forces During Two-Handed Push/Pull Exertions

Lateral off-axis forces measured during two-handed push/pull exertions were found to be smaller than vertical off-axis forces in 5 of the 6 push/pull conditions, with ninety percent of lateral off-axis forces being less than 34.3 N (~7.7 lbs) during all two-handed push/pull exertions (Figure 3.2). Because of the small magnitude of lateral off-axis forces, both absolute and relative to vertical off-axis forces, lateral off-axis forces were considered negligible during two-handed push/pull exertions.

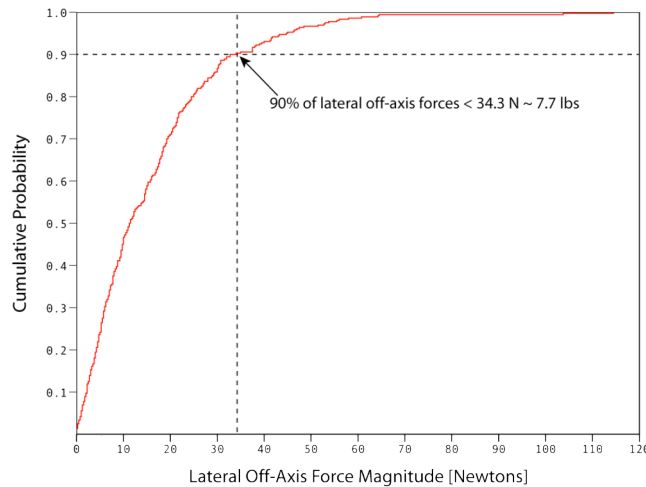


Figure 3.2. Cumulative distribution function for two-handed push/pull lateral off-axis force.

The relationship between requested horizontal push/pull force and vertical off-axis force was found to be highly significant ($p < 0.01$) for two-handed push exertions at elbow height but with different relationships existing for two-hand push exertions performed with flexed-elbows ($R^2 \text{ Adj} = 0.32$) versus extended elbows ($R^2 \text{ Adj} = 0.66$). Across both pushing strategies, a downward vertical force was observed during low-force pushes with the vertical force becoming upward during high-force exertions. On average,

when pushing with flexed-elbows vertical force was exerted upward, and downward when pushing with elbows extended. Horizontal force magnitude was not found to be a significant predictor of vertical off-axis force during two-handed elbow-height pulls. Similarly, vertical off-axis forces during two-handed push/pull exertions performed at the mid-thigh (Figure 3.4) and overhead (Figure 3.5) handle heights were not found to be significantly related to the requested hand force.

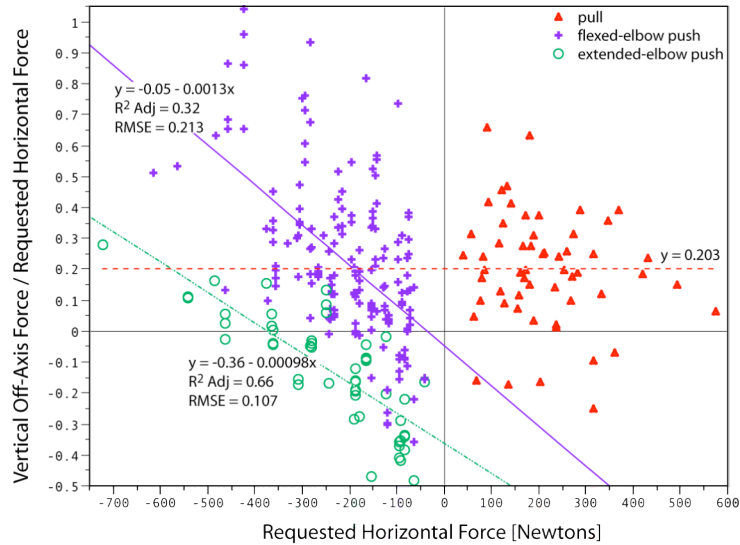


Figure 3.3. Vertical off-axis force during two-handed elbow-height push/pull exertions expressed as a percent of the magnitude of the requested horizontal force. Linear fits are highly significant ($p < 0.01$).

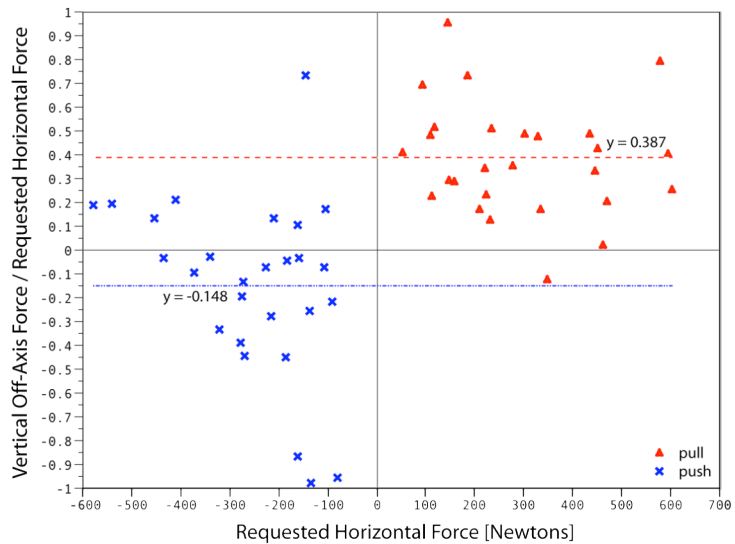


Figure 3.4. Vertical off-axis force during two-handed thigh-height push/pull exertions expressed as a percent of the magnitude of the requested horizontal force.

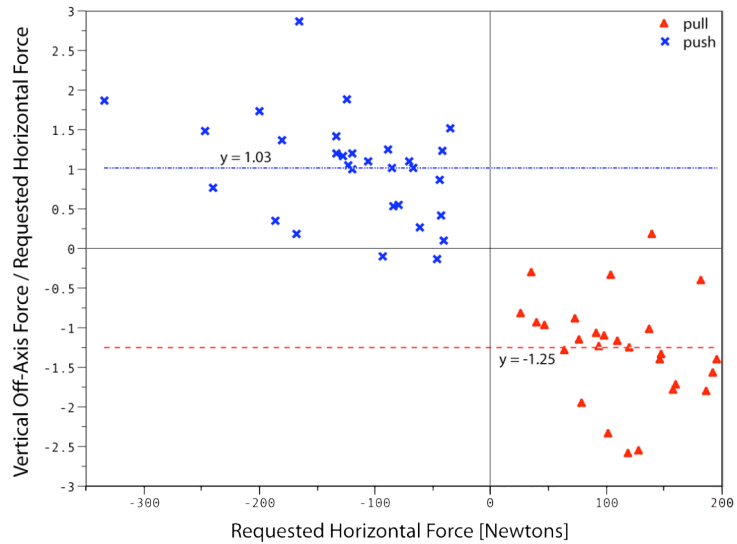


Figure 3.5. Vertical off-axis force during two-handed overhead push/pull exertions expressed as a percent of the magnitude of the requested horizontal force.

Off-Axis Forces During Two-Handed Up/Down Exertions

Off-axis forces exerted laterally during two-handed push down exertions did not exceed 36 N (~8.1 lbs). For two-handed upward exertions, lateral off-axis forces did not differ significantly across handle heights and were, on average, equal to 8% of the requested vertical force (Figure 3.7). Requested vertical force was not found to be a significant ($p < 0.05$) predictor of lateral off-axis force during two-handed up/down exertions. As with two-handed push/pull exertions, lateral off-axis forces during two-handed up/down exertions were small and considered negligible.

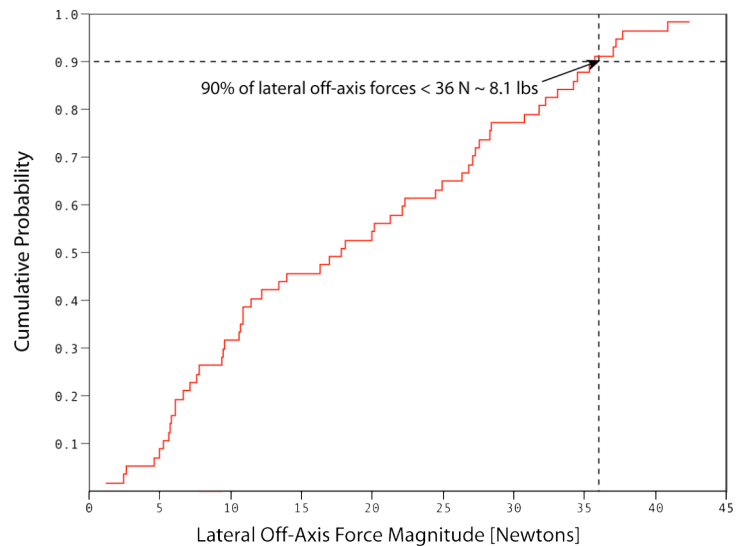


Figure 3.6. Cumulative distribution function for lateral off-axis forces during two-handed downward exertions at elbow-height.

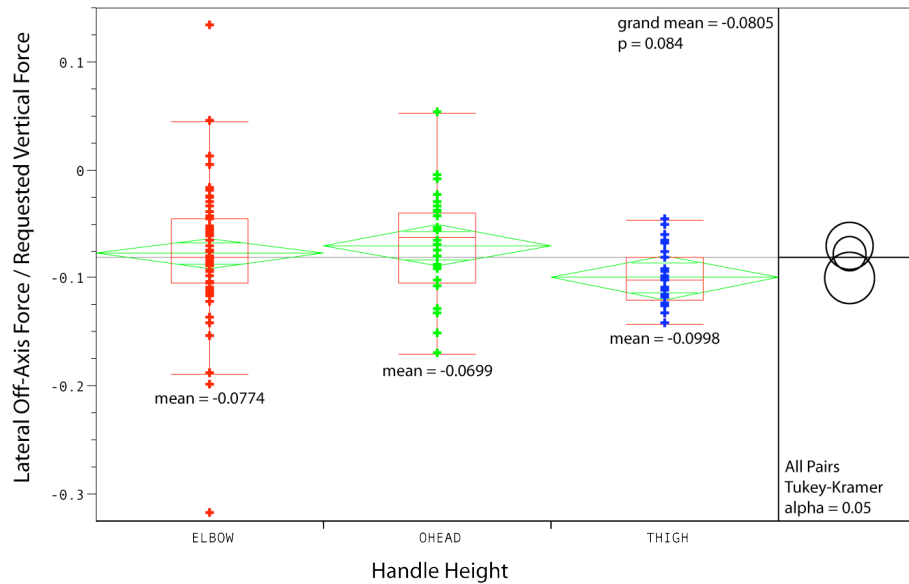


Figure 3.7. Lateral off-axis forces during upward exertions, when expressed as a fraction of the magnitude of the requested vertical force, are not significantly different across handle heights ($\alpha=0.05$).

The requested vertical force was found to be a significant predictor of fore-aft off-axis forces generated during two-handed elbow-height downward exertions, and thigh-height up exertions. The relationship is highly significant (R^2 Adj = 0.28, $p < 0.01$) for downward exertions and significant (R^2 Adj = 0.20, $p < 0.05$) for upward exertions performed at the mid-thigh handle height. When exerting force downward on an elbow-height handle, participants were found to push forward on the handle during low-force exertions, and pulled back on the handle as the level of vertical force required increased. Fore-aft off-axis forces are more variable during thigh-height upward exertions, with a tendency to transition from pulling back on the handle to pushing forward as the magnitude of upward force increases. Requested vertical force was not found to be a significant predictor of fore-aft off-axis force during elbow and thigh-height upward exertions. Elbow-height upward exertions were performed by pulling up on the handle or squatting down to get under the handle and push up. It was hypothesized that the presence of two distinct postural strategies accounted for the large variability in fore-aft off-axis force; however, ANOVA results indicated fore-aft forces were not significantly different across postural strategies.

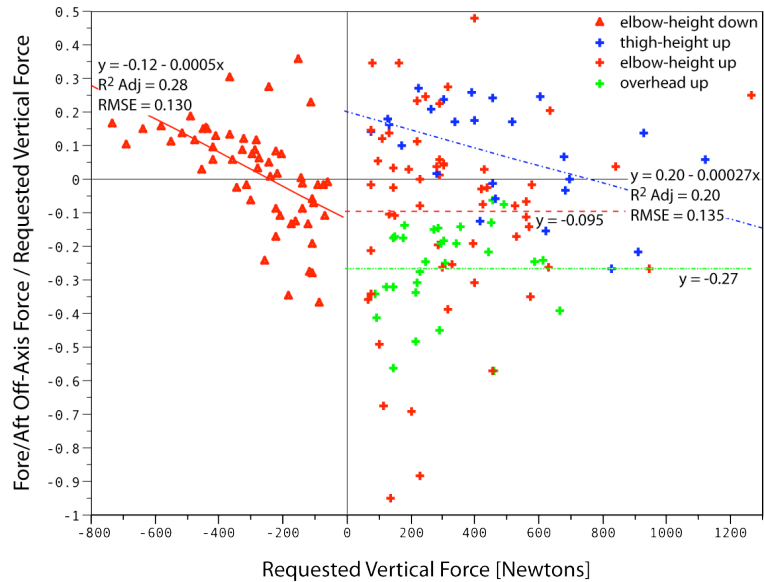


Figure 3.8. Fore-aft off-axis forces during two-handed up/down exertions. Linear fit is highly significant ($p < 0.01$) for two-hand downward exertions and significant ($p < 0.05$) for upward exertions at thigh-height.

Off-Axis Forces During One-Handed Push/Pull Exertions

One-handed force exertions to the right/left were grouped together with forward and back exertions, depending on whether people pushed or pulled to the left or right. Less than 2% (2 / 114) of exertions to the right were performed using a pushing strategy and thus were excluded from the analysis. Both push and pull strategies were prevalent when exerting force to the left. Comparison of lateral off-axis forces exerted during one-handed forward/back exertions to those exerted during one-hand exertions to the left and right indicates that lateral off-axis forces are more significant during left/right exertions. During forward/back exertions, lateral off-axis forces are less than 25.2 N (~5.7 lbs) during 90% of trials and thus considered negligible compared to vertical off-axis forces. Lateral off-axis forces are larger during exertions to the left and right with only 56% of left/right exertions having lateral off-axis forces less than or equal to 25.2 N.

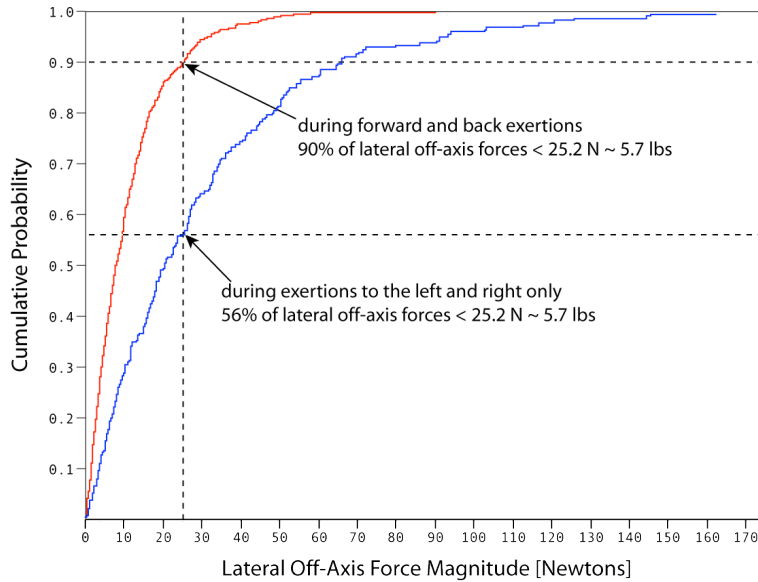


Figure 3.9. Cumulative distribution functions for lateral off-axis force magnitude during one-handed forward/back exertions and one-handed left/right exertions.

Within strategy, lateral off-axis forces generated during exertions to the left were not found to differ significantly across handle heights (Figure 3.10). On average, lateral off-axis forces were greater when pushing to the left as opposed to pulling to the left. For force exertions to the right, differences in lateral off-axis forces across handle heights were highly significant (Figure 3.11). Lateral forces are largest for thigh-height pulls to the right at approximately 25% of the requested force magnitude. During overhead pulls to the right lateral off-axis forces average 3.13 N (~0.7 lbs) and are considered negligible.

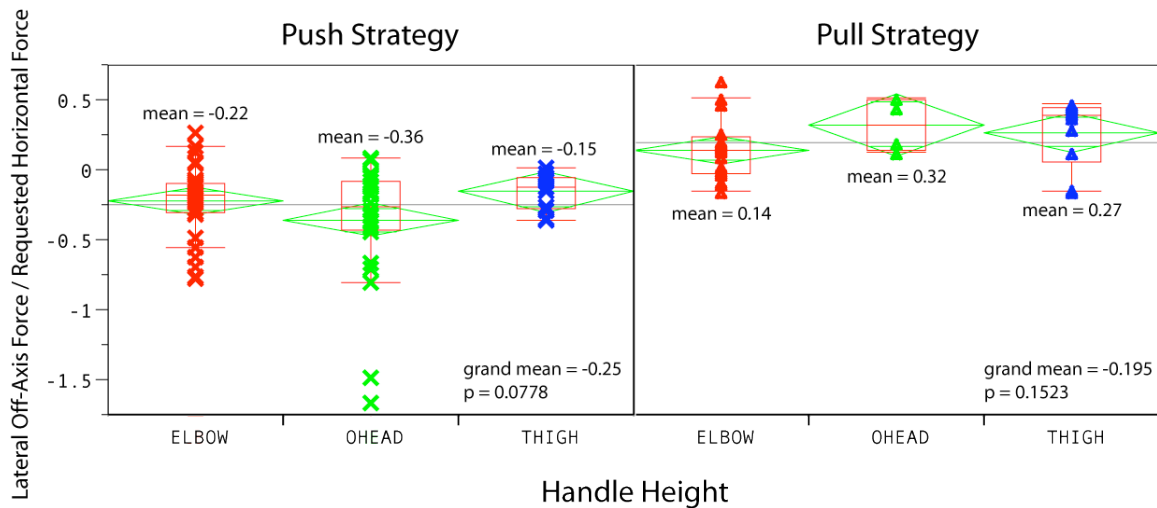


Figure 3.10. Lateral off-axis forces across handle heights during one-handed exertions to the left performed using a push or pull strategy. Within strategy, lateral off-axis forces are not significantly different across handle heights.

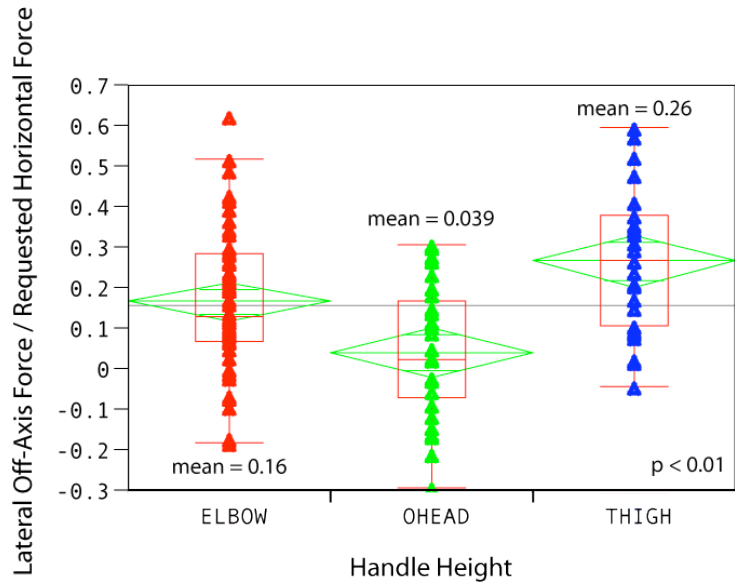


Figure 3.11. Lateral-off axis forces across handle heights during one-handed pulls to the right. Differences in lateral off-axis forces across handle heights are highly significant ($p < 0.01$). At the overhead handle height lateral off-axis forces are negligible, 3.13 N (0.7 lbs) on average.

Requested hand force is a significant predictor of vertical off-axis forces generated during forward exertions at elbow (Figure 3.12) and thigh-height (Figure 3.13). As with two-handed push exertions, relationships are significantly different between one-hand push exertions performed with a flexed versus extended-elbow strategy. For exertions performed with a flexed-elbow strategy, downward forces are observed during low-force push exertions with a transition to upward force occurring with increasing push force. When pushing with one hand at thigh-height, forces are directed more downward than during pushes at elbow-height. For extended-elbow pushes, a transition from downward to upward force also occurs for exertions at elbow-height, while vertical forces are predominantly downward when pushing at the mid-thigh handle location with one hand. It was also found that the requested force is not a significant predictor of vertical off-axis force when pushing overhead (Figure 3.14).

The relationship between vertical off-axis force and requested hand force is only significant for pulls performed at elbow height. When pulling at elbow-height, the trend is to pull back and up during low-force pulls and transition to a more horizontal pull as the required pull force increases (Figure 3.12). For pulls at thigh-height and overhead, vertical off-axis forces are best represented by mean values expressed as a percent of the requested hand force magnitude (Figure 3.13 and Figure 3.14).

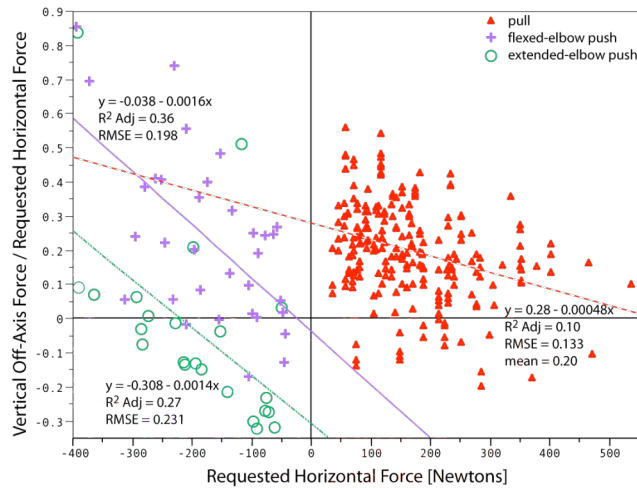


Figure 3.12. Vertical off-axis forces during forward and back exertions at elbow height. Differences in vertical off-axis forces are highly significant ($p < 0.01$) when pushing with flexed versus extended elbows.

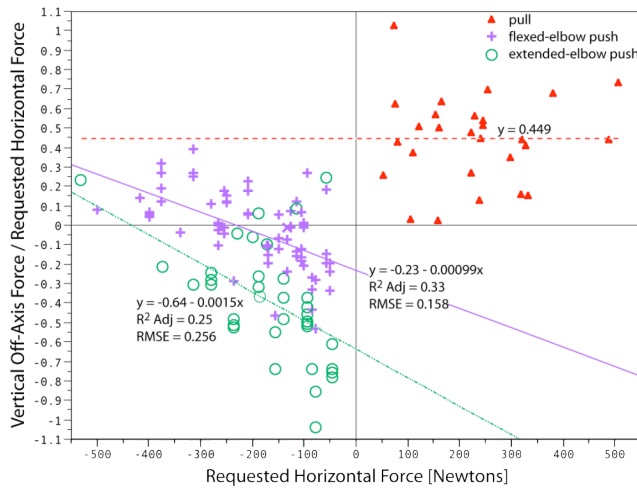


Figure 3.13. Vertical off-axis forces during forward and back exertions at thigh height. Differences in vertical off-axis forces are highly significant ($p < 0.01$) when pushing with flexed versus extended elbows.

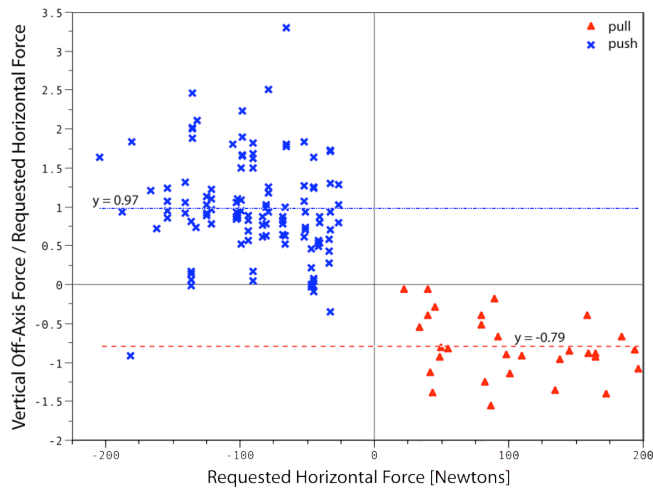


Figure 3.14. Vertical off-axis force during overhead forward and back exertions.

Off-Axis Forces During One-Handed Up/Down Exertions

Lateral forces were less than 31.6 N (~7.1 lbs) during 90% of one-handed down exertions performed at elbow-height and thus considered negligible (Figure 3.15). Lateral off-axis forces were larger during one-handed up exertions, and were found to be significantly predicted by requested vertical hand force for exertions performed at elbow-height (Figure 3.16). A weak but significant correlation showed that subjects exerted force to the left with lateral off-axis force increasing as the magnitude of vertical force required increased ($R^2 \text{ Adj} = 0.17$, $p < 0.01$). Requested hand force was not a significant predictor of lateral off-axis force for upward exertions performed at the thigh and overhead handle heights. Lateral forces at these heights are best represented by mean values expressed as a percent of the magnitude of the requested vertical hand force.

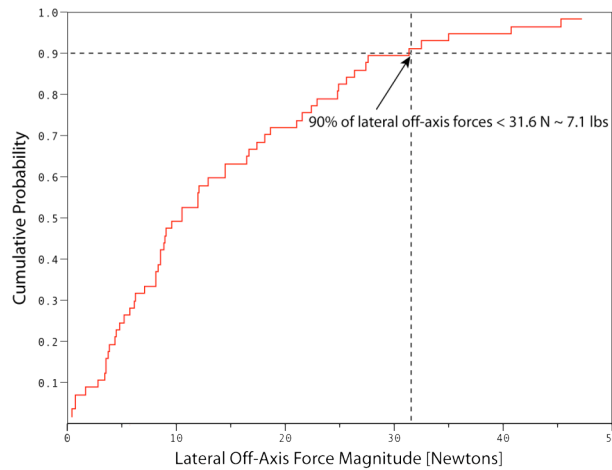


Figure 3.15. Cumulative distribution function for lateral off-axis forces during one-handed downward exertions at elbow-height.

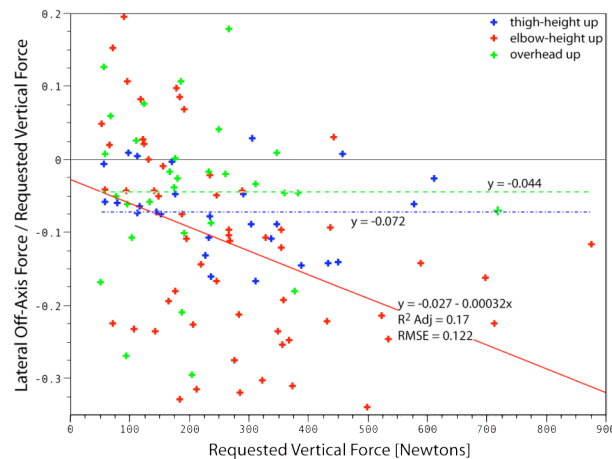


Figure 3.16. Lateral off-axis forces during one-handed upward exertions. Linear fit for elbow-height upward exertion is highly significant ($p < 0.01$).

Requested vertical force was found to be a significant predictor of fore-aft off-axis force during one-handed down exertions at elbow height (Figure 3.17). The actual force appears to be directed down and forward during low-force exertions, and down and back during high force exertions (R^2 Adj = 0.31, $p < 0.01$). Fore-aft off-axis force was not found to be predicted by the requested vertical force during up exertions. For upward exertions performed at thigh, elbow, and overhead heights, fore-aft forces are represented by mean values expressed as a fraction of the requested vertical hand force.

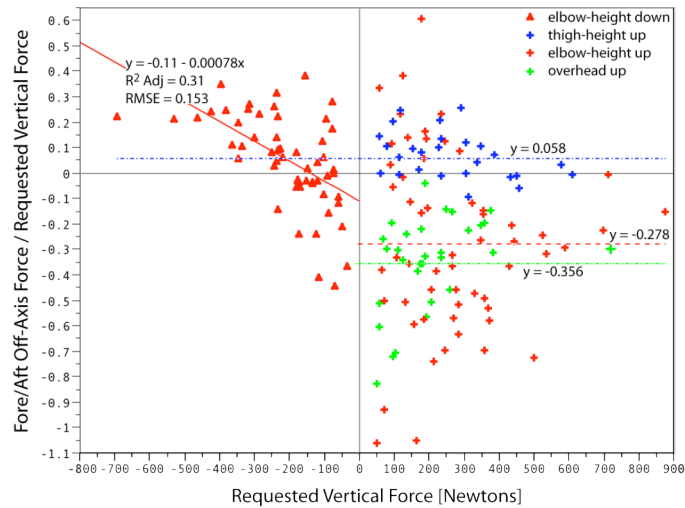


Figure 3.17. Fore-aft off-axis forces during one-handed up/down exertions. Linear fit is highly significant ($p < 0.01$) for one-hand downward exertions at elbow height.

3.5. Summary and Discussion

The laboratory data support the hypothesis that people exert hand forces in directions that are different from the ones requested, resulting in an overall magnitude of force substantially larger than the requested magnitude. The substantial off-axis loads observed in these data are generally consistent with other research on pushing and pulling (de Looze et al., 2000, Granata & Bennett, 2005, Boocock et al., 2006). For high-force push/pull exertions at elbow height, participants tended to push or pull upward on the handle as well as horizontally, increasing the vertical ground reaction force, and hence the magnitude of horizontal force available within the coefficient of friction of the shoe-floor interface (typical COF ~ 0.75). At mid-thigh and overhead handle heights, greater variability was observed in vertical off-axis forces, which can be explained in part by the kinematic difficulty of these tasks. For overhead exertions the high handle height reduces the number of kinematically feasible postures and limits the extent of postural

adjustments people can make. For low hand positions people sacrifice precision in force direction and are willing to exert a larger total force to keep their torsos more upright. Across all handle heights, vertical forces generated during push/pull exertions were consistent with the hypothesis regarding the direction of vertical force during push/pull exertions at handles below and above shoulder height. For pushes below shoulder height, a change in the vertical component from downward to upward with increasing force magnitude was not anticipated. Generation of upward forces when pushing would act to increase the available friction at the feet thereby increasing push force capability as discussed by Kerk (1994).

Previous work has not addressed lateral and fore-aft off-axis forces. While lateral forces were small, less than 44.5 N (~10 lbs) for all two-handed exertions and one-handed forward/back exertions, they were significantly greater than zero during requested one-handed push/pull exertions to the right and left. Lateral forces during exertions to the right and left are probably in part due to postural constraints imposed by the experimental apparatus. Participants were not easily able to stand directly to the left or right of the force handle causing them to exert a rearward force when pulling the right or left, and forward force when pushing to the left.

A lateral force to the left was observed during one-handed (always right-handed) upward exertions. Fore-aft forces were also observed during one-handed up/down exertions. Downward exertions at elbow height were characterized by a forward force component for low-force exertions, transitioning to a rearward component as the level of required force increased. This trend was also observed during two-handed downward exertions. For overhead and elbow-height upward exertions people tended to exert a forward force on the handle, whereas for thigh-height exertions the fore-aft force was directed rearward.

These findings show that the magnitude and direction of forces people exert can be substantially different from the nominal requirements, a finding that has important implications for ergonomic analysis. Requested hand force was found to be a significant predictor of off-axis forces for a subset of trial conditions suggesting that statistical models can be used to predict actual forces from required force data under certain conditions. Ergonomists often use product specification data to estimate the magnitude of

required force (for example, the nominal insertion force for a part) and infer hand force direction from part geometry or assume simple horizontal or vertical force directions when analyzing jobs using biomechanical modeling tools. The regression models relating required and actual hand forces presented in this chapter are a step towards allowing ergonomists to estimate the magnitude and direction of actual hand force from product data and knowledge of the assembly process (e.g. part insertion direction, constraints on direction of insertion, etc.).

This study has several limitations that affect the generalizability of the findings. Exertions were quasistatic and were held for only three seconds. In the field, workers often perform exertions dynamically to take advantage of inertial effects. Dynamic behaviors could accentuate or reduce the magnitude of the off-axis effects observed here. The laboratory environment was also largely free of kinematic constraints, allowing the participants to choose postures more freely than in some industrial situations. Adding postural constraints might affect the force directions.

Participants were provided continuous visual feedback regarding the magnitude of force in the requested direction. In typical application scenarios, e.g., inserting a part, the feedback to the worker is more binary and tactile. In those situations, the worker may overestimate the required force, in addition to applying an excessive magnitude due to off-axis components. More research is needed to determine the extent to which these factors contribute to loading in excess of the nominal values.

The participants in the laboratory study wore comfortable shoes on a high-friction surface. The off-axis forces during high-magnitude push-pull exertions are consistent the participants exerting upward force to increase ground reaction forces, thereby enabling higher fore-aft forces. A higher friction surface might have decreased the need for this action, and conversely a low-friction surface might accentuate the off-axis effects.

Finally, the nature of the coupling at the hand interface, and particularly the joint postures necessary to grasp the handle, may have affected the results. Other types of coupling, particularly those requiring a substantial frictional component to accomplish the task, may change the off-axis contribution. For example, pushing with an open hand against a flat surface may yield different off-axis forces than were observed with participants grasping a high-friction, cylindrical handle.

This study provides the first quantitative description of off-axis forces as a function of requested force magnitude and direction, for a wide range of magnitudes and force directions, and for men and women with a wide range of anthropometry and strengths (Table 3.5 and Table 3.6). These results should encourage caution by ergonomists in interpreting nominal required forces as those that a person would actually exert, and also suggest that more research is needed on how workers choose to generate force when the required force direction is not fully constrained. Such research should consider the effects of hand/object coupling and the foot/floor boundary condition, among other issues.

Table 3.5. Models for predicting two-hand off-axis forces from the requested hand force magnitude.

Hand Force Direction	Handle Height	Elbow Tactic	Off-Axis Force / Requested Force	R ² Adj	RMSE
Forward (Push)	Overhead	Extended	$F_z = 1.03$	-	-
	Elbow-height	Flexed	$F_z = -0.05 - 0.0013F_x^{Req.}$	0.32	0.213
		Extended	$F_z = -0.36 - 0.00098F_x^{Req.}$	0.66	0.107
	Thigh-height	All	$F_z = -0.148$	-	-
Back (Pull)	Overhead	Extended	$F_z = -1.25$	-	-
	Elbow-height	All	$F_z = 0.203$	-	-
	Thigh-height	All	$F_z = 0.387$	-	-
Up	Overhead	All	$F_x = -0.27$	-	-
	Elbow-height	All	$F_x = -0.095$	-	-
	Thigh-height	All	$F_x = -0.20 - 0.00027F_z^{Req.}$	0.20	0.135
Down	Elbow-height	All	$F_x = -0.12 - 0.0005F_z^{Req.}$	0.28	0.130

Table 3.6. Models for predicting one-hand off-axis forces from the requested hand force magnitude.

Hand Force Direction	Handle Height	Tactic (Push vs. Pull)	Elbow Tactic	Off-Axis Force / Requested Force	R ² Adj	RMSE
Forward (Push)	Overhead	Push	Extended	$F_z = 0.97$	-	-
	Elbow-height	Push	Flexed	$F_z = -0.038 - 0.0016F_x^{Req.}$	0.36	0.198
			Extended	$F_z = -0.308 - 0.0014F_x^{Req.}$	0.27	0.231
	Thigh-height	Push	Flexed	$F_z = -0.23 - 0.00099F_x^{Req.}$	0.33	0.158
			Extended	$F_z = -0.64 - 0.0015F_x^{Req.}$	0.25	0.256

Back (Pull)	Overhead	Pull	Extended	$F_z = -0.79$	-	-
	Elbow-height	Pull	All	$F_z = 0.28 - 0.00048F_x^{Req.}$	0.10	0.133
	Thigh-height	Pull	All	$F_z = 0.449$	-	-
Up	Overhead	-	All	$F_x = -0.356$ $F_y = -0.044$	-	-
	Elbow-height	-	All	$F_x = -0.278$ $F_y = -0.027 - 0.00032F_z^{Req.}$	0.17	0.122
	Thigh-height	-	All	$F_x = 0.058$ $F_y = -0.072$	-	-
Down	Elbow-height	-	All	$F_x = -0.11 - 0.00078F_z^{Req.}$	0.31	0.153
Left	Overhead	Push	All	$F_x = -0.36$	-	-
				$F_z = 0.97$	-	-
		Pull	All	$F_x = 0.32$ $F_z = -0.79$	-	-
	Elbow-height	Push	Flexed	$F_x = -0.22$	-	-
				$F_z = -0.038 - 0.0016F_y^{Req.}$	0.36	0.198
			Extended	$F_x = -0.22$ $F_z = -0.308 - 0.0014F_y^{Req.}$	0.27	0.231
		Pull	All	$F_x = 0.14$	-	-
				$F_z = 0.28 - 0.00048F_y^{Req.}$	0.10	0.133
				$F_x = -0.15$	-	-
Thigh-height	Push	Flexed	$F_z = -0.23 - 0.00099F_y^{Req.}$	0.33	0.158	
			Extended	$F_x = -0.15$ $F_z = -0.64 - 0.0015F_y^{Req.}$	0.25	0.256
	Pull	All	$F_x = 0.27$ $F_z = 0.449$	-	-	
Right	Overhead	Pull	All	$F_z = -0.79$	-	-
	Elbow-height	Pull	All	$F_x = 0.16$ $F_z = 0.28 - 0.00048F_y^{Req.}$	0.10	0.133
	Thigh-height	Pull	All	$F_x = 0.26$ $F_z = 0.449$	-	-

3.6. References

- Boocock, M. G., Haslam, R. A., Lemon, P., and Thorpe, S. (2006). Initial force and postural adaptations when pushing and pulling on floor surfaces with good and reduced resistance to slipping. *Ergonomics*, 49(9):801–821.
- de Looze, M. P., van Greuningen, K., Rebel, J., Kingma, I., and Kuijer, P. P. (2000). Force direction and physical load in dynamic pushing and pulling. *Ergonomics*, 43(3):377–390.
- Dempster, W. (1958). Analysis of two-handed pulls using free body diagrams. *J Applied Physiology*, 13(3):469–480.
- Granata, K. R. and Bennett, B. C. (2005). Low-back biomechanics and static stability during isometric pushing. *Hum Factors*, 47(3):536–549.
- Hoozemans, M. J. M., et al. (2004). Mechanical loading of the low back and shoulders during pushing and pulling activities. *Ergonomics*, 47(1):1–18.
- Kerk, C., Chaffin, D., and et al (1994). A comprehensive biomechanical model using strength, stability, and cof constraints to predict hand force exertion capability under sagittally symmetric static conditions. *IIE Transactions*, 26(3):57–67.
- Nussbaum, M., Chaffin, D., and Baker, G. (1999). Biomechanical analysis of materials handling manipulators in short distance transfers of moderate mass objects: joint strength, spine forces and muscular antagonism. *Ergonomics*, 42:1597–1618.
- Roebuck, J. A. (1995). *Anthropometric methods : designing to fit the human body*. Human Factors and Ergonomics Society, CA.

CHAPTER 4

PREDICTING TWO-HAND FORCE EXERTION POSTURES

4.1. Abstract

The objectives of this work were to quantify postural trends during two-handed standing hand force exertions and develop regression models to predict key aspects of task postures. Two-hand force exertion tasks were extracted from a larger dataset, and the effects of task parameters and anthropometrics on postures were examined. Force exertion postures were found to be consistent with a desire to reduce shoulder moments due to the hand force while maintaining an upright torso posture, within the limitations imposed by balance and kinematic constraints. People altered the location of their shoulder with respect to the point of force application or generated off-axis forces to direct the hand force vector towards the shoulder joint, resulting in a decrease or maintenance of shoulder moment despite increasing hand forces. It was found that the shoulder moment is strongly associated with task and postural variables, suggesting that shoulder flexion/extension moment can be used as part of a posture-prediction model. It was also found that torso inclination angle was predicted by change in shoulder location, as well as handle height, the interaction between handle height and change in shoulder height, and the vertical hand force component. An increase in the length of the base-of-support with increasing hand force magnitude was observed. This was consistent with the general balance hypothesis. The resulting data were used to develop predictive models two-handed push/pull exertions. In general, the postural trends and regression models presented in this chapter provide insight into the biomechanics of posture selection during two-handed hand force exertions. The findings are consistent with hypothesized biomechanical principles and behaviors, suggesting that these findings can be used as part of a posture-prediction model for standing hand force exertions.

4.2. Introduction

This chapter presents an investigation of the relationship between hand force and posture chosen by subjects during two-handed push/pull and up/down exertions. For the current analysis, data were extracted from a larger dataset wherein nineteen participants performed one- and two-handed exertions of various force magnitudes and directions at thigh, elbow, and overhead handle heights. The objective of this work was to identify underlying biomechanical principles that can predict key postural elements in relation to hand force and develop regression models for use in the posture prediction model discussed in Chapter 6.

Researchers have proposed several explanations for the observed posture and force-exertion trends in push/pull tasks. Granata et al. (2005) cited two reasons for applying an upward force when pushing that are related to posture: (1) to reduce moments at the low back and possibly at the shoulder, and (2) to recruit lower-body strength. The first reason is based on their observation that participants tend to align the force vector along their spine, passing the vector through their lumbosacral joint, by flexing their elbows and increasing torso flexion as the level of exertion increases. They showed that small L5/S1 moments during maximum push exertions support this explanation. Similarly, de Looze et al. (2000) explained small changes in shoulder moments over a range of handle heights and horizontal force levels by a tendency to maintain alignment of the resultant hand force vector through the shoulder joint. These observations suggest a strong relationship between hand force and posture during pushing exertions, although this relationship has not been systematically quantified.

High-Level Hypotheses

The following hypotheses were formulated based on review of the literature and observations from an automotive assembly plant study and laboratory pilot study:

1. People choose postures consistent with reducing the shoulder moment due to the hand force, within the limitations imposed by balance and kinematic constraints. External load effects are reduced by choosing postures such that the hand force vector is directed toward the shoulder joint center.
2. People incline their torsos from vertical the minimal amount necessary to generate the needed hand forces within the constraints of kinematics, except

as necessary to reduce shoulder moment. This is consistent with an objective to reduce lower-back extension moments.

Governing Constraints and Assumptions

The following assumptions and constraints are assumed to apply when analyzing force exertion postures and developing regression models to predict key postural metrics:

1. All force exertion postures of interest are quasistatic.
2. All postures are in static balance.
3. No moments are exerted at the feet, i.e., the ground reaction can be expressed solely as a three-dimensional force vector.
4. Moments exerted at the hands are negligible.
5. All transmission of force to/from the environment occurs at the floor and the load handle (no external bracing).

Hypothesized Biomechanical Principles

1. All hand force in the standing tasks of interest is inherently derived from body weight and ground reaction force. That is, no hand force can be exerted without an equal and opposite force generated by ground reaction.
2. To generate a force at the hand, the body mass must be located relative to the base of support (feet) to generate a moment to counter the reaction force applied to the hand.
3. People attempt to maintain postures as close to neutral standing as possible while still being able to exert the required force. Deviations from neutral standing postures occur due to:
 - a. the kinematic constraints of the task, i.e., to reach the force handle,
 - b. a desire or need to reduce shoulder moment.
4. People use three primary postural adaptations to produce hand force:
 - a. alter the base of support (foot placements)
 - b. incline the torso forward
 - c. squat (bend the knees)
5. Postures are selected to reduce rotational moments about the lumbar spine.

6. Postures are chosen to avoid having hand force limits dictated by elbow strength.

Hypothesized Behaviors

1. People produce forces in directions different than those requested, if permitted:
 - a. At low force levels, people will exert forces in directions that reduce shoulder moment while permitting a near neutral torso posture.
 - b. At high horizontal force levels, people will exert upward forces to generate increased vertical ground reaction force, which allows greater horizontal ground reaction force within the friction limitations of the interface.
2. People will alter their shoulder positions to reduce the moment, or alternatively to produce higher hand force with the same shoulder moment.
3. Shoulder moment and torso inclination will show a trade-off relationship when the objectives of reducing shoulder moment and maintaining an upright torso are in conflict.
4. Shoulder moments across individuals will be proportional to static isolated shoulder strength.
5. The position and orientation of the base of support relative to the hand force vector will be chosen to align the vertical plane in which the force vector lies with the L5/S1 joint.
6. The position of the active boundary of the base of support (e.g., rear foot for pushing, front foot for pulling) will be predictable using a planar static force- and moment-balance calculation. That is, the active boundary will be located such that the moment generated by body weight around the boundary will balance the moment generated by the hand force about the same point. This implies that people choose a base of support such that the center of pressure lies at the edge of the base of support.
7. Elbow postures are either (a) extended, reducing elbow moment, or (b) substantially flexed, positioning the hands close to the shoulders and using passively-generated elbow moment and internal bracing.

4.3. Methods

Participants

Nineteen participants performed trials at two of three handle heights and with a wide range of different force magnitudes and directions. One of the original twenty subjects, Subject 023, was identified as an outlier and excluded from the analysis. The experimental design and laboratory study are described in detail in Chapter 2 and two-handed test conditions summarized in Figure 4.1. For the current analysis, data from two-handed exertions at mid-thigh, elbow, and overhead handle heights were extracted from the larger dataset. As described in Chapter 2, the nineteen participants were young (median age 21 years) and relatively thin (median body mass index 23 kg/m²).

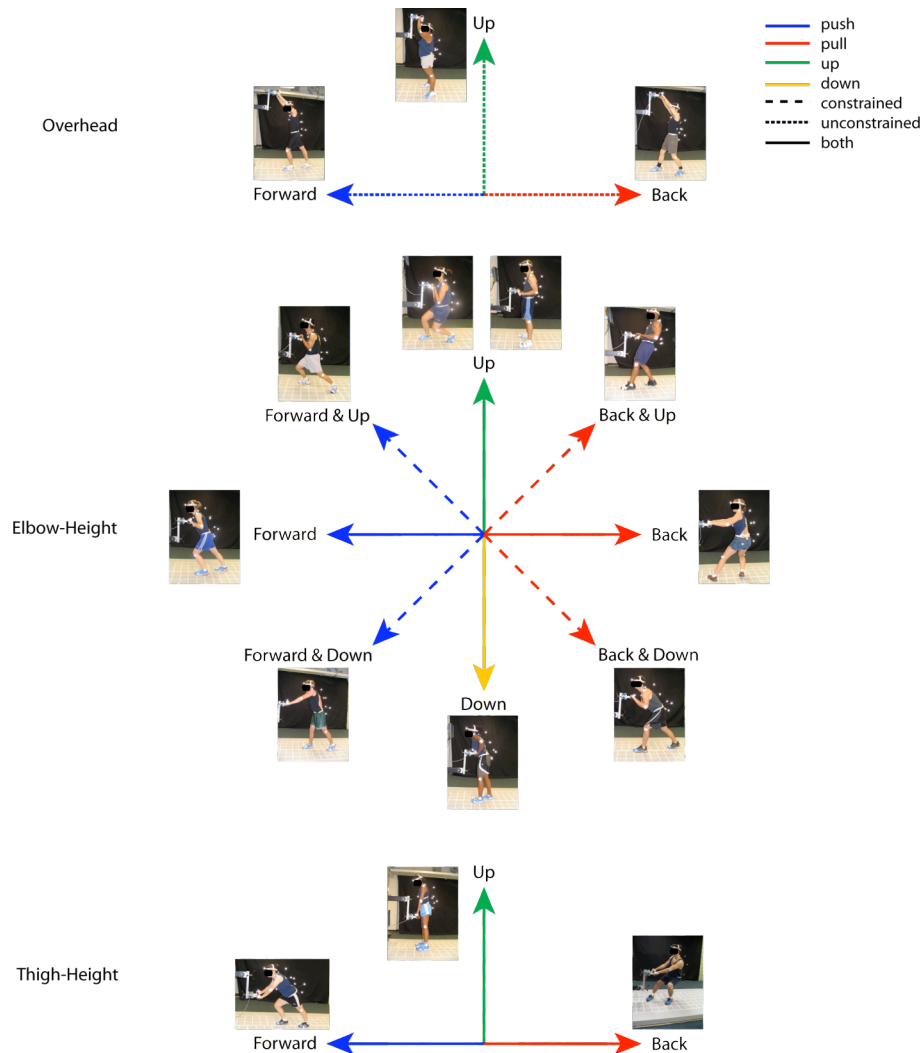


Figure 4.1. Hand force directions and force direction constraint conditions for two-handed thigh, elbow, and overhead height exertions. Forces levels were 25%, 50%, and 75% of maximum for all directions as well as maximal exertion for unconstrained force directions.

Test Conditions

Of the two-handed exertions collected as part of the experiment outlined in Chapter 2 and summarized in Figure 4.1, 80% were considered for analysis and the remaining 20% reserved for model validation. Participants were free to choose their preferred posture and encouraged during practice trials to try different postures in an effort to identify their preferred posture. Participants were instructed to exert a force in a specified direction but were free to choose how they completed the task. As a result, within a given task condition, different postural strategies were used. For example, upward exertions can be performed by pulling up from over top the force handle or by getting under the handle and pushing upward using the lower-extremities. Similarly, people can press downward from above the handle or pull downward from underneath the handle to exert the required downward force.

Two groups of outliers involving uncommon behaviors were identified and excluded. During pull exertions, a small subset of subjects adopted a less conservative strategy than others, in that the participants selected a side-by-side or parallel foot placement, with the torso located well rearward of both feet (Figure 4.2). This strategy is risky in that a sudden movement of the handle would likely lead to a fall. In this study, risky strategies were much less common than conservative strategies for positioning the feet and were excluded. A subset of thigh-height upward exertions was also excluded from the analysis. In some instances participants were able to generate larger than average upward forces by bracing their thighs against the underside of the force handle and using their lower-body to lift up on the handle. These trials were excluded from the analysis. Table 4.1 and Table 4.2 summarize the number of unconstrained and directionally constrained trials analyzed for women and men under each test condition.

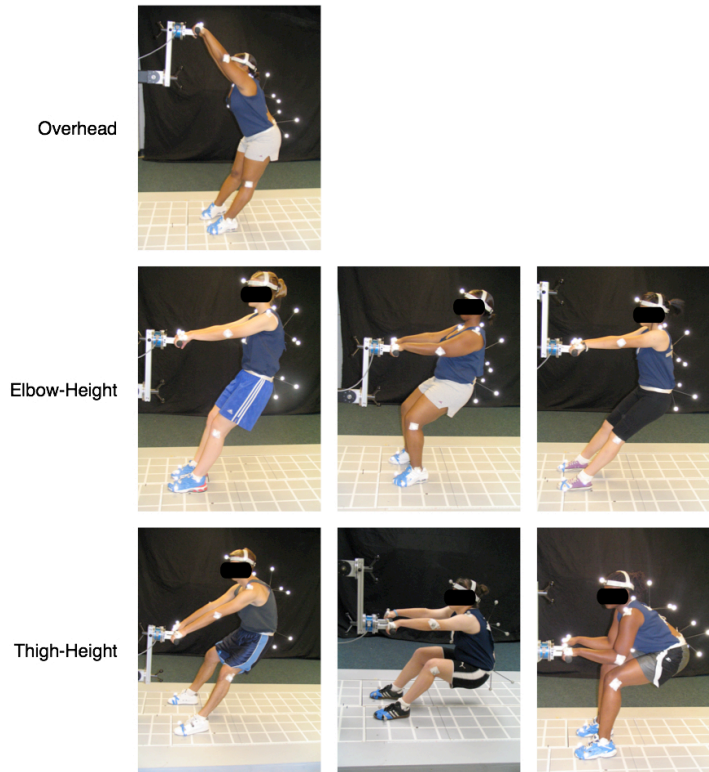


Figure 4.2. Examples of risky two-handed thigh-height, elbow-height, and overhead pulling strategies excluded from the analysis.

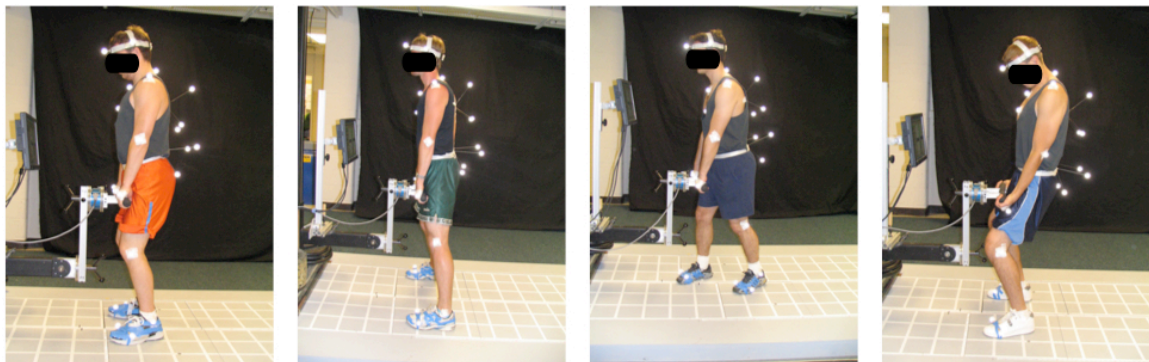


Figure 4.3. Examples of two-handed thigh-height up exertions excluded from the analysis.

Table 4.1. Test conditions and number of directionally unconstrained trials analyzed (women / men).

	Mid-Thigh				Elbow				Overhead				Total
	25%	50%	75%	100%	25%	50%	75%	100%	25%	50%	75%	100%	
Push	2/3	5/3	4/3	4/3	37/34	39/35	37/31	7/8	5/4	5/4	4/3	1/4	150/135
Pull	4/3	3/2	2/3	1/2	5/6	6/8	5/8	4/4	3/2	3/3	4/4	4/3	44/48
Up	4/1	3/0	4/0	4/0	9/8	4/7	10/6	7/6	3/3	5/5	3/4	4/3	60/43
Down	-	-	-	-	8/9	6/5	5/6	8/4	-	-	-	-	27/24
Total	10/7	11/5	10/6	9/5	59/57	55/55	57/51	26/22	11/9	13/12	11/11	9/10	281/250

Table 4.2. Test conditions and number of directionally constrained trials analyzed (women / men) with all hand force directions grouped as push, pull, up, or down exertions. Directionally constrained trials were not performed at the overhead handle height and all maximum exertions were directionally unconstrained.

	Mid-Thigh			Elbow			Total
	25%	50%	75%	25%	50%	75%	
Push	5/4	2/2	4/4	24/25	12/10	17/15	64/60
Pull	5/4	0/3	2/3	28/24	13/10	19/24	67/68
Up	5/4	3/0	5/0	10/9	7/7	9/8	39/28
Down	-	-	-	9/9	3/7	9/8	21/24
Total	15/12	5/5	11/7	71/67	35/34	54/55	191/180

Data Analysis

A hand force plane, defined as the vertical (x-z) plane containing the measured hand force vector, was determined for each data trial. By analyzing postures with respect to the hand-force plane, exertions in any force direction can be categorized as a push, pull, upward or downward exertion. Each data trial was categorized as a (1) push, (2) pull, (3) pull up, (4) push up, or (5) push down. Whole-body postures were quantified by a set of postural metrics defined with respect to the hand-force plane and analyses conducted within each postural category to determine the effects of worker and task parameters on posture.

Definition of Hand-Force Plane

For each data trial, components of the actual hand force vector measured via a 6 DOF load cell were used to define a hand-force plane (Figure 4.4). The z-axis of the hand-force frame was defined to be coincident with the global z-axis. The global orientation of the x and y-axes of the hand-force frame was obtained by rotating the global frame about the z-axis so that the x-axis lies in the vertical plane of the actual hand force vector. The rotation matrix mapping the global hand force vector to the hand-force plane was computed and used to map the three-dimensional kinematic data into the hand-force plane reference frame.

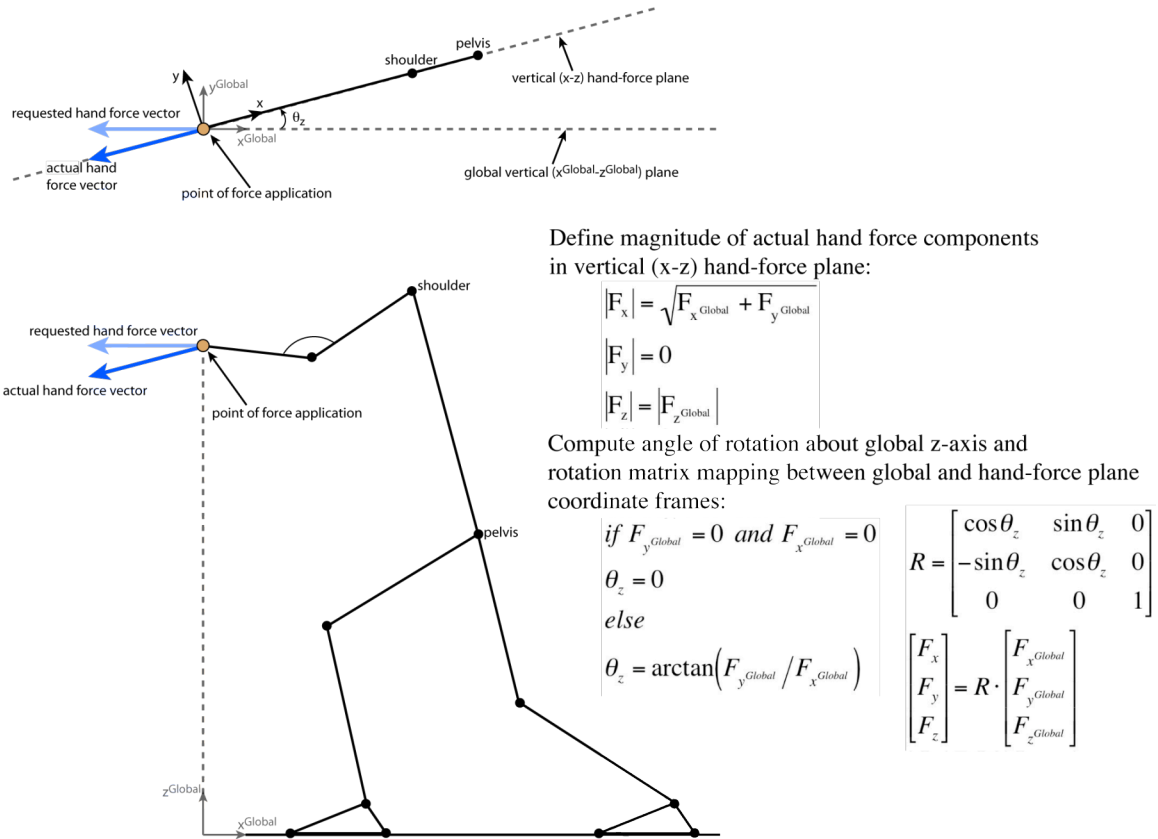


Figure 4.4. Top and side-view of hand-force plane defined as the vertical plane in which the actual hand-force vector lies. Transformation between the global and hand-force plane coordinate frames is performed by the rotation matrix, R, a pure rotation of θ_z about the global z-axis. As defined, the z-axis of the global and hand-force coordinate frame is coincident.

Postural Metrics

A set of postural metrics was developed to quantify whole-body postures with respect to the hand-force plane (Figure 4.6). Kinematic data was used to define a three-dimensional whole-body linkage and force exertion postures as the average whole-body linkage configuration during the final 3 seconds of each trial. By experimental design the last 3 seconds of each trial corresponded to the period during which the requested hand force had been achieved and maintained within the prescribed limits. Postural metrics were defined and computed as follows:

Included Elbow Angle (θ_{elbow}) – Included elbow angle is defined as the angle between the right upper arm and forearm vectors. The right upper arm vector is defined from the right elbow to right shoulder and the forearm from the right elbow to wrist.

Change in Shoulder Height from Neutral ($\Delta h_{shoulder}$) – Neutral standing shoulder height with respect to the ground was obtained for each subject by averaging over each

subject's trials the average shoulder height computed during the initial 20 frames of each trial. Change in shoulder height from neutral is then computed as the difference in shoulder height, while in the force exertion posture, from neutral standing shoulder height. Positive $\Delta h_{\text{shoulder}}$ values correspond to shoulder locations above, and negative values to shoulder locations below neutral standing height.

Shoulder Height with Respect to Hands (h_{shoulder}) – Shoulder height with respect to the hands (i.e. point of force application) was computed as the difference in vertical shoulder location and vertical location of the point of force application. Shoulder height is defined positive for shoulder locations above the point of force application.

Shoulder Flexion/Extension Moment (M_{shoulder}) – Flexion/extension moments about the right and left shoulders due to hand force and the mass of the upper-extremities were computed and averaged to obtain a shoulder flexion/extension moment. Shoulder extension moments are defined positive and shoulder flexion moments negative where shoulder extension corresponds to raising the arm, in the sagittal plane, from a resting posture along side the torso to overhead.

Planar Torso Inclination Angle (θ_{torso}) – A torso vector was defined from C7/T1 to the mid-hip location. Planar torso inclination angle is computed as the angle between the negative z-axis of the hand-force frame and the projection of the torso vector onto the vertical (x-z) plane of the hand-force frame. Positive values correspond to rearward torso inclination or torso extension and negative values to forward inclination or torso flexion.

Pelvis Pitch Angle (θ_{pelvis}) – Pelvis pitch angle is the anterior/posterior tilt of the pelvis with respect to the torso computed by subtracting planar torso inclination angle from pelvis pitch defined with respect to the hand-force frame. Pelvis orientation (roll, pitch, and yaw angles) was obtained from the rotation matrix defined by projecting the local pelvis coordinate axes onto the axes of the hand-force frame. To account for between-subject differences in pelvis pitch, due to differences in anatomy or marker placement, a neutral pelvis pitch angle was determined for each subject. For each subject, neutral pelvis pitch was defined by averaging across all trials the mean pitch angle computed over the initial 20 frames of each trial, when the subject was standing in a neutral posture. These values were used to normalize pelvis pitch prior to computing pelvis pitch angle. With respect to the hand-force frame, pelvis pitch is defined positive

for rearward tilt or extension, which is consistent with the definition for planar torso inclination angle. Positive pitch angles indicate extension or rearward tilt of the pelvis with respect to the thorax.

Lateral Pelvis Displacement (y_{pelvis}) – Lateral displacement of the pelvis out of the hand-force plane is defined by the y-location of the origin of the pelvis coordinate frame in the hand-force coordinate system. The pelvis coordinate system is defined by computed hip centers and digitized bony landmarks. The y-axis lies along the vector from the left to right hip joint and the x-axis defined along the vector from the mid-ASIS to mid-PSIS digitized points. The z-axis is obtained from the cross product of the x and y-axes.

Active Boundary of Base-of-Support ($x_{front\ boundary}$ or $x_{rear\ boundary}$) - The active boundary corresponds to the rear edge of the BOS when pushing and the forward edge when pulling. For exertions in the vertical direction, i.e. up/down exertions, the rear boundary is used. The active boundary is defined by the x-coordinate of the respective edge with the BOS defined as illustrated in the figure below.

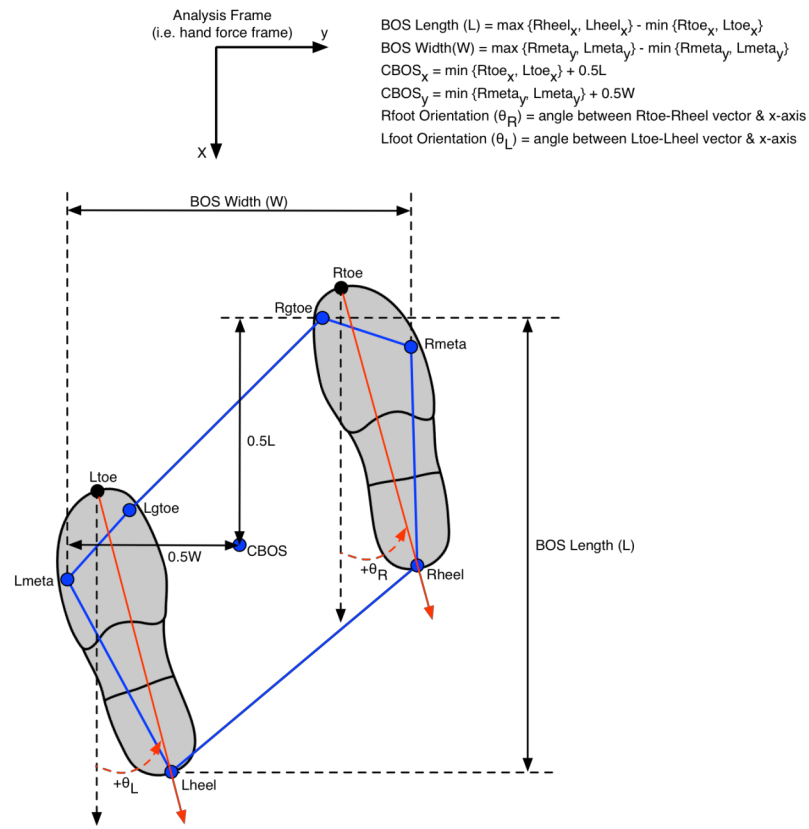


Figure 4.5. Definition of base-of-support and metrics used to quantify foot placements.

Length of Base-of-Support (L_{BOS}) – The length of the base-of-support (BOS) is defined as the distance, along the x-axis of the hand-force plane, between the front and rear boundaries of the BOS.

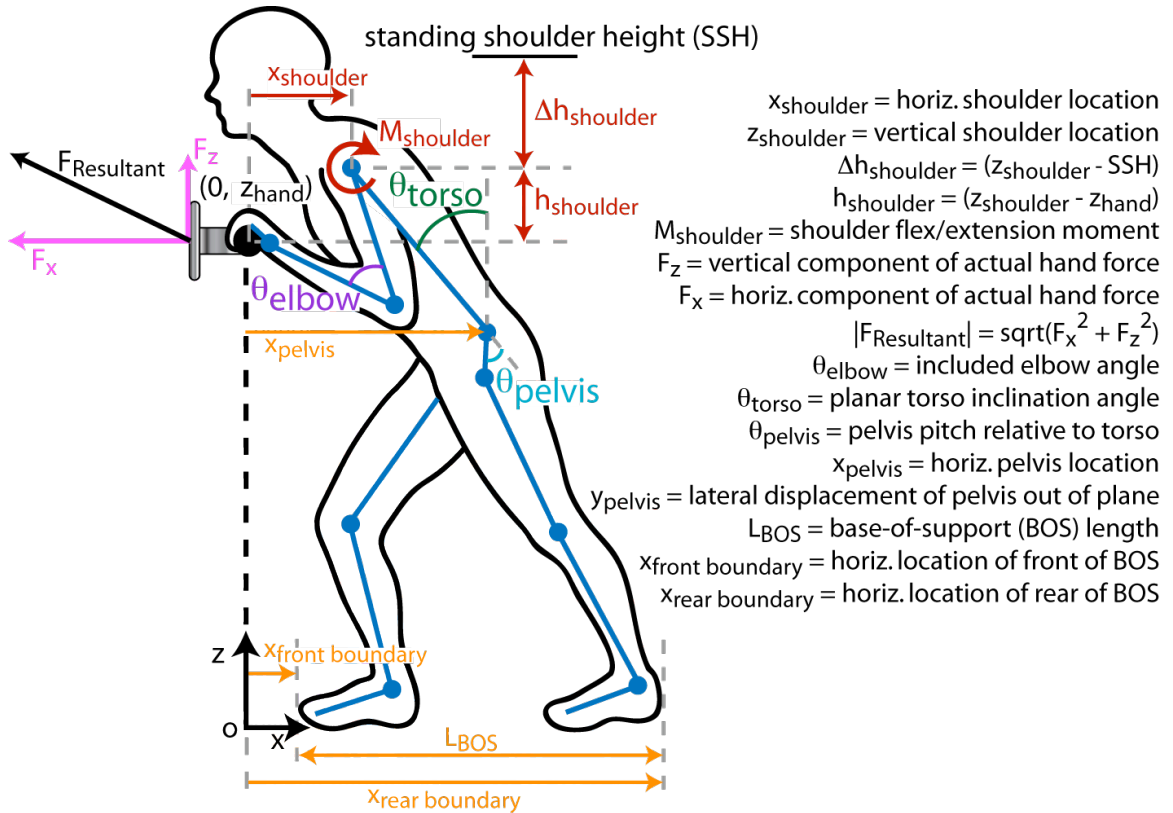


Figure 4.6. Postural metrics used to quantify whole-body postures with respect to the hand-force plane.

Statistical Analysis Approach

Analysis of data was conducted in two phases. The first phase explored trends in the data to determine if postures selected during hand force exertions were consistent with hypothesized biomechanical principles and behaviors. Results from this analysis are presented in Section 4.4. All linear and nonlinear trends presented in this section are highly significant ($p < 0.001$).

In the second phase regression models were developed to predict key postural metrics. Anthropometrics, task parameters, postural metrics, and second order interactions between covariates were considered as potential predictors. Regression models are presented in Section 4.5 and are highly significant ($p < 0.001$) as are all terms in the models. Non-significant terms were only included when second-order terms were

highly significant and inclusion of non-significant first-order terms required for a proper model. All potential predictors were added into the model and the model refined by sequentially removing the least significant covariate until only significant ($p < 0.05$) terms remained. In an effort to obtain simple models, models were further refined by, again starting with the least significant term, and removing variables contributing less than 0.02 to the adjusted R^2 value. All analyses were conducted using the JMP statistical software package (version 5.0).

4.4. Results: Posture Selection Trends

Trends in posture selection for two-handed force exertions were examined to determine if postures and postural adjustments are consistent with hypotheses. Relationships between postural metrics and the effects of task parameters on posture were investigated to test hypothesized biomechanical principles and behaviors.

Elbow Posture

Elbow angles in pushing tasks were hypothesized to follow a bimodal distribution, with most angles either fully flexed or fully extended, and the data are consistent with this hypothesis. People select between a flexed-elbow (included elbow angle < 90 degrees) and extended-elbow postural strategy (Figure 4.7). These distinct postural strategies are illustrated by the bimodal distribution of included elbow angle for two-handed pushes at elbow height. Differences in upper-extremity pushing postures across handle heights are in part captured by differences in the distribution of included elbow angle for exertions performed at each height (Figure 4.8). For exertions performed at elbow-height, a bimodal distribution is observed and supports the statement that people choose between two distinct strategies, pushing with elbows flexed versus elbows extended, with a preference towards the flexed-elbow posture (Figure 4.9). A preference (75%) towards flexed-elbow postures is also observed for push exertions at thigh-height. For overhead exertions, an extended-elbow strategy is used, due to the kinematic constraints of the handle position.

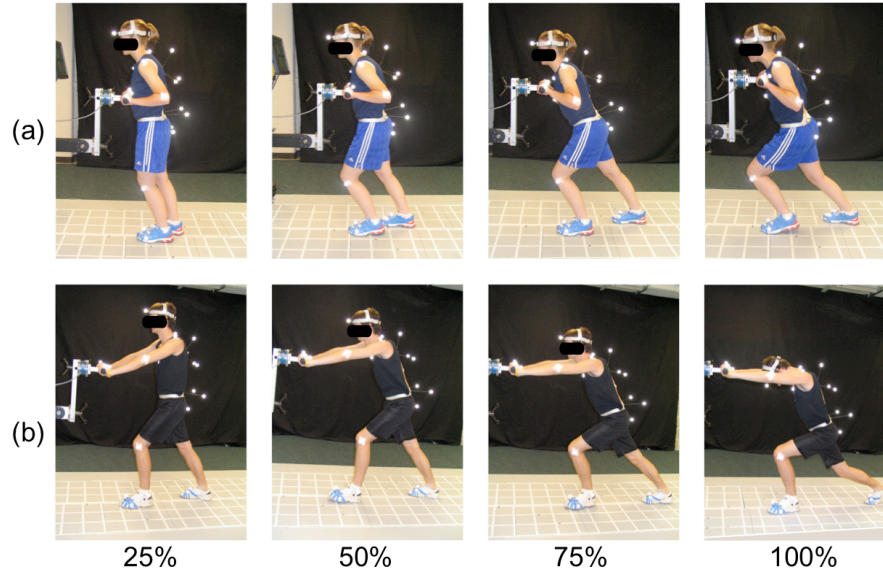


Figure 4.7. Two-handed pushing strategies: (a) elbows flexed; (b) elbows extended.

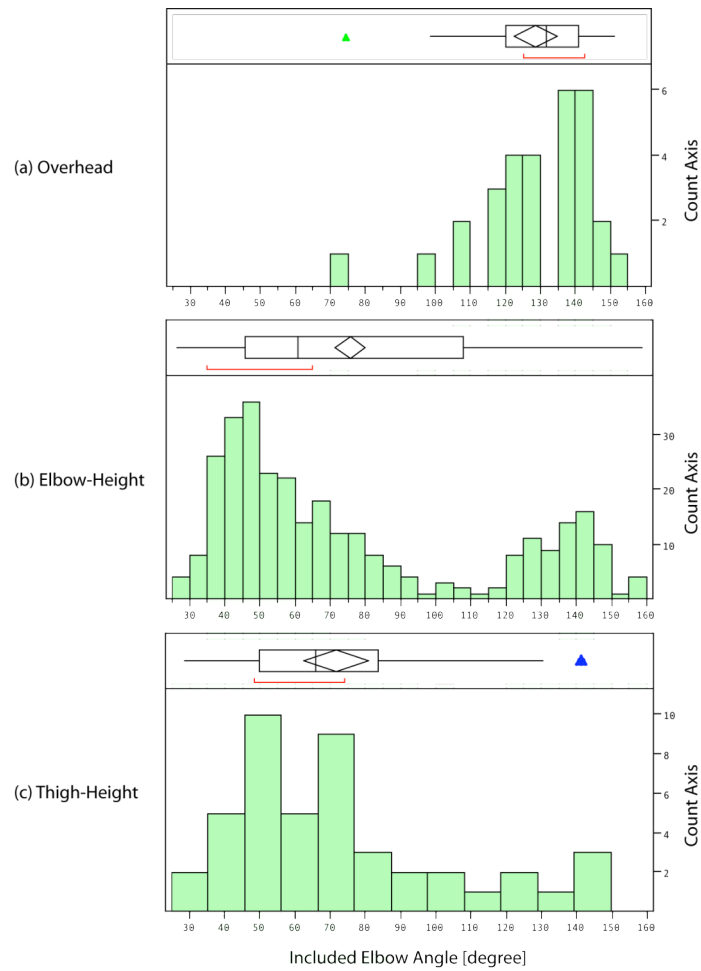


Figure 4.8. Distribution of included right elbow angle during two-handed push exertions at (a) overhead, (b) elbow, and (c) thigh-height.

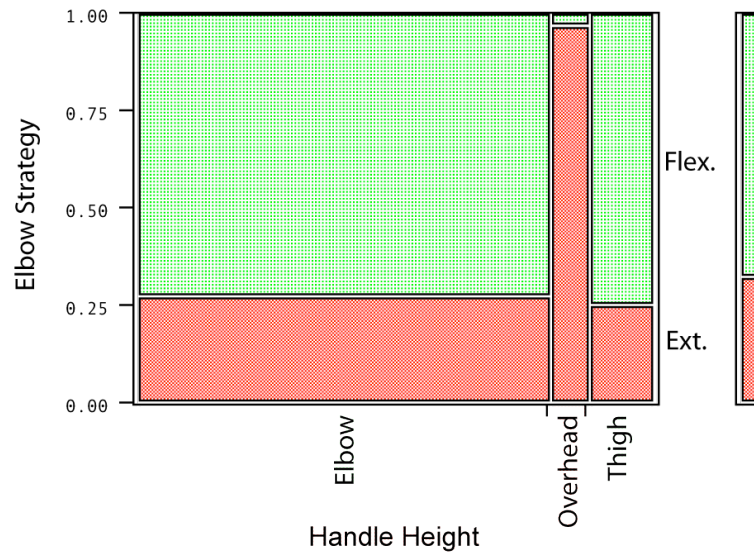


Figure 4.9. Prevalence of flexed (Flex.) and extended (Ext.) elbow pushing strategies across handle heights. A flexed elbow posture was used for 73%, 97% and 75% of push exertions at elbow, overhead, and mid-thigh handle heights.

Pull exertions are characterized by more extended elbow postures with included elbow angles greater than 90 degrees for 65% of the pulling postures analyzed (Figure 4.10). As shown in the following section, a preference towards extended-elbow pulling postures leaves subjects with two mechanisms for reducing moments about the shoulder: (1) reducing the vertical offset between the shoulder and point of force application (i.e. vertical moment arm) by lowering the shoulder (or raising it if the point of force application is above shoulder height), (2) generate significant vertical forces to direct the hand force vector towards the shoulder joint.

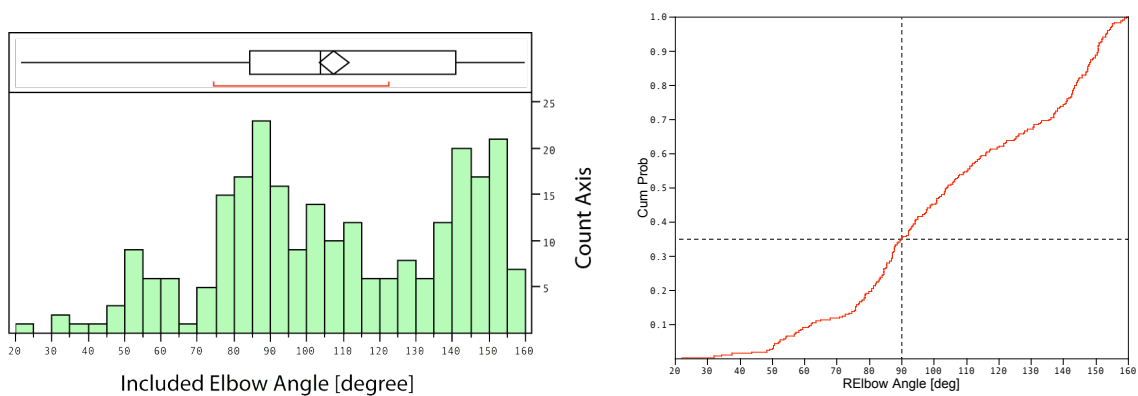


Figure 4.10. Distribution and cumulative distribution function for included right elbow angle during two-handed pulls at thigh, elbow, and overhead heights.

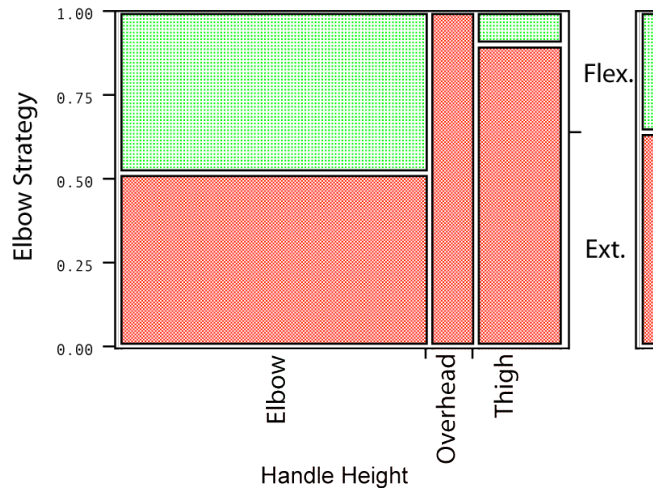


Figure 4.11. Prevalence of flexed (Flex.) and extended (Ext.) elbow postures during two-handed pulls at mid-thigh, elbow, and overhead handle height.

Effect of Shoulder Moment on Posture

Sensitivity to external shoulder moments is hypothesized to drive posture selection, leading to two behaviors: (1) generating off-axis forces to direct the hand force vector towards the glenohumeral joint center, and/or (2) altering shoulder location with respect to the point of force application to reduce the shoulder moment arm. The relationships between hand force, posture, and shoulder moment were investigated to determine if data are consistent with the hypothesized behaviors. Sensitivity to shoulder moment was quantified as changes in shoulder moment arm and force direction consistent with reducing moments about the shoulder.

Shoulder Location with Respect to Point of Force Application

Changes in shoulder location with respect to the point of force application were quantified for two-handed push/pull and up/down exertions. When pushing and pulling on a handle at or below shoulder level, people were expected to lower their shoulders as force magnitude increased. For overhead push/pull exertions the handle height prevents people from using a change in shoulder height to decrease shoulder moments. During vertical exertions, a decrease in the fore-aft location of the shoulder with respect to the point of force application is expected with increasing hand force magnitude. Changes in shoulder location were quantified by the fore-aft shoulder location (x_{shoulder}), shoulder height with respect to the point of force application (h_{shoulder}), and change in shoulder height from neutral standing height ($\Delta h_{\text{shoulder}}$). The effects of hand force on shoulder

location were first investigated for two-hand push exertions, followed by an analysis of two-handed pulls and up/down exertions. For each type of exertion the analysis was first conducted for trials performed at elbow-height and then expanded to trials performed at mid-thigh and overhead handle heights.

Elbow-height push exertions were grouped on elbow strategy and analyzed to quantify differences in shoulder location associated with selection of a flexed versus extended elbow tactic. People steadily drop their shoulder as the force magnitude increases when pushing with elbows extended resulting in a shoulder location below handle height for forces greater than approximately 50% of body weight (Figure 4.12). When pushing with a flexed-elbow posture, people lower their shoulders more gradually as force magnitude increases to approximately 60% of body weight. For forces exceeding 60% of body weight, shoulder height remains fairly constant at a height above hand height. This region of constant shoulder height corresponds to people reaching maximum elbow flexion (Figure 4.13) and is consistent with the nonlinear relationship between change in shoulder height and hand force magnitude for two-handed push exertions at elbow height. In this dataset, the flexed-elbow trend dominates since it is more prevalent (229 / 315 trials) than the extended-elbow strategy (86 / 315 trials) during push exertions at elbow height.

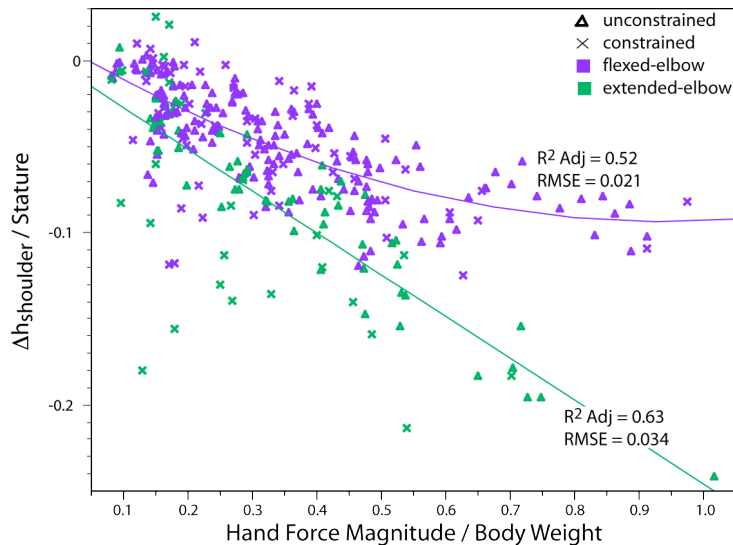


Figure 4.12. Differences in shoulder height adjustment with change in actual force (AF) magnitude when pushing at elbow-height with elbows extended (“E”) versus flexed-elbow (“F”) posture.

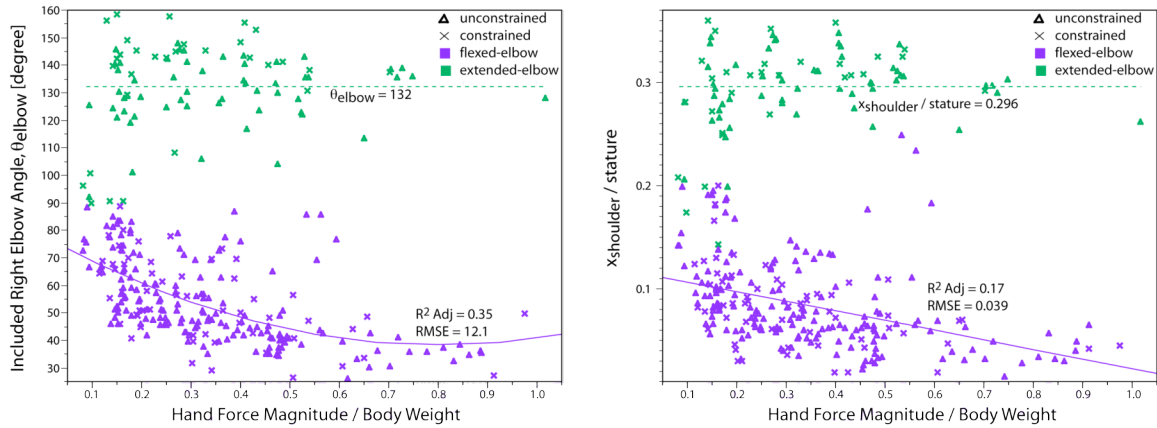


Figure 4.13. Change in included elbow angle and fore/aft distance from shoulder to point of force application with force magnitude when pushing with extended versus flexed-elbow posture.

The tendency to lower the shoulder as the level of force increases is observed across elbow and thigh-height trials for two-hand push exertions (Figure 4.14). For overhead exertions, shoulder height remains fairly constant near neutral standing shoulder height as the level of force increases. The data reflect a slightly elevated shoulder height associated with upward migration of the shoulders relative to the torso when arms are extended overhead. During overhead exertions, kinematic constraints prevent people from reducing shoulder moments by decreasing shoulder moment arm. People instead reduce the moment about the shoulder by directing the hand force vector towards the shoulder joint as illustrated in the following section. People’s reliance on this strategy in part explains why people were unable, in pilot testing, to perform high-force exertions overhead when hand force direction was constrained. For this reason only directionally unconstrained exertions were conducted at the overhead handle-height.

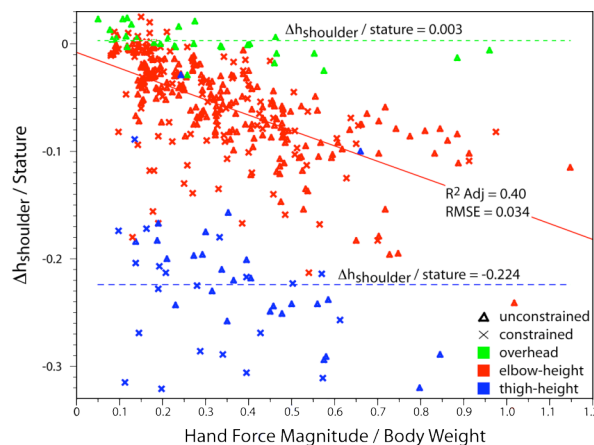


Figure 4.14. Change in shoulder height with increasing hand force magnitude during two-handed push exertions at mid-thigh, elbow, and overhead handle heights.

Similar to the trend observed for two-handed push exertions, a decrease in shoulder height with increasing hand force magnitude is also observed during two-handed elbow-height pulls (Figure 4.15).

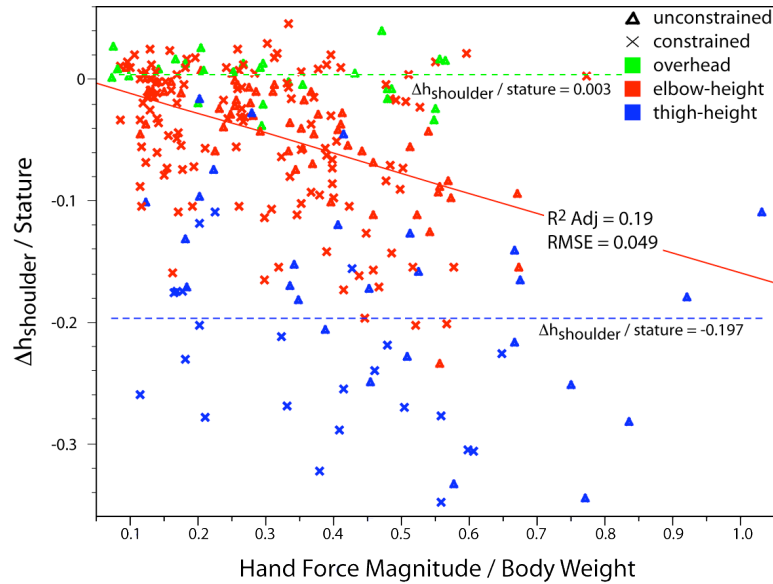


Figure 4.15. Change in shoulder height with increasing hand force magnitude during two-handed pulls at mid-thigh, elbow, and overhead handle heights.

During upward and downward exertions, people bring their shoulders toward the handle as force magnitude increases, decreasing the horizontal shoulder moment arm (Figure 4.16). When performing up/down exertions at elbow height, the fore/aft distance between the shoulder and handle remains fairly constant as force magnitude continues to increase past 60% of body weight. Downward exertions were not performed at the overhead or thigh-height handle. For upward exertions, the relationship between force magnitude and horizontal shoulder location is not significant for overhead or thigh-height exertions. When performing lifts at a low handle height people can either reach the handle by inclining their torso or standing close to the handle and maintaining a fairly upright torso posture. In the laboratory study people choose the latter approach, in some cases standing so close to the force handle that their thighs were in contact with the handle. Standing close to the handle was preferred over forward inclination of the torso for all force levels (consistent with biomechanical principle 3), which explains why force magnitude does not affect fore/aft shoulder location when lifting at thigh-height (Figure 4.17).

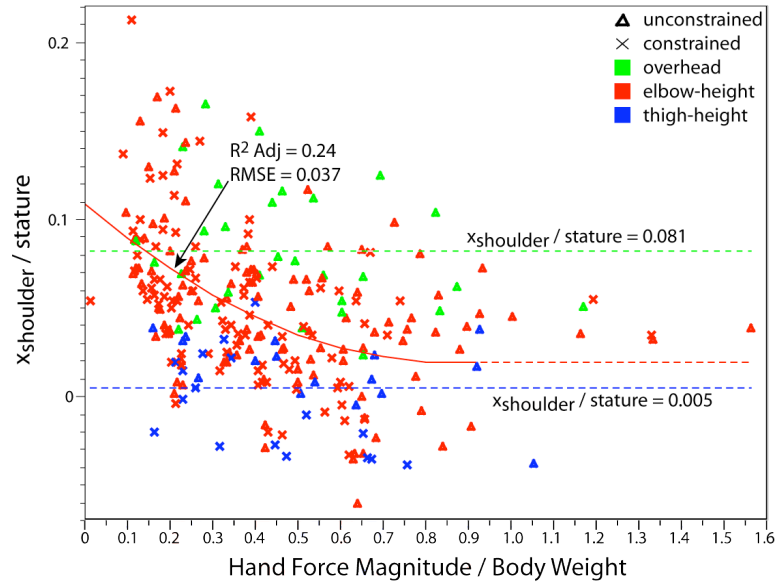


Figure 4.16. Change in fore/aft shoulder location with increasing hand force magnitude during up/down exertions at thigh, elbow, and overhead handle heights.

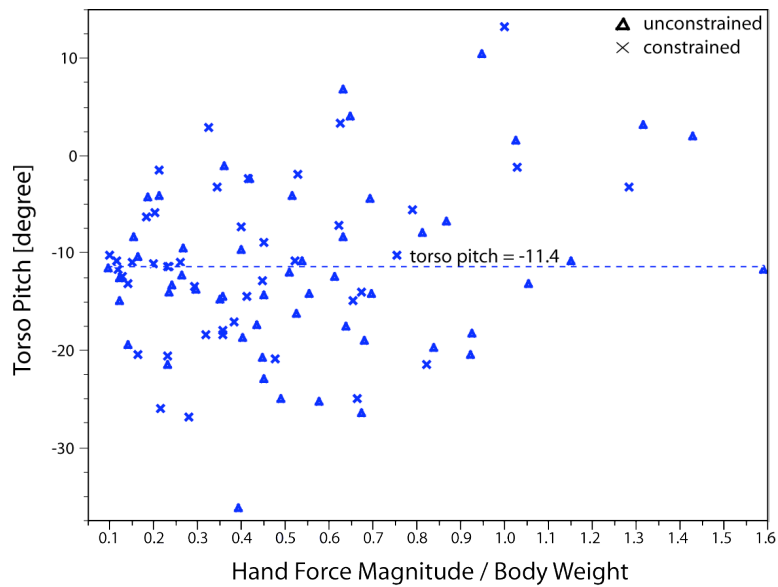


Figure 4.17. Torso pitch during thigh-height upward exertions.

For up/down exertions at elbow-height, shoulder height increases or decreases as a function of increasing force magnitude depending on which gross postural strategy people select. If pulling up or pushing down people locate their shoulders over the point of force application by decreasing the fore/aft distance between their shoulder and hands and raising their shoulders up over the handle. For downward exertions a significant relationship is not found between shoulder height and force magnitude suggesting that

people maintain an elevated shoulder location regardless of force level when pushing down. If pushing up or pulling down from underneath the handle people move closer to the handle while simultaneously dropping their shoulder to get under the handle and use their legs to generate the required upward force. A pull down strategy was used for only a small subset of the two-hand down trials (9 / 105) thus this strategy was not analyzed. Change in shoulder height with increasing force level is not significant for overhead or thigh-height upward exertions.

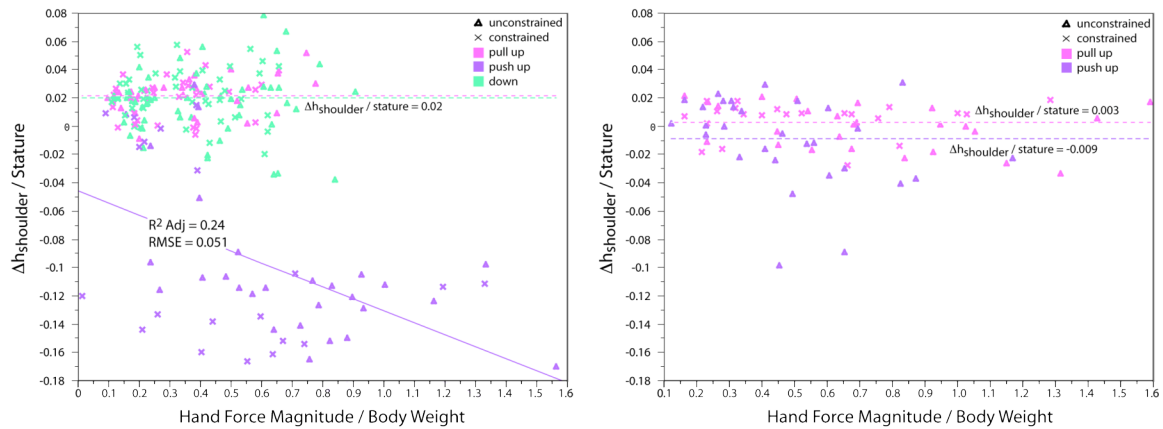


Figure 4.18. Relationship between change in shoulder height from neutral and hand force magnitude during elbow-height vertical up/down exertions (left) and thigh-height and overhead up exertions (right).

Relationship Between Off-Axis Forces and Posture

When hand force direction is unconstrained push/pull forces have a significant vertical component as quantified in Chapter 3. Comparison of force direction and the magnitude of vertical forces generated during two-handed push exertions at elbow height indicates that people generate larger vertical forces when pushing with flexed elbows. Vertical force increases as hand force magnitude increases, increasing more gradually for exertions performed with an extended-elbow posture than those performed with elbows flexed. When pushing with elbows extended the vertical force component is directed downward for low force exertions, corresponding to a shoulder location above the handle. For forces exceeding approximately 50% of body weight the vertical component is directed upward and the shoulder drops to or below the handle height.

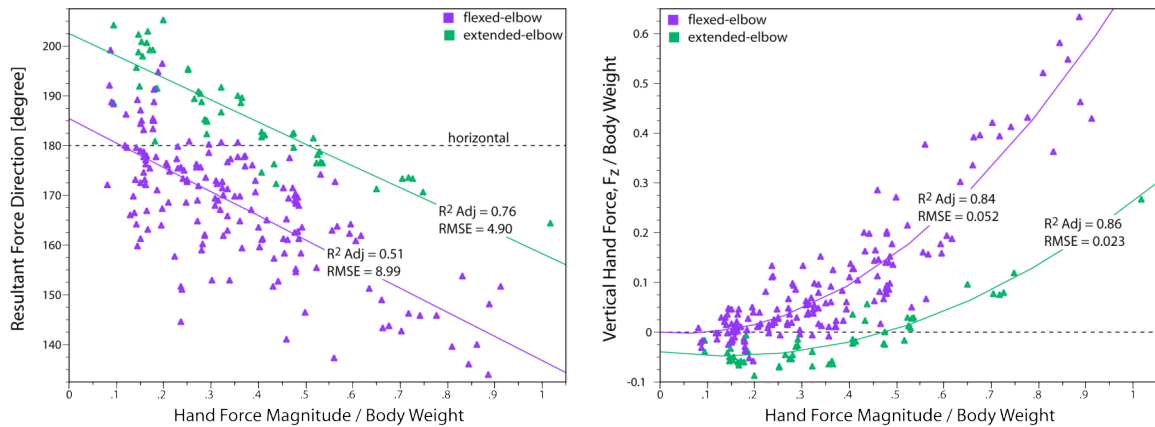


Figure 4.19. Relationship between magnitude and direction of resultant hand force vector and vertical force component during directionally unconstrained two-handed elbow-height push exertions performed with flexed versus extended elbow strategy.

Due to the kinematic constraint, an extended elbow posture is used for all overhead exertions. When pushing with elbows extended people can reduce moments about the shoulder by reducing the vertical offset between the point of force application and shoulder (i.e. the vertical moment arm) or generating a vertical force component to direct the hand force vector towards the shoulder. For overhead exertions, kinematics limit people's ability to reduce the vertical moment arm. This is reflected in significantly larger vertical hand forces when pushing overhead as compared to pushing with an extended elbow posture at elbow or thigh-height. Figure 4.20 shows data for unconstrained push exertions with extended elbow posture.

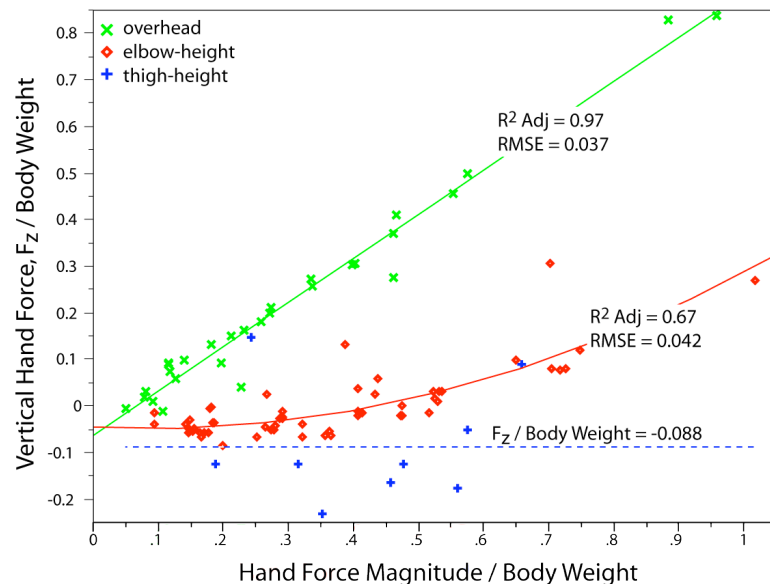


Figure 4.20. Vertical off-axis forces generated during directionally unconstrained two-handed push exertions performed at thigh, elbow, and overhead handle heights.

As with pushing, when pulling overhead people reduce the moment about the shoulder by generating a significant downward force that acts to direct the hand force vector towards the shoulder joint (Figure 4.21).

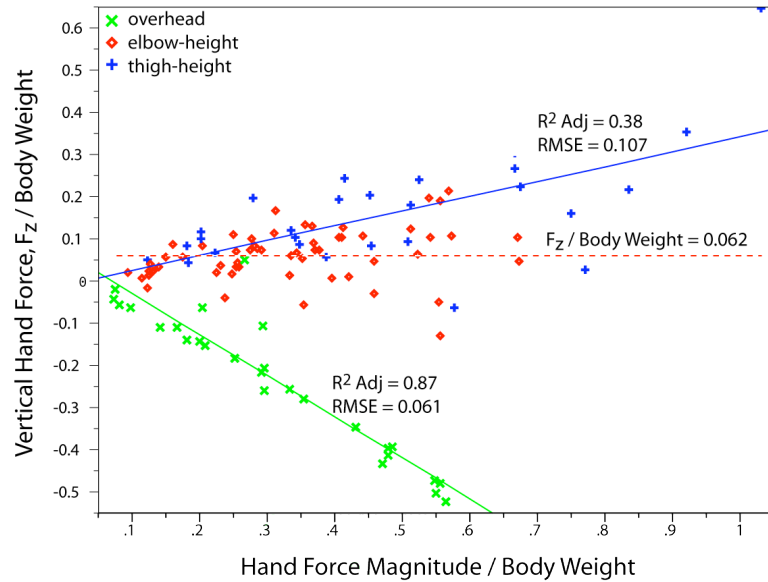


Figure 4.21. Vertical off-axis forces generated during directionally unconstrained two-handed pulls performed at thigh, elbow, and overhead handle heights.

Interaction Between Shoulder Location and Off-Axis Forces

An increase in force magnitude results in a larger drop in shoulder height during elbow-height pulls than when pulling at thigh-height. This drop in shoulder height coupled with a non-significant increase in vertical forces with increasing force magnitude (Figure 4.21) suggests that when pulling at elbow height lowering the shoulder is people's primary strategy for reducing shoulder moments.

The relationship between hand force magnitude and vertical hand force component is stronger for thigh-height pulls than elbow-height pulls, suggesting people are directing the hand force vector towards the shoulder to reduce shoulder moments. A drop in shoulder height also occurs during thigh-height pulls as the level of force increases suggesting people are also acting to minimize the shoulder moment by reducing the vertical offset between the shoulder and point of force application. However, when shoulder height is examined across all (directionally constrained and unconstrained) thigh-height pulls the change in shoulder height with increasing force level is highly variable (Figure 4.22). Closer inspection of these trials reveals a significant difference in the change in shoulder height with increasing hand force magnitude between

directionally unconstrained and constrained exertions. A smaller drop in shoulder height is observed during unconstrained exertions, suggesting people prefer not to lower their shoulder more than is required to successfully complete the task (i.e. satisfy the constraints on hand force magnitude & direction). This trend is consistent with the proposed tradeoff between maintaining a neutral torso posture and reducing shoulder moment.

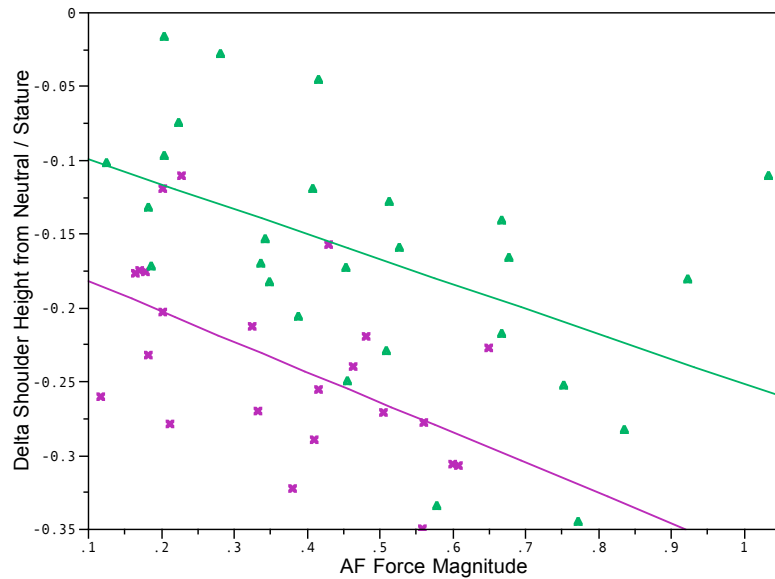


Figure 4.22. Comparison of change in shoulder height from neutral with actual hand force (AF) magnitude across directionally constrained (✕) versus unconstrained (▲) thigh-height pulls.

Higher shoulder locations during unconstrained pull exertions at thigh-height are associated with larger vertical hand force components (Figure 4.23). This suggests that people are willing to generate a larger hand force than requested rather than lower their shoulders to decrease the shoulder moment. Differences in shoulder moment across unconstrained and directionally constrained pulls at thigh-height are small indicating that when force direction is unconstrained people choose to generate an additional vertical force component to direct the hand force vector towards the shoulder instead of reducing shoulder moment by dropping the shoulder to decrease the moment arm (Figure 4.24). As was the case with thigh-height pulls, a higher shoulder location is associated with a larger upward vertical hand force component when pulling at elbow height (Figure 4.25).

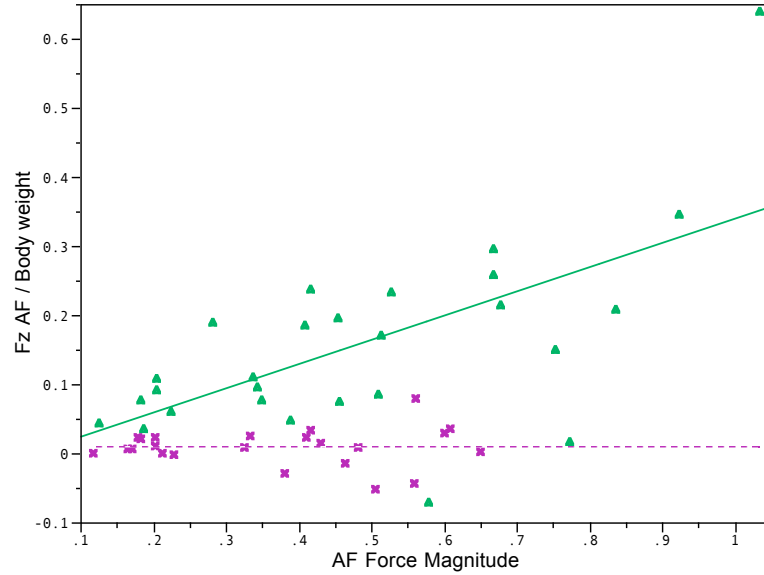


Figure 4.23. Actual vertical off-axis forces (F_z AF) expressed as a fraction of body weight generated during directionally constrained (x) versus unconstrained (\blacktriangle) thigh-height pulls. An increase in vertical off-axis force with increasing actual hand force (AF) magnitude is observed for unconstrained trials.

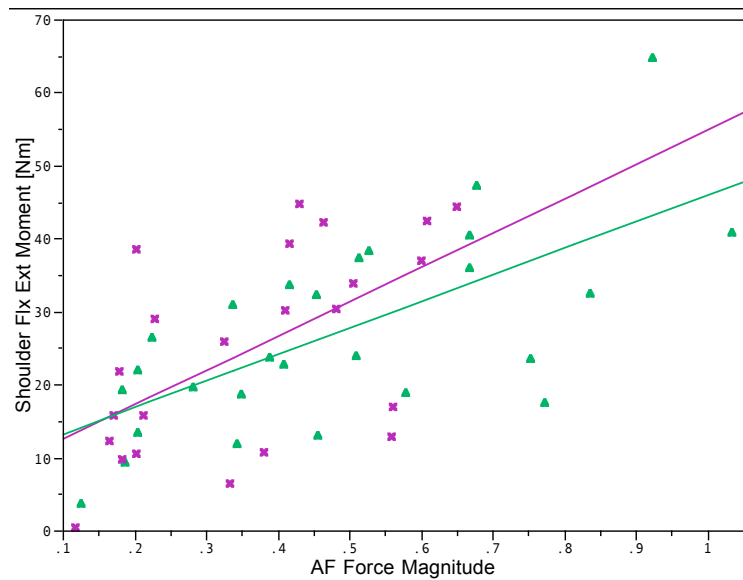


Figure 4.24. Comparison of shoulder flexion/extension moments across actual hand force (AF) magnitude during directionally constrained (x) versus unconstrained (\blacktriangle) thigh-height pulls.

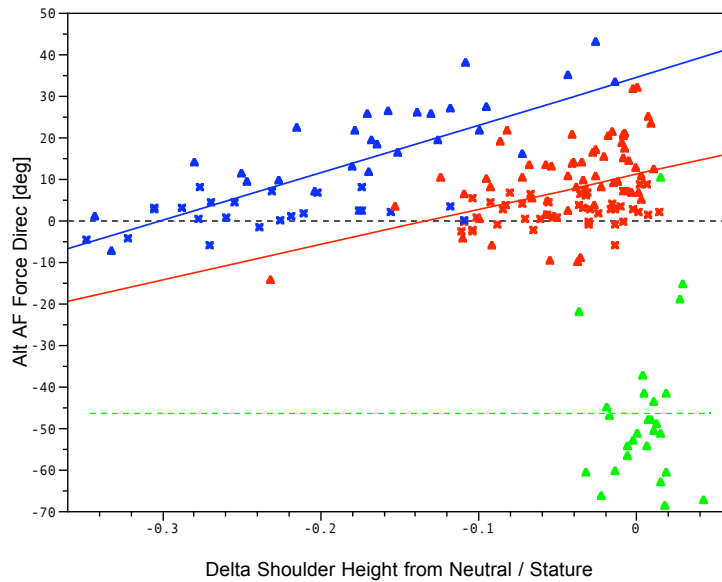


Figure 4.25. Change in actual hand force (AF) direction with change in shoulder height from neutral during two-handed pulls performed at mid-thigh (blue), elbow (red), and overhead (green) handle heights.

During overhead upward exertions people reduce shoulder moments by directing the hand force vector towards the shoulder joint as opposed to decreasing the moment arm (Figure 4.26).

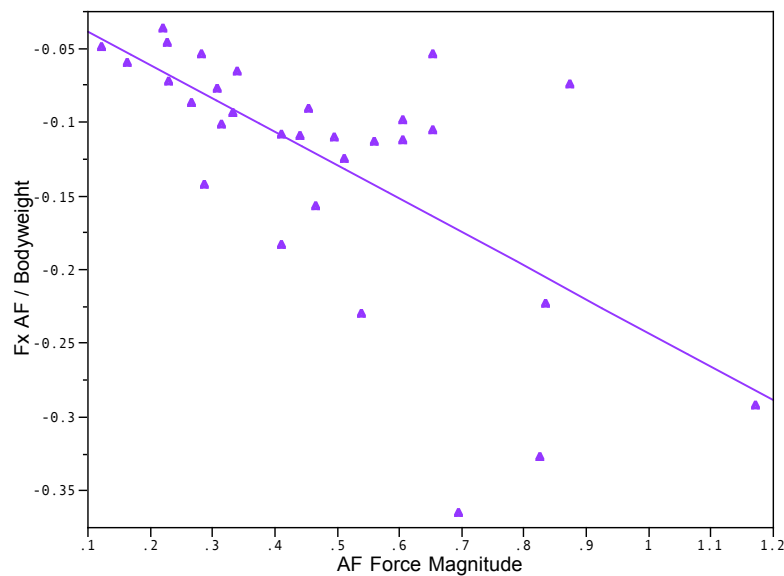


Figure 4.26. Actual horizontal off-axis forces (F_x AF) normalized to body weight generated during overhead upward exertions. An increase in horizontal off-axis force with increasing actual hand force (AF) magnitude is observed.

Level of Acceptable Shoulder Moment

Shoulder flexion/extension moment was computed as the average of the right and left shoulder moments. Shoulder extension moments are defined positive and shoulder

flexion moments negative where extension of the shoulder corresponds to raising the arm, in the sagittal plane, from a resting posture from along side the torso to overhead. Exerting a forward hand force with the hand in the neutral standing posture (hand hanging down) is a positive (flexion) moment.

Change in shoulder flexion/extension moment with hand force was analyzed for two-hand elbow-height pushes performed using a flexed-elbow strategy. The leftmost plot (Figure 4.27) shows that large vertical forces generated during unconstrained push exertions do not result in significant increases in shoulder flexion/extension moment when pushing with flexed elbows. This supports the proposition that a flexed elbow strategy allows people to generate large vertical forces without generating a large flexion/extension moment at the shoulder.

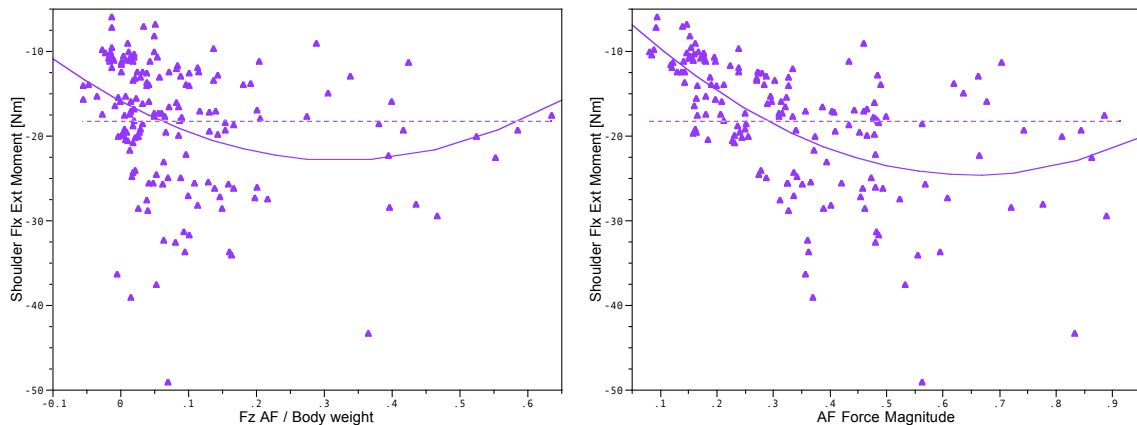


Figure 4.27. Change in shoulder flexion/extension moment with actual vertical hand force (F_z AF) and magnitude of resultant hand force vector, both normalized by body weight, for two-handed elbow-height pushes performed with a flexed-elbow strategy.

When pushing at elbow height with flexed or extended elbows, increasing force magnitude results in increasing shoulder flexion moments for push forces up to approximately one-half of body weight (Figure 4.28). As force magnitude continues to increase, on average, shoulder moments remain at or below a threshold of approximately 25 Nm of flexion with flexion moments of less than 30 Nm for 90% of elbow-height push exertions (Figure 4.29). Lowering the shoulder as the magnitude of requested hand force increases acts to maintain the shoulder moment below approximately 25 Nm (Figure 4.30).

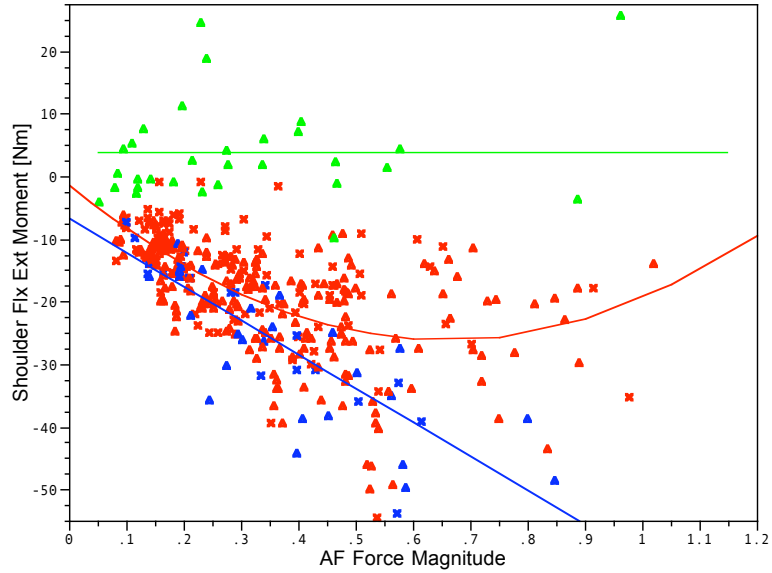


Figure 4.28. Change in shoulder flexion/extension moment with actual hand force (AF) magnitude for two-handed push exertions performed at mid-thigh (blue), elbow (red), and overhead (green) heights.

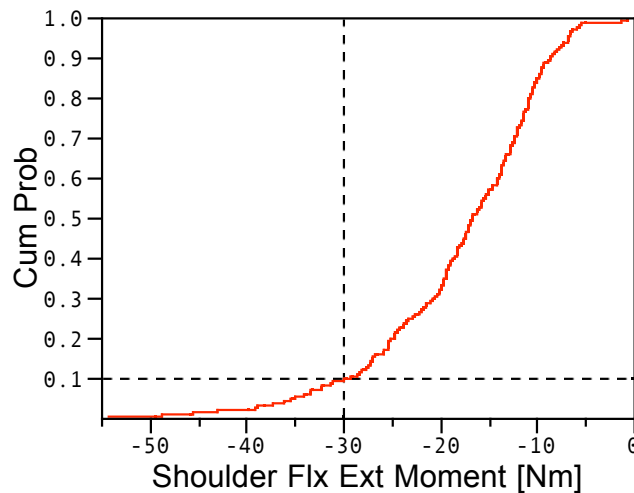


Figure 4.29. Cumulative distribution function for two-handed elbow-height pushes showing shoulder flexion moments are less than 30 Nm for 90% of trials.

Figure 4.30 shows the effectiveness of change in shoulder height for maintaining a stable moment during push exertions. Subject-specific relationships between shoulder moment and change in shoulder height do not show significant nonlinear trends but instead most show linear trends with different slopes. The combined data set suggests a nonlinear fit illustrating how pooling of subject data can mask what is really going on in the data. For this reason subject-specific trends were examined to verify that the significant trends were qualitatively similar to those observed in the individual subject's data.

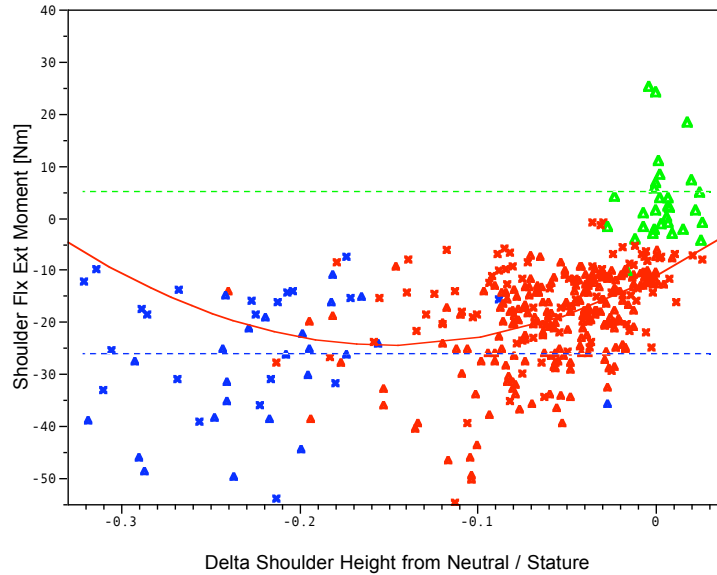


Figure 4.30. Relationship between shoulder flexion/extension moment and change in shoulder height from neutral standing height during two-handed thigh (blue), elbow (red), and overhead (green) push exertions.

Unlike exertions at elbow height, a significant relationship is not found between change in shoulder height and shoulder joint loads for push exertions overhead or at thigh-height. As previously discussed, a reduction in shoulder moment via a change in shoulder height is not kinematically feasible for exertions overhead. Alternatively, directing the hand force vector towards the shoulder during overhead push exertions maintains the shoulder moment at approximately 4 Nm of extension, on average, across exertions of increasing force magnitude (Figure 4.28).

For thigh-height exertions the trade-off between reducing shoulder moment and lowering the shoulder (by squatting or inclining the torso) is illustrated by the tendency to tolerate larger moments at the shoulder when pushing at thigh-height (Figure 4.30). However, despite larger flexion moments during thigh-height push exertions, in approximately 88% of all two-handed push exertions, shoulder flexion/extension moments do not exceed 30 Nm. This finding suggests that when pushing people alter their posture and/or the direction of the hand force vector to maintain shoulder moments below 30 Nm.

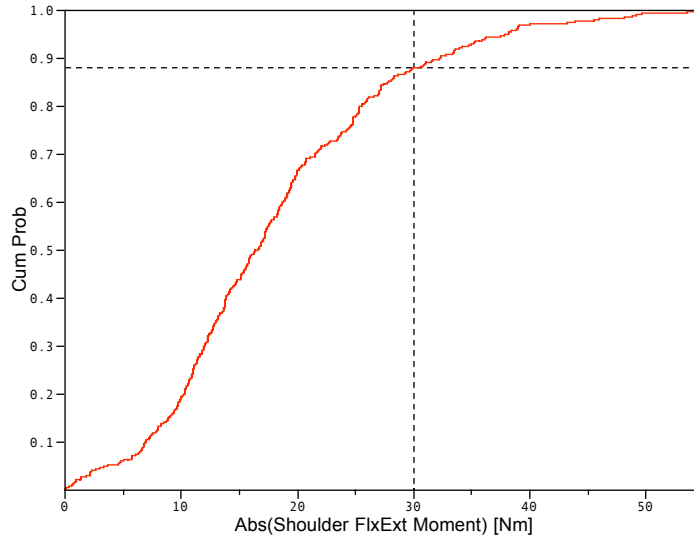


Figure 4.31. Cumulative distribution of magnitude of shoulder flexion/extension moments during two-handed push exertions at thigh, elbow, and overhead handle height.

Generating a downward force component during overhead pulls directs the hand force vector towards the shoulder and keeps the shoulder moment at approximately 10 Nm of flexion, on average, despite increasing force magnitude (Figure 4.32). For elbow and thigh-height pulls, an increase in force level results in increasing shoulder extension moments.

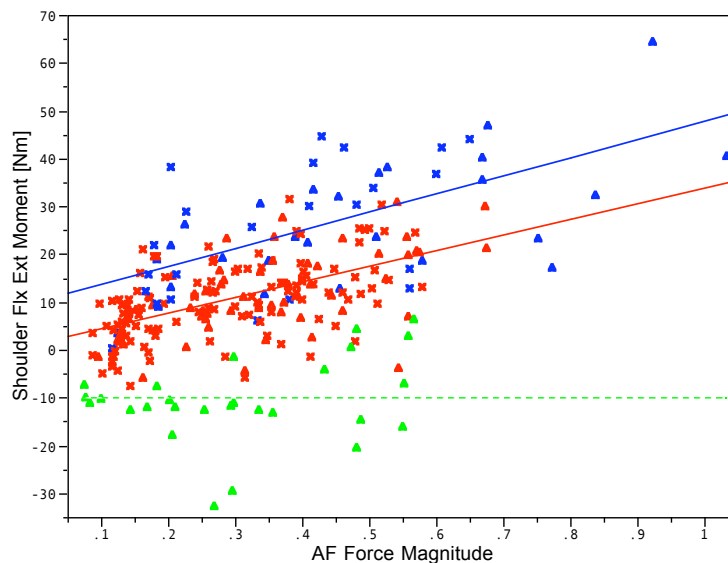


Figure 4.32. Change in shoulder flexion/extension moment with increase in actual magnitude of two-hand pull force (AF) for trials performed at mid-thigh (blue), elbow (red), and overhead (green) handle heights.

For pull exertions at elbow height, either flexion or extension shoulder moments are observed depending on whether subjects exert a downward or upward vertical force

component, respectively. For this reason the absolute value of external shoulder moment was used to generate the cumulative distribution function (Figure 4.33). For two-handed pulls at elbow height 90% of the trials result in shoulder moments equal or less than approximately 22 Nm. Higher shoulder moments are tolerated during thigh-height pulls with only 58% of trials having shoulder moments less than or equal to 30 Nm. To account for 90% of trials a shoulder moment criterion of approximately 42.5 Nm is required.

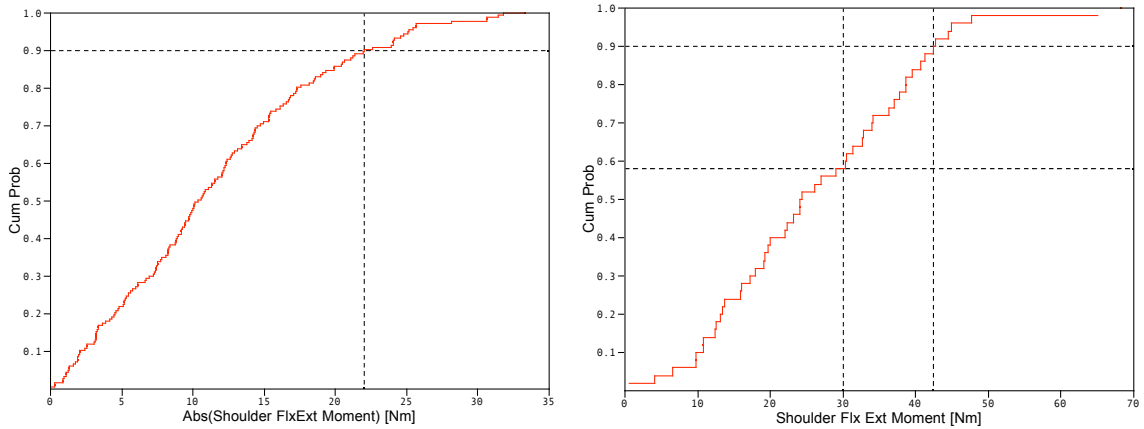


Figure 4.33. Cumulative distribution function for magnitude of shoulder flexion/extension moments during elbow-height (leftmost) and thigh-height (rightmost) pull exertions.

Shoulder moments were less than or equal to 33 Nm for 90% of all up/down trials (Figure 4.34). By decreasing the fore-aft distance from their shoulder to point of force application people are successful at keeping the shoulder moment below an acceptable level (Figure 4.35).

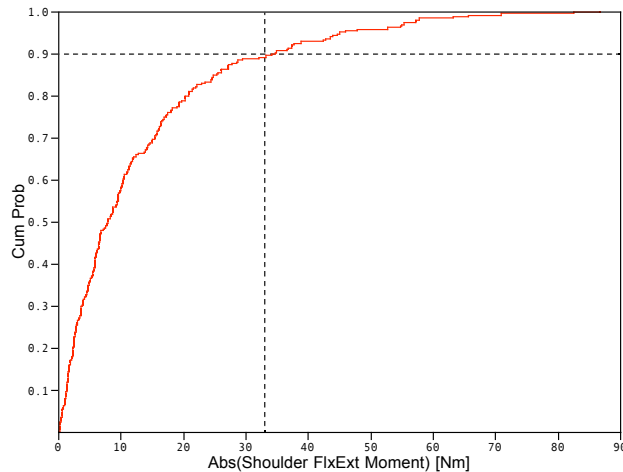


Figure 4.34. Cumulative distribution function of magnitude of shoulder moment during two-handed up down exertions showing shoulder moment is less than or equal to 33 Nm in 90% of all trials.

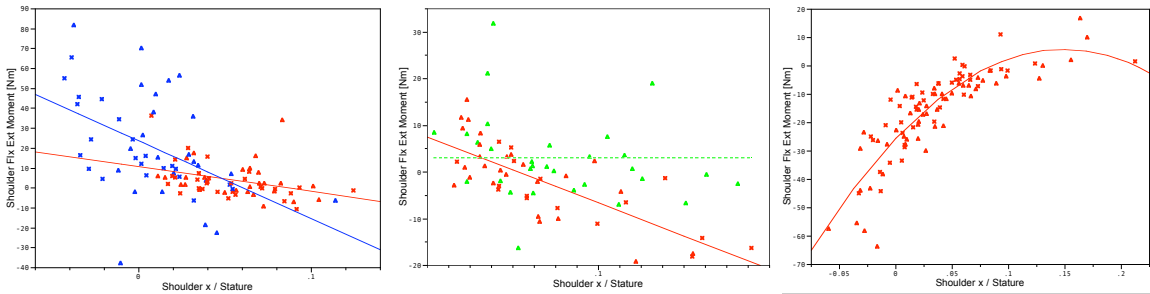


Figure 4.35. Relationship between shoulder moment and fore-aft shoulder location during pull-up (leftmost), push-up, and push-down (rightmost) vertical exertions.

Foot Placements during Two-Handed Force Exertions

During push and pull exertions the rear and front boundaries of the base-of-support, respectively, are considered the active boundary of the base-of-support. It is hypothesized that the rear foot when pushing and lead foot when pulling can be positioned with respect to the pelvis by assuming the center-of-pressure to lie on the active boundary of the BOS and computing the center-of-pressure location required for the posture to be in static balance. Given the location of the active boundary, placement of the passive foot can be determined by predicting the length of the base-of-support, which is hypothesized to increase with increasing push/pull force. The relationships between hand force and base-of-support length were examined for push/pull and up/down exertions. No relationship was found between hand force and BOS length during up/down exertions but hand force was found to have a significant effect on BOS during push/pull exertions.

Effect of Hand Force on BOS Length during Push Exertions

When pushing at mid-thigh and elbow-height a significant relationship is observed between BOS and push force which supports the hypothesis that BOS length increases with increasing hand force magnitude (Figure 4.36). Figure 4.37 suggests that the fore-aft distance along the x-axis of the hand-force frame from pelvis to the rear boundary of the BOS is a strong predictor of BOS length for push exertions at all three handle heights.

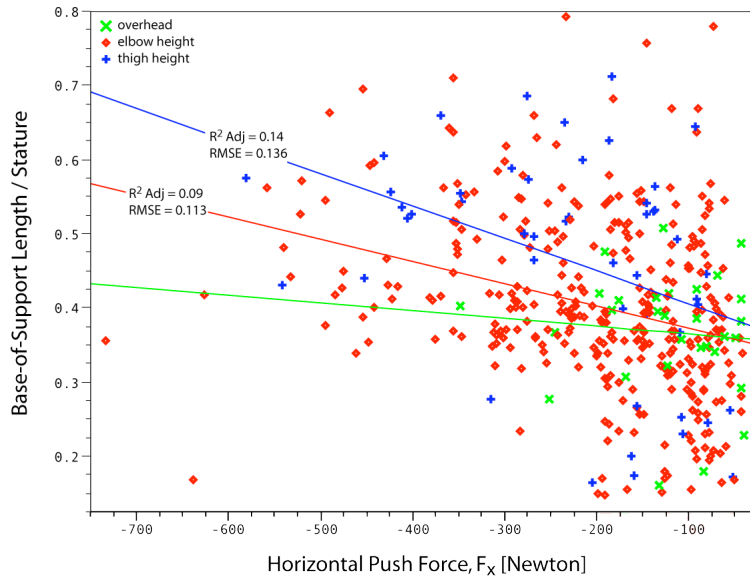


Figure 4.36. Lengthening of base-of-support with increasing push force. Linear relationship between horizontal push force and length of base-of-support is highly significant ($p < 0.01$) for two-handed push exertions at mid-thigh and elbow height. Relationship is not significant for overhead exertions.

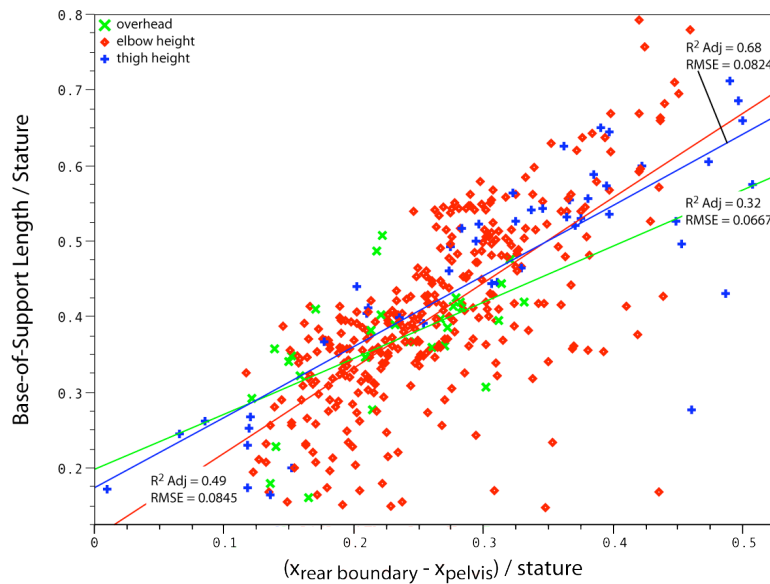


Figure 4.37. Length of base-of-support versus fore-aft distance from rear boundary of base-of-support to pelvis, both normalized by stature, for two-handed push exertions. For each handle height, linear relationship is highly significant ($p < 0.01$).

Comparison on mean offsets between the active boundary and pelvis across handle heights using the Tukey-Kramer HSD test for an alpha of 0.05 indicates that mean offsets are significantly different across handle heights (Figure 4.38). On average, the offset is largest when pushing at thigh-height and smallest during overhead exertions. Mean torso inclination angles are also significantly different when pushing at thigh,

elbow, or overhead handle heights with greater torso flexion during thigh-height push exertions (Figure 4.39).

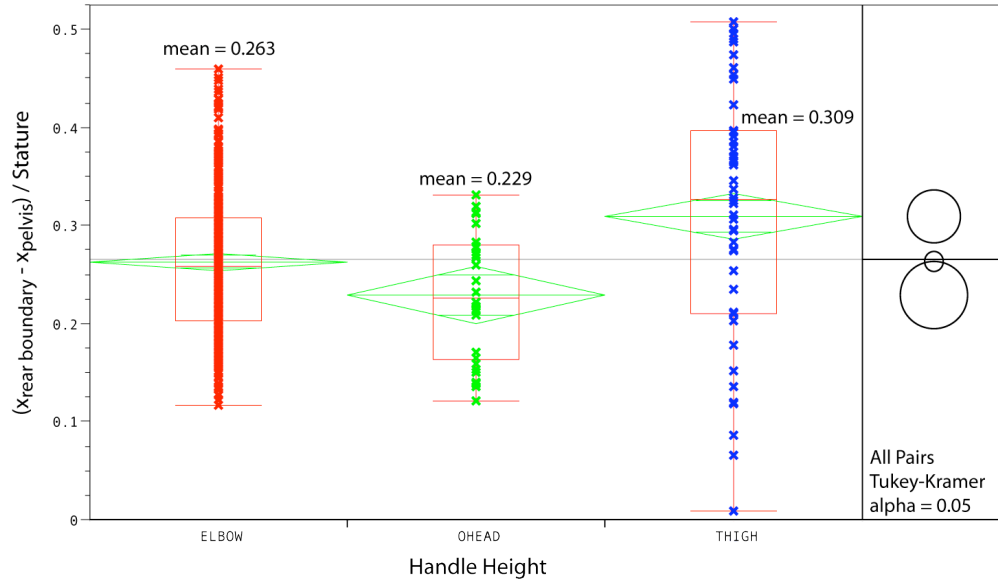


Figure 4.38. Fore-aft distance from rear boundary of base-of-support to pelvis, normalized by stature, for two-handed push exertions. Average offset for thigh-height push exertions is significantly different from mean offsets at elbow and overhead heights for alpha = 0.05.

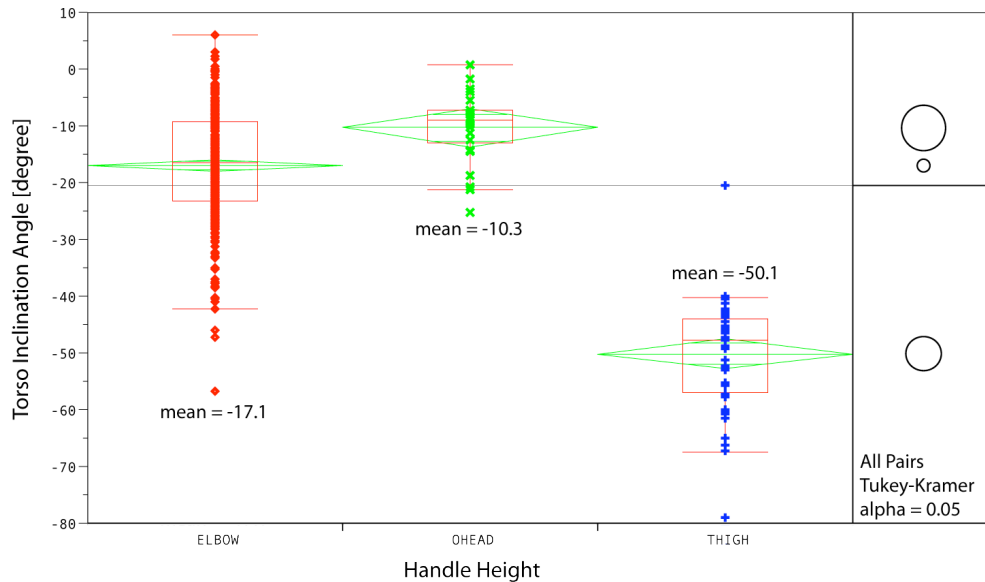


Figure 4.39. Mean torso inclination angle at each handle height during two-handed push exertions. On average, torso inclination angle is significantly different at each handle height for alpha = 0.05 with large forward flexion during thigh-height exertions and more upright torso posture during overhead trials.

Effect of Hand Force on BOS Length during Pull Exertions

As noted in the methods section a subset of high-force two-handed pulls were performed using a parallel stance. These trials were identified and excluded from the

analysis since this risky behavior was less common than the more conservative split-stance strategy for high-force pull exertions. The risky behaviors, though excluded from the analysis, are shown in grey in Figure 4.40.

As with pushing, the length of the base-of-support was also found to increase with increasing force magnitude during pull exertions (Figure 4.40). The relationship is highly significant at all three handle heights and is well predicted by the fore-aft offset from the pelvis to the front boundary of the BOS (Figure 4.41).

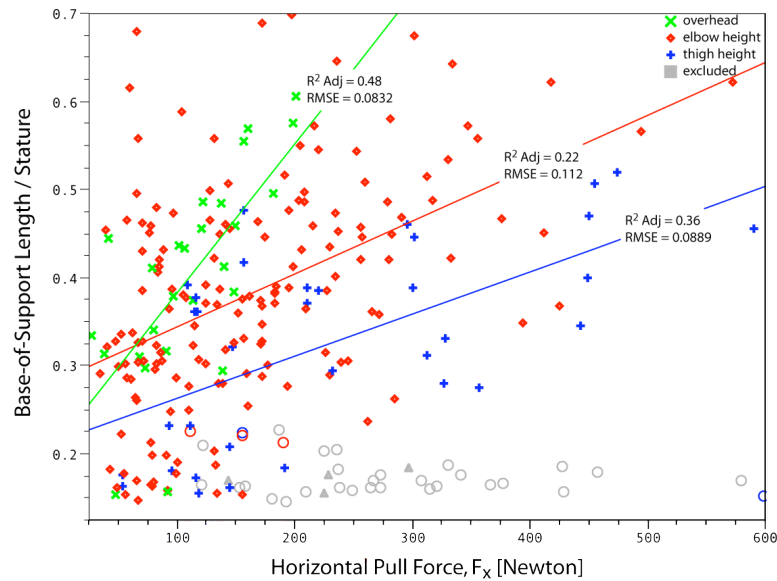


Figure 4.40. Lengthening of base-of-support with increasing hand force during two-handed pulls at mid-thigh, elbow, and overhead handle heights. Linear relationships are highly significant ($p < 0.01$). Grey markers denote high-force exertions performed with parallel stance identified as outliers and excluded from analysis.

The relationship between the distance from pelvis to front boundary of the BOS and length of the BOS at thigh-height pulls has a significant offset from the relationships at elbow and overhead heights. For a given BOS length, the offset between pelvis and the active edge of the BOS is larger during thigh-height exertions (Figure 4.42). The offset from the front boundary of the BOS to the whole-body center-of-mass location was however not found to be significantly different across handle heights. This can be explained by the significant difference in torso inclination for pulls at thigh-height compared to pulls at elbow or overhead heights. Significantly more forward torso inclination is observed when pulling at a low handle-height. Forward torso inclination shifts the center-of-mass (COM) forward countering the rearward shift in COM

associated with the larger offset between the pelvis and front boundary of the BOS. The canceling out of these effects explains why whole-body COM location with respect to the front boundary of the BOS is not significantly different when pulling at a mid-thigh, verses elbow, or overhead handle height.

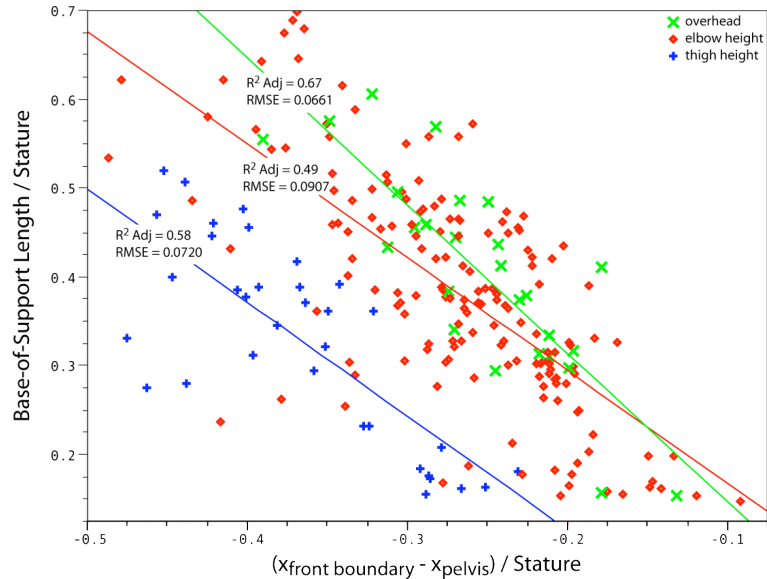


Figure 4.41. Length of base-of-support versus fore-aft distance from front boundary of base-of-support to pelvis, both normalized by stature, for two-handed pull exertions. For each handle height, linear relationship is highly significant ($p < 0.01$).

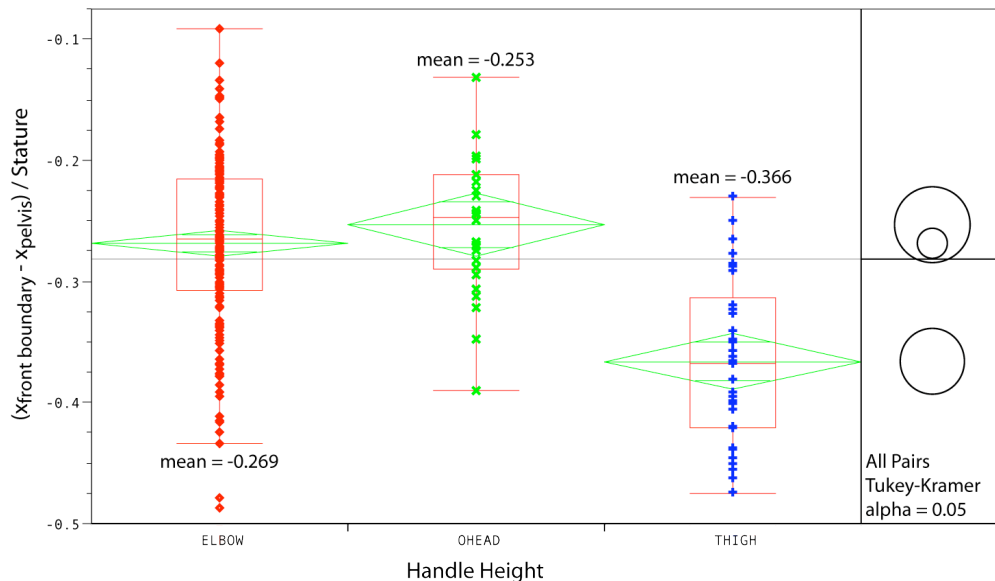


Figure 4.42. Mean fore-aft distance from front boundary of base-of-support to pelvis for two-hand pulls performed at mid-thigh, elbow, and overhead heights. On average, the fore-aft offset during thigh-height trials is significantly different from offsets during elbow and overhead exertions ($p < 0.01$).

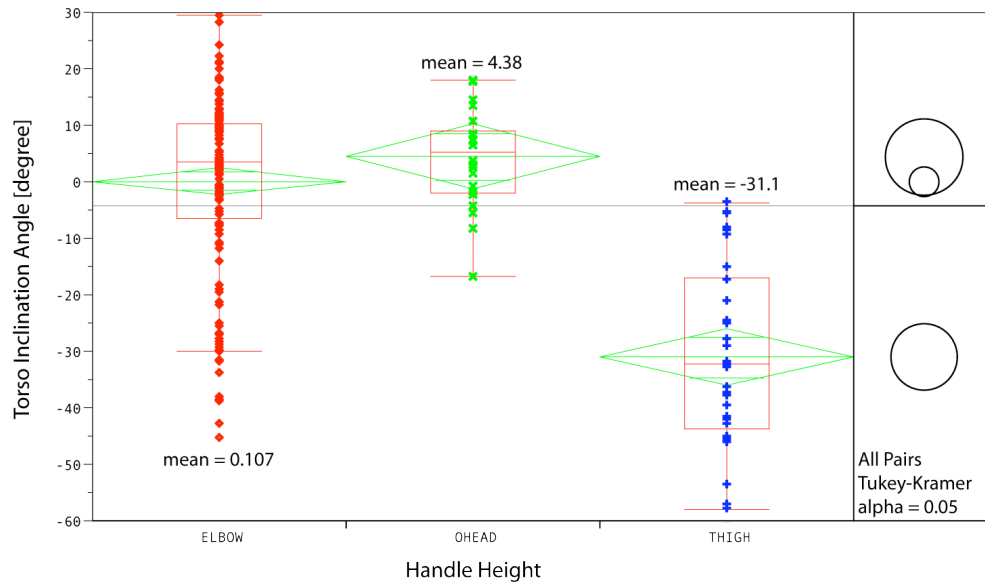


Figure 4.43. Mean torso inclination angle during two-hand pulls at mid-thigh, elbow, and overhead handle heights. Torso inclination angle is significantly different for thigh-height exertions, as compared to elbow and overhead exertions, for $\alpha = 0.05$.

4.5. Results: Regression Models

The preceding section demonstrated that the postural adaptations to hand force magnitude and direction are consistent with the biomechanical principles and hypothesized behaviors outlined at the beginning of this chapter. These observations guided the formulation of regression models to predict key postural variables. Although many possible regression models could be created, the choices of both dependent and independent variables were guided by the structure of the overall posture prediction model that is presented in Chapter 6. In particular, the sequence of computations in the prediction algorithm meant that certain variables could be predictors of others, but not vice versa. The choices of predictors in the regression models are not meant to imply causality, but rather associations that could be exploited to perform accurate, generalizable posture prediction.

The organization of this section parallels the computation sequence in the general posture prediction model presented later in Chapter 6. A shoulder flexion/extension moment target value, effectively the moment that a person is willing to generate, is computed as a function of force magnitude and shoulder position. Torso inclination is predicted as a function of shoulder position relative to the handle and the neutral position. Lumbar spine flexion (represented as pelvis inclination relative to torso inclination) is

predicted from handle position. Finally, the length of the base of support is predicted from the pelvis position and horizontal force.

In most cases, parsimonious models with fewer predictors were chosen over more complex models that provided slightly better fit. In general, the models presented here have adjusted R^2 values within 0.05 of the best model attainable.

Considerable analysis was conducted to determine when it was appropriate to produce separate models for different types of exertions. When the exertions represented qualitatively different behaviors that could not be well captured by a single model, separate regressions were performed. For example, separate models are presented for torso inclination in pushes, pulls, and up/down exertions.

Shoulder Moment Target Value

Relationships between posture and shoulder moment presented in the preceding section suggest that shoulder moment can be used to predict force exertion postures. Tightness of data within trial types suggests that once the postural tactic is known, the shoulder moment can be well predicted. Shoulder location with respect to the point of force application, quantified by h_{shoulder} and x_{shoulder} , (Figure 4.44) was found to capture the effect of postural strategy on the shoulder moments, thus these variables were considered as covariates in lieu of developing separate regression models for each postural tactic. Additional covariates considered include gender, stature, body mass index (BMI), horizontal and vertical hand force components, and an aggregate shoulder strength measure. Second-order interactions were also considered.

Individual shoulder strengths measured for each subject were used to define subject-specific aggregate shoulder strength. The aggregate measure was obtained by averaging horizontal shoulder flexion, horizontal shoulder extension, abduction, and adduction strengths. Shoulder internal/external rotation strengths were also measured but with a different humeral orientation, and thus were not included in the aggregate measure. Individual shoulder strengths were highly correlated, thus an average value was felt to be a good metric for quantifying total shoulder strength capability.

The resulting model is given by Equation (1) and performance by Figure 4.45.

$$\begin{aligned}
 M_{\text{shoulder}} = & 2.838 - 38.74(x_{\text{shoulder}}/\text{stature}) - 10.32(h_{\text{shoulder}}/\text{stature}) + 0.0915F_x \dots \\
 & + 0.6268(h_{\text{shoulder}}/\text{stature} - 0.10718)(F_x + 34.8169) - 0.0379F_z \dots \\
 & - 0.7126(x_{\text{shoulder}}/\text{stature} - 0.14069)(F_z - 43.8608)
 \end{aligned}
 \tag{1}$$

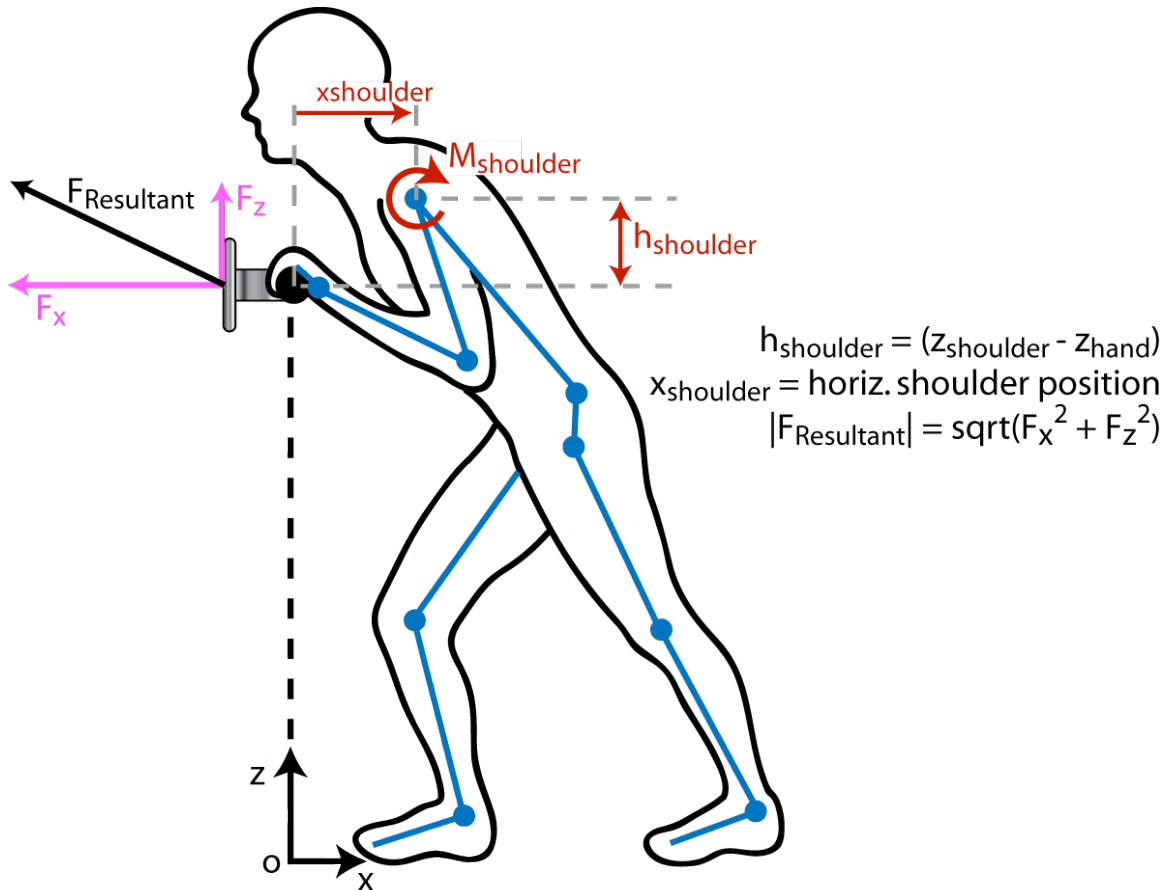


Figure 4.44. Definition of hand force components and postural metrics used to predict shoulder flexion/extension moment. Shoulder extension moments are defined positive where extension of the shoulder corresponds to raising the arm, in the sagittal plane, from a resting posture along side the torso to overhead.

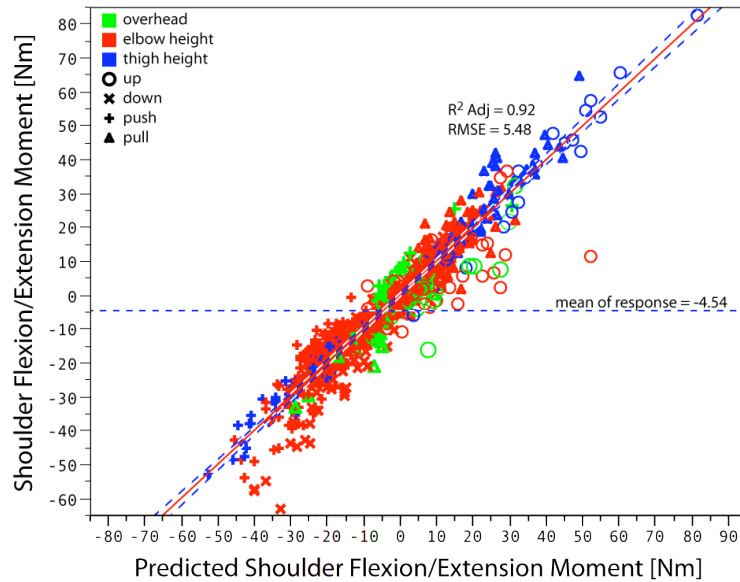


Figure 4.45. Actual versus predicted shoulder flexion/extension moment for two-handed push, pull, up, and down exertions at mid-thigh, elbow, and overhead handle heights ($p < 0.001$).

Aggregate shoulder strength was not found to be a significant predictor of shoulder flexion/extension moment despite a weak relationship between the maximum shoulder moment computed for a given shoulder and subject-specific aggregate shoulder strength. Analysis of data within subjects does not support a moment threshold or plateauing of shoulder moment with increasing hand force and thus supports a linear model. A linear model can however predict physically impossible shoulder flexion/extension moments if inputs, specifically hand forces, are unreasonable. Furthermore, across subjects, a tendency to reduce or maintain shoulder flexion / extension moments below an acceptable value suggests that a shoulder moment threshold could be used as part of a posture-prediction model to predict task postures.

Relationships between residual shoulder flexion/extension moment and task parameters were investigated to assess model performance across trial conditions. Plots of residuals verse horizontal hand force, vertical hand force, BMI, stature, gender, handle height normalized to stature, nominal hand force direction, postural tactic, and aggregate shoulder strength were generated. A small bias was observed across handle heights for push and pull exertions. The model was found to overpredict (mean residual of 3.15 Nm) shoulder moment for pulls at thigh-height and underpredict (mean residual of -2.13 Nm) for overhead pull exertions. For overhead push exertions the model, on average, overpredicts (mean residual of 4.15 Nm) shoulder moment. Mean residual values were

also found to differ significantly ($\alpha = 0.05$) for select hand force directions with a maximum mean residual of 4.16 Nm. Weak (adjusted $R^2 < 0.06$) trends were also found between select anthropometrics and residuals and are likely attributable to having distinctly different subjects perform the thigh-height and overhead exertions.

While biases were observed across a select of trial conditions and anthropometrics biases are small (< 5 Nm) and thus will not have a significant effect on shoulder location or subsequently the predicted task posture.

Torso Inclination in the Hand-Force Plane

Changes in torso inclination across test conditions were found to be qualitatively different for push, pull, and up/down exertions. For this reason a separate regression model was developed for each type of exertion to predict planar torso inclination angle. Gender, stature, and BMI were considered as potential predictors as were hand force (vertical and horizontal components), drop in shoulder from neutral standing height, shoulder height with respect to the point of force application, handle height, and second-order interactions.

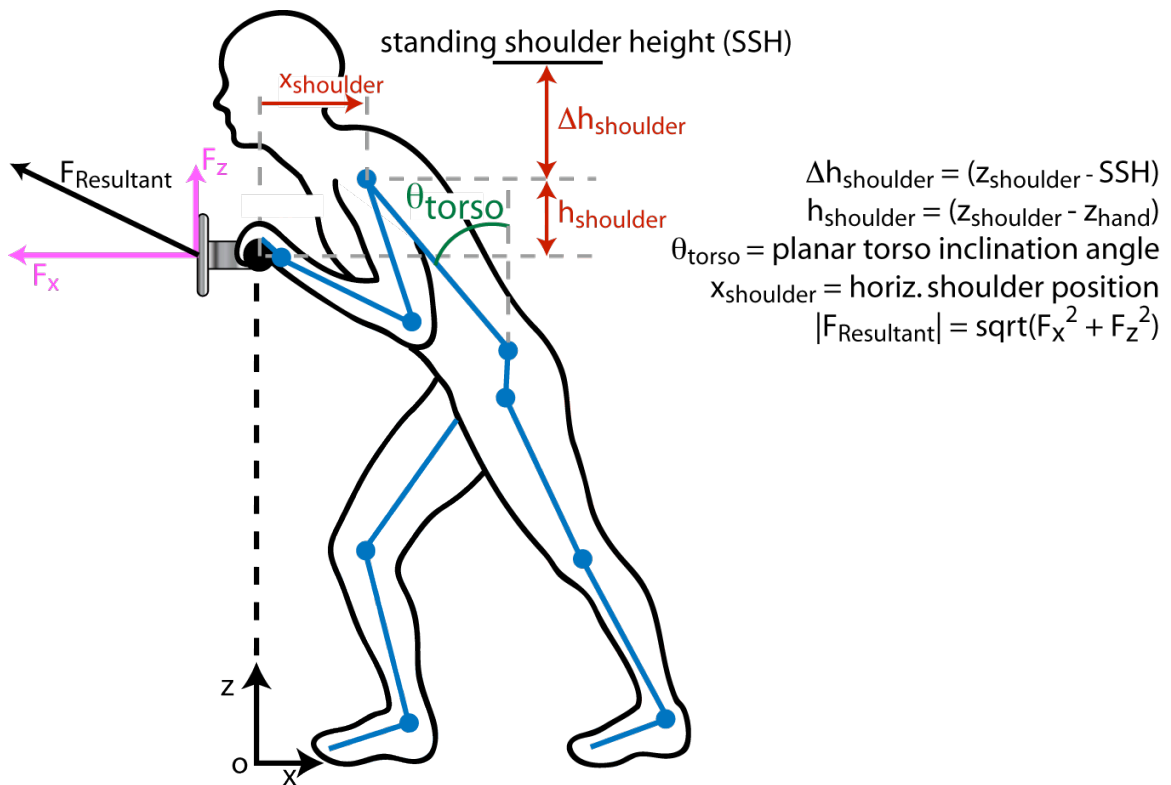


Figure 4.46. Hand force and postural metrics used to predict torso inclination in the hand-force plane. Torso inclination angle is with respect to the vertical and defined positive rearward.

Torso Inclination Angle Regression Model for Up/Down Exertions

Fore/aft shoulder location, shoulder height with respect to the point of force application, vertical hand force, and handle height were found to be the strongest predictors of torso inclination during two-handed vertical up/down exertions. The predictive equation is given by Equation (2) and model performance shown in Figure 4.47.

$$\theta_{torso} = -72.17 + 129.9(x_{shoulder}/stature) + 65.58(h_{shoulder}/stature) \dots + 0.0131F_z + 71.71(z_{handle}/stature) \quad (2)$$

Down exertions were only performed at elbow-height and thus residuals cannot be used to assess model performance across handle heights for down exertions. For upward exertions relationships between residuals and covariates were examined and no significant biases found.

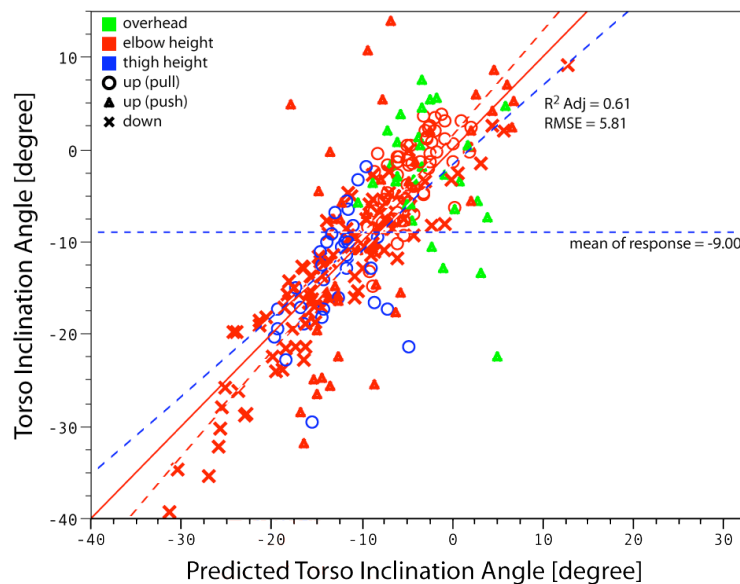


Figure 4.47. Actual versus predicted torso inclination angle for two-handed exertions in the vertical up/down direction spanning mid-thigh to overhead handle heights ($p < 0.001$).

Torso Inclination Angle Regression Model for Pull Exertions

Planar torso inclination angle during two-handed pulls is predicted by vertical hand force, handle height, change in shoulder height from neutral, and the interaction between the latter to variables. Change in shoulder height alone is not a significant predictor but the interaction with handle height is highly significant thus the first-order term was included to have a proper model. All other terms in the model are highly significant ($p < 0.001$). Anthropometrics were not found to be significant predictors.

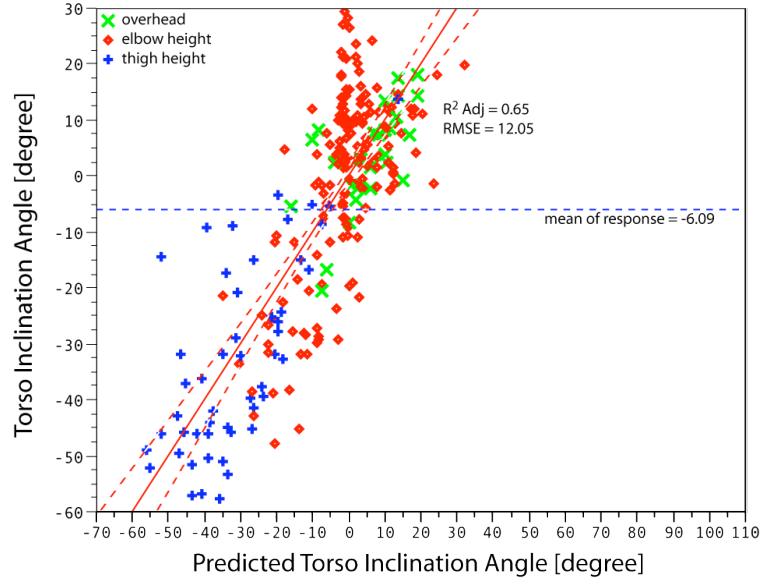


Figure 4.48. Actual versus predicted torso inclination angle for two-handed pulls spanning mid-thigh to overhead handle heights ($p < 0.001$).

$$\begin{aligned} \theta_{torso} = & -57.0 + 87.71(z_{handle}/stature) + 11.52(\Delta h_{shoulder}/stature) \dots \\ & -464.7(z_{handle}/stature - 0.6262)(\Delta h_{shoulder}/stature + 0.0692) + 0.0874F_z \end{aligned} \quad (3)$$

Residuals were examined to assess model performance across trial conditions and full range of subject anthropometrics. The model was found to perform well for all conditions with no significant biases.

Torso Inclination Angle Regression Model for Push Exertions

Two-handed push exertions yielded the strongest regression model for torso inclination angle with an adjusted R^2 value of 0.72 and root-mean-square error (RMSE) of 7.64 degrees. The model is also the simplest with change in shoulder height from neutral being the sole predictor of torso inclination angle (Equation 4). Gender, stature, BMI, vertical and horizontal hand force components, handle height, and all second-order interactions were also considered but none were found to be significant predictors.

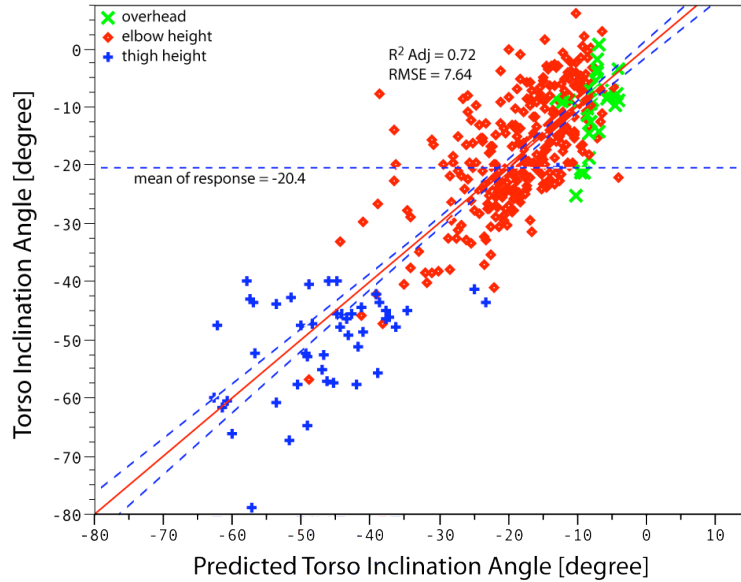


Figure 4.49. Actual versus predicted torso inclination angle for two-handed push exertions performed at mid-thigh, elbow, and overhead handle heights ($p < 0.001$).

$$\theta_{torso} = -8.175 + 169.3(\Delta h_{shoulder} / stature) \quad (4)$$

Residuals were used to assess model performance across trial conditions and a significant difference was found in mean residual values across handle heights (Figure 4.50). Although biases at mid-thigh and overhead handle heights are small, separate models were developed for each handle height and compared to the above model to determine if individual models performed significantly better. The combined model was found to have an adjusted R^2 value equivalent to or higher than R^2 values of the individual models. The RMSE of the combined model was also equal to or less than that of the individual models for each handle height. Based on this comparison of model performance the combined model was determined to be the best model for predicting torso inclination angle during two-handed push exertions.

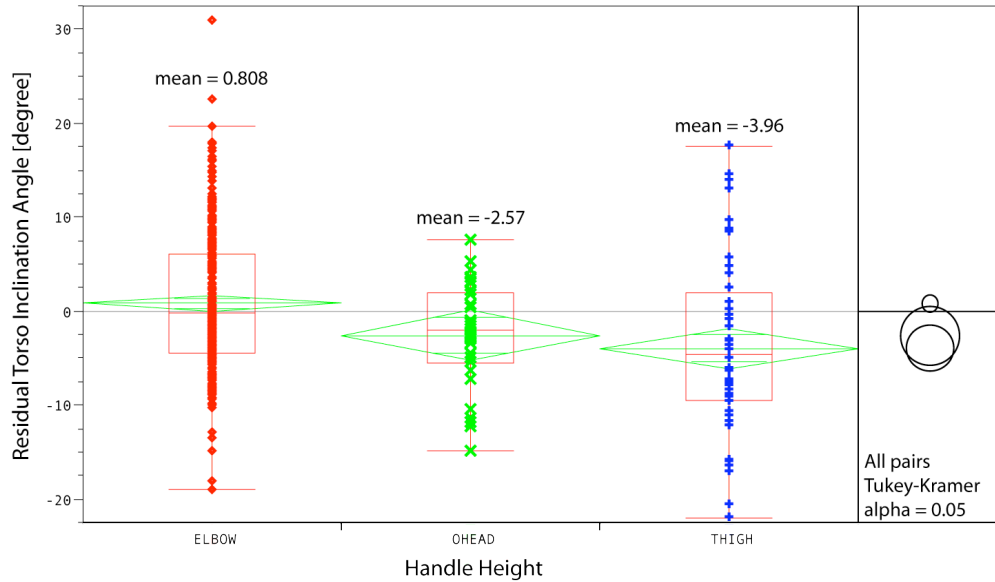


Figure 4.50. Residual torso inclination angle across handle heights for two-handed push exertions. Mean residuals at overhead and mid-thigh handle heights are significantly different from mean residual at elbow height for $\alpha = 0.05$.

Pelvis Pitch with Respect to Torso Inclination

Pelvis pitch with respect to the hand-force frame and torso inclination angle are highly correlated, thus pelvis pitch was predicted relative to torso inclination as opposed to predicting pelvis pitch relative to the hand-force frame. Torso inclination angle, handle height, and the interaction between handle height and torso inclination were found to be the strongest predictors of pelvis pitch angle (Equation 5).

$$\begin{aligned} \theta_{pelvis} = & 19.35 - 0.1902\theta_{torso} - 28.08(z_{handle}/stature)\dots \\ & + 0.5590(\theta_{torso} + 13.21)(z_{handle}/stature - 0.6338) \end{aligned} \quad (5)$$

The plot of actual versus predicted pelvis pitch angle (Figure 4.51) shows rearward extension of the pelvis with respect to the torso for exertions at thigh-height and forward flexion when exerting force overhead. The RMSE is relatively large compared to the range of pelvis pitch angles observed in the data but anthropometrics and additional task variables were not found to significantly improve model performance and the model was found to perform equally well across all test conditions.

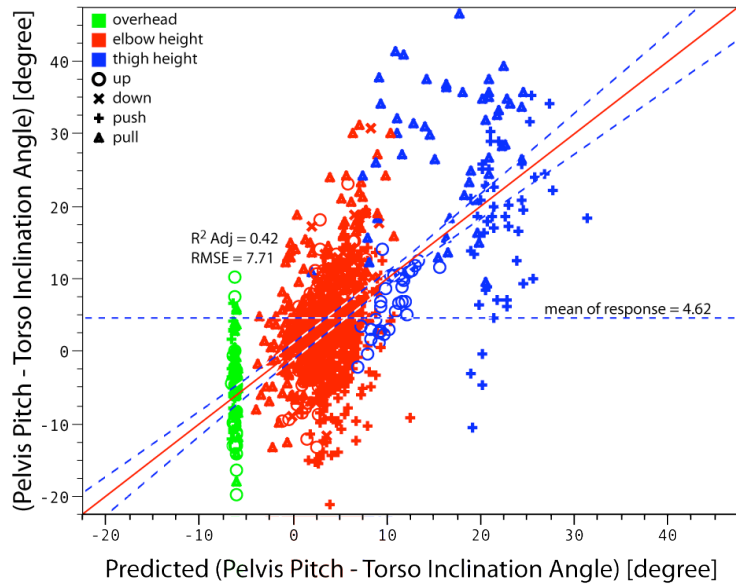


Figure 4.51. Actual versus predicted pelvis pitch with respect to torso inclination for two-handed exertions ($p < 0.001$).

Lateral Pelvis Displacement

Displacement of the pelvis laterally out of the hand-force plane was investigated by looking at the distribution in lateral pelvis location across trials. Variance in lateral pelvis location was found to be small thus displacement of the pelvis out of the hand force plane was determined to be negligible during two-handed exertions. This finding supports the hypothesis that people choose foot placements that allow them to align the vertical plane in which the force vector lies with the L5/S1 joint.

Base-of-Support (BOS) Length

For both push and pull exertions the distance along the x-axis of the hand-force frame from the pelvis to active boundary of the BOS was found to be the strongest predictor of BOS length. When pushing the rear boundary of the BOS acts as the active boundary whereas for pulling the front boundary is active thus separate models were developed to predict the length of the BOS for push and pull exertions. For up/down exertions the variance in BOS length across trials was small and thus not predictable but instead represented by a mean value equal to approximately twice the offset from the pelvis to the rear boundary of the BOS. This suggests that during up/down exertions people center their pelvis over their BOS.

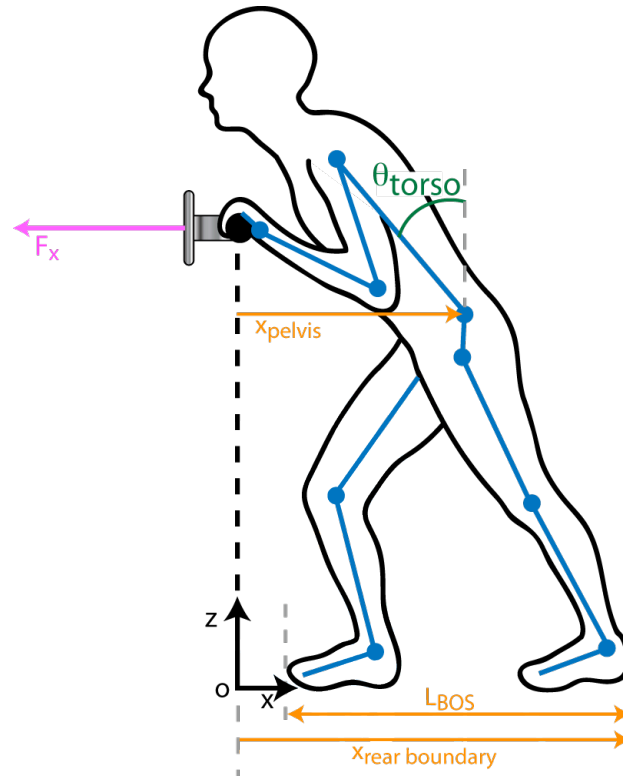


Figure 4.52. Definition of metrics used to predict base-of-support length for two-hand push exertions. The active boundary of the base-of-support is the rear boundary when pushing and front boundary when pulling.

BOS Length Regression Model for Push Exertions

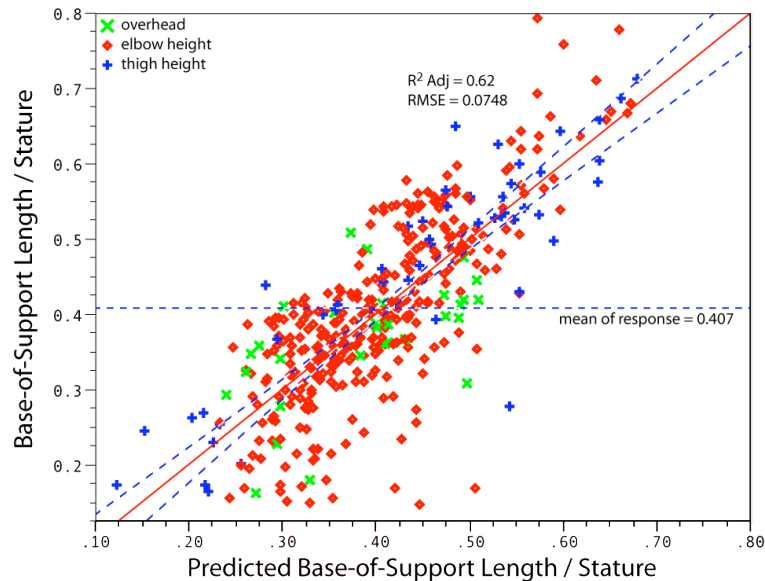


Figure 4.53. Actual versus predicted base-of-support length normalized by stature for two-handed push exertions performed at mid-thigh, elbow, and overhead handle heights ($p < 0.01$).

$$L_{BOS} = -0.4495 + 0.00036 \text{ stature} + 1.151 \left(x_{\text{active boundary}} - x_{\text{pelvis}} \right) / \text{stature} + 0.00027 F_x \quad (6)$$

BOS Length Regression Model for Pull Exertions

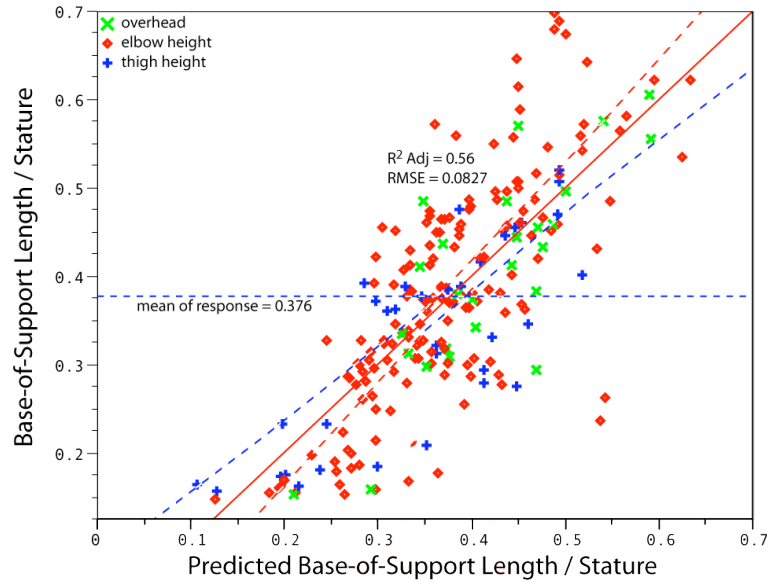


Figure 4.54. Actual versus predicted base-of-support length for two-handed pull exertions ($p < 0.01$).

$$L_{BOS} = -0.5853 + 0.00029stature + 0.2428(z_{handle}/stature) + 0.00076\theta_{torso} \dots - 0.00989(z_{handle}/stature - 0.6340)(\theta_{torso} + 4.187) - 1.157(x_{front\ boundary} - x_{pelvis})/stature \quad (7)$$

4.6. Discussion

The foregoing analysis demonstrates that postures for hand force exertions are consistent with the proposed biomechanical principles and behavioral hypotheses. Two factors dominate the posture selection behavior: first, the base of support must be adjusted to allow the body weight to generate sufficient moment to counteract the hand reaction force, and, second, upper body actions are coordinated to compensate for the relative weakness of the shoulder. The findings are consistent with three main hypotheses:

1. People choose postures consistent with reducing or maintaining shoulder moments below an acceptable level, within the limitations imposed by balance and kinematic constraints.
2. Deviations from a neutral standing posture, specifically changes in torso inclination, are only as large as is required to:
 - a. satisfy kinematic constraints (i.e. reach the force handle),
 - b. generate the required hand force, and/or
 - c. reduce shoulder moments.

3. The location of the base-of-support with respect to the pelvis is determined by the moment due to body weight required to counter the moment resulting from the applied hand force.

Sensitivity to Shoulder Moment

Posture selection during standing hand-force exertions was hypothesized to be driven in part by sensitivity to shoulder moments. Postural analyses are consistent with this hypothesis and suggest that moments at the shoulder are managed by:

1. inclining and lowering the torso to decrease the vertical offset between the shoulder and point of force application (i.e. reduce the vertical moment arm) during push/pull exertions or decrease the horizontal offset between the shoulder and point of force application (i.e. reduce horizontal moment arm) during up/down exertions,
2. exerting a substantial vertical component to direct the hand force vector towards the shoulder joint, and
3. decreasing the hand force moment arm around the shoulder by flexing the elbows to bring the shoulder close to the force handle.

Across all two-handed exertions, absolute shoulder flexion/extension moments were found to be less than or equal to 31 Nm during 90% of trials. This finding is consistent with a study by Schibye et al. (2001) regarding mechanical loading of the low-back and shoulders when pushing and pulling two-wheeled waste containers. Schibye et al. reported shoulder flexion/extension torques ranging from 38 Nm to -35 Nm (flexion torques defined positive) with no significant relationship between shoulder moments and the magnitude of the horizontal push/pull force for individual workers. Similarly, shoulder torque values were reported by de Looze et al. (2000) to be less than 32 Nm with little effect of handle height or horizontal force on shoulder moments when pushing and pulling on a fixed handle and moving cart. The lack of relationship between shoulder moments and horizontal force is also supported in a study by Hoozemans et al (2004) wherein correlations between exerted force and shoulder moments during pushing and pulling were found to be low (0.32 to 0.54). In the current study, shoulder flexion/extension moment was found to increase with horizontal force, but the relationship was not significant for all subjects, especially during pull exertions. Schibye

et al. explained the independence of shoulder moments from horizontal push/pull force by deviations in push/pull forces from horizontal and a tendency for people to direct the resultant push/pull force towards the shoulder joint. This explanation has been proposed by several other researchers (Hoozemans, et al 2004, de Looze et al. 2000, Granata et al. 2005) and is consistent with the significant vertical off-axis forces observed during this work and quantified in Chapter 3.

Depending on the trial conditions (e.g. constraint on hand force direction) one or more of the above mentioned strategies are used to keep the shoulder moment below an acceptable limit. For overhead exertions, kinematics and a sensitivity to shoulder moments cause people to use, almost exclusively, an extended-elbow strategy that allows people to reduce shoulder moments by directing the hand force vector towards the shoulder joint without incurring large moments about the elbow. Of the 30 overhead push (forward) exertions analyzed only one trial was performed using a flexed elbow strategy (Figure 4.55). This trial was performed by one of the strongest subjects. Out of the nineteen participants in the study, this subject had the greatest elbow extension strength (71.5 Nm) and aggregate shoulder strength (38.97 Nm) measures.



Figure 4.55. Unusual flexed-elbow forward overhead exertion.

The bimodal distribution in elbow angle observed for two-hand push exertions at elbow and thigh-height is consistent with the hypothesis that elbow postures are either (a) extended, reducing elbow moment, or (b) substantially flexed, positioning the hands close to the shoulders and using passively-generated elbow moment and internal bracing. When pushing with flexed elbows people reduce the shoulder moment by increasing elbow

flexion as force magnitude increases to bring the shoulders closer to the point of force application. The resulting decrease in horizontal (fore/aft) shoulder moment arm allows people to generate a larger vertical force component with little or no increase in shoulder moment. This trend is illustrated by the plot of vertical hand force expressed as a percent of body weight by force magnitude (Figure 4.19) where the vertical force component is significantly larger for flexed elbow postures than for extended elbow postures when hand force direction is unconstrained. When pushing at high-force levels, most people adopt a flexed-elbow strategy that allows them to generate the vertical forces necessary to increase the friction at the feet to the level required by the requested push force. This explanation is consistent with a study by Dempster (1958) whereby horizontal hand force capability was found to decrease significantly with a reduction in the available friction at the shoe-floor interface. As shown by Boocock et al (2006), people can reduce the required coefficient of friction by generating large vertical force components thus allowing them to generate the required horizontal hand force. A change in elbow posture from an extended to flexed-elbow strategy eliminates the need for subjects to lower their shoulders as much as would be required with the extended-elbow strategy to achieve the same shoulder moment and allows significant vertical hand forces to be generated, and thus the available friction at the feet increased, without a significant change in shoulder moment.

The vertical force component also increases with increasing force magnitude when pushing with elbows extended but increases more gradually. When pushing with elbows extended the vertical force component is directed downward for low-force exertions when the shoulder is located above the handle and directed upward for forces exceeding approximately 50% of body weight as the shoulder approaches and drops below handle height. Again this change in hand force direction is consistent with directing the resultant push force towards the shoulder joint and increases the available friction at the shoe-floor interface by increasing the vertical ground reaction force.

An extended elbow strategy was observed for 65% of two-hand pull exertions and the average included elbow angle during flexed-elbow pulls found to be significantly greater than that during flexed elbow push exertions (72 degrees versus 54 degrees, respectively). Extended elbow pulling postures are consistent with the hypothesis that

elbow postures are selected to reduce elbow moment thus avoiding having hand force limits dictated by elbow strength. This preference towards an extended-elbow pulling postures leaves people with two mechanisms for reducing shoulder moments: (1) decrease the vertical offset from the shoulder to point of force application, and/or (2) generate significant vertical off-axis force components to direct the hand force vector towards the shoulder joint. Shoulder height was found to decrease with increasing hand force magnitude during pulls at mid-thigh and elbow height. Significant vertical forces also were generated across all handle heights with the largest forces generated during overhead pulls. This suggests that during overhead exertions, kinematic constraints force people to rely more heavily on the change in hand force direction as a means for reducing shoulder moments. Although both strategies are used for pull exertions at mid-thigh and elbow heights, people are fairly successful at managing shoulder moment through a change in shoulder location and appear to use change in force direction as a secondary mechanism. Slightly larger vertical forces during thigh-height pulls suggests greater reliance on change in force direction than during elbow-height pulls.

Shoulder flexion/extension moment was found to be well predicted (R^2 Adj = 0.92, RMSE = 5.48 Nm) by the location of the shoulder with respect to the point of force application as well as horizontal and vertical hand force components. Note that a strong relationship is to be expected, because these geometric and force parameters could be used to calculate moment directly. The structure of this regression model (Equation 1), rather than attempting to explain the behavior, was selected for its utility in the posture-prediction model in chapter 6. Anthropometrics and subject-specific aggregate strength measures were not found to be significant predictors of shoulder flexion/extension moment.

Preference Towards Neutral Posture

Because the trunk accounts for approximately half of total body mass, forward inclination of the torso is relatively costly in the sense that significant moments at the low-back are needed to maintain an inclined posture. Furthermore, trunk flexion has been associated with increased levels of co-contraction as compared to co-contraction during equivalent trunk extension tasks (Granata et al., 2005). Using a biomechanical model to estimate muscle forces from recorded EMG data, Granata et al. found that co-contraction

during torso flexion accounted for 47% of total spinal loads. Low-back loads associated with the mechanics of forward torso inclination coupled with loads resulting from increased co-contraction with torso flexion serve as a basis for the hypothesis that people only incline their torso the minimal amount necessary. Analysis of thigh-height upward exertions in the current study is consistent with this hypothesis in that torso inclination angle was not found to vary with force magnitude. When exerting upward force at low handle heights people can either reach the handle by inclining their torso or standing close to the handle and maintaining a fairly upright torso posture. In the current study, people usually chose to stand close to the handle, indicated by no significant change in shoulder fore/aft location with increasing force magnitude, instead of inclining their torsos. A preference towards upright torso postures is also supported by a willingness to tolerate higher shoulder moments during push/pull exertions at the low handle height.

Predicting Foot Placements from Balance Requirements

All postures analyzed were assumed to be in static balance and the equilibrium conditions required by static balance were hypothesized to be sufficient to predict foot placements. Specifically, the location of the base-of-support with respect to the pelvis expected to be chosen such that the moment generated by body weight about the active edge of the base-of-support counters the moment due to the applied hand forces. Analysis of data found a significant relationship between the magnitude of horizontal push/pull forces and the fore-aft offset from the pelvis to the active boundary of the BOS (i.e. front edge when pulling and rear edge when pushing). This result is consistent with the idea that people are recruiting their body weight to generate the required hand force by shifting the location of their whole-body center-of-mass with respect to the active boundary of their base-of-support. Conservative foot placements, i.e. foot placements for which the projected COM location lies within the BOS, were found to be more prevalent, with only a small subset of participants selecting foot placements which resulted in their COM lying outside of their BOS. The prevalence of conservative foot placements is consistent with the finding that BOS length is highly predicted by the offset from the pelvis to active boundary of the BOS. Horizontal hand force and the offset from the pelvis to rear boundary of the BOS were found to be the sole predictors of BOS length for two-hand push exertions ($\text{Adj } R^2 = 0.62$, $\text{RMSE} = 0.07$). BOS length was slightly less

well predicted for two-hand pulls ($\text{Adj } R^2 = 0.56$, $\text{RMSE} = 0.08$) with stature, handle height, and torso inclination being significant predictors of BOS length, in addition to the offset from the pelvis to front boundary of the BOS.

Limitations and Future Work

The generality of the results presented in this chapter is limited by the characteristics of the participants and the test conditions. The participants were young, thin, and fit, and hence do not represent a typical worker population. The force-exertion handle was equipped with a high-friction surface and was a size easily gripped. Workers gripping parts that required a more awkward grip or one producing little friction might adopt different tactics. Similar to many carts and materials handling devices, the handle provided the opportunity for symmetric two-handed postures, but the observed postures might not be typical of those that would be observed for asymmetric two-hand postures.

The postures were held for only a short period of time (three seconds). Tasks requiring longer exertions might be accomplished using different postures. The friction characteristics of the floor surface and the participants' shoes (which were self-selected and varied) also likely affected both the participants' maximum forces and the associated postures. Nonetheless, the general type of footwear (athletic shoes) is common in industry, as are painted floor surfaces.

Further research in this area should include similar tasks in which the handle moves, e.g., pushing a cart or moving a lift-assist/materials handling device. Subjects should be more diverse, particularly with respect to age and body weight. Studies could also examine the effects of floor friction and the handle characteristics. A larger range of task conditions should also be examined, including those with additional constraints on posture. For example, many industry settings include benches, tables, bins, or other constraints on foot position that may affect posture selection. Video from auto assembly plants also shows a large number of one-hand force-exertion tasks in which the other hand is braced against an object in the environment. Future work should consider whether the postural tactics used for bracing are similar to those used to exert task forces.

4.7. References

- Boocock, M. G., Haslam, R. A., Lemon, P., and Thorpe, S. (2006). Initial force and postural adaptations when pushing and pulling on floor surfaces with good and reduced resistance to slipping. *Ergonomics*, 49(9):801–821.
- de Looze, M. P., van Greuningen, K., Rebel, J., Kingma, I., and Kuijer, P. P. (2000). Force direction and physical load in dynamic pushing and pulling. *Ergonomics*, 43(3):377–390.
- Dempster, W. (1958). Analysis of two-handed pulls using free body diagrams. *J Applied Physiology*, 13(3):469–480.
- Granata, K. P., Lee, P. E., and Franklin, T. C. (2005). Co-contraction recruitment and spinal load during isometric trunk flexion and extension. *Clin Biomech (Bristol, Avon)*, 20(10):1029–1037.
- Granata, K. R. and Bennett, B. C. (2005). Low-back biomechanics and static stability during isometric pushing. *Hum Factors*, 47(3):536–549.
- Hoozemans, M. J. M., et al. (2004). Mechanical loading of the low back and shoulders during pushing and pulling activities. *Ergonomics*, 47(1):1–18.
- Schibye, B., Sogaard, K., Martinsen, D., and Klausen, K. (2001). Mechanical load on the low back and shoulders during pushing and pulling of two-wheeled waste containers compared with lifting and carrying of bags and bins. *Clin Biomech (Bristol, Avon)*, 16(7):549–559.

CHAPTER 5

PREDICTING ONE-HAND FORCE EXERTION TASK POSTURES

5.1. Abstract

The objectives of this work were to quantify postural trends during one-handed standing hand force exertions and to develop regression models to predict key aspects of task postures. One-hand force exertion tasks were extracted from a larger data set, and the effects of task parameters and anthropometrics on postures were then examined. Force exertion postures were found to be consistent with a desire to reduce shoulder moments while maintaining a relatively upright torso posture, within the limitations imposed by balance and kinematic constraints. People were found to alter the location of their shoulder with respect to the point of force application, or they generated off-axis forces to direct the hand force vector towards the shoulder joint, resulting in a decrease or maintenance of shoulder moment, despite increasing hand forces. It is shown that the shoulder moment is constrained to a narrow range across a large range of hand force magnitudes. The postural analysis suggests that this restricted shoulder moment range can be exploited to predict force exertion postures. It was also found that torso inclination angle is associated with changes in shoulder location as well as handle height, hand force, and an interaction between handle height and shoulder location. The location and orientation of the pelvis with respect to the hand-force plane were consistent with a tendency to decrease moments about L5/S1. Finally, as hypothesized, an increase in the length of the base-of-support with increasing hand force magnitude was observed for pushing exertions. For pulls however, the BOS length remained fairly constant as the level of force increased. In general the postural trends and regression models presented in this chapter provide insight into the biomechanics of posture selection during one-handed hand force exertions. The findings are consistent with previously hypothesized

biomechanical principles and behaviors, and it is shown that these principles can be modeled and used to predict whole-body postures for one-handed standing hand force exertions.

5.2. Introduction

As discussed in Chapter 4 several researchers have examined postural changes in response to hand forces, and have proposed explanations regarding the observed trends. Granata et al (2005) hypothesized that people exert off-axis forces to align the force vector along the spine. Similarly, de Looze et al. (2000) explained small changes in shoulder moments over a range of task conditions by a tendency for people to direct the resultant hand force vector towards their shoulder. Observations from the literature regarding posture selection and postural changes during forceful exertions suggest a strong relationship between hand force and posture (Haslegrave et al., 1997), although this relationship has not been systematically quantified. Furthermore, past research has mainly focused on two-handed tasks.

This chapter presents an investigation of the relationship between hand force and posture during one-hand standing force-exertions. The current analysis is of data extracted from a larger data set wherein nineteen participants performed one- and two-hand exertions of various force magnitudes and directions at thigh, elbow, and overhead handle heights. The objective of this work was to identify underlying biomechanical principles that can predict key postural elements in relation to the hand force, and develop regression models for use in the posture prediction algorithm discussed later in Chapter 6.

High-Level Hypotheses

The following hypotheses were formulated based on a review of the literature as well as from observations in an automotive assembly plant and laboratory pilot study:

1. People choose postures consistent with reducing the shoulder moment, within the limitations imposed by balance and kinematic constraints. External load effects are reduced by choosing postures such that the hand force vector is directed toward the shoulder joint center,
2. People incline their torsos forward from vertical the minimal amount necessary to generate the needed hand forces within the constraints of

anthropometrically defined kinematics, except as necessary to reduce the shoulder moment. This is consistent with an objective to reduce lower-back extension moments.

Governing Constraints and Assumptions

The following assumptions and constraints are assumed to apply when analyzing force exertion postures and developing regression models to predict key postural metrics:

1. All force exertion postures of interest are quasistatic.
2. All postures are in static balance.
3. No moments are exerted at the feet, i.e., the ground reaction can be expressed solely as a three-dimensional force vector.
4. Moments exerted at the hands are negligible.
5. All transmission of force to/from the environment occurs at the floor and the load handle (no external bracing).

Hypothesized Biomechanical Principles

1. All hand force in the standing tasks of interest is inherently derived from body weight and ground reaction force. That is, no hand force can be exerted without an equal and opposite force generated by ground reaction.
2. To generate a force at the hand, the body mass must be located relative to the base of support (feet) so as to generate a moment to counter the reaction force applied to the hand.
3. People attempt to maintain postures as close to neutral standing as possible while still being able to exert the required force. Deviations in torso inclination and foot placements from neutral standing postures occur due to:
 - a. the kinematic constraints of the task, i.e., to reach the force handle,
 - b. a desire or need to reduce shoulder moment,
 - c. need to increase the moment generated by body weight.
4. Postures are selected to reduce rotational moments about the lumbar spine.
5. Postures are chosen to avoid having hand force limits dictated by elbow strength.

Hypothesized Behaviors

1. People produce forces in directions different than those requested, if permitted:
 - a. At low force levels, people will exert forces in directions that reduce shoulder moment while choosing a torso posture near neutral (i.e. erect).
 - b. At high horizontal force levels, people will exert upward forces to generate increased vertical ground reaction forces, which allows greater horizontal ground reaction forces within the friction limitations of the shoe-floor interface.
2. People will alter their shoulder positions to reduce the shoulder moments, or alternatively to produce higher hand force with the same shoulder moment.
3. Shoulder moment and torso inclination will show a trade-off relationship when the objectives of reducing shoulder moment and maintaining an upright torso are in conflict.
4. Shoulder moments across individuals will be proportional to a static isolated subject-specific shoulder strength.
5. The position and orientation of the base of support relative to the hand force vector will be chosen to align the vertical plane in which the force vector lies with the L5/S1 joint.

5.3. Methods

Participants

Nineteen participants performed trials at three handle heights and with a wide range of different force magnitudes and directions. The experimental design and laboratory study are described in detail in Chapter 2. For the current analysis, data from one-handed exertions at mid-thigh, elbow, and overhead handle heights were extracted from the larger dataset. As described in Chapter 2, all nineteen participants analyzed were young (median age 21 years) and relatively thin (median body mass index 23 kg/m²).

Test Conditions

Of the one-handed exertions collected as part of the experiment outlined in Chapter 2, 80% were considered for analysis, with the remaining 20% withheld for model

validation. Subjects exerted forces spanning from 25% to 100% of their maximum capability in the forward, back, up, down, left, and right directions. Forces were also exerted on the diagonals (forward and left, forward and right, back and left, back and right). The force handle was oriented vertically during all exertions except those in the forward, back, up, and down directions. During those trials a horizontal handle orientation was used (Figure 5.1).

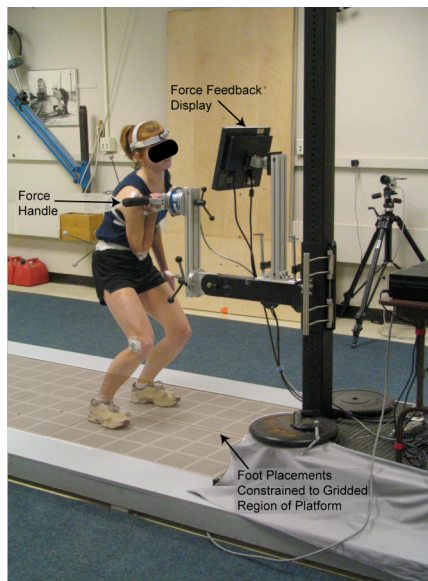


Figure 5.1. Participant in the laboratory performing an upward exertion on a fixed force handle while receiving visual feedback on hand force via an LCD screen. The force handle is shown in a horizontal orientation. Minimal constraints were imposed on foot placements by requiring subjects to keep their feet within the gridded area of the platform.

During all trials participants were free to choose their preferred posture and provided with practice trials during which to identify their preferred posture. The only postural constraints imposed were that subjects were not allowed to brace externally off of the experimental setup, and were required to keep their feet within the gridded area of the raised platform (Figure 5.1).

Data Analysis

A hand force plane, defined as the vertical plane containing the measured hand force vector, was determined for each data trial. Whole-body postures were quantified by a set of postural metrics defined with respect to the hand-force plane. Statistical analyses within each postural category were then performed to determine the effects of worker and task parameters on each posture. The hand-force plane is defined in Chapter 4.

Postural Metrics

A set of postural metrics was developed to quantify whole-body postures with respect to the hand force plane and is presented in Chapter 4. In addition, the following metric was used to quantify one-handed force exertion postures.

Out-of-Plane Rotation Angle (α_{torso}) – The angle between the lateral (y-axis) of the hand-force plane and the projection of a vector from the left to right shoulder in the horizontal plane. Positive rotation out of the plane corresponds to rotating to the left, i.e. turning away from the handle or “opening up” the torso for these right-handed exertions. Conversely, a negative rotation angle corresponds to rotating the left (contralateral) shoulder toward the force handle, “closing up” the torso rotation angle.

Statistical Analysis Approach

Analysis of the postural data was conducted in three phases. The first phase involved qualitative analysis of postures to identify the postural strategies used (Section 5.4). The second phase explored statistical trends in the data to determine if postures selected during hand force exertions were consistent with hypothesized biomechanical principles and behaviors. Results from this analysis are presented in Section 5.5. All linear and nonlinear trends selected for presentation in this section are highly significant ($p < 0.001$). In the third phase regression models were developed to predict key postural metrics. Anthropometrics, task parameters, postural metrics, and second order interactions between covariates were considered as potential predictors. Regression models are presented in Section 5.6 and are highly significant ($p < 0.001$) as are all terms in the models. Non-significant terms were only included when second-order terms were highly significant and inclusion of the non-significant first-order term was required for a proper model. All potential predictors were added into the model, and the model refined by sequentially removing the least significant covariate until only significant terms remained. In an effort to obtain simple models, models were further refined by starting with the least significant term, and removing variables contributing less than 0.02 to the adjusted R^2 value. All analyses were conducted using the JMP statistical software package (version 5.0).

5.4. Results: Postural Strategies Observed

During the experiment participants were asked to exert a force in a specified direction (e.g. forward, right, left) but were not instructed how to perform the exertion (e.g. push, pull). Participants were also encouraged to select their preferred posture. As a result, within a given task condition, different postural strategies were used.

Push Versus Pull Exertions

When instructed to exert a force to the left or right or in one of the non-principal force directions some participants chose to push while others pulled (Figure 5.2). A preference towards pulling was observed for force exertions to the right, back and left, and back and right whereas people preferred to push to the left, forward and left, and forward and right (Figure 5.3).

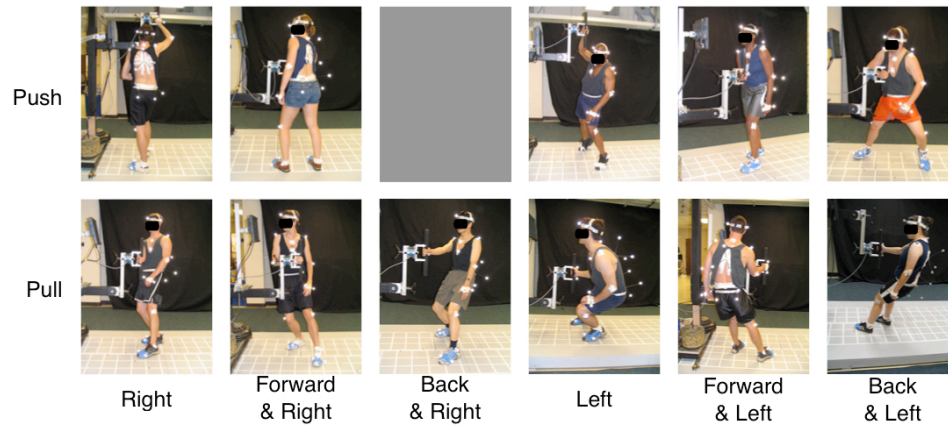


Figure 5.2. One-hand force exertions performed using push versus pull strategy. All participants chose to pull back and to the right thus a picture of a push back and to the right is not shown.

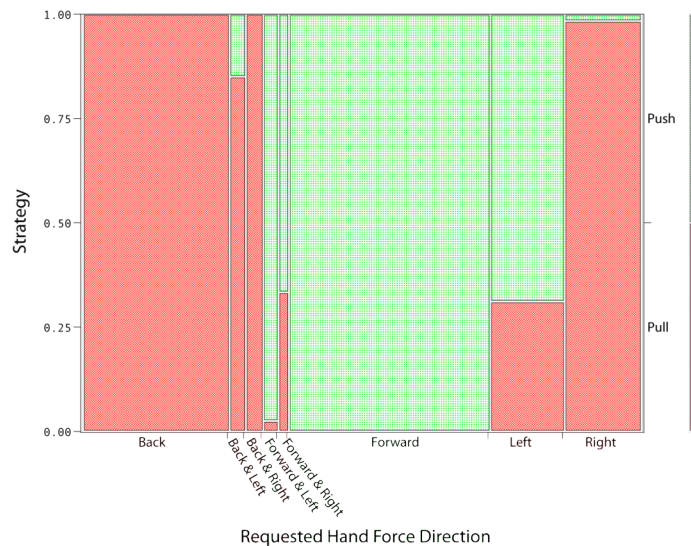


Figure 5.3. Prevalence of push and pull strategies across hand force directions.

Open Versus Closed Orientation

The out-of-plane rotation angle and base-of-support (BOS) orientation were used to categorize a posture as being open or closed. Postures with a positive out-of-plane rotation angle, positive pelvis yaw angle, and BOS rotated towards the left, with respect to the hand-force plane, were defined as open. A closed posture corresponds to rotation of the torso, pelvis, and BOS to the right. Postures are considered neutral if torso, pelvis and BOS rotations are in opposite directions.

Prevalence of open, closed, and neutral strategies across different types of exertions was quantified (Figure 5.4). All three strategies were observed during push, pull, and up exertions (Figure 5.5). A closed strategy was not observed for downward exertions.



Figure 5.4. Open, neutral, and closed torso strategies used across different hand force directions. All downward exertions were performed using a neutral or open strategy thus a picture of closed downward exertion is not shown.

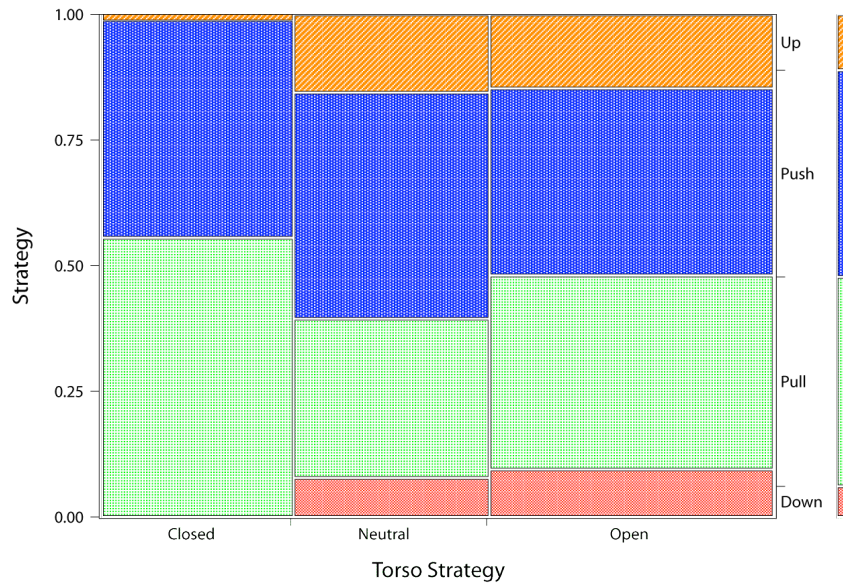


Figure 5.5. Prevalence of torso orientation strategies within push, pull, up and down exertions.

5.5. Results: Posture Selection Trends

Trends in posture selection for one-handed sagittal plane exertions were examined to determine if postures and postural adjustments are consistent with earlier hypotheses. Relationships between postural metrics and the effects of task parameters on posture were investigated to test hypothesized biomechanical principles and behaviors. Many of the results were found to be consistent with those for two-handed postures presented in Chapter 4. Only a general explanation of these findings is given here, while those findings unique to one-handed tasks are explained in detail.

Elbow Posture

As with two-handed tasks, both flexed and extended elbow postures were observed during push exertions at thigh and elbow height (Figure 5.6). Overhead tasks are characterized by an extended elbow posture. A preference towards the flexed-elbow strategy was observed for pushes at thigh and elbow-height (Figure 5.7).

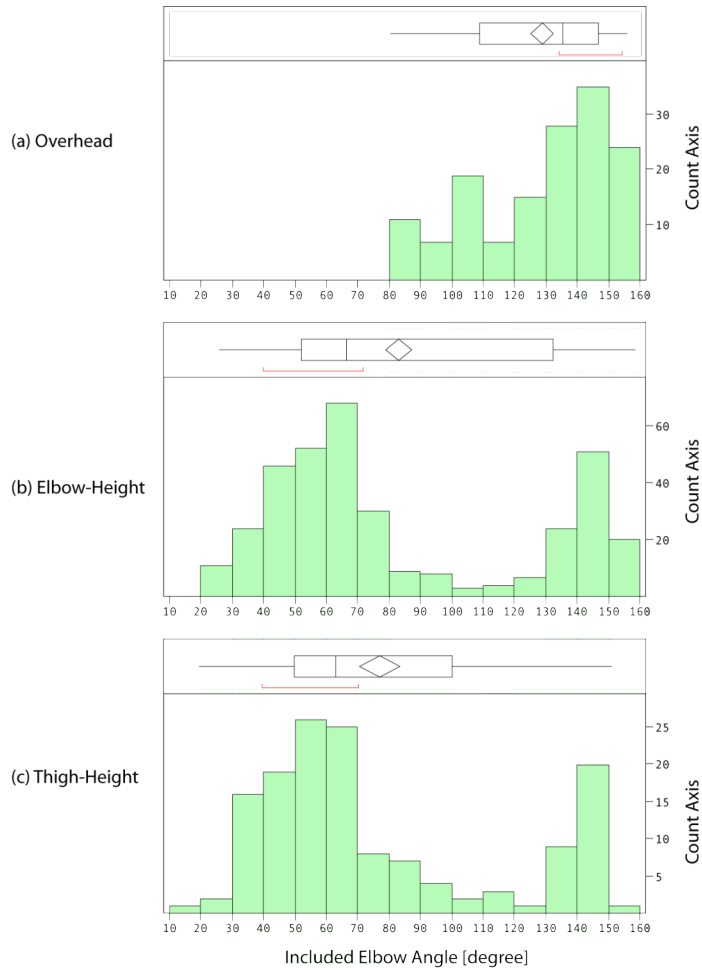


Figure 5.6. Distribution of included right elbow angle during one-handed push exertions at (a) overhead, (b) elbow, and (c) thigh-height.

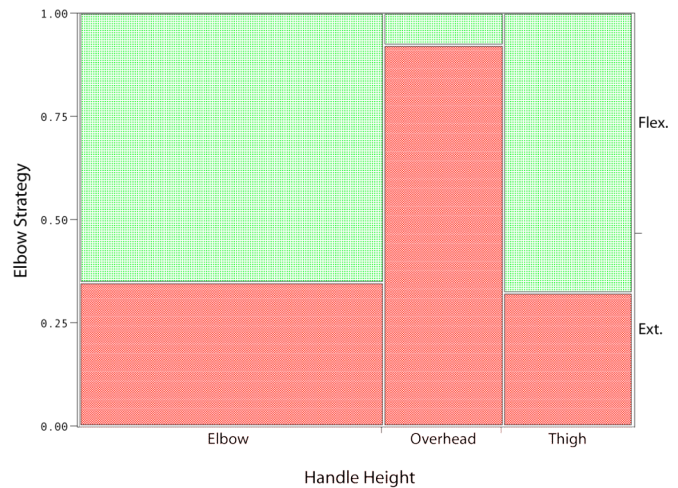


Figure 5.7. Prevalence of flexed (Flex.) and extended (Ext.) elbow pushing strategies across handle heights.

Pull exertions are characterized as often having more extended elbow postures, with 74% of one-hand pulls having an included elbow angle greater than or equal to

ninety degrees (Figure 5.8). This preference is observed across all three handle heights (Figure 5.9). As discussed in Chapter 4 and shown in the following section, a preference towards extended-elbow pulling postures leaves subjects with two mechanisms for reducing moments at the shoulder: (1) decrease the vertical offset between the shoulder and point of force application (i.e. vertical moment arm) by altering shoulder location, and/or (2) generate significant vertical forces to direct the hand force vector toward the shoulder joint.

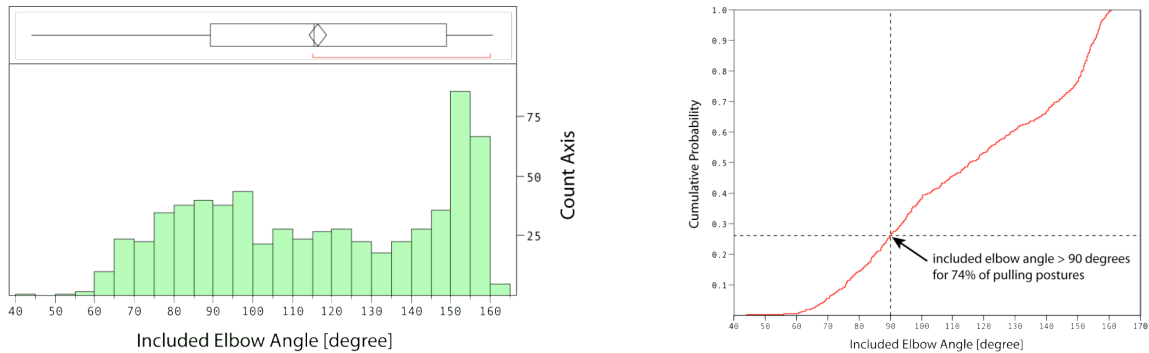


Figure 5.8. Distribution and cumulative distribution function for included right elbow angle during one-handed pulls at thigh, elbow, and overhead heights.

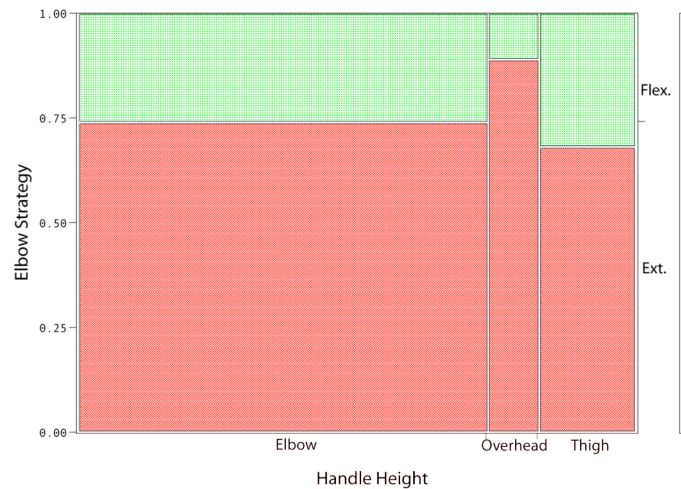


Figure 5.9. Prevalence of flexed (Flex.) and extended (Ext.) elbow postures during one-handed pulls at mid-thigh, elbow, and overhead handle height.

Effect of Shoulder Moment on Posture

A sensitivity to external shoulder moments has been hypothesized to drive posture selection, leading to two behaviors: (1) generating off-axis forces to direct the hand force vector towards the glenohumeral joint center, and/or (2) altering shoulder location with respect to the point of force application to reduce the shoulder moment arm. The

relationships between hand force, posture, and shoulder moment were investigated in these one-hand exertions to determine if data are consistent with the hypothesized behaviors. Sensitivity to shoulder moment was quantified as changes in shoulder moment arm, and in force direction consistent with reducing moments about the shoulder.

Shoulder Location with Respect to Point of Force Application

Changes in shoulder location with respect to the point of force application were quantified for one-handed push/pull and up/down exertions. When pushing and pulling on a handle at or below shoulder level, people were expected to lower their shoulders as force magnitude increased. For overhead push/pull exertions the handle height prevents people from using a change in shoulder height to decrease shoulder moments. During vertical exertions, a decrease in the fore-aft location of the shoulder with respect to the point of force application is expected with increasing hand force magnitude. Changes in shoulder location were quantified by the fore-aft shoulder location (x_{shoulder}), shoulder height with respect to the point of force application (h_{shoulder}), and change in shoulder height from neutral standing height ($\Delta h_{\text{shoulder}}$). These postural metrics are illustrated in Figure 5.37.

For push exertions at elbow and thigh height a drop in shoulder height was observed with increasing horizontal hand force (Figure 5.10). This is consistent with a tendency to reduce shoulder moment as the level of required force increases by decreasing the shoulder moment arm. The same trend is observed for one-hand pulls at elbow-height (Figure 5.11). A significant change in shoulder height with increasing force is not observed for pulls at thigh-height.

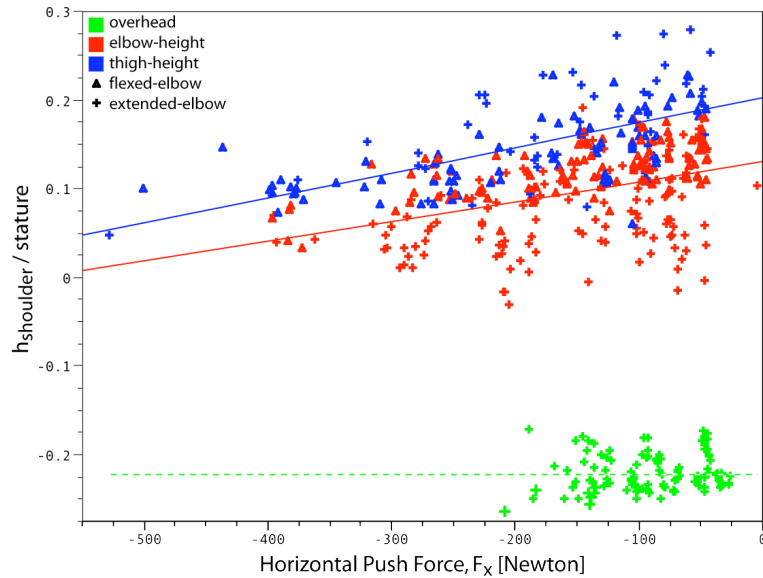


Figure 5.10. Change in shoulder height, relative to point of force application, with increasing hand force during one-handed **push** exertions at mid-thigh, elbow, and overhead handle heights.

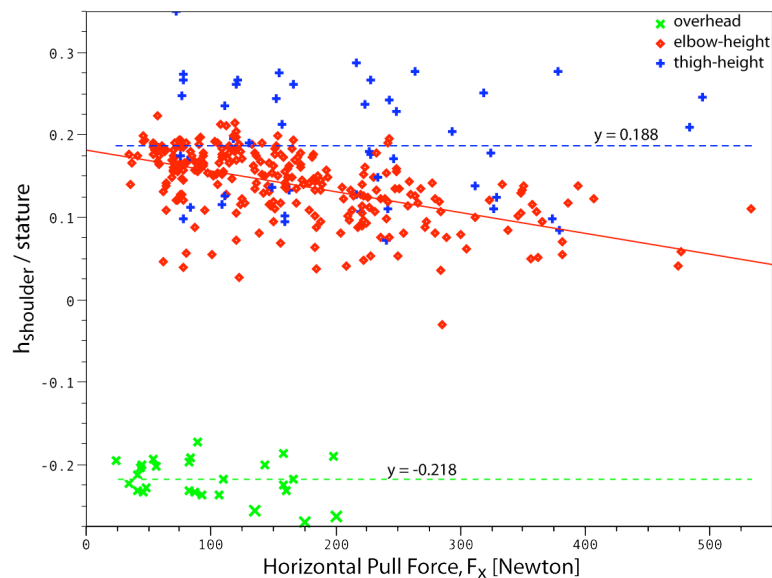


Figure 5.11. Change in shoulder height, relative to point of force application, with increasing hand force during one-hand **pulls** at mid-thigh, elbow, and overhead handle heights.

Shoulder moments are reduced during vertical hand force exertions by decreasing the fore-aft offset from the shoulder to the point of force application (Figure 5.12). During upward and downward exertions at elbow height, people appear to bring their shoulder closer to the handle as the vertical force increases. For overhead and thigh-height exertions a relationship is not found between shoulder location and hand force. During upward thigh-height exertions people stood close to the point of force application

with their shoulders over the handle, which explains why a relationship was not observed between shoulder location and hand force. It is hypothesized that standing close to the handle was preferred over inclining the torso forward to reach the handle (Figure 5.13).

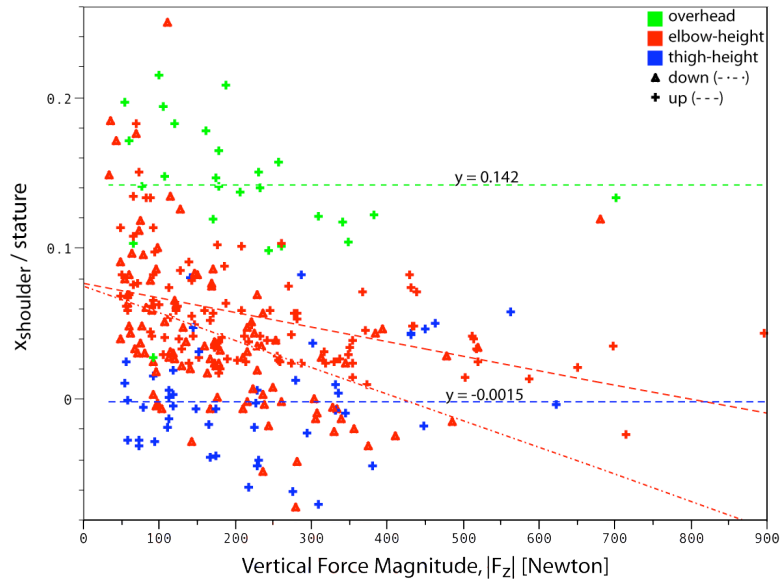


Figure 5.12. Change in fore/aft shoulder location with increasing hand force magnitude during up/down exertions at thigh, elbow, and overhead handle heights.

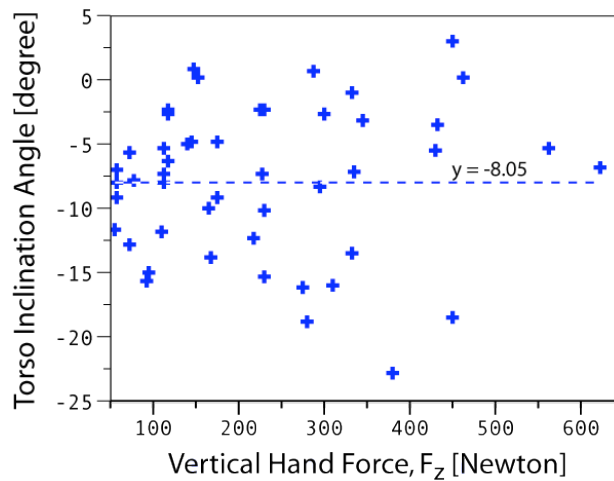


Figure 5.13. Torso inclination angle during thigh-height upward exertions.

Relationship Between Off-Axis Forces and Posture

When hand force direction is unconstrained, push/pull forces have a significant vertical force component, as quantified in Chapter 3. Analysis of push exertions indicates that vertical forces are largest when pushing overhead and that vertical forces differ when pushing with flexed versus extended elbows (Figure 5.14). Large vertical forces during overhead trials are consistent with reducing shoulder moments by directing the hand

force vector towards the shoulder since the anthropometrics based kinematics prevent reduction in moments through a change in shoulder location.

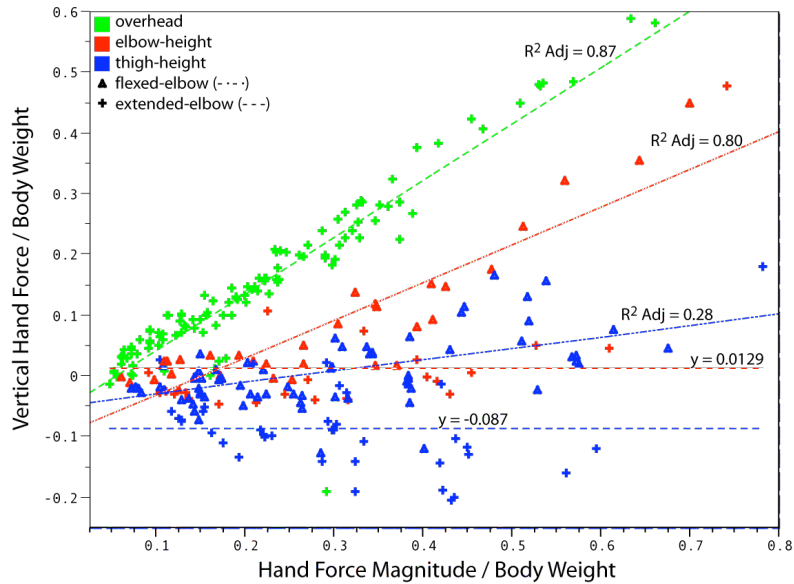


Figure 5.14. Vertical off-axis forces generated during one-handed push exertions performed at thigh, elbow, and overhead handle heights.

Large vertical forces are also observed during one-hand pulls. As with push exertions, vertical components are largest during overhead trials. The smallest vertical forces are observed during elbow-height pulls suggesting people are readily able to reduce moment through a change in shoulder location when pulling at elbow-height.

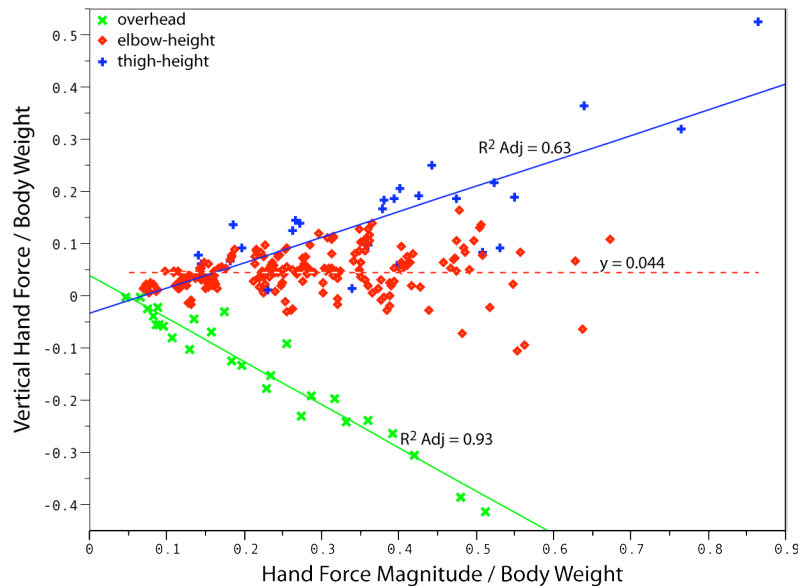


Figure 5.15. Vertical off-axis forces generated during one-hand pulls at thigh, elbow, and overhead handle heights.

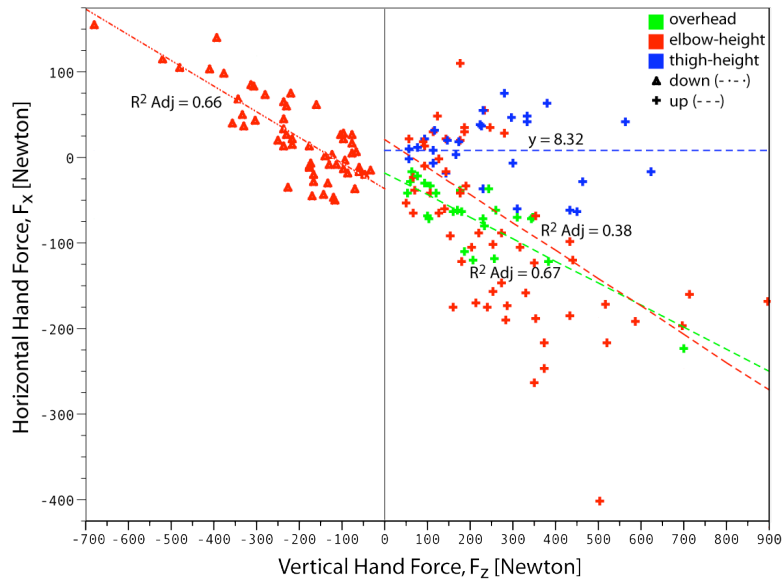


Figure 5.16. Horizontal off-axis forces generated during elbow-height down exertions and upward exertions at mid-thigh, elbow, and overhead handle heights.

Interaction Between Shoulder Location and Off-Axis Forces

When force direction is unconstrained people choose to maintain a higher shoulder location and generate large vertical hand forces instead of lowering the shoulder, as during directionally constrained trials (Figure 5.17). The same relationships are observed for elbow-height pulls (Figure 5.18). These relationships combined with Figure 5.19 illustrate how two different mechanisms, a change in shoulder location and generation of off-axis forces, can be used to maintain the shoulder moments at an acceptable level.

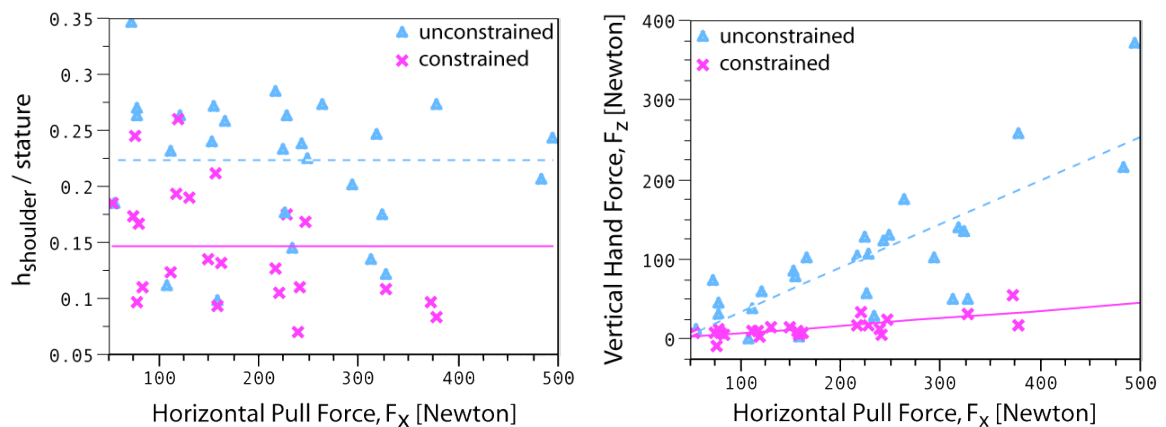


Figure 5.17. Shoulder height, relative to point of force application, and vertical off-axis forces generated during directionally constrained and unconstrained **thigh-height** pull exertions.

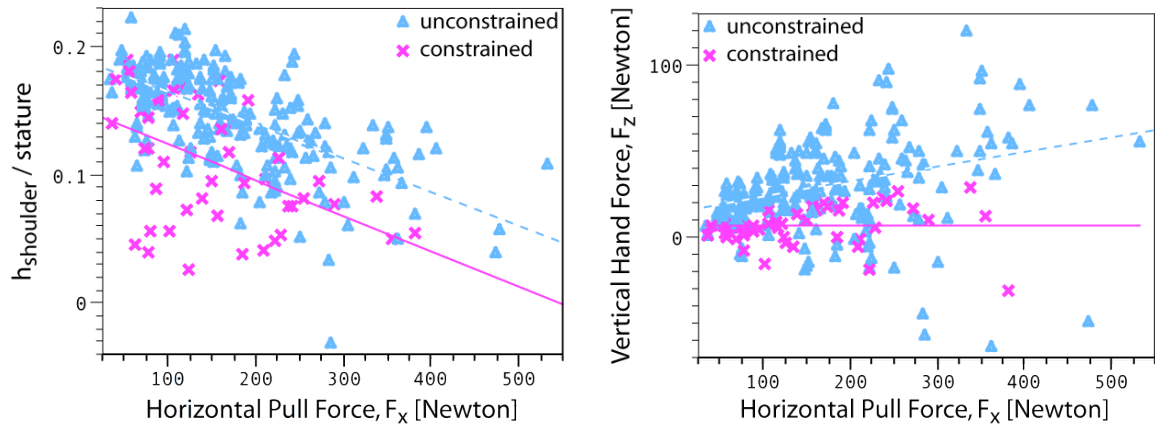


Figure 5.18. Shoulder height, relative to point of force application, and vertical off-axis forces generated during directionally constrained and unconstrained **elbow-height** pull exertions.

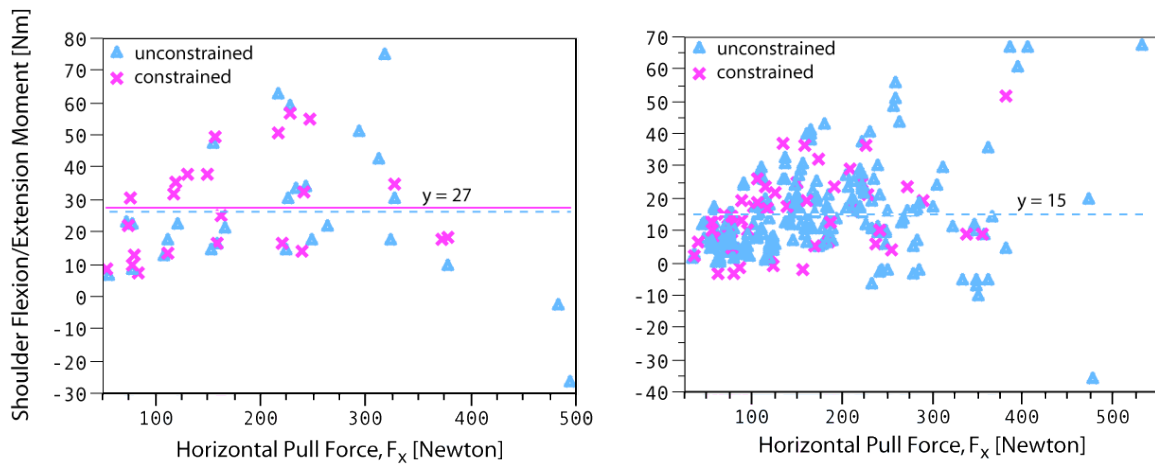


Figure 5.19. Shoulder flexion/extension moments during directionally constrained and unconstrained thigh (leftmost plot) and elbow-height (rightmost plot) pulls.

Level of Acceptable Shoulder Moment

The relationship between shoulder flexion/extension moment and posture was investigated to test the hypothesis that postural changes are consistent with maintaining the shoulder moment at or below an acceptable level. Higher shoulder moments observed during a subset of one-hand forward exertions were attributed to trials in which participants braced their right arm against their body. This tactic unloads the shoulder by transmitting the force to the torso, allowing greater hand force by bypassing the moment-generating limits of the shoulder. Braced trials are indicated by black and grey data points in Figure 5.21 and were excluded from the analysis.

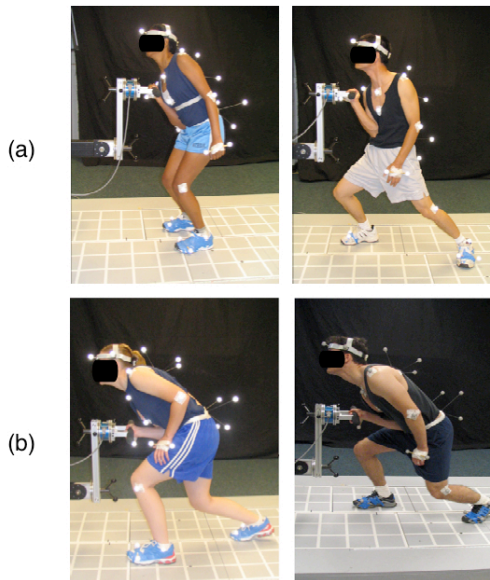


Figure 5.20. Utilization of internal bracing during (a) elbow-height upward exertions and (b) thigh-height forward exertions.

The relationship between change in shoulder height and shoulder flexion extension moment indicates that people are successful at reducing shoulder moments by altering their shoulder location with respect to the point of force application. For 90% of trials in which bracing was not used, shoulder flexion/extension moment was less than or equal to approximately 37 Nm (Figure 5.22).

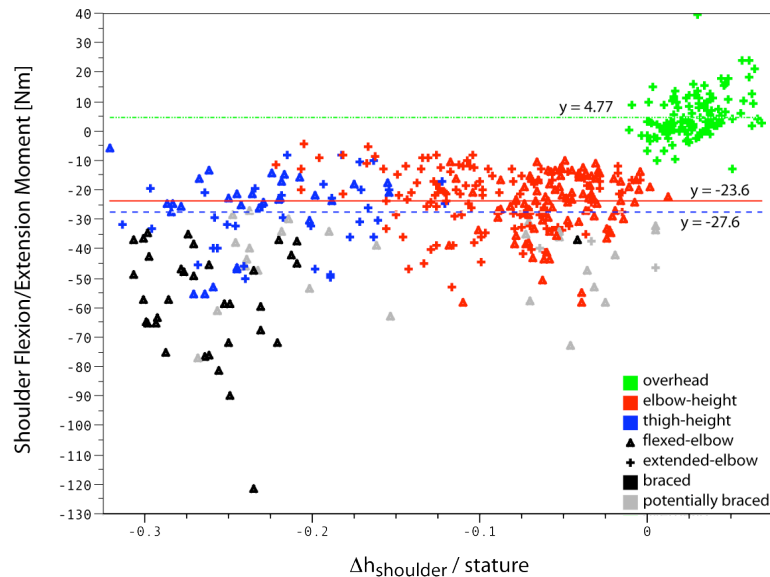


Figure 5.21. Relationship between shoulder flexion/extension moment and drop in shoulder height for one-hand push exertions at mid-thigh, elbow and overhead handle heights. Black and grey data points correspond to trials in which bracing was or may have been used and were excluded from the analysis.

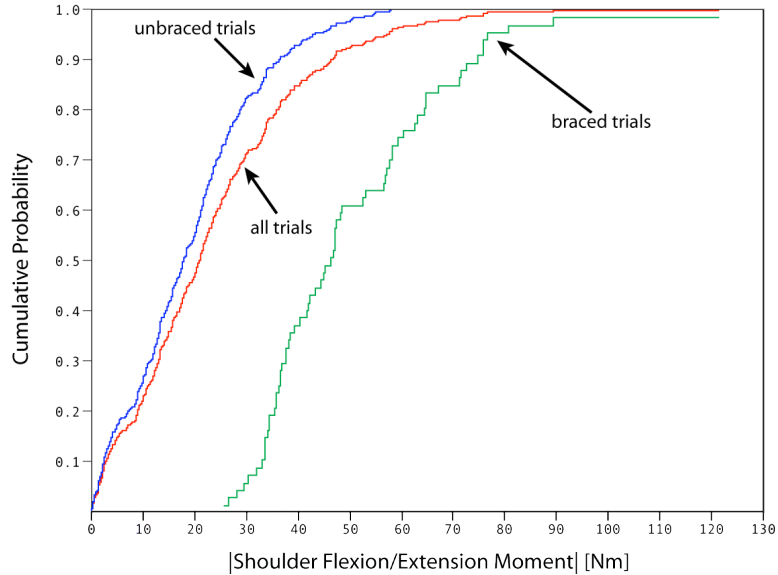


Figure 5.22. Cumulative distribution function for absolute value of shoulder flexion/extension moments during forward exertions. 90% of unbraced trials had moments less than or equal to ~37 Nm as compared to 75 Nm for braced trials and 47 Nm for both braced and unbraced trials combined.

Similarly, shoulder moments were less than or equal to 35 Nm during 90% of all pull exertions (Figure 5.25). The relationships among hand force, shoulder moment, and shoulder location show people are equally as successful at reducing moment when pulling as when pushing (Figure 5.23 and Figure 5.24). On average, during low force (25%) elbow-height pulls, the shoulder is located 27.3 cm above the handle. If people were to maintain that shoulder height as the level of force required increased, an average maximum one-hand pull force of 314 N would result in a shoulder moment of approximately 86 Nm. The average shoulder moment during one-hand pulls is 21 Nm, approximately 25% of the calculated value, indicating that by lowering their shoulder people are reducing the potential shoulder moment by 75%.

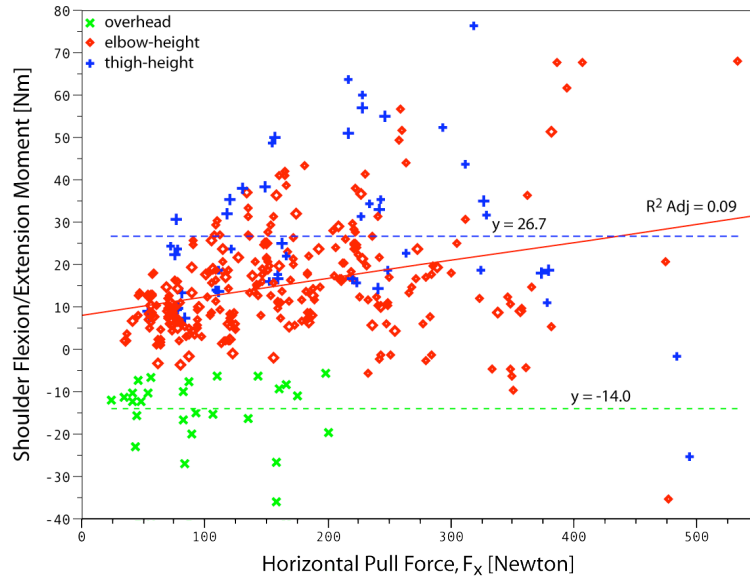


Figure 5.23. Change in shoulder flexion/extension moment with horizontal pull force for one-handed back exertions at mid-thigh, elbow and overhead handle heights.

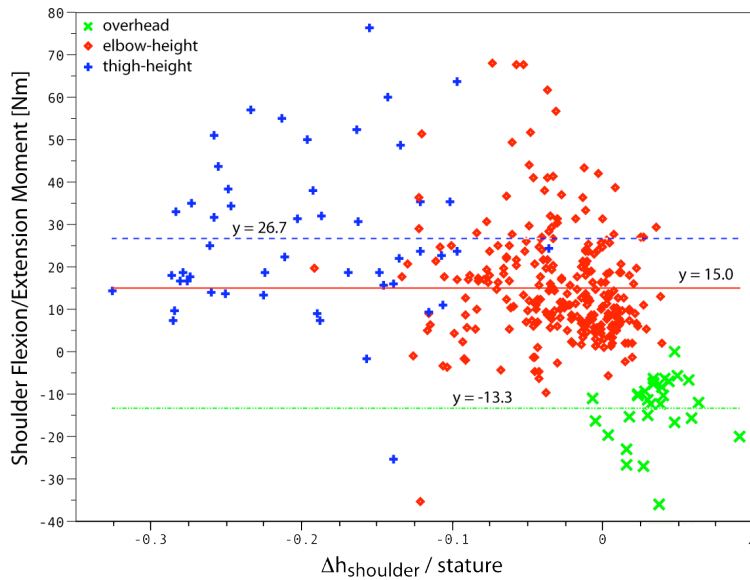


Figure 5.24. Relationship between shoulder flexion/extension moment and drop in shoulder height during one-handed pulls at thigh, elbow, and overhead handle heights.

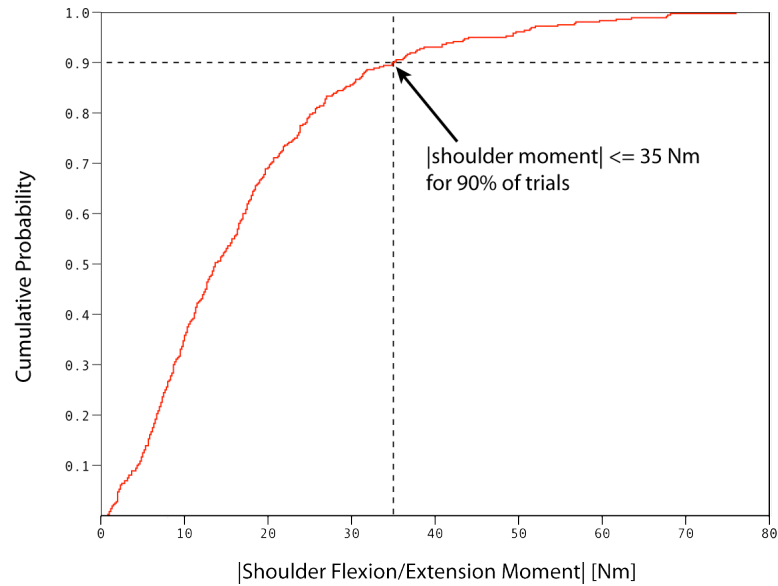


Figure 5.25. Cumulative distribution function for one-hand pulls showing magnitude of shoulder flexion/extension moment is less than or equal to 35 Nm for 90% of trials.

Pelvis Location and Orientation with Respect to Hand-Force Plane

It was hypothesized that people shift their pelvis laterally such that L5/S1 lies on the hand-force plane, thereby reducing low-back torsion moments due to the hand force. Pelvis location and orientation during one-hand exertions were quantified and the relationship between hand force and posture quantified to test this hypothesis.

Lateral Pelvis Displacement

During push and pull exertions at elbow height a shift in pelvis location towards the hand-force plane (i.e. toward zero lateral displacement) was observed with increasing hand force (Figure 5.26 and Figure 5.27). The same trend was observed when pushing overhead. For push and pull exertions at thigh-height no relationship was observed between lateral pelvis displacement and force and a larger mean offset was observed for pulls at thigh-height as compared to pulls overhead or at elbow-height.

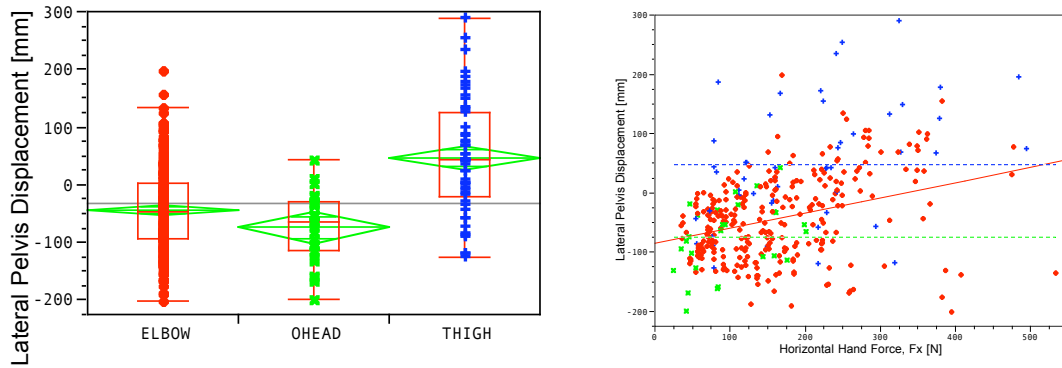


Figure 5.26. Variation in lateral displacement of the pelvis out of the hand-force plane across handle heights and with horizontal hand force during one-hand pulls.

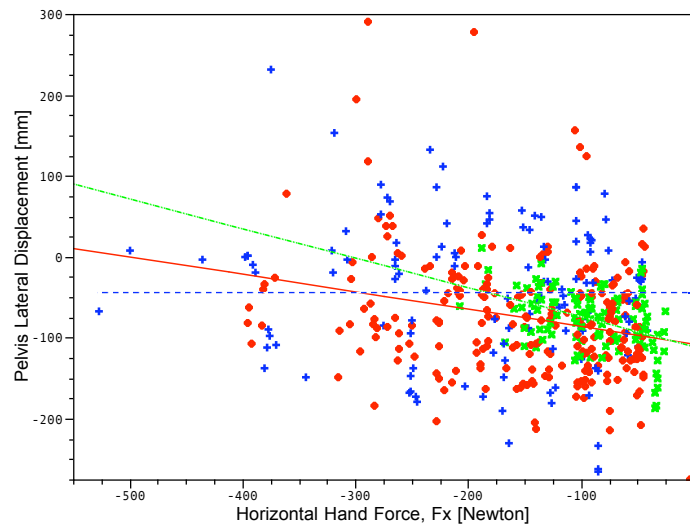


Figure 5.27. Change in lateral displacement of the pelvis with horizontal hand force for **push** exertions at mid-thigh (mean = -43 mm), elbow (R2 Adj = 0.06), and overhead (R2 Adj = 0.19) heights.

Out-of-Plane Rotation Angle

The distribution of out-of-plane rotation angles during one-hand exertions was examined to determine if postures are consistent with the hypothesis of reducing low-back rotation moments by rotating the torso to reduce the rotational moment arm. The distribution of low-back moments computed for one-hand exertions is presented in Figure 5.28. On average, out-of-plane rotation angles were found to be small during push exertions but significantly different from zero during other one-hand exertions (Figure 5.29). When pulling at elbow and thigh-heights an increase in out-of-plane rotation angle was observed with increasing pull force (Figure 5.30). This is consistent with the hypothesis that people are opening up (i.e. rotating towards the left) to reduce the low-

back rotational moment. This strategy also acts to shift the L5/S1 joint laterally towards the hand-force plane. No significant relationships were found between hand force and out-of-plane rotation angle for one-hand push exertions.

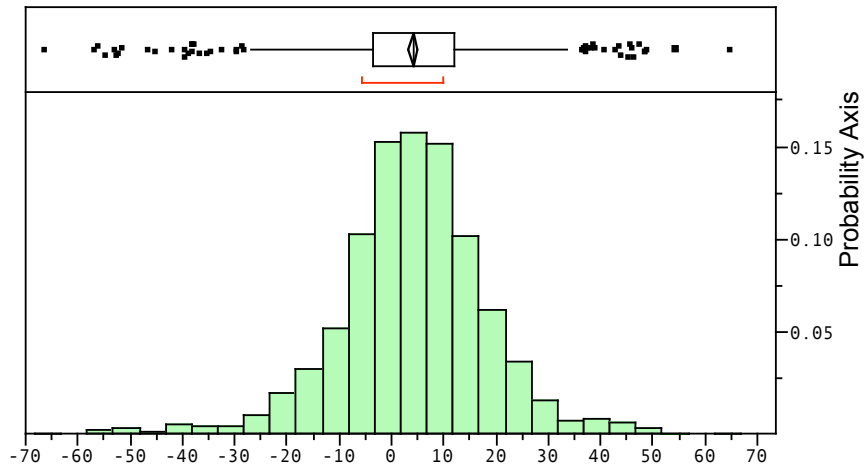


Figure 5.28. Distribution of axial rotation moments [Nm] about the lumbar spine during one-hand exertions (mean = 2.3 Nm, Std.Dev. = 14.9 Nm).

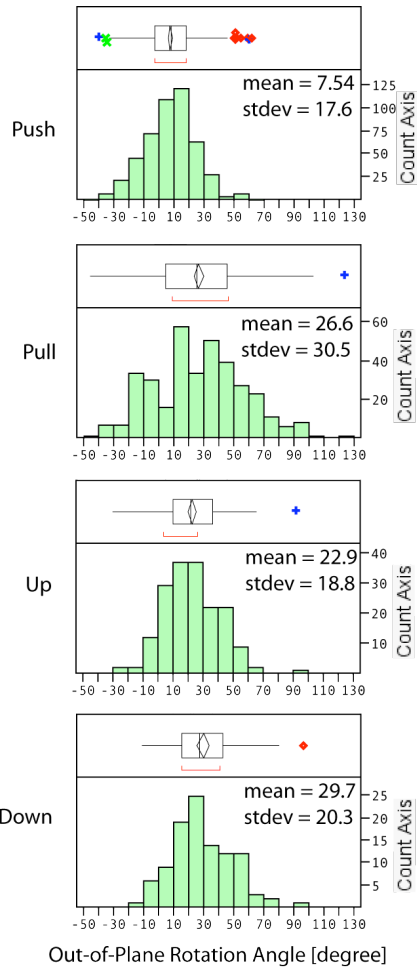


Figure 5.29. Distribution of out-of-plane rotation angle during one-hand push, pull, up, and down exertions performed at mid-thigh, elbow, and overhead handle heights.

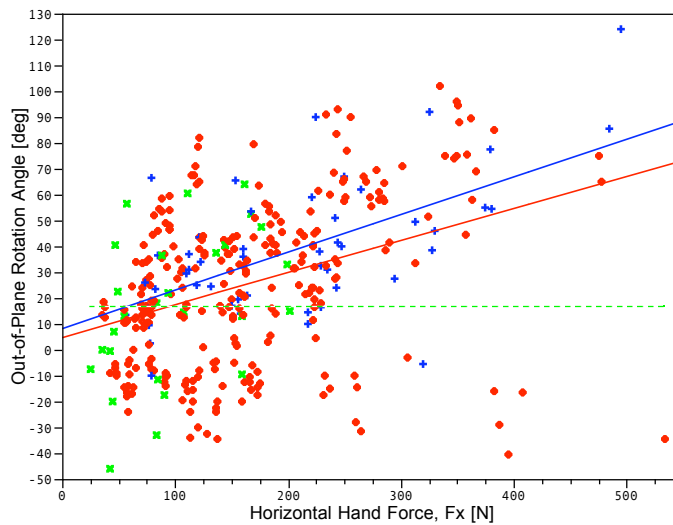


Figure 5.30. Relationship between out-of-plane rotation angle and horizontal hand force during one-hand pulls at thigh (R^2 Adj = 0.36), elbow (R^2 Adj = 0.13), and overhead (mean = 17 degrees) handle heights.

Out-of-plane rotation angle also was found to vary with hand force during downward exertions at elbow height (Figure 5.31). As the required vertical force increases people appear to bring their shoulder towards the point of force application, while at the same time opening up (i.e. rotating to the left).

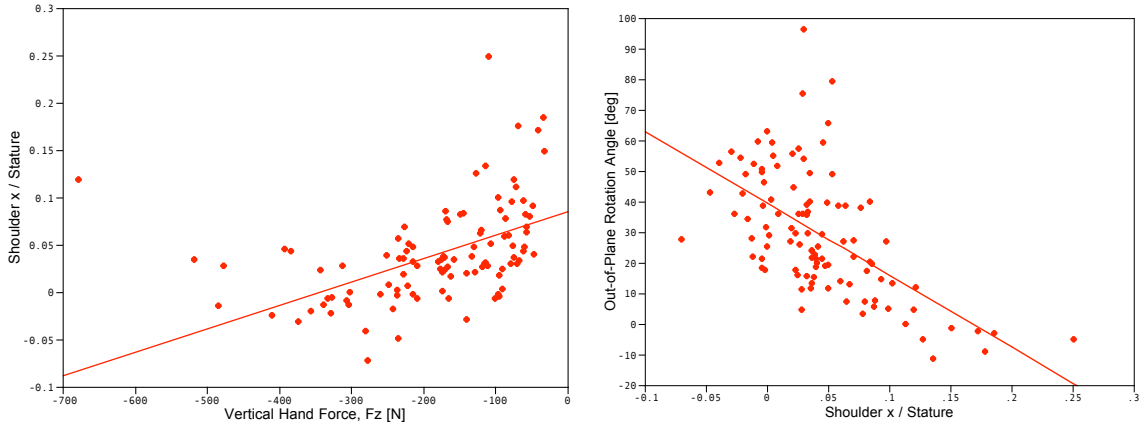


Figure 5.31. Change in shoulder fore-aft location with vertical hand force and associated change in out-of-plane rotation angle during elbow-height downward exertions.

For upward exertions, out-of-plane rotation angle was found to vary significantly with fore-aft shoulder location. During thigh-height upward exertions people tended to stand close to the handle, bringing their shoulder directly over or forward of the handle, and opening up, rotating their body away from the handle (i.e. to the left). For higher handle locations the force-aft offset between the shoulder and point of force application is larger and on average, people adopt a more neutral torso orientation.

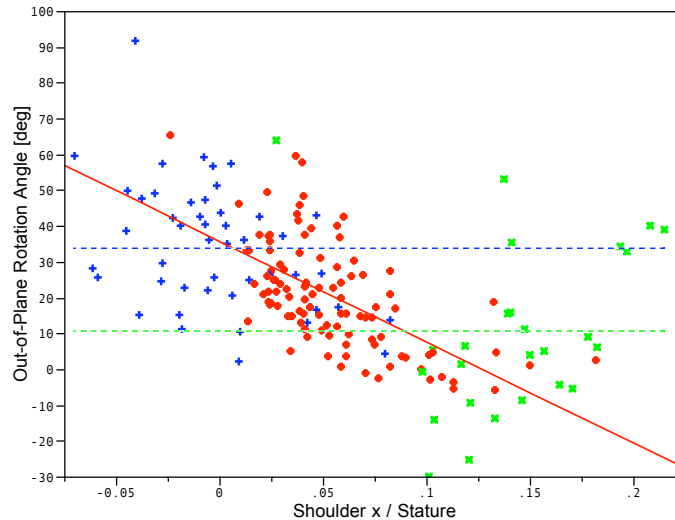


Figure 5.32. Relationship between out-of-plane rotation angle and shoulder fore-aft location during **upward** exertions performed at thigh (mean = 34 degrees), elbow (R^2 Adj = 0.37), and overhead (mean = 10.6 degrees) handle heights.

Foot Placements during One-Hand Force Exertions

Effect of Hand Force on BOS Length during Push Exertions

BOS length increases with increasing horizontal force during one-handed push exertions across all handle heights (Figure 5.33). The offset from the active boundary (i.e. rear edge of BOS) to the pelvis is a strong predictor of the length of the BOS across all push trials.

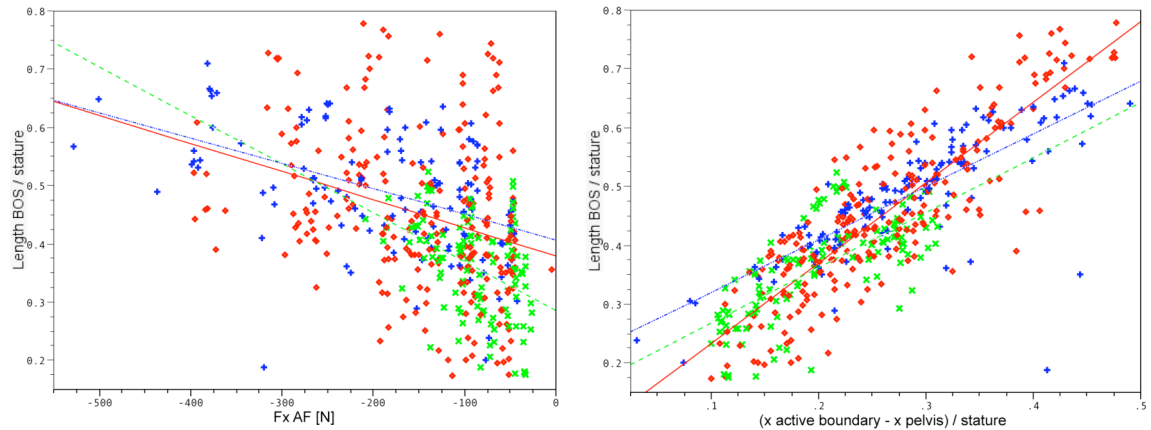


Figure 5.33. Relationship between horizontal hand force and BOS length and fore-aft distance from rear boundary and BOS length during one-hand push exertions.

Effect of Hand Force on BOS Length during Pull Exertions

High-force (75% to 100% of maximum) one-hand pulls performed with a parallel stance were uncommon, and therefore were excluded from the analysis. Parallel stance was defined as BOS length equal to or less than 1.5 foot lengths. Excluded trials are shown in grey in Figure 5.34. Length of the base-of-support is more variable during one-hand pulls. A significant ($p < 0.0001$) relationship was found between pull force and BOS length for pulls at elbow-height, but no relationship was found for exertions at thigh and overhead heights. Unlike when pushing, people tend to open up when pulling, rotating their bodies to their left as the level of force increases. Figure 5.34 indicates that when using this tactic people do not increase their BOS but instead maintain a fairly constant BOS length and increase the offset between their pelvis and forward edge of the BOS (active margin).

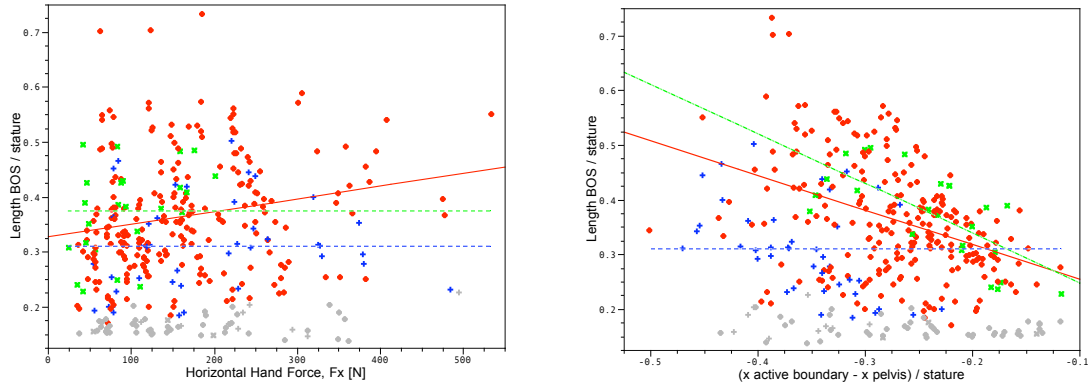


Figure 5.34. Change in length of BOS with pull force and relationship between BOS length and offset from front edge of BOS and pelvis during one-hand pulls. Grey data points correspond to 75% and maximal exertions performed with a parallel stance (BOS length \leq 1.5 foot lengths), and were excluded from the analysis.

5.6. Results: Regression Models

The preceding section demonstrated that the postural adaptations to hand force magnitude and direction are consistent with the biomechanical principles and hypothesized behaviors outlined at the beginning of this chapter. These observations guided the formulation of regression models to predict key postural variables. Although many possible regression models could be created, the choices of both dependent and independent variables were guided by the structure of the overall posture prediction model that is presented in Chapter 6. In particular, the sequence of computations in the prediction algorithm means that certain variables could be predictors of others, but not vice versa. The choices of predictors in the regression models are not meant to imply causality but rather associations that could be exploited to perform accurate, generalizable posture prediction.

The organization of this section parallels the computation sequence in the posture-prediction model presented later in Chapter 6. The resulting algorithm includes the following steps: (1) A shoulder flexion/extension moment target value, effectively the moment that a person is willing to generate, is computed as a function of force magnitude and shoulder position. (2) Torso inclination is predicted as a function of shoulder position relative to the handle and the neutral position. (3) Lumbar spine flexion (represented as pelvis inclination relative to torso inclination) is predicted from handle position. Finally, the length of the base of support is predicted from the pelvis position and horizontal

force. (The position of the base of support is predicted from balance considerations -- see Chapter 6.)

In most cases, parsimonious models with fewer predictors were chosen over more complex models that provided only slightly better fit. In general, the models presented here have adjusted R^2 values within 0.05 of the best model attainable.

Considerable analysis was conducted to determine when it was appropriate to produce separate models for different types of exertions. When the exertions represented qualitatively different behaviors that could not be well captured by a single model, separate regression models were generated. For example, separate models are presented for torso inclination in pushes, pulls, and up/down exertions.

Shoulder Moment Target Value

Relationships between posture and shoulder moment presented in the preceding section suggest that shoulder moment can be used to predict force exertion postures. Tightness of data within trial types suggests that once the postural tactic is known, shoulder moment can be well predicted. Shoulder location with respect to the point of force application, quantified by h_{shoulder} and x_{shoulder} , (Figure 5.37) was found to capture the effect of postural strategy on shoulder moment, thus these variables were considered as covariates in lieu of developing separate regression models for each postural tactic. Additional covariates considered include gender, stature, body mass index (BMI), horizontal and vertical hand force components, and an aggregate shoulder strength measure. Second-order interactions were also considered. The resulting model is given by Equation (1) and performance by Figure 5.36.

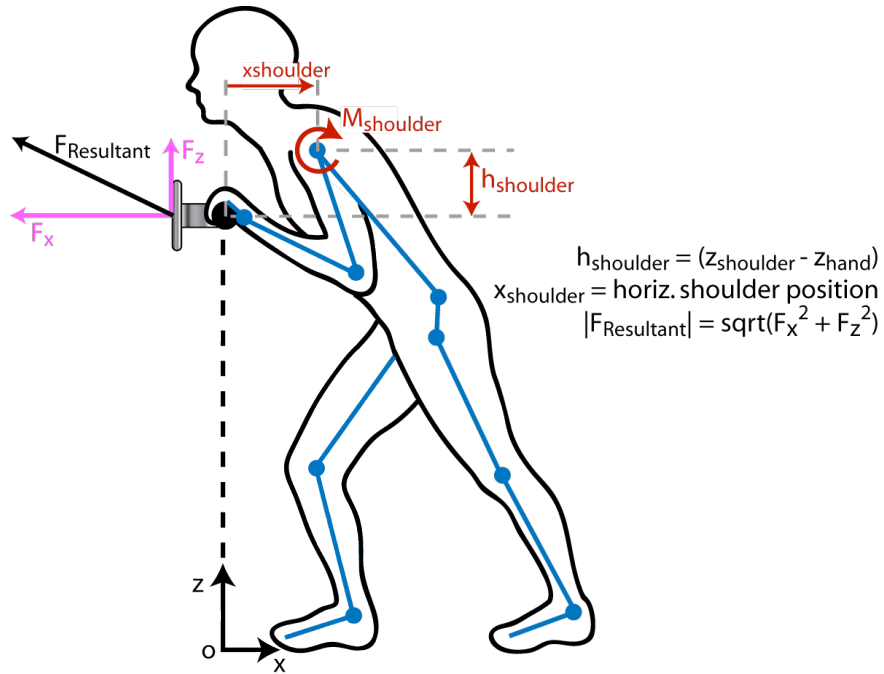


Figure 5.35. Definition of hand force components and postural metrics used to predict shoulder flexion/extension moment. Shoulder extension moments are defined positive where extension of the shoulder corresponds to raising the arm, in the sagittal plane, from a resting posture along side the torso to overhead.

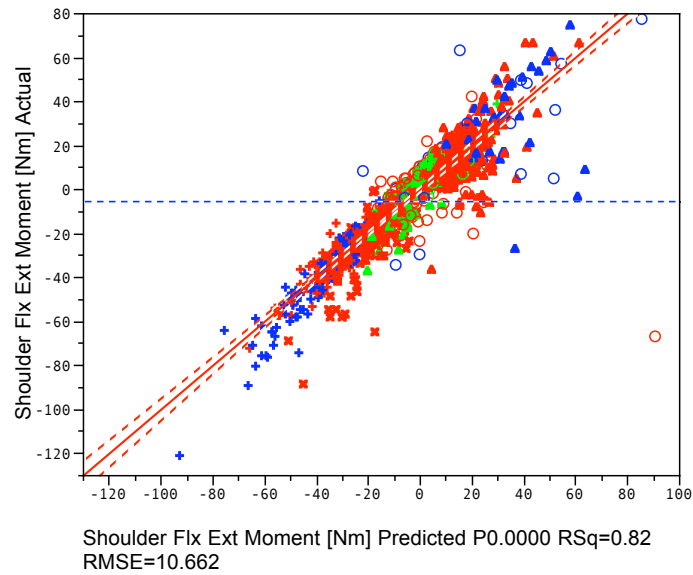


Figure 5.36. Actual versus predicted shoulder flexion/extension moment (Eqn 1) for **one-handed push, pull, up, and down** exertions at **mid-thigh, elbow, and overhead handle heights** ($p < 0.001$).

$$\begin{aligned}
 M_{\text{shoulder}} = & 3.484 - 43.21(x_{\text{shoulder}}/\text{stature}) - 23.56(h_{\text{shoulder}}/\text{stature})\dots \\
 & + 0.1277F_x + 1.288(h_{\text{shoulder}}/\text{stature} - 0.08835)(F_x + 11.1042)\dots \\
 & - 0.1588F_z - 1.338(x_{\text{shoulder}}/\text{stature} - 0.19226)(F_z - 27.8348)
 \end{aligned} \tag{1}$$

Relationships between residual shoulder flexion/extension moment and task parameters were investigated to assess model performance across trial conditions. Plots of residuals versus horizontal hand force, vertical hand force, BMI, stature, gender, handle height normalized to stature, nominal hand force direction, postural tactic, and aggregate shoulder strength were generated. No significant biases were found at $p \leq 0.05$.

Torso Inclination in the Hand-Force Plane

Changes in torso inclination across test conditions were found to be qualitatively different for push, pull, and up/down exertions. For this reason a separate regression model was developed for each type of exertion to predict torso inclination angle in the force plane. Gender, stature, and BMI were considered as potential predictors as were hand force (vertical and horizontal components), drop in shoulder from neutral standing height, shoulder height with respect to the point of force application, handle height, and second-order interactions.

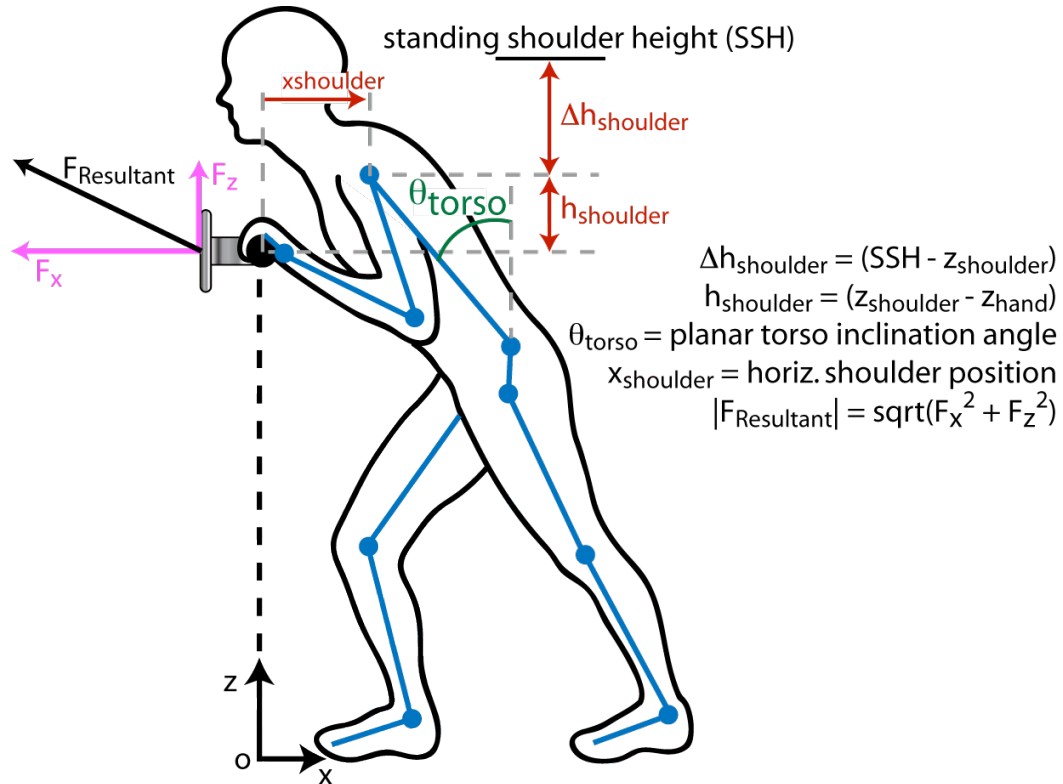


Figure 5.37. Hand force and postural metrics used to predict torso inclination in the hand-force plane. Torso inclination angle is with respect to the vertical and defined positive rearward.

Torso Inclination Angle Regression Model for Up/Down Exertions

Fore/aft shoulder location, change in shoulder height from neutral standing height, vertical hand force, and handle height were found to be the strongest predictors of torso inclination during two-handed vertical (up/down) exertions. The predictive equation is given by Equation (2), and model performance is shown in Figure 5.38. In general, torso inclination angle had less range during up/down exertions than during push/pull exertions but was not as well predicted.

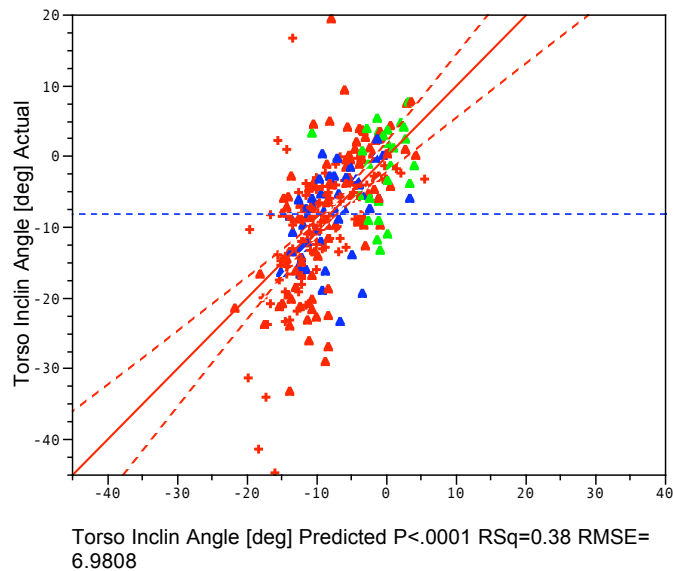


Figure 5.38. Actual versus predicted torso inclination angle (Eqn 2) for one-handed exertions in the vertical up/down direction spanning mid-thigh to overhead handle heights (R^2 Adj = 0.37, RMSE = 6.98, $p < 0.001$).

$$\theta_{torso} = -11.94 + 77.75(x_{shoulder}/stature) + 19.06(\Delta h_{shoulder}/stature) + 0.0163F_z + 0.0402F_x \quad (2)$$

Torso Inclination Angle Regression Model for Pull Exertions

Planar torso inclination angle during one-handed pulls is predicted by vertical hand force, handle height, change in shoulder height from neutral, and the interaction between the latter two variables. Change in shoulder height alone is not a significant predictor but the interaction with handle height is highly significant, thus the first-order term was included to have a proper model. All other terms in the model are highly significant ($p < 0.001$). Subject characteristics were not found to be significant predictors.

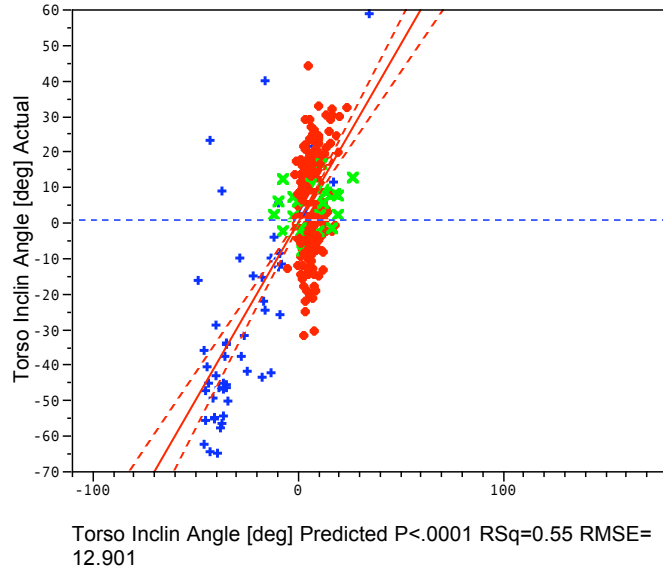


Figure 5.39. Actual versus predicted torso inclination angle (Eqn 3) for **one-handed pulls** spanning mid-thigh to overhead handle heights (R^2 Adj = 0.54, RMSE = 12.9. $p < 0.0001$).

$$\begin{aligned} \theta_{torso} = & -74.98 + 118.2(z_{handle} / stature) - 51.91(\Delta h_{shoulder} / stature) \dots \\ & -675.9(z_{handle} / stature - 0.62724)(\Delta h_{shoulder} / stature + 0.04815) + 0.1806F_z \end{aligned} \quad (3)$$

Residuals were examined to assess model performance across trial conditions and full range of subject anthropometrics. The model was found to perform well for all conditions with no significant biases.

Torso Inclination Angle Regression Model for Push Exertions

Two-handed push exertions yielded the strongest regression model for torso inclination angle with an adjusted R^2 value of 0.72 and root-mean-square error (RMSE) of 9.78 degrees. The model is also the simplest with change in shoulder height from neutral being the sole predictor of torso inclination angle (Equation 4). Gender, stature, BMI, vertical and horizontal hand force components, handle height, and all second-order interactions were also considered but none were found to be significant predictors.

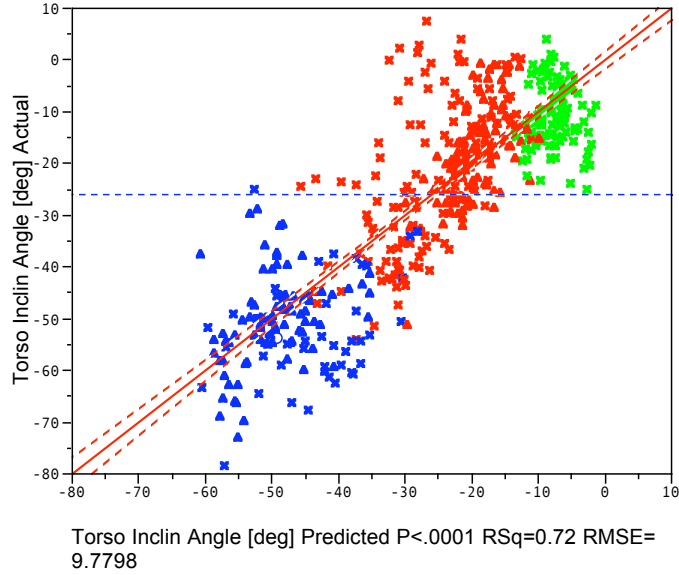


Figure 5.40. Actual versus predicted torso inclination angle (Eqn 4) for one-handed push exertions performed at mid-thigh, elbow, and overhead handle heights (R2Adj = 0.72, RMSE = 9.78 deg, p < 0.001).

$$\theta_{torso} = -12.02 + 152.42(\Delta h_{shoulder} / stature) \quad (4)$$

Pelvis Pitch with Respect to Torso Inclination

Pelvis pitch with respect to the hand-force frame and torso inclination angle are highly correlated thus pelvis pitch was predicted relative to torso inclination as opposed to predicting pelvis pitch relative to the hand-force frame. Torso inclination angle, handle height, and the interaction between handle height and torso inclination were found to be the strongest predictors of pelvis pitch angle (Equation 5).

$$\begin{aligned} \theta_{pelvis} = & 17.09 - 0.2067\theta_{torso} - 21.48(z_{handle} / stature) \dots \\ & + 0.3942(\theta_{torso} + 12.96)(z_{handle} / stature - 0.6422) \end{aligned} \quad (5)$$

The plot of actual versus predicted pelvis pitch angle (Figure 5.41) shows rearward extension of the pelvis with respect to the torso for exertions at thigh-height and forward flexion when exerting force overhead. The RMSE is relatively large compared to the range of pelvis pitch angles observed in the data but anthropometrics and additional task variables were not found to significantly improve model performance and the model was found to perform equally well across all test conditions.

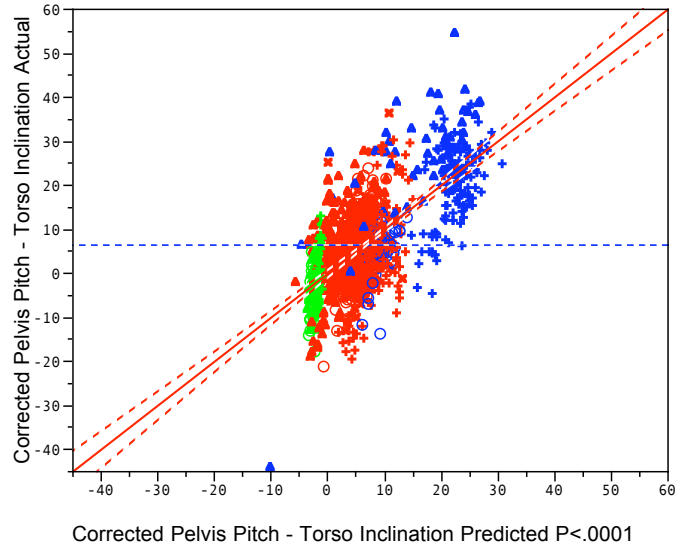


Figure 5.41. Actual versus predicted pelvis pitch with respect to torso inclination (Eqn 5) for one-handed exertions (R^2 Adj = 0.47, RMSE = 8.02, $p < 0.001$).

Base-of-Support (BOS) Length

For both push and pull exertions the distance along the x-axis of the hand-force frame from the pelvis to active boundary of the BOS was found to be the strongest predictor of BOS length. When pushing the rear boundary of the BOS acts as the active boundary whereas for pulling the front boundary is active, thus separate models were developed to predict the length of the BOS for push and pull exertions. For up/down exertions the variance in BOS length across trials was small and thus not predictable but instead represented by a mean value equal to approximately twice the offset from the pelvis to the rear boundary of the BOS. This suggests that during up/down exertions people center their pelvis over their BOS.

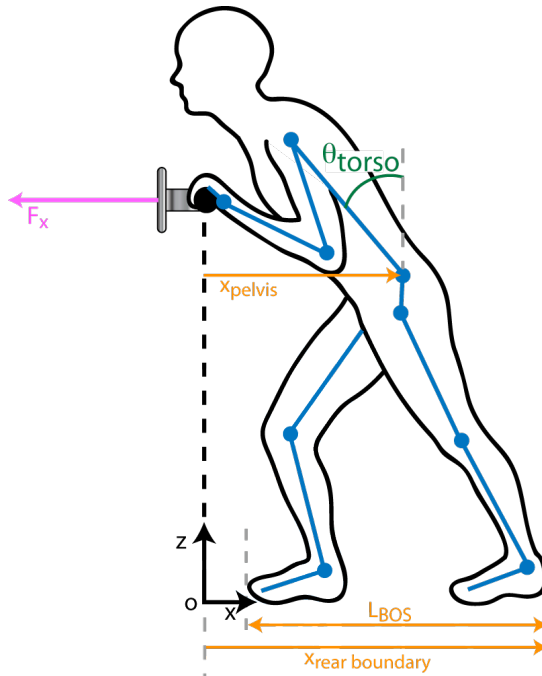


Figure 5.42. Definition of metrics used to predict base-of-support length for two-hand push exertions. The active boundary of the base-of-support is the rear boundary when pushing and front boundary when pulling.

BOS Length Regression Model for Push Exertions

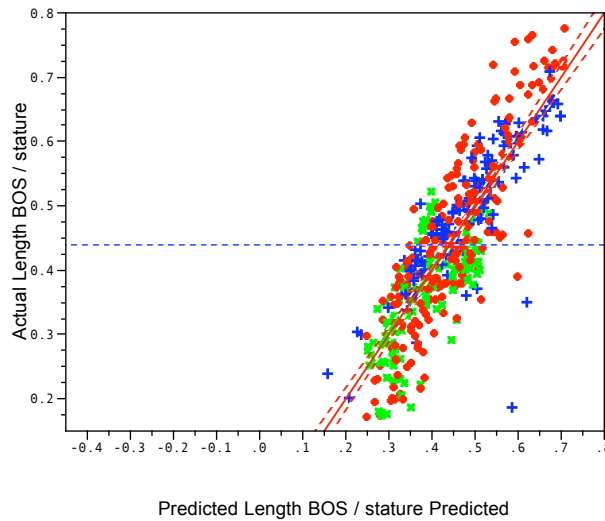


Figure 5.43. Actual versus predicted base-of-support length normalized by stature for one-handed push exertions performed at mid-thigh, elbow, and overhead handle heights (R^2 Adj = 0.72, RMSE = 0.066, $p < 0.001$).

$$L_{BOS} = -0.2176 + 0.00022stature + 1.120(x_{active\ boundary} - x_{pelvis})/stature \quad (6)$$

BOS Length Regression Model for Pull Exertions

$$L_{BOS} = -0.6308 + 0.2143(z_{handle}/stature) - 0.7178(x_{active\ boundary} - x_{pelvis})/stature... \quad (7)$$

$$+0.00039stature - 0.000766\alpha_{torso}$$

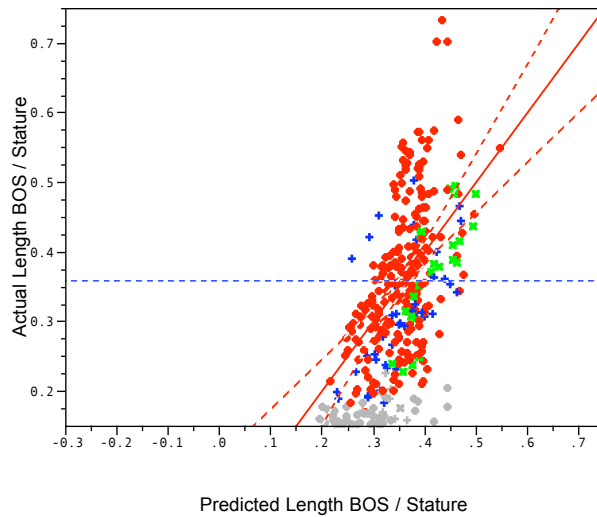


Figure 5.44. Actual versus predicted length of base-of-support for one-handed pulls (R^2 Adj = 0.27, RMSE = 0.087, $p < 0.001$).

5.7. Discussion

Analysis of one-hand force exertions is consistent with that of two-handed exertions presented in Chapter 4 and further supports the hypothesized biomechanical principles and behaviors. As with two-handed exertions, changes in one-handed postures in response to increasing hand forces were found to be consistent with the maintenance of shoulder flexion/extension moments below approximately 30 Nm. The only exception was for one-handed exertions in which internal bracing was used. Internal bracing was most prevalent during forward exertions at thigh-height. Shoulder flexion/extension moments were significantly larger for trials in which internal bracing was used. An increase in moment with bracing is not surprising since bracing the arm against the torso essentially unloads the shoulder, removing any limitations in force production capability associated with shoulder weakness.

As with two-handed postures, a preference towards neutral standing postures was also observed. In addition to low-back flexion/extension moments, it was hypothesized that rotational moment about the low-back is a significant determinant of posture during one-hand force exertions. As the level of force increased participants appeared to shift

their pelvis towards the hand force plane and/or rotate the torso in a manner consistent with reducing the low-back rotation moment. Rotational moments about the low-back were quantified and found to be small with moments less than or equal to +/-10 Nm during most trials. Maximum twisting moments in both symmetric and asymmetric postures have been quantified by Marras et al. (1998) and shown to range from approximately 50 to 60 Nm with maximum moments being greatest in symmetric postures. These values suggest that the rotational moments observed during this study are small and perhaps consistent with the strategy of minimizing the low-back rotational moment. However, the effect of pelvis twist on asymmetric loading of the low-back was examined by Kingma et al. (1998) and change in pelvis orientation was not found to produce a significant reduction in low-back loads.

The findings of this chapter suggest, that as with two-handed tasks, the biomechanics of one-hand force exertions can be used to predict key postural metrics required for development of a whole-body posture prediction model. Postural trends unique to one-hand exertions include axial rotation of the trunk, particularly during high-force pulls. This behavior reduces the moment arm from the point of force application to L5/S1 and is consistent with a desire to reduce low-back rotational moments. Rotation is not significant during one-hand push exertions and moment about the low-back instead may be reduced by shifting the pelvis laterally towards the hand-force plane as the level of required force increases.

Internal bracing is an additional and unexpected finding of this work and an area that is rarely addressed in the literature. During a study involving force exertion in awkward working postures Haslegrave et al. (1997) noted the tendency for subjects to use their free hand, wrist, or elbow to brace against their body. This study was similar to the work presented in this dissertation in that minimal constraints were placed on posture and subjects were encouraged to practice different techniques and strategies in order to identify their preferred posture. The prevalence of self-bracing or internal bracing in the work presented here and in the work of Haslegrave et al. suggests self-bracing is a worthwhile area for future research. Furthermore, external bracing, a behavior prevalent in industry also has not been well documented or studied and is a natural extension of this work.

5.8. References

- de Looze, M. P., van Greuningen, K., Rebel, J., Kingma, I., and Kuijer, P. P. (2000). Force direction and physical load in dynamic pushing and pulling. *Ergonomics*, 43(3):377–390.
- Granata, K. R. and Bennett, B. C. (2005). Low-back biomechanics and static stability during isometric pushing. *Hum Factors*, 47(3):536–549.
- Haslegrave, C. M., Tracy, M. F., and Corlett, E. N. (1997). Force exertion in awkward working postures—strength capability while twisting or working overhead. *Ergonomics*, 40(12):1335–1362.
- Kingma, I., van Dieen, J. H., de Looze, M., Toussaint, H. M., Dolan, P., and Baten, C. T. (1998). Asymmetric low back loading in asymmetric lifting movements is not prevented by pelvic twist. *J Biomech*, 31(6):527–534.
- Kumar, S., “Isolated planar trunk strengths measurement in normals: Part III – Results and database,” *International Journal of Industrial Ergonomics* 17:103-111 (1996).
- Marras, W. S., Davis, K. G., and Granata, K. P. (1998). Trunk muscle activities during asymmetric twisting motions. *J Electromyogr Kinesiol*, 8(4):247–256.

CHAPTER 6

DEVELOPMENT AND VALIDATION OF A THREE-DIMENSIONAL BIOMECHANICAL POSTURE PREDICTION MODEL FOR STANDING HAND FORCE EXERTIONS

6.1. Abstract

Task postures have a strong effect on ergonomic analyses with digital human models because posture is a significant determinant of key outcome measures such as joint loads and balance assessment. A model that accurately predicts whole-body postures for standing hand-force exertions would improve the utility and repeatability of job analyses. Importantly, a model should be able to perform accurately across a substantial percentage of force exertion conditions encountered in industry while reproducing most of the tactics that workers use.

This chapter presents a new modeling approach based on a small set of biomechanical principles. The overarching hypothesis is that a well-designed biomechanical model can make accurate predictions with only minimal reliance on empirical findings. The resulting model has a high level of generality, producing accurate predictions for a wide range of one-hand and two-hand standing force exertions, is computationally simple, and is robust to interpolation and extrapolation. The only model inputs are worker body dimensions and the force exertion location, direction, and related measures.

This chapter demonstrates that postural behaviors quantified in the laboratory are consistent with proposed biomechanical principles. Rather than beginning with data fitting, the model was developed using a qualitative, knowledge-based process, yielding a model that could reproduce with good fidelity the major characteristics of human behavior for the tasks of interest without relying on parameters fit from data. The model

was then tuned using data from 80% of the laboratory trials and validated against the remaining 20%. A qualitative assessment of model performance showed that the model produced a good subjective correspondence between observed and predicted postures. Moderate to high correlations were observed between the model predictions and observed shoulder locations, pelvis locations, and torso inclinations. The model has substantial utility for predicting force-exertion postures for analysis of industrial tasks, particularly for push and pull exertions. The error distributions reported here can be used to bound the confidence of those analyses.

6.2. Introduction

Requirements for Posture Prediction Models used for Ergonomics

Accurate representation of working postures is critical for ergonomic assessments with digital human models because posture has a dominant effect on analysis outcomes. Most current digital human modeling tools require manual manipulation of the digital human to simulate force-exertion postures or rely on optimization procedures that have not been validated. Automated posture prediction based on human data would improve the accuracy and repeatability of analyses. A model intended for ergonomic evaluation of industry jobs must only require, as input, information which is readily available to ergonomists. The model must produce accurate postures for the range of task conditions observed in industry and be capable of replicating the different postural strategies prevalent in industry. Model performance should be assessed based on the model's ability to yield, for a predicted posture, ergonomic outcome measures consistent with analysis of actual working postures.

Previous Approaches to Posture Prediction for Standing Tasks

Several strength-based posture-prediction models have recently been developed suggesting a high level of interest in this area. At the Technische Universität München in Germany, measures of forces, internal and external, and discomfort are being used to predict posture (Seitz et al., 2005). Work regarding posture prediction is also ongoing at the University of Pennsylvania where strength is used as a 'naturalness' constraint to ensure that predicted postures look realistic (Liu, 2003 & Zhao et al., 2005). This shared interest in strength-based posture prediction speaks towards the significance of the

problem and the lack of validation of existing posture-prediction models supports the need for additional research in this area. Seitz et al. (2005) acknowledge that while computed postures are “plausible,” a comparison has not been made between predicted and actual postures to assess the accuracy of the predictions. Similarly, the work by Liu (2003) and Zhao et al. (2005) has proven capable of predicting “natural” as opposed to “awkward” postures but, naturalness is not a quantitative measure and again predicted postures have not been compared against postures actually used by workers.

Statistics-based models have been used extensively for posture prediction. These models use regression equations to define a posture based on a set of input variables identified from data as significant determinants of posture. The University of Michigan’s 3D Static Strength Prediction Program (3DSSPP) posture prediction feature is based on this type of approach. Regression equations based on data from Kilpatrick and Snyder et al. were assimilated to form a behavioral inverse kinematics algorithm (Beck, 1992). This algorithm defines whole-body postures by predicting body segment positions based on hand location and orientation (supine, semi-prone, or prone), and worker height and weight.

The limited predictive capability of statistics-based models is illustrated by 3DSSPP’s inability to predict realistic postures for high-exertion tasks. As with all statistics-based models the behavioral inverse kinematics algorithm is based on a finite data set collected under a small number of conditions, relative to the possible application domain. Using the regression equations to predict postures for conditions not included in the data set often results in inaccurate postures; however, a data set which contains all possible conditions of interest is unrealistic suggesting this is not a robust approach to posture prediction.

An important point to emphasize is that the fundamental problem with previous statistical approaches to standing posture prediction is not that they are empirical, but that the parameterization that is used does not allow good interpolation and extrapolation, that is, it does not model the underlying behavior well. For example, linear statistical models are often used to predict postural variables that are not likely to be truly linear in a larger dataset. A proposition of the current work is that empirical models are most effective when placed within a model structure that predicts most of the behavior by applying

biomechanical principles. Because the model structure incorporates most of the nonlinearities and physics-based effects, relatively few empirical tuning models for selected parameters are all that is required to provide good performance for a large range of task conditions.

Biomechanical Posture Prediction: Overview of Approach

Posture prediction based on biomechanical principles is an alternative approach proposed by this research. Behaviors observed during pilot work and an automotive plant study, and results from a simulation study using 3DSSPP suggest posture selection is largely driven by biomechanics. Observations from the literature also support this approach. A biomechanical approach to posture prediction is preferable in that the predictive capability will not be limited to a specific data set but instead will be applicable to a wide range high-force standing exertions.

Support for Biomechanical Approach

Knowledge of postural behaviors acquired through a laboratory study and review of the literature has been coupled with human-body kinematics and the mechanics of force exertion and balance to develop the model. Predictions are driven by sensitivity to external shoulder loads and static balance requirements, subject to the constraints of upper- and lower-extremity kinematics.

Postural Behaviors Observed in Laboratory and Industry

Behaviors observed in the laboratory and automotive plants suggest posture-selection during standing hand-force exertions is driven by biomechanics and basic mechanics. Statistical analyses of data quantifying the effects of hand force location, magnitude, and direction on standing task postures (Chapters 4 and 5) support these observations as does work by Gaughran and Dempster (1956) and Kerk et al (1994). In these studies basic mechanics and task constraints, coupled with knowledge of strength and balance limitations were shown to be indicators of preferred postures.



Figure 6.1. Laboratory and industry postures consistent with hypothesized biomechanical principles.

Explanations of Hand Force and Posture from Literature

Researchers have proposed several biomechanical explanations for the observed posture and force-exertion trends in push/pull tasks with a focus on posture and hand force direction. Granata et al. (2005) hypothesized that people apply an upward force when pushing: (1) to reduce moments at the low back and possibly at the shoulder, and (2) to recruit lower-body strength. The first reason is based on their observation that participants tend to align the force vector along their spine, passing the vector through their lumbosacral joint, by flexing their elbows and increasing torso flexion as the level of exertion increases. Small L5/S1 moments observed during maximum push exertions support this explanation. Similarly, de Looze et al. (2000) explained small changes in shoulder moments over a range of handle heights and horizontal force levels by a tendency to maintain alignment of the resultant hand force vector through the shoulder joint. Friction has also been cited as an explanation for changes in hand force magnitude and direction (Dempster, 1958, Boocock, et al., 2006). These observations suggest a strong relationship between hand force and posture during pushing exertions that supports development of a biomechanics-based posture-prediction model.

6.3. Model Development

Human body kinematics and the constraint of static balance were combined with select empirical models to develop a three-dimensional biomechanics-based posture-prediction model. A linkage representation of the human body was created to impose kinematic constraints on the predicted posture. For the purpose of implementation a

kinematic linkage was defined using the Denavit-Hartenberg convention and is described in Section 6.4. Given the kinematics of the linkage, the hand location(s) specified by the task bound the solution space of feasible postures. Predicted postures must be in static balance, which further constrains the problem. Task hand location(s) and the required hand force define the applied moment that must be countered by the linkage for the posture to be in static equilibrium. Given a pelvis location, defined by upper-extremity and torso kinematics, a shoulder moment threshold, and select postural metrics (e.g. elbow angle, torso and pelvis orientations), a target center-of-pressure (COP) location is computed. The target COP location is defined relative to the pelvis location and is the point of the ground about which the moment due to body weight balances the moment due to the applied hand forces. From this target COP location the active boundary of the BOS (the front boundary if pulling, rear boundary if pushing) is set and the remaining postural metrics (e.g. BOS length) predicted from empirical models. This process of using kinematics and static balance requirements in combination with postural metrics predicted from data to define task postures for standing hand-force exertions is illustrated in Figure 6.2. The structure of the model and postural metrics selected for prediction are based on a set of biomechanical hypotheses derived from observation and review of the literature and supported by analysis of laboratory data.

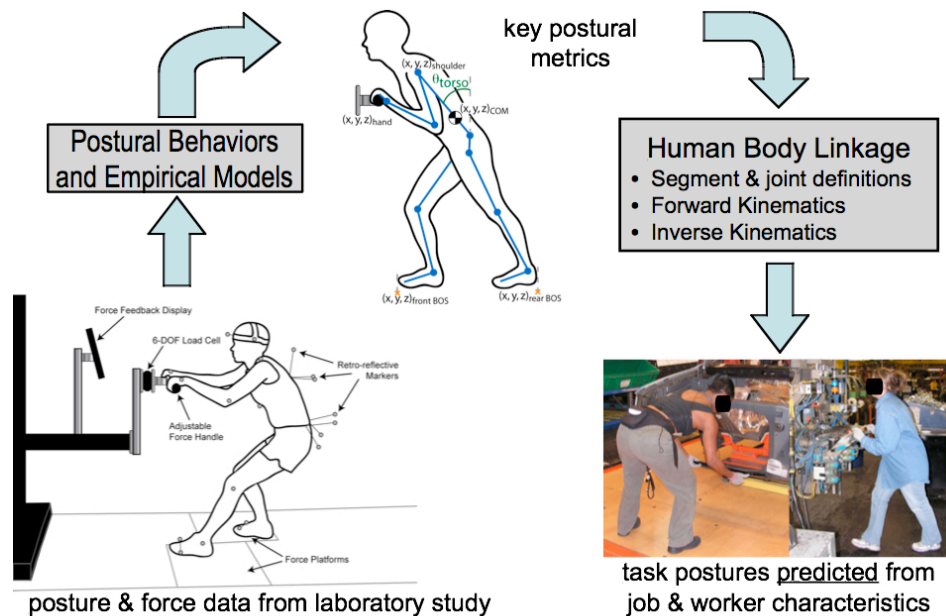


Figure 6.2. High-level model development process: postural behaviors (sensitivity to joint loads, standing balance requirements and aversion to slips and falls) and empirical models from data are used to predict key postural metrics, which coupled with kinematics, define task postures.

Underlying Biomechanical Principles

The analysis of laboratory data presented in chapters 3, 4, and 5 largely supported the proposed hypotheses concerning posture-selection behavior. Hence, the model structure that was developed in conjunction with these hypotheses was retained with only minor adjustments. The principal findings from the laboratory data that were used in model development are:

1. A desire to maintain shoulder moment within an acceptable range leads to two complementary behaviors:
 - a. When permitted by the task conditions, people exert substantial off-axis forces, producing higher-than-required load magnitudes but directing the force vector toward the shoulder. Across subjects and trials, 90% of calculated shoulder moments were below 31 Nm.
 - b. When permitted by the task conditions, people position and orient their torsos to place their shoulders closer to the hand force vector. The data showed strong associations between force magnitude and shoulder position with respect to the hands, particularly for thigh-height tasks where lowering the shoulder requires increased torso inclination.
2. The position and length of the base of support changes with hand force magnitude and direction, consistent with the need to use the moment generated by body weight around the active margin of the base of support to generate the required hand force.

Overview of Model Structure and Posture Prediction Sequence

Model inputs were restricted to task parameters and worker characteristics readily available to ergonomists analyzing industrial tasks. Inputs include the hand applying the force (right or both), required hand force magnitude and direction, whether or not hand force direction is constrained, and the height of the point of force application with respect to the ground. Worker inputs include gender, stature, and body mass. Worker-specific strengths are not generally known by ergonomist and thus were not included as potential model inputs. The exclusion of strength, specifically an aggregate measure of shoulder strength, as a model input is supported by analyses in Chapter 4 and Chapter 5 where individual isolated shoulder strengths and an aggregate measure of isolated shoulder

strength were not found to be significant determinants of posture. Given task and worker descriptors, the model predicts the actual hand force exerted and three-dimensional whole-body standing task posture.

Predictions are dependent on model parameter values, most of which are set based on the analysis of the laboratory data. The parameters are given in Table 6.1 and illustrated in Figure 6.3 and regression equations for predicting postural metrics presented in subsequent sections.

Table 6.1. Empirical parameters used in the posture-prediction model.

Variable	Definition	Value
Shoulder Moment Threshold	Maximum magnitude of shoulder flexion/extension moment	20 Nm
Center of Pressure Margin	Distance from active edge of base of support to center of pressure	0 for initial model assessment; to be set to fraction of BOS length
Neutral Standing Shoulder Height	Height of the shoulder with respect to ground when standing in an upright, neutral posture	computed as the sum of lower-extremity and torso link lengths
Squat Limit	Minimum allowable vertical pelvis location with respect to the ground.	40% of stature (pelvis height < 40% of stature in only 10% of all trials)

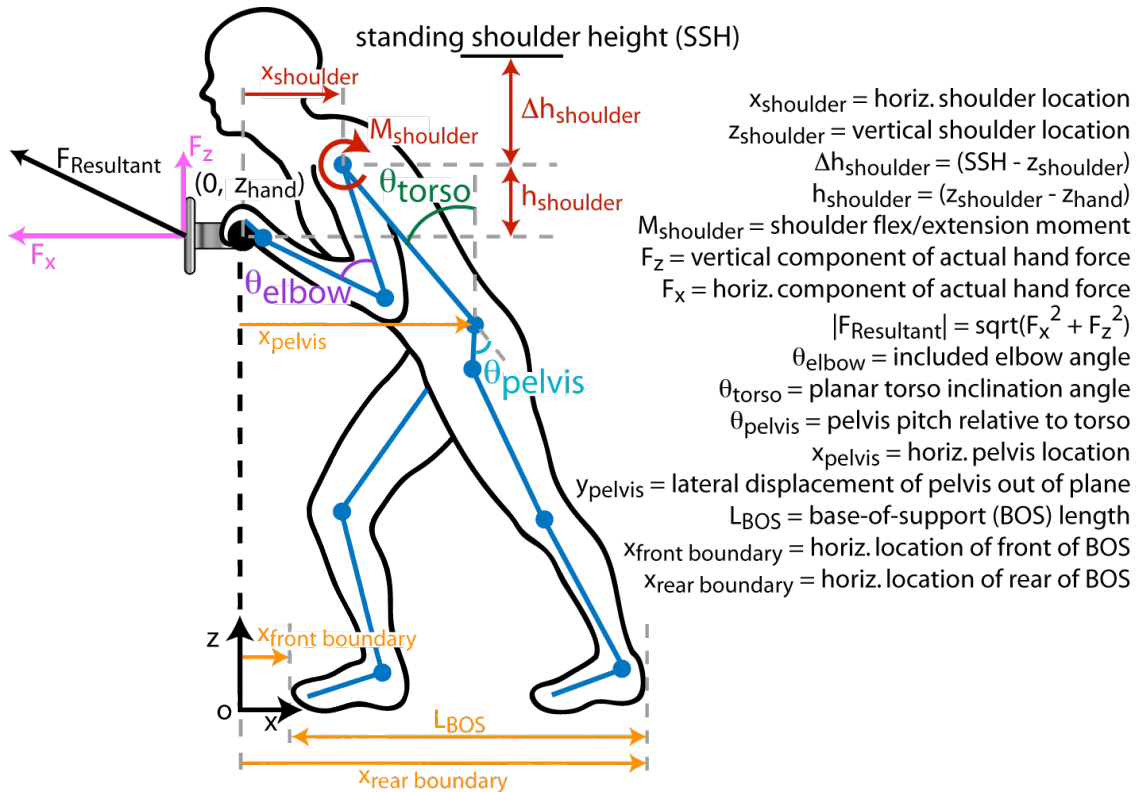


Figure 6.3. Definition of postural metrics used to define standing hand-force postures.

Predictions are also dependent on the tactic or postural strategy selected. For a given set of inputs the most probable postural strategy is selected. Alternatively, users may also choose to predict a certain postural strategy by specifying a tactic vector. Via the tactic vector users can specify an open (rotation to the left) or closed (rotation to the right) torso posture, flexed versus extended elbow posture, and whether the right or left foot leads. As discussed in Chapters 4 and 5, tactic was not well predicted by task or subject variables.

Figure 6.4 shows the model posture prediction sequence and process for mapping predicted postural metrics onto the kinematics linkage to ensure predicted postures are kinematically consistent. The task and worker variables, along with the user-specified tactic vector, is input to the computational model.

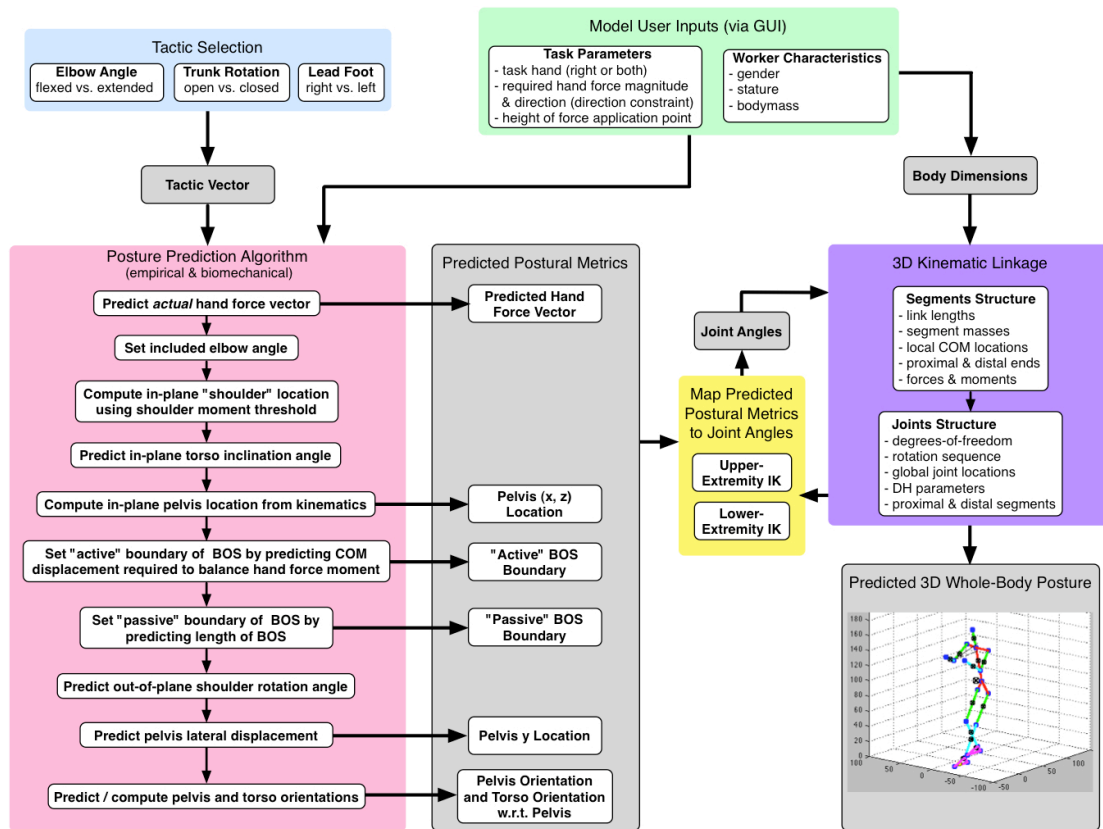


Figure 6.4. Main components and overall flow of the model.

Model Formulation

The posture prediction algorithm is comprised of a series of steps that define key aspects of posture and is explained in detail by sequentially describing each step in the process.

1. Compute Actual Hand Force Vector and Define Hand-Force Plane

Simple linear regression models relating actual and requested hand forces were developed in Chapter 3 and are implemented in the model to predict actual hand forces from the requested hand force vector. If the force direction is unconstrained (off-axis forces are permitted, but the on-axis force must reach the specified magnitude), the actual hand force is computed from the regression models in Chapter 3. Because separate regression models were obtained for each handle height, linear interpolation is used to estimate actual forces for intermediate handle heights (as a fraction of stature). For tasks in which force direction is constrained, the actual and requested hand force vectors are assumed to be equivalent. The actual hand force vector is then used to define the hand-force plane and the rotation matrix relating the global and hand-force plane coordinate frames (Figure 6.5). All postural metrics are defined with respect to the hand-force plane and a simplified planar linkage used for predicting key postural metrics in this vertical plane.

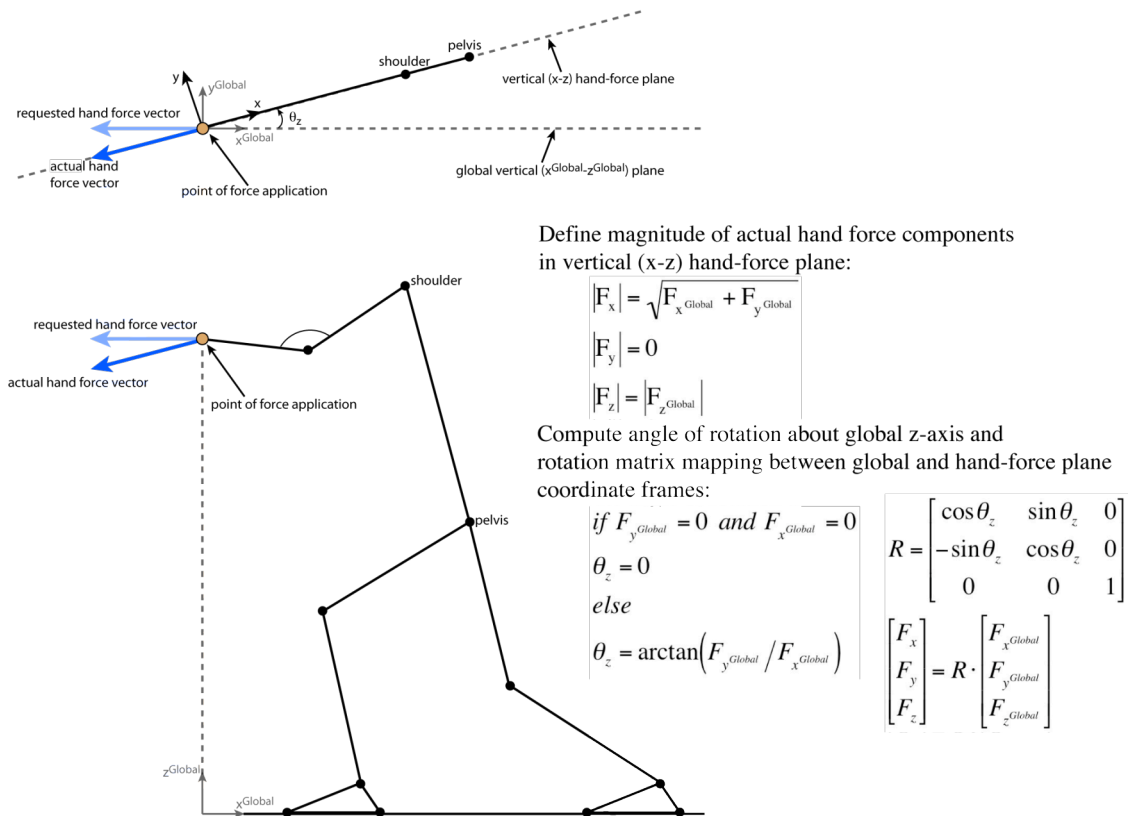


Figure 6.5. Top and side-view of hand-force plane defined as the vertical plane in which the actual hand-force vector lies. Transformation between the global and hand-force plane coordinate frames is performed by the rotation matrix, R , a pure rotation of θ_z about the global z -axis. As defined, the z -axis of the global and hand-force coordinate frame is coincident.

2. Predict Included Elbow Angle

Given a set of task descriptors and tactic vector, included elbow angle is set to the corresponding mean value from data (Table 6.2). Within handle handles, different mean values were used for trial conditions in which included elbow angle was found to be significantly different ($p < 0.0001$). Linear interpolation of mean values is used to compute an included elbow angle for tasks with hand location(s) between handle heights tested in the laboratory. For one-handed tasks, the idle arm was specified to be in a neutral posture along side the body with an included elbow angle of 170 degrees.

Table 6.2. Mean included elbow angles [degrees] specified for different task conditions.

Number of Hands	Simplified Hand Force Direction	Handle Height	Additional Specifier (tactic, constraint, etc)	Included Elbow Angle
Two	Push	All	Flexed-elbow	54
			Extended-elbow	130
	Pull	Overhead		136
		Elbow-height		114
		Thigh-height	Directionally constrained	114
			Directionally unconstrained	142
	Up	Overhead		113
		Elbow-height	$F_z \geq 80\% \text{ BW}$ (push up)	34
			$F_z < 80\% \text{ BW}$ (pull up)	70
	Thigh-height		154	
	Down	All		75
One	Push	All	Flexed-elbow (male / female)	45 / 61
			Extended-elbow (open / closed)	138 / 123
	Pull	Overhead		140
		Elbow-height	Open/neutral torso	138
			Closed torso	97
		Thigh-height	Directionally constrained	121
	Directionally unconstrained		151	
	Up	Overhead		128
		Elbow-height	$F_z \geq 80\% \text{ BW}$ (push up)	38
			$F_z < 80\% \text{ BW}$ (pull up)	74
	Thigh-height		155	
	Down			78

3. Position Shoulder with Respect to Point of Force Application

Elbow angle and upper-extremity segment lengths constrain the shoulder to an arc centered at the point of force application (Figure 6.6). Starting from a neutral standing shoulder height, the planar shoulder is incrementally lowered along the arc defined by the kinematics of the upper-extremity until the shoulder moment threshold is satisfied. If the threshold cannot be satisfied, the two-dimensional shoulder location yielding the smallest absolute moment is selected and the user notified.

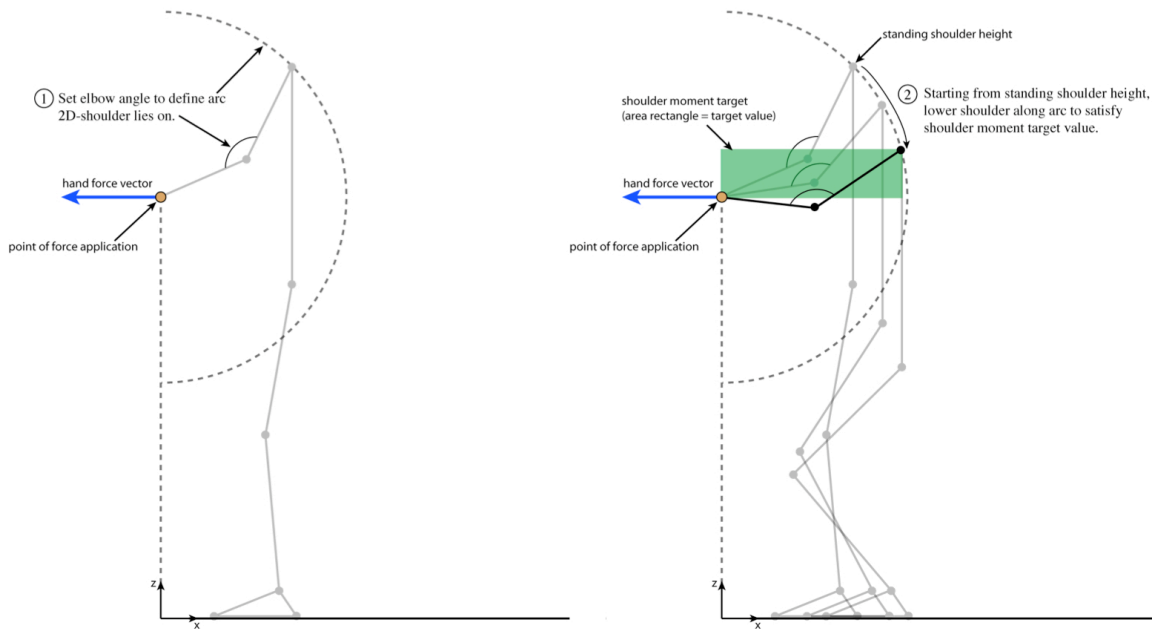


Figure 6.6. Use kinematics of upper-extremity (1) and shoulder moment threshold (2) to set two-dimensional shoulder location in the hand-force plane.

4. Set Torso Inclination in the Hand-Force Plane

Torso inclination angle in the hand force plane, a measure of torso flexion/extension for two-handed tasks and lateral bending for one-handed tasks, is predicted empirically to define pelvis location in the hand force plane (Figure 6.7). Separate regression models were developed in Chapter 4 and Chapter 5 for torso inclination during two and one-hand up/down, push, and pull exertions and are summarized in Table 6.3. Pelvis location in the vertical hand-force plane is determined by rotating the torso vector, defined by the planar shoulder location and torso segment, through the predicted torso inclination angle (rearward extension defined positive).

Table 6.3. Regression equations for predicting torso inclination in the hand-force plane.

Number Hands	Simplified Hand Force Direction	Regression Equation for Planar Torso Inclination Angle [deg]	R ² Adj	RMSE [deg]
Two	Up/Down	$\theta_{torso} = -72.17 + 129.9(x_{shoulder}/stature) + 65.58(h_{shoulder}/stature) \dots + 0.0131F_z + 71.71(z_{handle}/stature)$	0.61	5.81
	Push	$\theta_{torso} = -8.175 + 169.3(\Delta h_{shoulder}/stature)$	0.72	7.64
	Pull	$\theta_{torso} = -57.0 + 87.71(z_{handle}/stature) + 11.52(\Delta h_{shoulder}/stature) \dots - 464.7(z_{handle}/stature - 0.6262)(\Delta h_{shoulder}/stature + 0.0692) + 0.0874F_z$	0.65	12.1
One	Up/Down	$\theta_{torso} = -11.94 + 77.75(x_{shoulder}/stature) + 19.06(\Delta h_{shoulder}/stature) \dots + 0.0163F_z + 0.0402F_x$	0.37	6.98
	Push	$\theta_{torso} = -12.02 + 152.42(\Delta h_{shoulder}/stature)$	0.72	9.78
	Pull	$\theta_{torso} = -74.98 + 118.2(z_{handle}/stature) - 51.91(\Delta h_{shoulder}/stature) \dots - 675.9(z_{handle}/stature - 0.62724)(\Delta h_{shoulder}/stature + 0.04815) + 0.1806F_z$	0.54	12.9

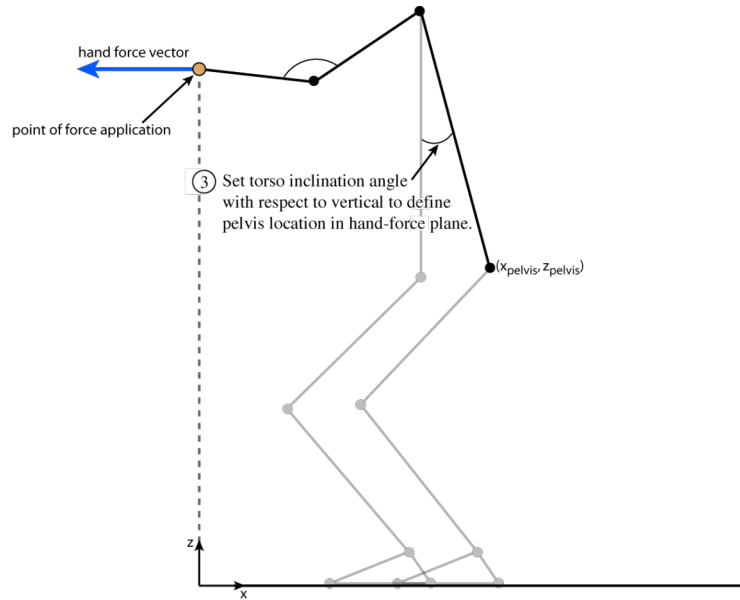


Figure 6.7. Set torso inclination angle to obtain pelvis location in the hand-force plane.

5. Compute Foot Placements in the Hand-Force Plane

Foot placements are set to satisfy balance requirements. Static balance requirements, and the assumption that people push off their rear foot and pull off their front foot, are used to compute a target center-of-pressure (COP) location:

$$x_{COP} = \frac{bodymass \cdot g \cdot x_{COM} - z_{handle} \cdot F_x}{F_z + bodymass \cdot g} \quad (1)$$

In Equation (1) whole-body center-of-mass location (x_{COM}) is unknown since the task posture is not yet fully defined and is approximated by torso center-of-mass location. Within the hand-force plane, the active foot (the rear foot if pushing and forward foot if pulling) is placed such that the target COP lies a prescribed distance (defined by the BOS margin) from the active edge (heel if pushing, toe if pulling) of the foot (Figure 6.8). In the current implementation the BOS margin is set to zero but will be defined as a fraction of BOS length in future implementations to capture the shift in COP location from the center to active edge of the BOS with increasing hand force.

Placement of the passive foot in the hand-force plane is defined by the length of the base-of-support, which is predicted from data (Figure 6.8). Base-of-support length during push/pull exertions is predicted as a percent of stature from the equations developed in Chapter 4 and Chapter 5 and provided in Table 6.4. For vertical (up/down) exertions base-of-support length was found, on average, to be equal to approximately twice the offset from the pelvis to the rear edge of the base-of-support. These postural metrics, in combination with kinematics, fully define the task posture in the hand-force plane. The task posture is expanded into the third dimension through the prediction of subsequent postural metrics.

Table 6.4. Regression equations used to compute base-of-support length as a fraction of stature.

Number Hands	Simplified Hand Force Direction	Regression Equation for BOS Length / Stature	R ² Adj	RMSE
Two	Up/Down	$L_{BOS} = 2 x_{rear\ boundary} - x_{pelvis} /stature$	-	-
	Push	$L_{BOS} = -0.4495 + 0.00036stature \dots$ $+1.151(x_{rear\ boundary} - x_{pelvis})/stature + 0.00027F_x$	0.62	0.075
	Pull	$L_{BOS} = -0.5853 + 0.00029stature + 0.2428(z_{handle}/stature) + 0.00076\theta_{torso} \dots$ $-0.00989(z_{handle}/stature - 0.6340)(\theta_{torso} + 4.187) - 1.157(x_{front\ boundary} - x_{pelvis})/stature$	0.56	0.083
One	Up/Down	$L_{BOS} = 2 x_{rear\ boundary} - x_{pelvis} /stature$	-	-
	Push	$L_{BOS} = -0.2176 + 0.00022stature + 1.120(x_{rear\ boundary} - x_{pelvis})/stature$	0.72	0.066
	Pull	$L_{BOS} = -0.6308 + 0.2143(z_{handle}/stature) \dots$ $-0.7178(x_{front\ boundary} - x_{pelvis})/stature + 0.00039stature - 0.000766\alpha_{torso}$	0.27	0.087

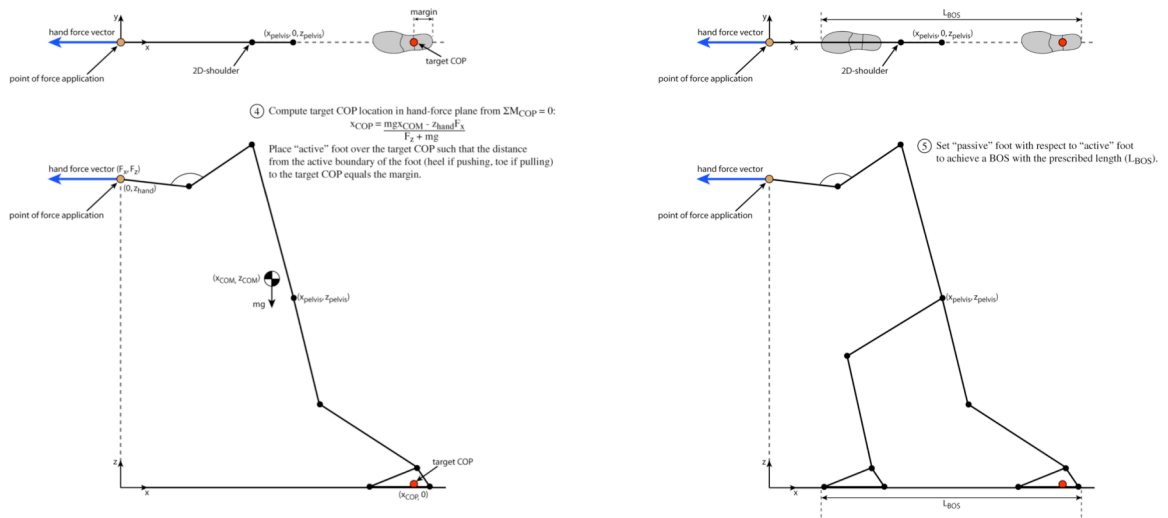


Figure 6.8. Use target COP location computed from static equilibrium condition to position “active” foot (4). Set “passive” foot with respect to “active” foot to achieve desired BOS (5).

6. Set Out-of-Plane Shoulder Rotation Angle

Open versus closed torso postures are specified by the shoulder rotation angle defined with respect to the y-axis of the hand-force coordinate frame (Figure 6.9). During two-hand exertions the out-of-plane rotation angle was found to be small and is assumed zero in the model. Out-of-plane rotation angle during one-hand exertions is predicted by the regression equations presented in Table 6.5.

Table 6.5. Regression equations developed to predict out-of-plane rotation angle during one-hand exertions.

Number Hands	Simplified Hand Force Direction	Torso Tactic	Regression Equation for Out-of-Plane Shoulder Rotation Angle [deg]	R ² Adj	RMSE
Two	All		0	-	-
One	Push	Open	$\alpha_{\text{torso}} = -46.3 + 0.041 \text{stature} \dots$ $-20.9(z_{\text{handle}}/\text{stature}) + 45.6(x_{\text{shoulder}}/\text{stature})$	0.23	10.7
		Neutral	2.8 (left foot leads) / -2.8 (right foot leads)	-	-
		Closed	$\alpha_{\text{torso}} = -72.2 + 177(x_{\text{shoulder}}/\text{stature}) \dots$ $+45.1(h_{\text{shoulder}}/\text{stature}) - 0.05F_x$	0.38	21.24
	Pull	Open / Neutral	$\alpha_{\text{torso}} = -169 + 0.114 \text{stature} + 0.102F_x$	0.56	14.3
		Closed	$\alpha_{\text{torso}} = -72.2 + 177(x_{\text{shoulder}}/\text{stature}) \dots$ $+45.1(h_{\text{shoulder}}/\text{stature}) - 0.05F_x$	0.38	21.24
	Up/Down		$\alpha_{\text{torso}} = 35.8 + 195(x_{\text{shoulder}}/\text{stature}) - 0.013F_z$	0.33	16.0

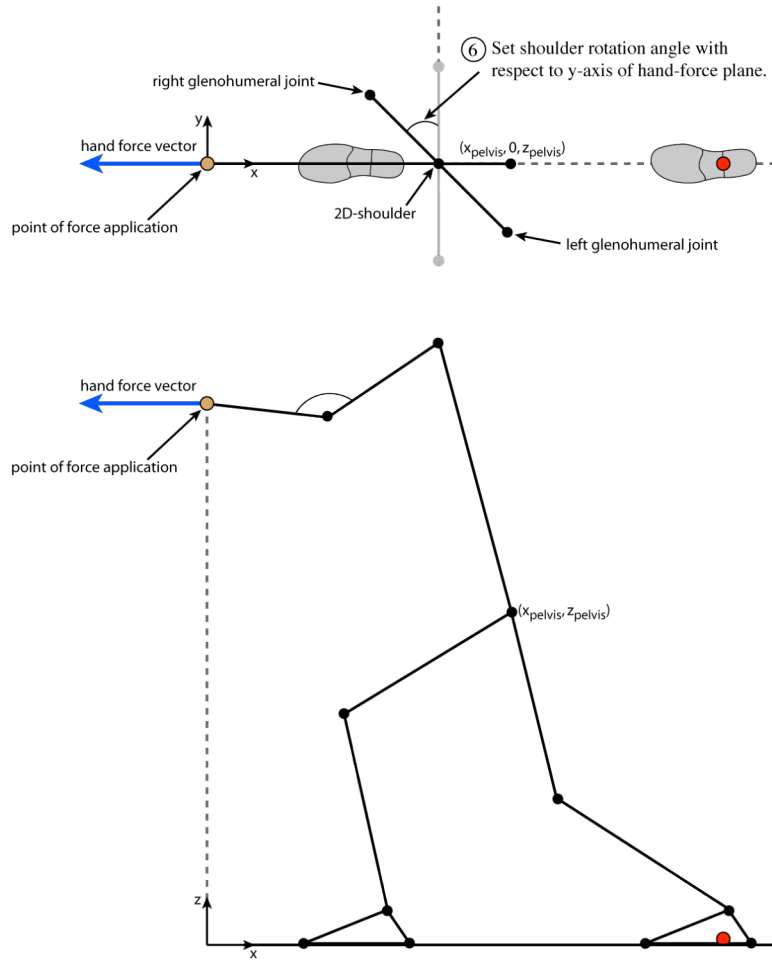


Figure 6.9. Orientation of shoulder vector with respect to hand-force plane used to define pelvis and torso orientations with respect to the hand-force plane.

7. Lateral Displacement of Pelvis out of Hand-Force Plane

Lateral displacement of the pelvis out of the hand-force plane defines pelvis location in three-dimensional space (Figure 6.1). In Chapter 4 lateral displacement of the pelvis during two-handed exertions was found to be small and thus is assumed zero. Lateral displacement of the pelvis was found to be significant for a subset of one-hand tasks and is predicted by the equations presented in Table 6.6

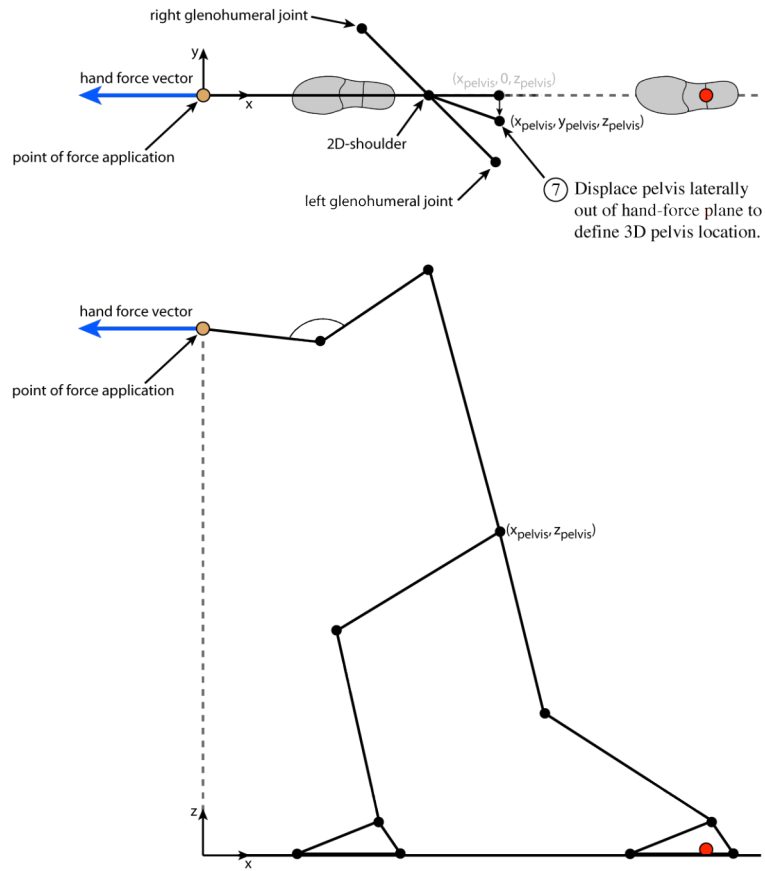


Figure 6.10. Lateral displacement of the pelvis out of the hand-force plane to define 3D pelvis location.

Table 6.6. Predictive equations and mean values used to define lateral displacement of the pelvis during one-hand exertions.

Simplified Hand Force Direction	Handle Height	Regression Equation for Lateral Pelvis Displacement [cm]	R ² Adj	RMSE [cm]
Down		$y_{pelvis} = 0$	-	-
Up		$y_{pelvis} = -34.1 - 294(x_{shoulder}/stature)$	0.08	54.0
Push	Overhead	$y_{pelvis} = -110 - 0.365F_x$	0.19	31.8
	Elbow-height	$y_{pelvis} = -107 - 0.214F_x$	0.06	71.7
	Thigh-height	$y_{pelvis} = -43.2$	-	-
Pull	Overhead	$y_{pelvis} = -74.5$	-	-
	Elbow-height	$y_{pelvis} = -85.5 - 0.257F_x$	0.09	67.3
	Thigh-height	$y_{pelvis} = 47.1$	-	-

8. Compute Pelvis and Torso Orientations

Pelvis pitch relative to the torso, defined in Figure 6.11, is predicted from planar torso inclination angle and the vertical location of the hand(s) (Table 6.7). Pelvis pitch in

three-dimensional space is then computed as the sum of the relative pelvis pitch angle and planar torso inclination angle (Equation 2). Based on the data analysis in Chapters 4 and 5, pelvis yaw is set to zero during two-handed exertions and predicted by Equation 3 for one-handed exertions. Similarly, pelvis roll is set to zero during all exertions.

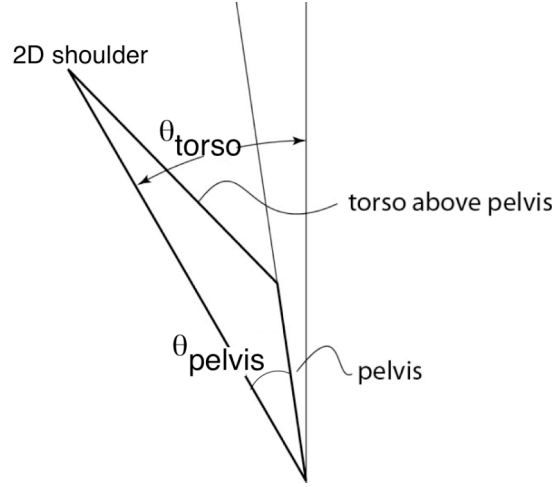


Figure 6.11. Definition of pelvis pitch angle (θ_{pelvis}) relative to the torso.

Table 6.7. Regression equations for pelvis pitch angle [deg] relative to the torso.

Number Hands	Regression Equation for Relative Pelvis Pitch	R ² Adj	RMSE [deg]
Two	$\theta_{pelvis} = 19.35 - 0.1902\theta_{torso} - 28.08(z_{handle}/stature) \dots$ $+ 0.5590(\theta_{torso} + 13.21)(z_{handle}/stature)$	0.42	7.71
One	$\theta_{pelvis} = 17.09 - 0.2067\theta_{torso} - 21.48(z_{handle}/stature) \dots$ $+ 0.3942(\theta_{torso} + 12.96)(z_{handle}/stature - 0.6422)$	0.47	8.02

$$\theta_{pelvis}^{Global} = \theta_{pelvis} + \theta_{torso} \quad (2)$$

$$\psi_{pelvis}^{Global} = -1.34 + 1.11\alpha_{torso} - 0.052F_x \quad (3)$$

Torso orientation is defined by lumbar flexion/extension, axial rotation, and lateral bending angles. Trigonometric relations are used to compute a lumbar flexion/extension angle (β_{flxext}) from the relative pelvis pitch angle (Equation 4). Axial rotation of the torso (ψ_{pelvis}^{Global}) is assumed zero for two-hand exertions and predicted by Equation 5 for one-hand exertions (R^2 Adj = 0.83, RMSE = 5.72 degrees). The predicted axial rotation angle is then used to distribute the predicted lumbar flexion/extension angle between torso flexion/extension (θ_{torso}^{Global}) and lateral bending (ϕ_{torso}^{Global}) according to Equation 6 and Equation 7, respectively. These relationships are defined such that, for zero axial rotation, torso flexion/extension is equal to the lumbar flexion/extension angle

and for axial rotation of 90 degrees the lumbar flexion/extension angle defines lateral bending of the torso.

$$\beta_{flxext} = - \left[|\theta_{pelvis}| + \sin^{-1} \left(\frac{L_{Mhip\ L5S1}}{L_{L5S1\ C7T1}} \sin(|\theta_{pelvis}|) \right) \right] \left(\frac{\theta_{pelvis}}{|\theta_{pelvis}|} \right) \quad (4)$$

$$\psi_{torso}^{Global} = 12.4 - 18.5(z_{handle} / stature) - 0.83(\varphi_{pelvis}^{Global} - \alpha_{torso}) \quad (5)$$

$$\theta_{torso}^{Global} = \beta_{flxext} - \phi_{torso}^{Global} \quad (6)$$

$$\phi_{torso}^{Global} = \beta_{flxext} \sin(|\varphi_{torso}^{global}|) \quad (7)$$

9. Kinematic Constraints and Adjustments

Given the predicted postural metrics, upper- and lower-extremity inverse kinematics algorithms are used to compute feasible elbow and knee locations. If the predicted pelvis location obtained by the preceding computations produces a kinematically infeasible combination of hip locations and foot placements the torso is lowered to satisfy lower-extremity kinematics constraints. Similarly, if the shoulder and hand location(s) are kinematically inconsistent the pelvis is shifted towards the point of force application until the kinematics of the upper-extremities are satisfied. This problem of kinematically inconsistent predicted postures is uncommon, arising only in high force circumstances. If task constraints and static equilibrium requirements make it kinematically impossible to generate the requested hand force the level of force is reduced to the maximum attainable and the user notified. In addition to balance requirements, an available coefficient of friction could be implemented, limiting ground friction and thus restricting the attainable hand force

6.4. Matlab Implementation

An implementation of the posture-prediction model was created in the Matlab programming environment for use as a testbed for model development and validation. The Matlab implementation is not intended to be an end-user tool. As discussed above, the model is designed to be readily implemented in any human modeling environment with minimal coding requirements. Consequently, most of the Matlab code creates the linkage and user interface. The model can be readily applied to other human body linkages without modification, since all kinematic models will have the components used here.

Predicted postural metrics are used to define a whole-body posture by integrating the posture-prediction algorithm into the larger model structure. The model structure ensures that predicted postures are kinematically feasible and in static balance by using inverse kinematics algorithms and static equilibrium checks to iterate on predicted postural metrics. In addition to kinematic constraints the structure also enforces postural constraints defined by model parameters. Current postural constraints include a squat limit or minimum pelvis height above the ground.

Three-Dimensional Human Body Linkage Definition

A three-dimensional linkage representation of the human body was defined by anatomical joint centers and anthropometric measures (Figure 6.12). Segment lengths and masses are defined from subject data or literature values. If literature values are used total body mass is distributed across segments and segment center-of-mass (COM) locations defined as a percent of segment length according to de Leva (1996). The linkage consists of seventeen links and has thirty-five degrees of freedom. Joint ranges of motion are not implemented, because the prediction process precludes postures that violate typical joint ranges of motion.

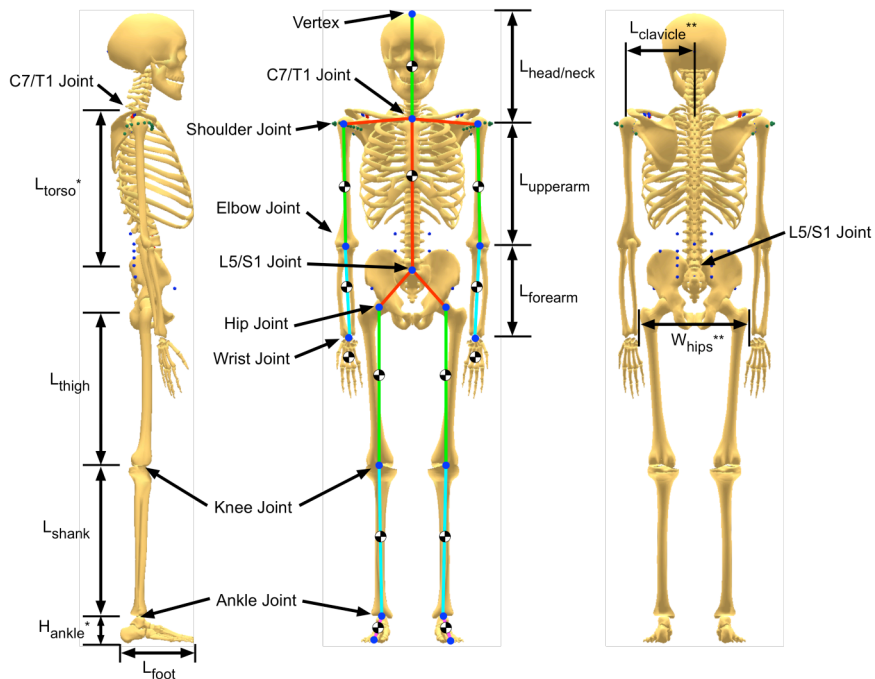


Figure 6.12. Anatomical landmarks and measures used to define linkage representation of human body.

Table 6.8. Segment lengths as a percent of stature, mass as a percent of total body mass, and COM location with respect to proximal end as a percent of segment length (male / female) from de Leva (1996), *subject data, and **UGS Jack Human figure model.

Segment	Length [% stature]	Mass [% body mass]	COM Location [% segment length]
Hand	10.8 / 9.80	0.61 / 0.56	36.2 / 34.3
Forearm	15.4 / 15.2	1.62 / 1.38	45.7 / 45.6
Upper arm	16.2 / 15.9	2.71 / 2.55	57.7 / 57.5
Clavicle**	12.0 / 12.0	-	-
Head/neck	14.0 / 14.0	6.94 / 6.68	50.0 / 48.4
Torso	34.7 / 35.4	43.5 / 42.6	51.4 / 49.6
Alt Torso*	26.0 / 26.0	-	38.6 / 36.4
Pelvis (W_{hips})**	10.0 / 10.0	-	-
Thigh	24.3 / 21.2	14.2 / 14.8	41.0 / 36.1
Shank	24.9 / 24.9	4.33 / 4.81	44.6 / 44.2
Foot	14.8 / 13.2	1.37 / 1.29	44.2 / 40.1
Foot (H_{ankle})*	4.0 / 4.0	-	-

Given the complexity of the human body the Denavit-Hartenberg (DH) method was used to minimize the number of parameters needed to define the system. DH frames were assigned to each degree-of-freedom as illustrated in Figure 6.13. Axes of rotation were defined to be consistent with anatomical joint motions with reduced degrees-of-freedom at the wrist and ankle joints. DH parameters are summarized in Table 6.9 and Table 6.10 for the upper-body and lower-body respectively. The posture depicted in Figure 6.13 corresponds to the zero-posture joint angle values (θ_i^0) presented in Table 6.9 and Table 6.10.

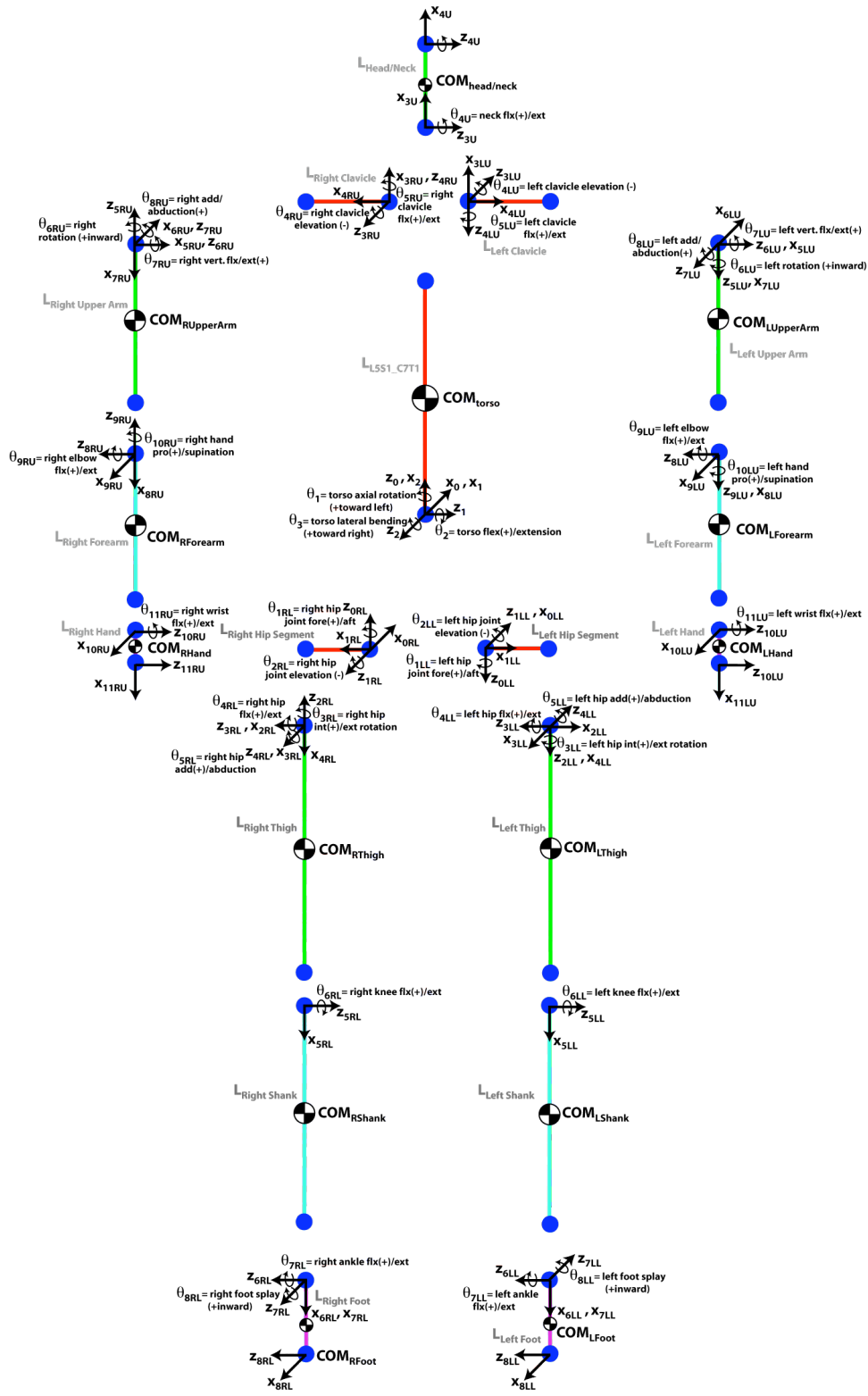


Figure 6.13. Linkage representation of the human body exploded to show DH frames.

Table 6.9. Denavit-Hartenberg parameters and zero-posture joint angles (θ_i^0) for the upper-body (RU=right upper-body, LU=left upper-body).

i	Joint	DOF, θ_i	θ_i^0	d_i	a_i	α_i
1	L5/S1	$\theta_1 =$ torso axial rotation	0	0	0	$\pi/2$
2	L5/S1	$\theta_2 =$ torso flex/extension	$\pi/2$	0	0	$-\pi/2$
3	C7/T1	$\theta_3 =$ torso lateral bending	0	0	L_{torso}	0
3U	C7/T1	zero transformation	0	0	0	$\pi/2$
3LU	C7/T1	zero transformation	0	0	0	π
4U	C7/T1	$\theta_{4U} =$ neck flex/extension	0	0	$L_{\text{head/neck}}$	0
4RU	C7/T1	$\theta_{4RU} =$ right clavicle elevation	$\pi/2$	0	0	$\pi/2$
4LU	C7/T1	$\theta_{4LU} =$ left clavicle elevation	$\pi/2$	0	0	$-\pi/2$
5RU	R. Shoulder	$\theta_{5RU} =$ right clavicle flex/extension	π	0	$-L_{\text{clavicle}}$	0
5LU	L. Shoulder	$\theta_{5LU} =$ left clavicle flex/extension	0	0	L_{clavicle}	0
6RU	R. Shoulder	$\theta_{6RU} =$ right humeral rotation	$\pi/2$	0	0	$\pi/2$
6LU	L. Shoulder	$\theta_{6LU} =$ left humeral rotation	$-\pi/2$	0	0	$-\pi/2$
7RU	R. Shoulder	$\theta_{7RU} =$ right shoulder flex/extension	$3\pi/2$	0	0	$-\pi/2$
7LU	L. Shoulder	$\theta_{7LU} =$ left shoulder flex/extension	$3\pi/2$	0	0	$\pi/2$
8RU	R. Elbow	$\theta_{8RU} =$ right shoulder ad/abduction	0	0	L_{upperarm}	$-\pi/2$
8LU	L. Elbow	$\theta_{8LU} =$ left shoulder ad/abduction	0	0	L_{upperarm}	$\pi/2$
9RU	R. Elbow	$\theta_{9RU} =$ right elbow flex/extension	$\pi/2$	0	0	$-\pi/2$
9LU	L. Elbow	$\theta_{9LU} =$ left elbow flex/extension	$\pi/2$	0	0	$\pi/2$
10RU	R. Wrist	$\theta_{10RU} =$ right hand pro/supination	0	$-L_{\text{forearm}}$	0	$-\pi/2$
10LU	L. Wrist	$\theta_{10LU} =$ left hand pro/supination	0	L_{forearm}	0	$\pi/2$
11RU	R. Grip	$\theta_{11RU} =$ right wrist flex/extension	$\pi/2$	0	L_{hand}	0
11LU	L. Grip	$\theta_{11LU} =$ left wrist flex/extension	$\pi/2$	0	L_{hand}	0

Table 6.10. Denavit-Hartenberg parameters and zero-posture joint angles (θ_i^0) for the lower-body (RL=right lower-body, LL=left lower-body, Bof = ball-of-foot).

i	Joint	DOF, θ_i	θ_i^0	d_i	a_i	α_i
0RL	L5/S1	zero transformation	0	0	0	0
0LL	L5/S1	zero transformation	0	0	0	π
1RL	L5/S1	θ_{1RL} = right hip segment fore/aft	$\pi/2$	0	0	$-\pi/2$
1LL	L5/S1	θ_{1LL} = left hip segment fore/aft	$\pi/2$	0	0	$\pi/2$
2RL	R. Hip	θ_{2RL} = right hip segment elevation	0	0	$L_{\text{hipsegment}}$	$\pi/2$
2LL	L. Hip	θ_{2LL} = left hip segment elevation	0	0	$L_{\text{hipsegment}}$	$-\pi/2$
3RL	R. Hip	θ_{3RL} = right hip in/external rotation	$\pi/2$	0	0	$\pi/2$
3LL	L. Hip	θ_{3LL} = left hip in/external rotation	$\pi/2$	0	0	$-\pi/2$
4RL	R. Hip	θ_{4RL} = right hip flex/extension	$-\pi/2$	0	0	$-\pi/2$
4LL	L. Hip	θ_{4LL} = left hip flex/extension	$-\pi/2$	0	0	$\pi/2$
5RL	R. Knee	θ_{5RL} = right hip ad/abduction	0	0	L_{thigh}	$-\pi/2$
5LL	L. Knee	θ_{5LL} = left hip ad/abduction	0	0	L_{thigh}	$\pi/2$
6RL	R. Ankle	θ_{6RL} = right knee flex/extension	0	0	L_{shank}	π
6LL	L. Ankle	θ_{6LL} = left knee flex/extension	0	0	L_{shank}	π
7RL	R. Ankle	θ_{7RL} = right ankle flex/extension	0	0	0	$-\pi/2$
7LL	L. Ankle	θ_{7LL} = left ankle flex/extension	0	0	0	$\pi/2$
8RL	R. Bof	θ_{8RL} = right foot splay	0	0	L_{foot}	0
8LL	L. Bof	θ_{8LL} = left foot splay	0	0	L_{foot}	0

Code was written in Matlab to create the human body linkage defined above. A flowchart of the Matlab code is presented in Figure 6.14. The code takes as input joint angles, stature, body mass, and a start location on the linkage chosen to be the L5S1 joint and uses the pre-defined DH frames to compute the forward kinematics of the linkage. Forward kinematics is performed by using knowledge of the linkage structure to traverse the linkage, computing and updating global rotations and locations at every step in the process. This process begins at the root of the linkage, the pelvis, and propagates outward along each branch of the linkage. The result is a three-dimensional graphical representation of the postured linkage.

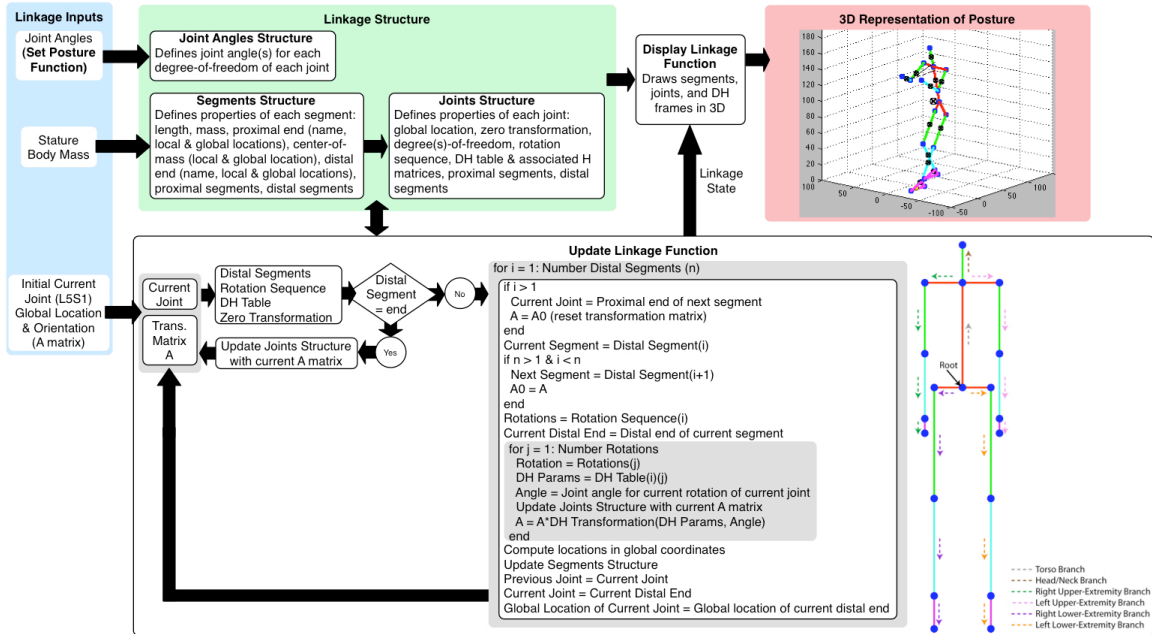


Figure 6.14. Linkage structure and update linkage function used to generate three-dimensional representation of posture. Linkage is rooted at pelvis and recursion is used to traverse each branch of the linkage computing forward kinematics and continuously updating joint and segment properties needed to display linkage.

In addition, inverse kinematics functions were written in Matlab for the upper and lower-extremity to compute feasible elbow and knee locations. Use of these functions allows one to compute a feasible elbow location for a given shoulder and hand location, and similarly a knee location when the hip and ankle location are known. These computations are carried out using trigonometric relations in conjunction with knowledge of segment lengths. This type of geometric approach to inverse kinematics is simpler and faster than searching for a feasible kinematic solution.

Graphical User Interface

A graphical user interface (GUI) was developed in Matlab to allow users to easily interact with the model. Model inputs are specified via text fields, radio buttons, and drop-down lists and the predicted posture displayed graphically (Figure 6.15). Top, front, side, and three-dimensional views of the predicted posture are provided with the ability to interactively rotate each view. The GUI also allows the user to annotate the predicted posture with the requested hand force vector, predicted/actual hand force vector, segment COM locations, whole-body COM location, center-of-gravity and center-of-pressure

locations. Additional model outputs including the components of the predicted hand force vector, joint torques, and ground reaction forces are provided to the user via text fields.

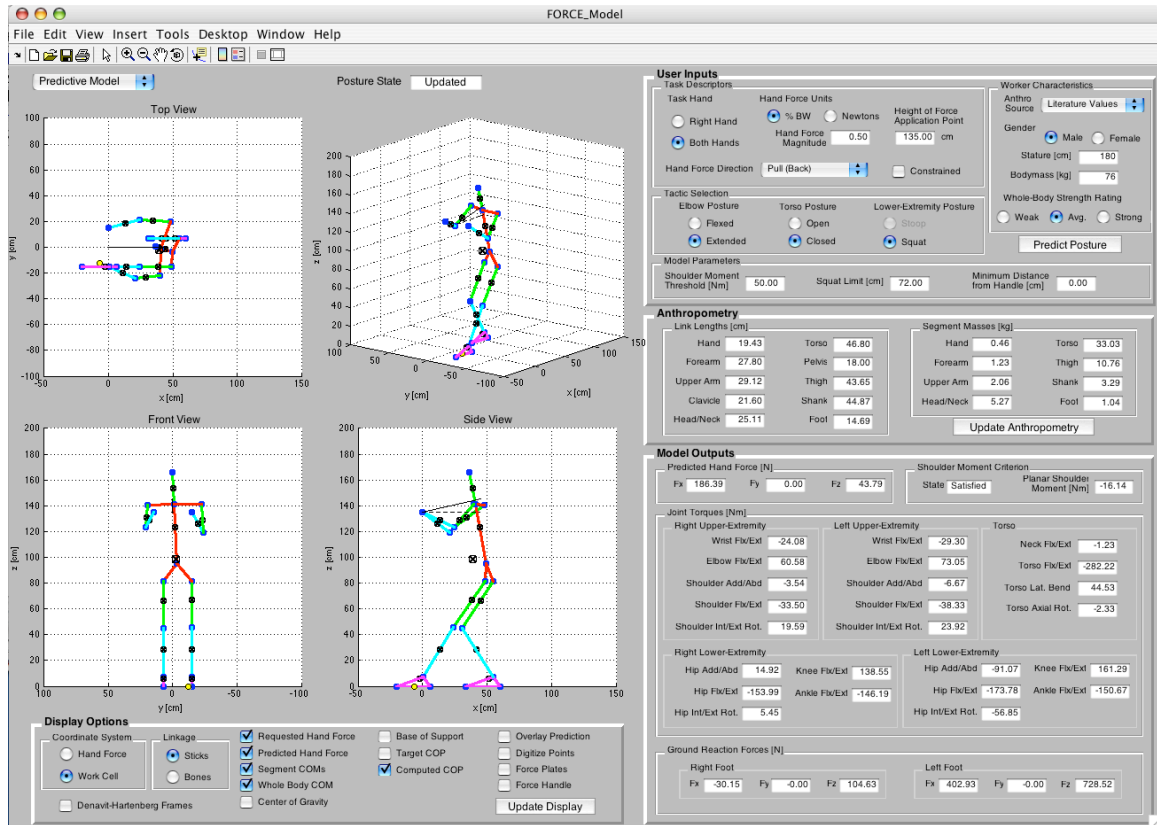


Figure 6.15. Graphical user interface (GUI) developed in Matlab.

6.5. Model Performance

Model performance was evaluated by exercising the Matlab implementation for the task conditions of a subset of the total trials that were withheld during the development of the regression models in Chapters 3, 4, and 5. Twenty percent of trials were withheld for each subject, randomly sampling within handle-height and force-direction blocks.

The model linkage was set to match the subject's data in the terminal posture, so potential modeling errors due to calculation of segment lengths were avoided. The body segment mass estimation procedure described in Section 2.6 was used to compute subject-specific body segment masses and applied to the linkage using segment COM locations from de Leva (1996). Because posture comparisons are not meaningful across different tactics, the actual tactic vector, consisting of the elbow posture (flexed or extended), open/neutral/closed torso orientation for one-hand trials, and lead foot (right

or left) was used as input. The measured hand force vector was also used during the initial assessment of model performance to eliminate inaccuracies in posture predictions associated with errors in the predicted hand force vector.

Qualitative Model Performance

A whole-body posture was predicted for each of the trials withheld for model validation. A subset of the resulting predictions for one and two-hand exertions, spanning a range of test conditions, are presented in Figure 6.16 and Figure 6.17. Predicted postures (shown in dark blue) are qualitatively similar to actual task postures (shown in light blue), and changes in predicted postures across force levels and hand force directions are consistent with postural changes captured in the laboratory.

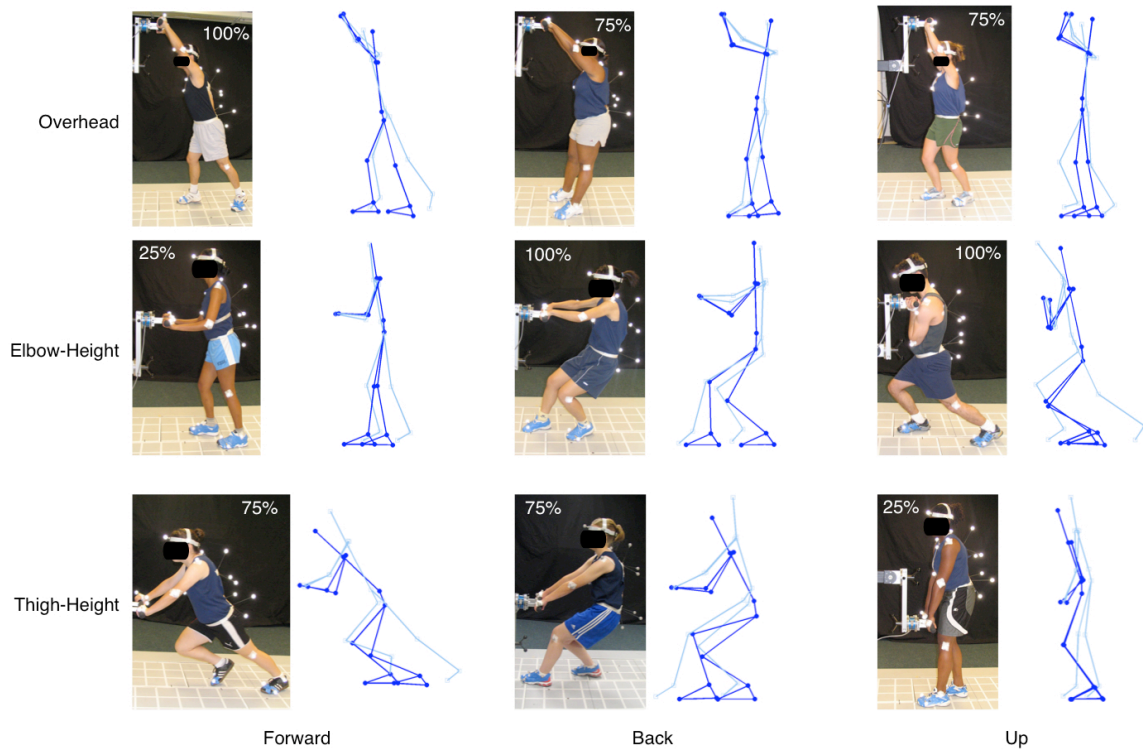


Figure 6.16. Comparison of select, actual (light lines, ■) and predicted (dark lines, ●) **two-hand** postures across handle heights for a subset of directionally unconstrained trial conditions. Actual task postures correspond to individual data trials (i.e. data points) selected from dataset reserved for model validation.

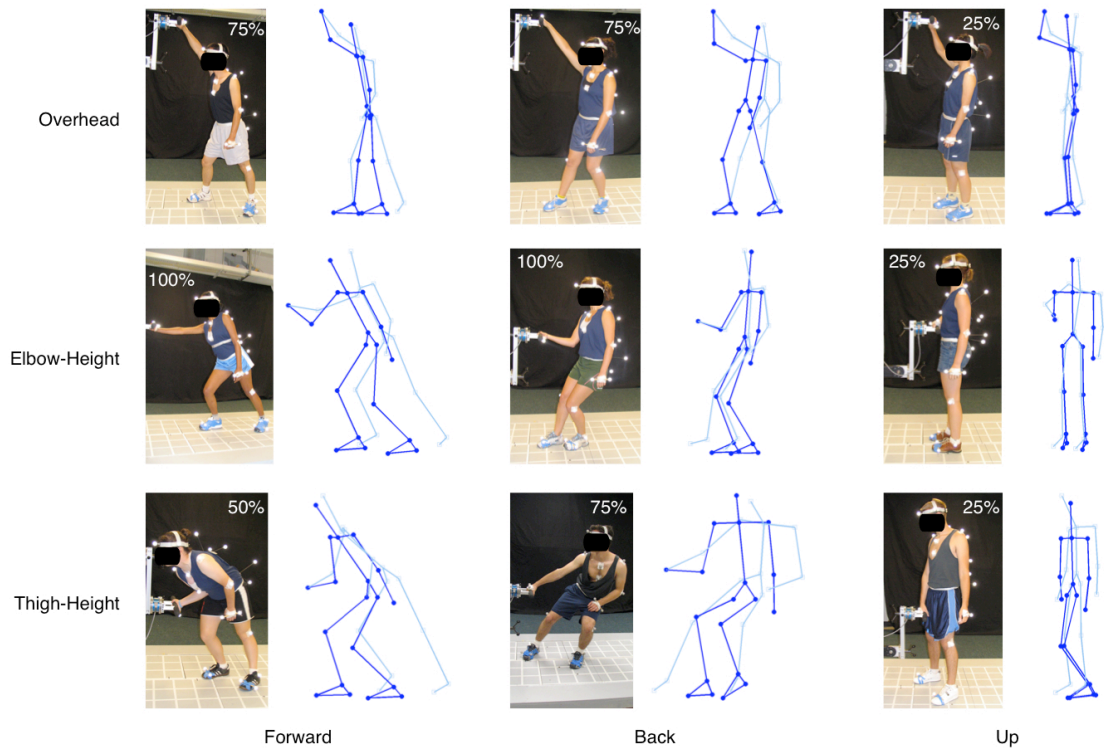


Figure 6.17. Comparison of select, actual (light lines, ■) and predicted (dark lines, ●) one-hand postures across handle heights for a subset of directionally unconstrained trial conditions. Actual task postures correspond to individual data trials (i.e. data points) selected from dataset reserved for model validation.

Changes in actual and predicted two-hand push/pull postures with increasing hand force are illustrated by Figure 6.18 and Figure 6.19. For two-hand push exertions, a drop in shoulder height with increasing push force is predicted for elbow- and thigh-height exertions. Across all three handle heights a lengthening of the base-of-support with increasing hand force is predicted. A forward shift in pelvis relative to the rear boundary of the base-of-support is also predicted for push exertions and is consistent with increasing the moment generated by body weight to counter the moment due to the applied hand force and satisfy the requirements of static balance. Smaller postural changes with increasing hand force are predicted for exertions at thigh and overhead heights than for exertions at elbow height. This is consistent with postures being more kinematically constrained at the low and high handle heights.

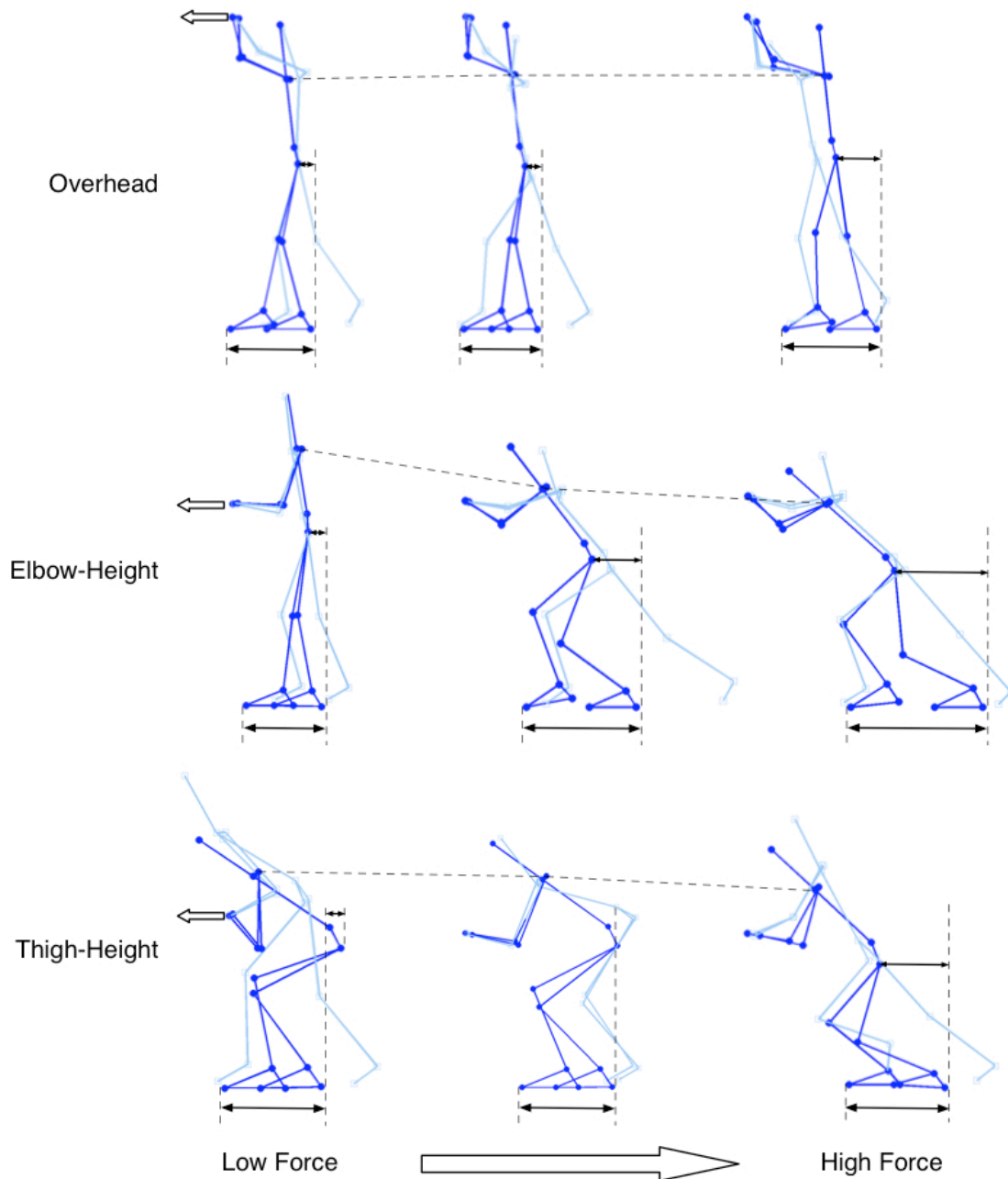


Figure 6.18. Actual (■) and predicted (●) two-hand elbow-height pushing postures showing drop in shoulder height and lengthening of base-of-support with increasing hand force magnitude. Forces are relative with low force corresponding to 25% of a subject's maximum and high force corresponding to 75% of their maximum. Actual task postures correspond to individual data trials (i.e. data points) selected from dataset reserved for model validation.

Similar to predicted pushing postures, a drop in shoulder height is also predicted with increasing hand force for pulls at elbow and thigh-height. A slight increase in shoulder height is predicted for two-hand pulls overhead. As the level of force increases predicted pulling postures show an increase in the fore-aft offset from the pelvis to the

forward edge of the base-of-support. As with push exertions, this shift in predicted pelvis location is consistent with the need to increase the moment generated by body weight to counter the increasing moment due to the applied hand force. An increase in hand force also results in a lengthening of the base-of-support.

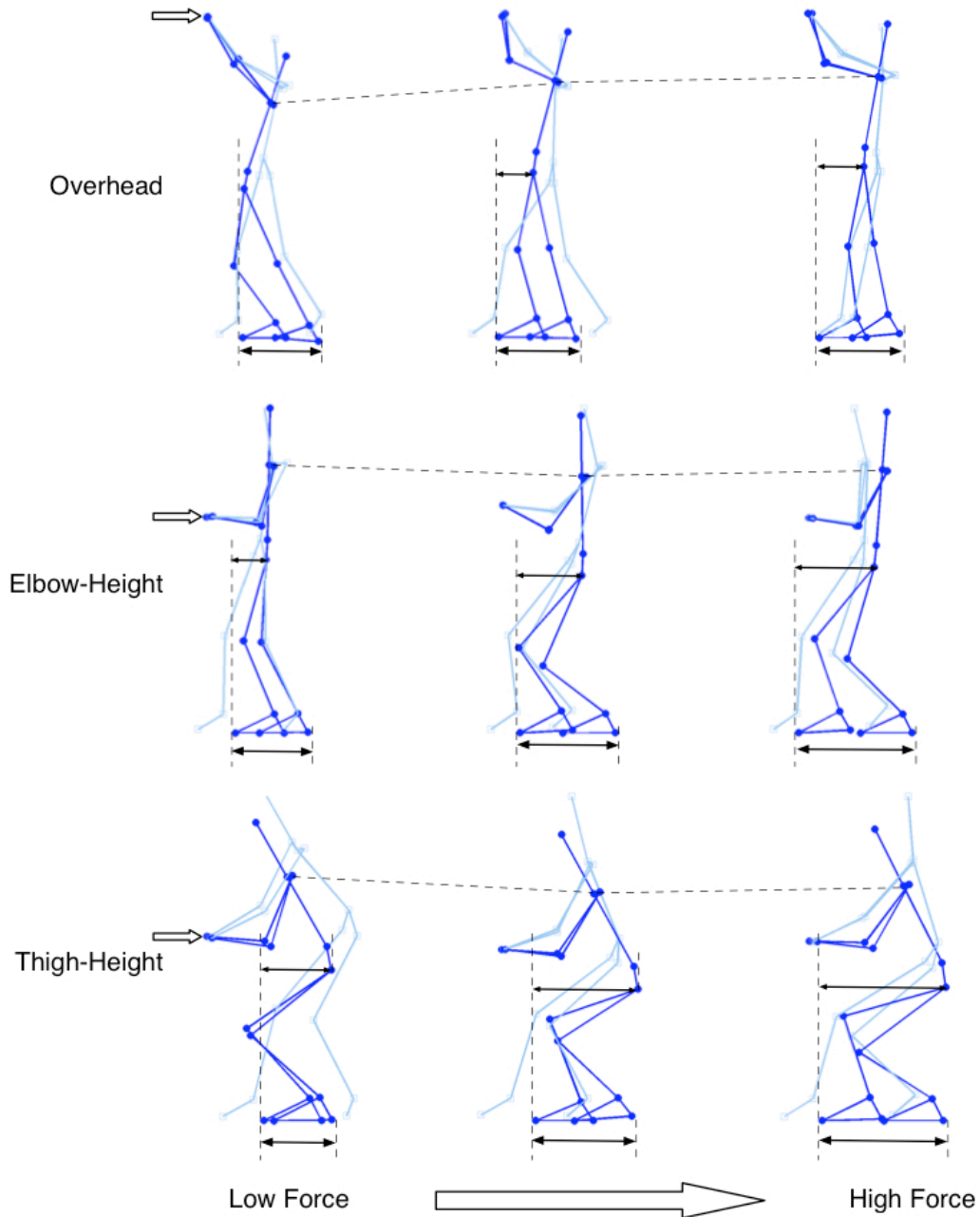


Figure 6.19. Changes in actual (■) and predicted (●) two-hand pulling postures with change in handle height and hand force magnitude. Forces are relative with low force corresponding to 25% of a subject's maximum and high force corresponding to 75% of their maximum. Actual task postures correspond to individual data trials (i.e. data points) selected from dataset reserved for model validation.

Comparison of actual two-hand pulling postures from individual data trials with predicted two-handed pulling postures shows that as hand force magnitude increases changes in predicted postures are qualitatively consistent with the postural changes quantified in the laboratory. Both actual and predict postures show the lowering of the shoulder and lengthening of the base-of-support with increasing hand force magnitude.

When pushing, participants in the laboratory study selected either an extended-elbow or flexed-elbow strategy. By specifying the elbow strategy via the tactic vector both postural strategies can be predicted by the model as illustrated by Figure 6.16 and Figure 99.18. Although some discrepancies are noted, the qualitative analysis suggests that the modeling approach is capable of predicting realistic task postures from worker characteristics and task parameters for a wide range of one- and two-hand force exertions.

Quantitative Performance: Validation Against Withheld Data

The performance of the model was evaluated by comparing the predicted values for selected variables against those observed in the withheld data. The evaluations focused on variables that are most important for ergonomic analysis, namely torso inclination, shoulder position, and foot placements. In this section, plots of the observed versus predicted values show the qualitative relationships, and the quantitative relationships are evaluated using the correlation coefficient (r) and the standard deviation of the residuals (root mean square error). Correlations greater than 0.7 indicate a strong linear relationship between the observed and predicted values. However, because the correlation coefficient is affected by the range of the data, the RMSE is sometimes a more useful measure of performance. In each case, the RMSE has the same units as the variable and can be take as the standard deviation of the distribution of the model errors.

Table 6.11 and Figure 6.20 show the model performance on torso flexion/extension angle (torso inclination). Recall that torso flexion/extension angle is predicted using regression equations (see Table 6.3 in the model development section, above), so this evaluation is primarily an assessment of how well these models perform against the validation dataset, and when integrated into the whole-body prediction. Across all trials, and for the one- and two-hand subsets, the correlations are strong, but the RMSE are fairly large, about 15 degrees. Figure 6.20 shows that the errors are similar across the range of torso angles in the validation dataset. Table 6.11 shows that the

correlations are relatively poor for upward exertions. Examination of the data shows that the poor performance is due to a blending of tactics, with some subjects moving their pelvis close to the handle and pulling upward with a near-vertical torso orientation, while others bend down to get their shoulders closer to the handle.

Table 6.11. Model performance for torso flexion/extension angle [deg] measured by correlation coefficient (r) and standard deviation of model residuals (RMSE).

Group	Number of Hands	Simplified Force Direction	r (RMSE)
All Trials			0.727 (14.5)
	One		0.734 (14.0)
		Push	0.657 (14.0)
		Pull	0.786 (13.8)
		Up	0.107 (10.4)
		Down	0.529 (7.39)
	Two		0.757 (13.9)
		Push	0.598 (16.9)
		Pull	0.796 (12.1)
		Up	0.171 (13.3)
		Down	0.567 (10.5)

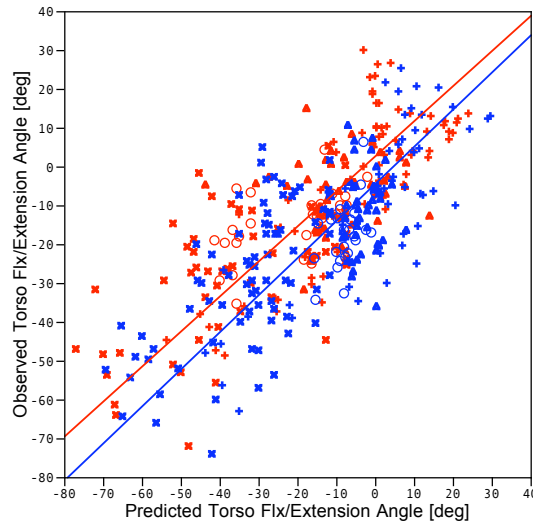


Figure 6.20. Observed versus predicted torso flexion/extension angle across all trials grouped on task hand (one-hand = blue, two-hand = red). Marker style denotes force direction: ▲ = up, ✖ = push, + = pull, O = down.

Table 6.12 and Figure 6.21 show the model performance for fore-aft shoulder location with respect to the handle. The overall correlation is strong and correlations for one- and two-handed pushes exceed 0.8. Low correlations were observed for both one- and two-handed pulls, but this resulted more from a restriction of range than poor model performance. The RMSE values for pulls are similar to the overall model performance.

The fore-aft shoulder location for downward exertions was not well predicted due to a mix of tactics among the subjects, particularly for one-hand downward exertions.

Table 6.12. Model performance for fore/aft shoulder location [cm] (x_{shoulder}).

Group	Number of Hands	Simplified Force Direction	r (RMSE)
All Trials			0.769 (11.8)
	One		0.770 (12.5)
		Push	0.863 (12.0)
		Pull	0.057 (11.7)
		Up	0.468 (10.7)
		Down	0.010 (14.3)
	Two		0.792 (10.6)
		Push	0.815 (10.6)
		Pull	0.210 (11.9)
		Up	0.474 (7.56)
		Down	-0.016 (9.52)

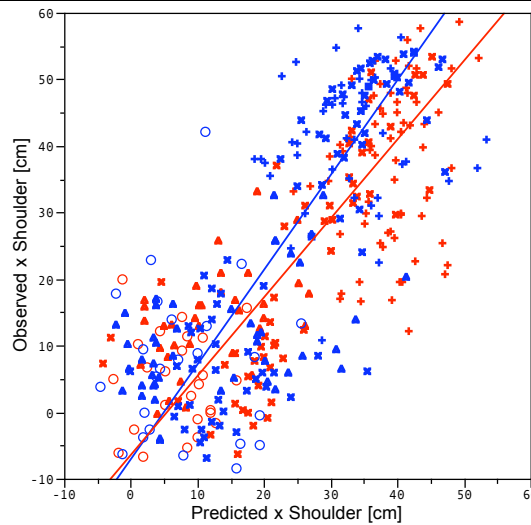


Figure 6.21. Observed versus predicted shoulder fore/aft location across all trials grouped on task hand (one-hand = blue, two-hand = red). Marker style denotes force direction: ▲ = up, ✖ = push, + = pull, O = down.

Table 6.13 and Figure 6.22 show model performance for the prediction of shoulder height above the handle. The correlations are generally very strong, but benefit from the large range of the variable due to the range of handle positions (from mid thigh to overhead). The best performance in terms of RMSE was found for pull exertions with both one- and two-hands. These are the trials in which the trend of shoulder height adjustment to control shoulder moment was most clearly observed. Shoulder vertical position was predicted most poorly for downward exertions, again reflecting a diversity of tactics not well captured by the model.

Table 6.13. Model performance for shoulder height relative to point of force application [cm] (h_{shoulder}).

Group	Number of Hands	Simplified Force Direction	r (RMSE)
All Trials			0.847 (13.3)
	One		0.857 (12.4)
		Push	0.894 (8.47)
		Pull	0.962 (6.83)
		Up	0.921 (13.2)
		Down	0.121 (18.2)
	Two		0.843 (14.0)
		Push	0.899 (10.3)
		Pull	0.916 (8.90)
		Up	0.946 (12.5)
		Down	-0.312 (23.0)

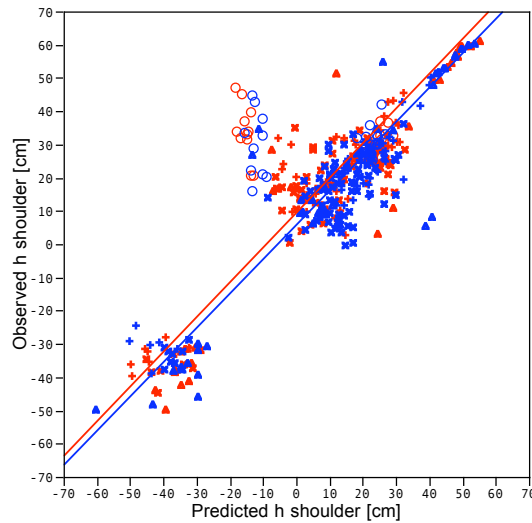


Figure 6.22. Observed versus predicted shoulder height with respect to the point of force application across all trials grouped on task hand (one-hand = blue, two-hand = red). Marker style denotes force direction: \blacktriangle = up, \times = push, $+$ = pull, O = down.

The model predicts the position of the active boundary of the base of support (front foot placement for pulls, rear foot placement for pushes) solely from balance considerations. That is, the active foot placement is chosen to have the smallest deviation from neutral that can generate the required moment to stabilize the hand force. Figure 6.23 shows that, on average, the distance between the pelvis and the active BOS margin was larger in the data than in the model predictions. Nonetheless, the model did well for pull exertions, with high correlations and relatively low RMSE values. For pushes, the participants tended to place their rear (active) foot further rearward than required. Considered in conjunction with the results for fore-aft shoulder positioning, it appears that participants place their BOS conservative, giving themselves more than enough margin, and then fine-tune the force by flexing the elbow as they move their COM fore-

aft along the force plane. Note that the model includes a parameter for the offset between the active boundary and the target center of pressure, but the parameter was set to zero for this initial model evaluation.

Table 6.14. Model performance for (x active edge of BOS – x pelvis) [cm].

Group	Number of Hands	Simplified Force Direction	r (RMSE)
All Trials			0.531 (12.0)
	One		0.363 (31.5)
		Push	0.210 (18.0)
		Pull	0.721 (10.1)
		Up	-0.344 (23.5)
		Down	0.042 (12.8)
	Two		0.652 (27.1)
		Push	0.484 (15.5)
		Pull	0.846 (8.34)
		Up	0.051 (22.4)
		Down	0.274 (9.74)

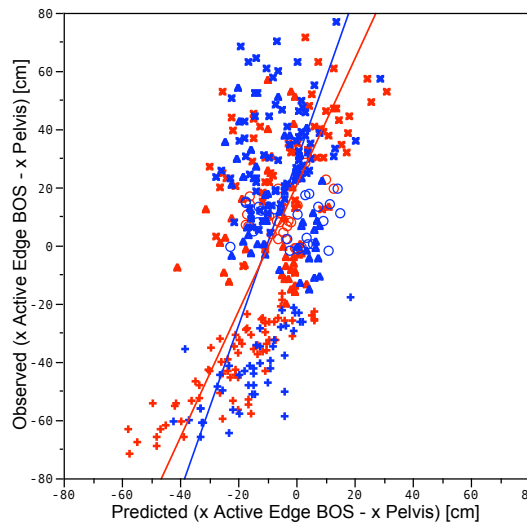


Figure 6.23. Observed versus predicted fore-aft offset from pelvis to active boundary of BOS across all trials grouped on task hand (one-hand = blue, two-hand = red). Marker style denotes force direction: ▲ = up, ✕ = push, + = pull, O = down.

Sensitivity Analysis

The sensitivity of model predictions for two-hand push/pull exertions to body weight and the shoulder moment threshold is illustrated in Figure 6.24 and Figure 6.25. The fore-aft offset from the pelvis to active edge of the BOS increases with increasing hand force magnitude during both push and pull exertions with the magnitude of offset required for a given force magnitude decreasing as body weight increases (Figure 6.24). A larger drop in shoulder height with increasing hand force magnitude is observed for a shoulder moment threshold of 10 Nm as compared to a threshold of 40 Nm.

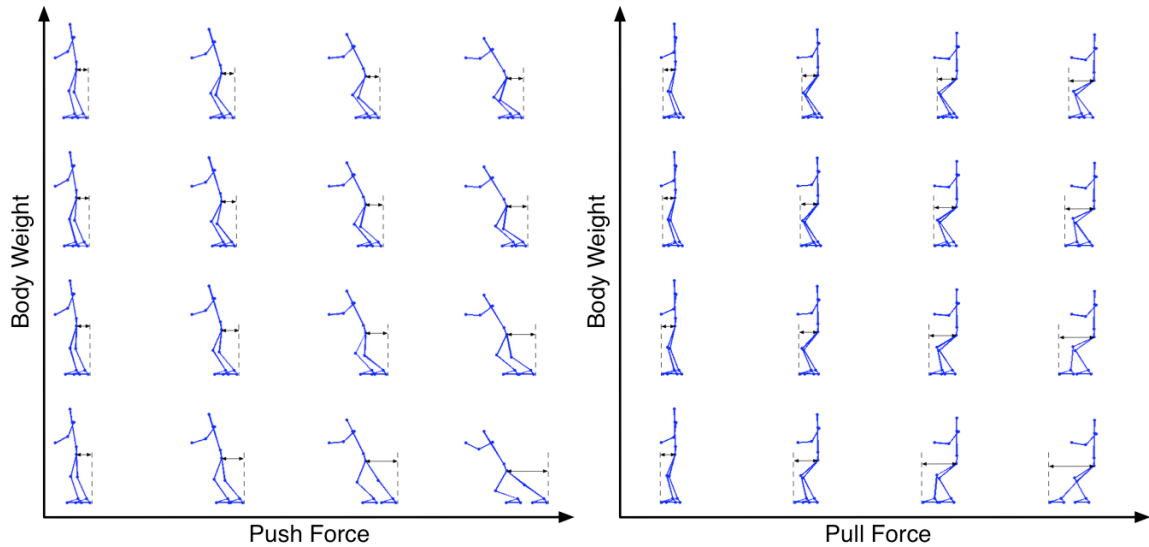


Figure 6.24. The effects of body weight and hand force magnitude on two-hand push / pull model predictions. Body weight spans from 445 N (100 lbs) to 890 N (200 lbs) and hand force magnitude from 44.5 N (10 lbs) to 223 N (50 lbs).

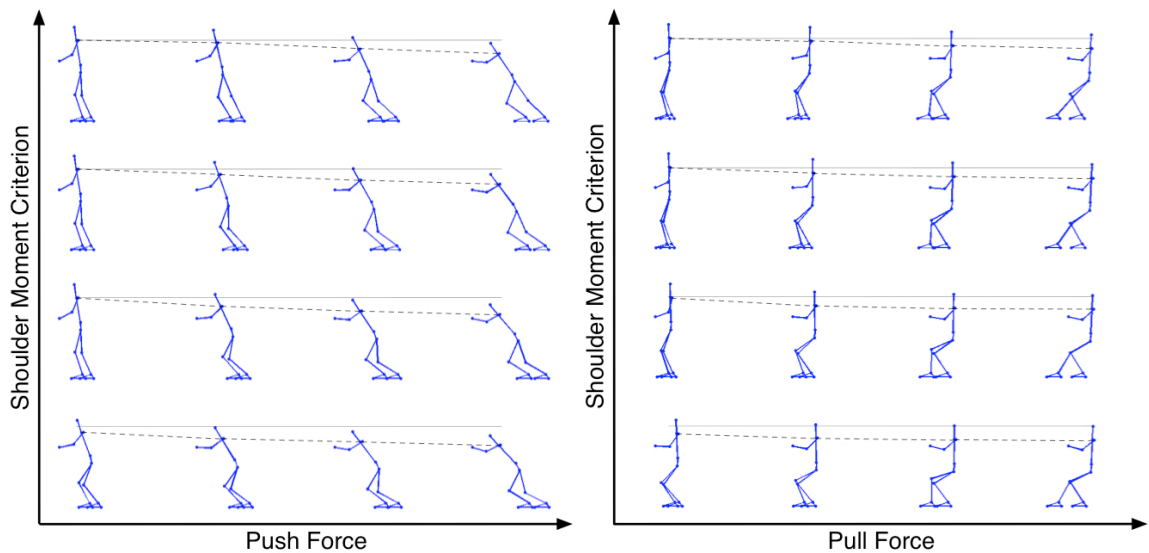


Figure 6.25. Sensitivity of model predictions for two-hand push/pull exertions to shoulder moment criterion. The shoulder moment criterion spans from 10 Nm to 40 Nm and body weight spans from 445 N (100 lbs) to 890 N (200 lbs).

6.6. Discussion

Summary

A new hybrid approach to predicting three-dimensional, whole-body postures for hand-force-exertion tasks was introduced. The model is based on (1) a static biomechanical analysis that incorporates force and moment balance and (2) empirical models to predict actual hand force and critical degrees of freedom. The model concept is

based on a concise set of hypotheses concerning posture-selection behavior that have been supported by data from a laboratory experiment. The model is designed to be very general and was both constructed and validated on a wider set of data than any model of hand force postures previously appearing in the literature.

Model Structure

By design, the current model is much simpler in structure and content than most other approaches to three-dimensional posture prediction. For example, Seitz et al. (2005) perform global optimization of joint angles to predict a posture. That approach requires a specific manikin linkage and joint angle definition, along with specialized computation code. In contrast, the model presented here uses simple, closed-form computations that can be readily implemented in any existing human modeling software system. As such, it is more likely to have an influence on the practice of ergonomics than more complex systems. The current model was developed for integration into the Human Motion Simulation Framework, a modular system for predicting and analyzing task-oriented postures and motions (Reed et al. 2006). A reference implementation of the Human Motion Simulation Framework is already in use in several companies.

Model Performance

The model was able to exhibit the many of the qualitative characteristics of force-exertion postures. The hand force direction and approximate magnitude are subjectively apparent from the predicted postures in Figure 6.16 and Figure 6.17. The quantitative performance of the model was extensively evaluated using data withheld from the parameter fitting process. Across subjects and trials, high correlations were observed for most force directions.

Model performance was weakest for up and down exertions, largely due to the large range of tactics employed by the subjects. These actions differed from the lifting motions that have been studied extensively in that the handle did not move. In general, the behaviors were consistent with the hypothesized objective of reducing shoulder moments, but the actual positioning of the shoulder, and the supporting torso inclinations, varied considerably. More work is needed to determine if an alternative approach to computing the shoulder position for these tasks would yield better results.

Overall, the model performed best when the participant tactics were most consistent, namely for horizontal pulls with both one and two hands. The contrast between the success in predicting pulling postures and the difficulty with vertical exertions highlights the central challenge of predicting tactics. Previous researchers have noted the critical importance of tactic selection as a first step in predicting postures (Park et al., 2005). Yet, in the current work, tactics were not found to be well predicted by task or subject variables, or their interaction. From a model development perspective, this leaves two unsatisfying alternatives. One can create individualized models for a variety of tactics, such as open/closed torso for one-hand exertions, and bent/flexed elbow for two-hand pushes (the approach chosen here for several common tactics). Alternatively, one can create a model that averages across a range of tactics, which risks predicting a behavior that does not exist. The lack of ability to clarify a small number of alternative tactics for vertical exertions led to an aggregate approach for in the current model that produced unsatisfying performance.

The range of tactics that are employed by workers performing similar tasks is a critical topic for future research. In studies of lifting, a large amount of effort has been directed at quantifying the relative loading for squat and stoop lifting approaches, and training programs have attempted to encourage tactics that produce lower spine loading. However, for proactive ergonomics, predictions of the distribution of tactics that workers will use are needed. These analyses might lead to the design of a job to preclude the use of one or more tactics judged to be risky, but a failure to anticipate a range of tactics would undermine the utility of proactive ergonomics. Wagner et al. (2005, 2006) has shown that a relatively small number of foot movement patterns account for a clear majority of foot movements during materials handling tasks in automotive assembly workcells, and the current work (see Chapters 4 and 5) show that a small number of quantifiable tactics are observed for push and pull exertions in a laboratory setting. Nonetheless, considerably more research is needed to document, classify, and predict tactics for hand force exertions.

Limitations and Future Work

Model Linkage

The model was constructed with a minimally complex linkage to permit a focus on the primary degrees of freedom. Non-anatomical links from the C7T1 vertebrae to the shoulder and from the L5S1 vertebrae to the hip were used to achieve fore/aft and up/down locations of the shoulder and hip joints with respect to C7T1 and L5S1 joint locations, respectively. Two complications associated with the use of these non-anatomical links are: (1) the length and orientation of these links are not defined and had to be approximated and (2) shoulder and hip joint angles are defined with respect to the torso and thus the DH frames associated with these non-anatomical links are only used to compute the global locations of the shoulder and hip joints. The orientation of these links with respect to the torso were fixed and defined by average angle values computed across all subjects.

The linkage was further simplified by exclusion of the hand segment. This decision resulted from insufficient postural data collected for the hand during the laboratory study. Hand orientation (i.e. overhand versus underhand grip) was captured but the marker set used was not sufficient for compute wrist angles. Ankle joints were also simplified by modeling only two degrees-of-freedom at the ankle (flexion/extension and outward/inward foot splay). Ankle eversion/inversion were ignored. Lastly, the torso is represented by two links and the feet by a single link. Simplification of the torso linkage and limited pelvis and torso data prevent behaviors such as the hyperextension of the lumbar spine shown in Figure 6.26 from being quantified and modeled. These simplifications, along with exclusion of the hand, limit how accurately the model can represent whole-body postures since only gross foot, and torso postures are possible with the current linkage.

Future work should include implementing the model on a more complex linkage, such as within a commercial human modeling software system used for ergonomics. Two candidates for such an implementation are the 3D Static Strength Prediction Program (3DSSPP) published by the University of Michigan Center for Ergonomics and the Reference Implementation of the Human Motion Simulation Framework, which uses the commercial JackTM human modeling software system.

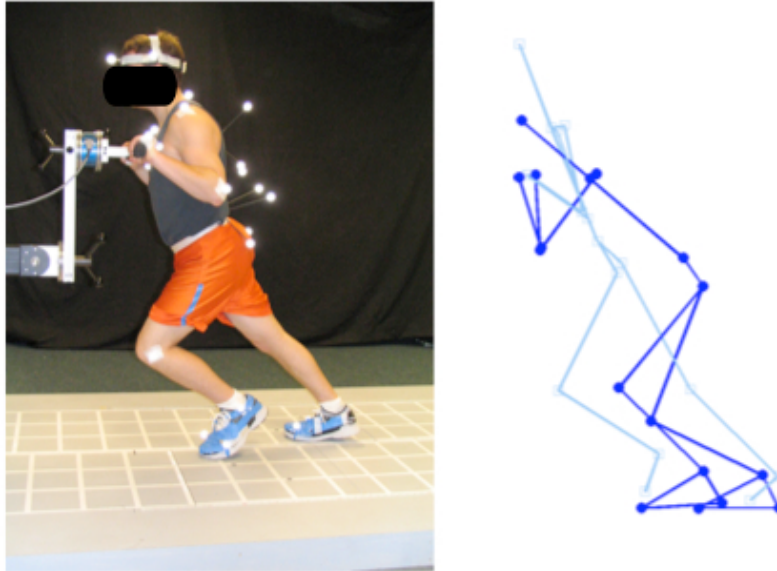


Figure 6.26. Hyperextension of the lumbar spine used by a subset of subjects during high-force exertions.

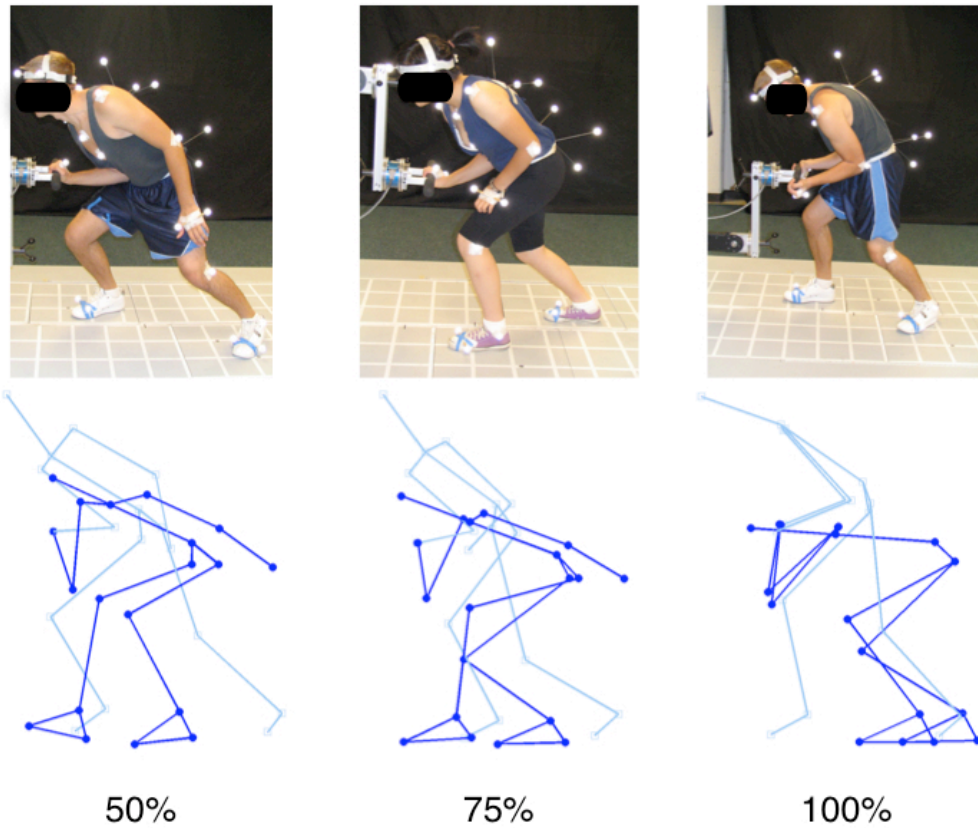


Figure 6.27. Discrepancies between actual and predicted postures associated with internal bracing.

Model Structure

The current model algorithm has been designed to be deterministic and to avoid the use of optimization and a requirement to use a particular joint angle description. In particular, unlike nearly all previous whole-body posture-prediction models, the current model is not based on a particular joint-angle definition. These choices help to ensure that the model can be readily implemented in a wide range of human modeling systems. Yet, it is possible that a slightly more complex solution formulation would yield better results. The data support the proposed hypotheses that people try to maintain shoulder moments within a narrow range of acceptable values while also trying to maintain a relatively upright torso orientation. The presence of these potentially conflicting objectives suggests a simple optimization formulation that would attempt to trade off these two considerations while selecting shoulder position and torso inclination. Future research should examine this possibility while maintaining the joint-angle independence of the current formulation and minimizing the amount of special purpose optimization code that would be required.

The current model lacks explicit consideration of strength because the analysis of the laboratory data did not find that strength, as measured in static laboratory trials, was a meaningful predictor of task postures. Nonetheless, this finding should be interpreted cautiously, because the young, fit subject population may not have included a sufficiently wide range of strengths. The treatment of strength is also complicated by the likelihood that strength influences tactic selection as well as, potentially, behavior within tactic. The current model could be augmented by adding joint-specific strength as a constraint on posture. Yet, the shoulder and elbow are the only joints that are likely to be close to their moment-generating limits in these tasks, and the posture-prediction algorithm already operates to reduce moments at these joints through posture selection. Hence, it seems unlikely that adding joint-strength limits would affect a large percentage of the predictions.

The model has the capability of predicting force-exertion capability. For these relatively unconstrained tasks, force capability is limited primarily by body weight and the coefficient of friction on the floor, not by strength. Hence, for a particular force direction and worker characteristics, the model can predict the maximum force-

generating capability, limited by floor friction, for both constrained and unconstrained directions. As with other aspects of the model predictions, the performance is likely to be best for primarily horizontal pushes and pulls, with poorer performance for upward exertions where joint strength is likely to be more limiting than friction on the floor. For downward exertions, body weight is the primary limiting factor and model performance of maximum capability is likely to be good.

6.7. References

- Beck, D. (1992). Human factors of posture entry into ergonomics analysis systems. PhD thesis, The University of Michigan, Ann Arbor, MI.
- Boocock, M. G., Haslam, R. A., Lemon, P., and Thorpe, S. (2006). Initial force and postural adaptations when pushing and pulling on floor surfaces with good and reduced resistance to slipping. *Ergonomics*, 49(9):801–821.
- de Leva, P. (1996). Adjustments to zatsiorsky-seluyanov's segment inertia parameters. *J Biomech*, 29(9):1223–1230.
- de Looze, M. P., van Greuningen, K., Rebel, J., Kingma, I., and Kuijer, P. P. (2000). Force direction and physical load in dynamic pushing and pulling. *Ergonomics*, 43(3):377–390.
- Dempster, W. (1958). Analysis of two-handed pulls using free body diagrams. *J Applied Physiology*, 13(3):469–480.
- Center for Ergonomics (2005). Three dimensional static strength prediction program (3DSSPP). The University of Michigan, Ann Arbor, MI, v 5.0.3 edition.
- Gaughran, G. and Dempster, W. (1956). Force analysis of horizontal two- handed pushes and pulls in the sagittal plane. *Human Biology*, 28(1):67–92.
- Granata, K. R. and Bennett, B. C. (2005). Low-back biomechanics and static stability during isometric pushing. *Hum Factors*, 47(3):536–549.
- Kerk, C., Chaffin, D., and et al (1994). A comprehensive biomechanical model using strength, stability, and cof constraints to predict hand force exertion capability under sagittally symmetric static conditions. *IIE Transactions*, 26(3):57–67.
- Liu, Y. (2003). Interactive reach planning for animated characters using hardware acceleration. PhD thesis, The University of Pennsylvania, Philadelphia, PA.
- Park, W., Martin, B. J., Choe, S., Chaffin, D. B., and Reed, M. P. (2005). Representing and identifying alternative movement techniques for goal-directed manual tasks. *J Biomech*, 38(3):519–527.
- Reed, M. P., Faraway, J., Chaffin, D. B., and Martin, B. J. (2006). The HUMOSIM framework: A new approach to human motion simulation for ergonomic analysis. Technical Report 2006-01-2365, SAE International, Warrendale, PA.
- Seitz, T., Recluta, D., Zimmermann, D., and Wirsching, H.-J. (2005). Focopp - an approach for a human posture prediction model using internal / external forces and discomfort. Technical Report 2005-01-2694, SAE International, Warrendale, PA.

- Wagner, D., Reed, M., and Chaffin, D. (2006). A task-based stepping behavior model for digital human models. In SAE Transactions: Journal of Passenger Cars - Electronic and Electrical Systems, volume 115, Warrendale, PA.
- Wagner, D., Reed, M., and Chaffin, D. (2005). Predicting foot positions for manual materials handling tasks. Technical Report 2005-01-2681, SAE International, Warrendale, PA.
- Zhao, L., Liu, Y., and Badler, N. (2005). Applying empirical data on upper torso movement to real-time collision-free reach tasks. Technical Report 2005-01-2685, SAE International, Warrendale, PA.

CHAPTER 7

DISCUSSION

7.1. Overview

The work presented in this dissertation focused on understanding and modeling the effects of hand force magnitude and direction on whole body standing hand force postures. The main objective of this work was to combine kinematics and static balance requirements with a set of hypothesized biomechanical principles and behaviors to predict standing hand force exertion postures.

Summary of Principal Empirical Findings

- Significant vertical off-axis forces were quantified during one- and two-hand exertions. One-hand exertions were also characterized by significant lateral off-axis forces.
- Pushing postures were characterized by either flexed or extended-elbow postures. A preference towards extended-elbow postures was observed for pulls, with 65% of two-hand pulls and 74% of one-hand pulls having included elbow angles greater than 90 degrees.
- Shoulder flexion/extension moments were found to be a significant determinant of posture. Changes in shoulder location with respect to the point of force application and/or changes in hand force direction consistent with reducing or maintaining an acceptable level of shoulder moment were quantified.
- A preference towards neutral standing postures was observed with people inclining their torso and/or changing their base-of-support only when required to generate the requested hand force. Torso inclination angle was

found to be well predicted across all trials with slightly lower R^2 values for torso inclination angles during vertical (up/down) exertions. Torso inclination is largely determined by kinematic constraints with shoulder height relative to handle location, change in shoulder height from neutral, fore-aft shoulder location, handle height, an interaction between handle height and change in shoulder height, and horizontal and vertical hand force components being the significant ($p < 0.0001$) predictors.

- Low-back rotation moments were quantified and found to be less than 21 Nm in 90% of all trials. Flexion/extension, twisting, and lateral bending moments about L5/S1 were used to estimate low-back compression force (McGill et al, 1996) and compression forces found to be less than or equal to 1,756 N for 90% of all trials.
- One-hand exertions were characterized by axial rotation of the torso and lateral displacement of the pelvis relative to the hand-force plane. Rotation angles were smallest during one-hand push exertions with a mean value of 7.5 degrees and standard deviation of 17.6 degrees. The largest variation in torso rotation angles was observed for one-hand pulls with a standard deviation of 30.5 degrees. Lateral displacement of the pelvis was largest for one-hand push exertions with an average displacement of approximately 67 mm to the left. Across all conditions, lateral displacements varied significantly with standard deviations ranging from 56.3 mm to 83.0 mm.
- Foot placement, specifically the location of the active boundary of the base-of-support (BOS) with respect to the pelvis, was found to be fairly well predicted by assuming that the applied moment due to hand force is countered by the moment generated by body weight. A strong relationship was also found between the fore-aft offset from the pelvis to active edge of the BOS and BOS length, with a stronger relationship observed for push exertions than for pull exertions.

Unexpected Findings

- Internal bracing was found to be a prevalent strategy when performing one-hand push exertions at a mid-thigh handle height. This phenomenon was not expected and is not well documented in the current literature. Possible explanations for this behavior include: (1) an unloading of the shoulder joint, allowing for higher shoulder locations (i.e. more upright, neutral posture) without the associated cost of higher shoulder moment, (2) stabilization of the arm for more precise control of hand force.
- Gender was not found to be a significant predictor of the postural metrics analyzed. Across all trial conditions kinematic constraints imposed by the handle locations were a significant determinant of postural metrics and may have masked gender effects. Also, only 19 subjects (9 males and 10 females) were analyzed. A gender effect may have been observed with a larger sample size, which would have provided greater statistical power.

Summary of Principal Contributions

- Developed and conducted an experiment to collect postural and force data for one- and two-handed exertions under a large number of test conditions.
- Quantified actual hand force vectors and developed regression equations to predict the actual hand force vector from the requested hand force.
- Developed a set of biomechanical explanations that appear to account for a wide range of force exertion behaviors observed in the laboratory and automotive assembly plants.
- Analyzed force exertion postures with respect to the hand-force plane based on the observation that, when possible, people tend to align themselves with the actual hand force vector.
- Developed and validated a three-dimensional whole-body posture prediction model capable of predicting realistic force-exertion postures for a large range of task conditions.

7.2. Principal Contributions

The principal contributions of this work are discussed within the context of the five research objectives outlined in Chapter 1. The findings associated with each

objective are interpreted, the implications and limitations discussed, and alternative hypotheses considered.

1. Classify standing hand-force exertion postures by gross postural technique and investigate the effects of worker and task characteristics on tactic selection.

Gross postural techniques used during two- and one-handed force exertions were presented in Chapter 4 and Chapter 5. All horizontal exertions were categorized as a push or pull with a preference towards pulling for one-hand exertions to the right, back and left, and back and right. A preference towards pushing was observed for one-hand exertions to the left, forward and left, and forward and right. Four postural techniques were identified for vertical (up/down) exertions: (1) push up, (2) pull up, (3) push down, and (4) pull down. Restriction of the pull down strategy to a few participants for only a small subset of trials precluded analysis of this strategy. Classification of standing hand-force exertion postures by gross postural technique aided analysis of data by reducing force exertions in various directions to a minimal set of fundamentally different exertion types. Data trials were divided into push, pull, and up/down exertions for all subsequent analyses.

Within push exertions both flexed and extended-elbow strategies were observed and were analyzed separately when elbow posture was found to have a significant effect on hand force and/or other aspects of posture. Elbow angle had a bimodal distribution for thigh and elbow-height push exertions whereas the kinematics of reaching the overhead handle required an extended-elbow posture. Extended-elbow postures were preferred when pulling with 65% of two-hand and 74% of one-hand pulls having an included elbow angle greater than 90 degrees. The observed elbow postures are consistent with the hypothesis that elbow postures are selected to reduce elbow moment or position the hands close to the shoulder, using passively-generated elbow moment and internal bracing, such that hand forces are not limited by elbow strength. Extending the elbow during push/pull exertions acts to reduce the moment about the elbow while pushing with maximally flexed elbows utilizes the passive tension. Alternatively, bracing the elbow against the thorax allows push forces to be transmitted along the forearm and through the elbow joint resulting in minimal moments about the elbow. Haslegrave (1992) also found force exertion postures to be characterized by two distinct elbow postures: (1) “near fully

extended” and (2) “arm tightly bent with the hand close to the shoulder”. Furthermore, elbow postures were found to be consistent across exertions with and without constraints imposed on reach distance with participants making considerable whole-body postural adjustments to maintain similar arm postures despite reach distance constraints. She hypothesized that fully extended postures were selected to stabilize the elbow joint, a potentially “weak link”, and allow high forces to be generated by the shoulder and back muscles. Less discussion was dedicated to the flexed-elbow strategy with Haslegrave simply commenting that maximally flexing the elbow places the shoulder joint close to the point of force application. The flexed-elbow strategy was further investigated in this dissertation, in the context of push exertions, by examining the relationship between included elbow angle and shoulder location, and quantifying the effect of upper-extremity postures on shoulder moment. Analyses of one- and two-hand pushing postures conducted as part of this work support the hypothesis that a flexed-elbow posture is selected to allow for a large vertical force component without the cost of increased moments at the shoulder.

One-hand force exertions were characterized by different trunk orientations. Three strategies were observed: (1) open trunk rotation defined as axial rotation of the trunk to the left, (2) closed orientation whereby participants rotated to the right such that their right arm which was exerting the force was across their chest, (3) neutral trunk orientation corresponding to the trunk and shoulders being approximately square to the force handle. Variation in trunk rotation was largest across one-hand pull exertions with a mean rotation angle of 26.6 degrees and standard deviation of 30.5 degrees with positive values corresponding to rotation to the left (i.e. open trunk orientation). Trunk rotation was found to be a strong predictor of the lead foot with the right foot leading in 94% of exertions characterized by an open torso orientation, and the left foot leading in 99% of exertions performed with a closed torso posture.

Tactic selection was found to be subject-specific and attempts to predict a tactic from task parameters and worker characteristics were unsuccessful. As discussed by Park et al. (2005), tactics or alternative postural and movement techniques are an important aspect of human motion and posture prediction. In this paper the authors make the point that, although optimization-based posture and motion prediction models may be capable

of producing observed behaviors, the concept of producing an optimal human behavior is flawed in the sense that the natural variability in human motion is ignored. Park et al. argue that instead an effort should be made to qualitatively identify and study alternative movement techniques with the objective of incorporating this source of variability into posture and motion models to enhance model performance. Future work could include using a method such as the joint contribution vector developed by Park et al. to quantitatively identify the different tactics, which at present have been qualitatively identified in the current data set. Such a method could allow for more accurate and consistent identification of tactics. Furthermore, from an application standpoint it would be interesting to quantify the workspace or work envelope associated with each postural strategy. Knowledge of the work envelope provided or required for each tactic might be used to determine which tactic would be selected to perform jobs with restrictions on available workspace.

2. Quantify the relationship between actual and requested hand force and develop a model that predicts the actual hand force vector from worker characteristics and task parameters.

Actual hand force vectors were quantified for one- and two-hand exertions over a range of test conditions. A set of regression equations were then developed to predict actual hand force vectors from requested hand forces.

Previous studies have reported large vertical off-axis forces during push/pull exertions and noted that actual hand force vectors are consistent with the hypothesis that the force vector is directed toward the glenohumeral joint (Schibye et al., 2001; Hoozemans et al., 2004; de Looze et al., 2000; Granata et al., 2005). In the current study, the vertical force component was directed downward when pushing for postures in which the shoulder was positioned above the force handle, and upward for shoulder locations below the handle. This relationship is somewhat complicated by elbow posture in that shoulder locations above the handle were associated with a large upward force component during high-force push exertions in which the elbow was maximally flexed. By flexing the elbow(s), the horizontal distance from the point of force application to shoulder(s) (i.e. moment arm) is reduced allowing large vertical forces to be exerted without an increase in shoulder moments. When pulling, the opposite relationship is

observed in that an upward vertical force component is observed for shoulder locations above the handle, and a downward component when the shoulder is positioned below the handle. These findings are consistent with the literature as is the transition from a downward to upward vertical component during high-force push exertions (de Looze et al., 2000; Granata et al., 2005).

The use of a vertical hand force component when pushing or pulling also affects the required coefficient of friction (COF) at the feet. All exertions were performed on a painted wood platform with a COF of approximately 0.75. All participants wore their own shoes and thus the available friction at the shoe-floor interface may have differed across subjects. A few participants were observed to slip during high-force exertions, suggesting that frictional requirements may have affected hand force capability and/or posture during a subset of trials. The large vertical hand force component quantified during high-force push exertions is consistent with exertions being limited by friction and a need to decrease the required COF. However, upward exertions were characterized by a large downward hand force component that acts to decrease the amount of friction at the feet. This finding suggests that the desire to direct the hand force vector toward the glenohumeral joint may take precedence over increasing ground reaction force when a relatively high-traction floor is present.

3. Identify and analyze biomechanically critical aspects of postures to determine if task postures are consistent with hypothesized biomechanical principles.

A set of biomechanical postural metrics was developed and the effects of task and worker characteristics on these metrics were analyzed. The defined metrics quantify shoulder location, torso inclination, elbow angle, pelvis location and orientation, and foot placements, and were considered biomechanically critical in that balance, and the moments about the shoulder and low-back are closely related to these measures. In general, the relationships between postural metrics and task parameters were found to support the following hypothesized biomechanical principles.

Shoulder Location with Respect to Point of Force Application & Shoulder Moment

Data were found to be consistent with the hypothesis that postures are chosen to maintain the shoulder moment at an acceptable level. Analysis of data suggests that moments at the shoulder are managed by: (1) inclining and lowering the torso to decrease

the vertical offset between the shoulder and point of force applications (i.e. reduce the vertical moment arm) during push/pull exertions or decrease the horizontal offset between the shoulder and point of force application (i.e. reduce the horizontal moment arm) during up/down exertions, (2) exerting a substantial vertical component to direct the hand force vector towards the shoulder joint center, (3) flexing the elbows to bring the shoulder close to the force handle thereby decreasing the hand force moment around the shoulder. Across all test conditions, shoulder flexion/extension moments were less than or equal to 37 Nm in 90% of trials.

Sensitivity to moments about the shoulder and a desire to select postures, which reduce or maintain a certain level of shoulder moment, can be explained in part by the instability of the joint. High joint loads and awkward postures are of particular concern for the shoulder since the biomechanical structure of the joint makes it inherently unstable and thus highly susceptible to injury (Sommerich and Hughes, 2005; Sommerich et al. 1993). Within the United States, estimated annual costs associated with occupational shoulder injuries are \$1 – 2 billion (Reynolds, 1999). Excessive force is one of the main risk factors for upper extremity disorders (Gil Coury et al., 1998). Risk of injury is also greater when joints are stressed near the ends of their range-of-motion (Soderberg and Blaschak, 1987). The large range-of-motion afforded by the biomechanical structure of the shoulder makes it possible for jobs to be designed that encourage stressful postures and place the shoulder at greater risk of injury.

In the current study, participants were observed to alter the location of the shoulder relative to the point of force application in a manner that acted to reduce moments about the shoulder. Changes in shoulder location with increasing hand force were especially strong during trials in which the direction of the hand force vector was constrained. These findings are consistent with the hypothesis that participants will alter their shoulder location as the required force magnitude increases to maintain an acceptable level of shoulder moment; however, several alternative explanations could account for this behavior. For example, changes in shoulder location may simply be the consequence of the kinematic constraints imposed by the task. A lengthening of the base-of-support and inclination of the torso are associated with increasing hand force magnitude and offer an alternative explanation for changes in shoulder location. Flexing

the elbows during high-force push exertions also alters shoulder location in a manner consistent with reducing moments about the shoulder, but may instead be motivated by a desire to reduce the amount of elbow strength required by the task. However, flexed-elbow pushing postures were associated with an increased vertical hand force component, which in an extended-elbow posture would demand greater shoulder strength not elbow strength, suggesting that the posture is adopted to allow greater vertical forces to be exerted on the handle without incurring increased moments about the shoulder.

Shoulder strength, specifically isolated shoulder joint strengths and an aggregate measure of these strengths, were not found to be significant predictors of postural metrics. The relative weakness of the shoulder may cause people to choose postures that protect the shoulder from high voluntary moments whenever possible. The design of the experiment placed minimal constraints on posture allowing people to recruit their lower-body strength and to adopt postures in which shoulder moments were minimal.

Postures selected for the upward exertions would likely be different and might depend more on strength if participants were required to lift and carry an object rather than pull or push up on a fixed handle. Similarly, postures would probably differ and may depend on strength capability if the task requires greater precision, or if workplace constraints precluded shoulder locations inline with the point of force application and/or hand force vector. Furthermore, strength could be a determinant of posture in that the combination of shoulder and surrounding muscle lengths may be optimal in the selected postures. Postures may be chosen to maximize the overall force-producing capability of the shoulder and/or maximize shoulder stability. Directing hand force vectors towards the shoulder joint center so the force acts to keep the humeral head within the glenohumeral joint, as opposed to causing migration of the humeral head towards the periphery of the socket, is one way of increasing shoulder stability and avoiding dislocation of the joint (Sommerich and Hughes, 2005; Dickerson, 2005). However, this strategy of directing the hand force vector towards the shoulder to increase shoulder stability is also consistent with the hypothesized reduction or maintenance of low shoulder moment. Sensitivity to shoulder loading is also supported by the work of Thompson (1993) who found subjects to be better at perceiving stress in the shoulder than in the back.

When the adjustments in shoulder location required to maintain an acceptable level of shoulder moment are relatively small (e.g. changes in shoulder location during elbow-height exertions), a preference towards this strategy is observed. When reduction in shoulder moment requires large deviations from a neutral standing posture, and/or task constraints prevent a reduction in moment arm and hand force direction is unconstrained, a preference towards redirecting the hand force vector towards the shoulder as a means of managing moments about the shoulder is observed. The fact that both shoulder location and the direction of the hand force vector are consistent with reducing moments about the shoulder further supports the hypothesis that postures are selected to reduce moments about the shoulder.

Vertical forces were largest during overhead pulls, despite lower two and one-hand pull strengths at the overhead handle height (average of 0.26*body weight), as compared to two and one-hand pull strengths at the elbow (0.51 and 0.47*body weight) and mid-thigh (0.73 and 0.56*body weight) handle locations. A downward vertical force during overhead pulls could be attributed to using body weight (i.e. hanging on the handle), as opposed to a desire to direct the hand force vector towards the shoulder. Kinematic constraints on posture prevent people from effectively using body weight to generate larger pull forces when exerting the force on a handle located overhead. Furthermore, large downward forces actually act to decrease horizontal hand force capability by reducing the available friction at the feet through a reduction in normal force, and yet large downward forces were quantified, suggesting that there is a benefit in directing the hand force vector downwards, which outweighs this cost. Again, one possible benefit is a reduction in shoulder moment.

An alternative explanation for generating vertical off-axis forces is the need to increase the available friction at the shoe-floor interface. Upward forces were measured during high-force push exertions and are consistent with this explanation. This explanation is also supported by the fact that some participants were observed to slip during a few high-force trials. Loss of traction indicates that friction may have been a limiting factor in these trials, and thus participants may have generated large upward forces for the sole purpose of obtaining larger horizontal forces within the available coefficient of friction (COF). However, while participants did slip during some trials,

traction was not a problem during the majority of trials in which upward forces were observed, suggesting that friction was not the limiting factor for a significant subset of the exertions. One possible explanation is that participants were generating the minimal amount of vertical force required for adequate friction. This seems unlikely given the magnitude of vertical forces observed, but could be tested by comparing the required and available COF values, where the required COF is quantified from ground reaction force data. An available COF of 0.75 was determined for the experimental setup using the Big Foot.

Recall that, the main objective of this work was to develop an algorithm that accurately predicts postures for a wide range of standing hand-force exertions. In this context the true causes of the observed behavior are less critical than good predictive performance. Of course, a model that incorporated accurate assumptions about posture selection tactics would be more likely to be accurate and robust across conditions. From a modeling standpoint, the critical observation is that a strong trend toward postures with minimal shoulder moments can be used to accurately predict task postures, provided that the actual hand force vector can be computed from empirical relationships, like those in Chapter 3.

Torso Inclination

The laboratory data are consistent with the hypothesis that neutral or upright torso postures are preferred. Torso inclination was not found to vary significantly with force magnitude during thigh-height upward exertions. Participants instead stood close to the handle, their thighs at times contacting the handle, allowing them to reach the handle without inclining the torso. An alternative strategy would be to flex the torso forward and then pull up or lift up on the handle in a manner similar to that used when performing a deadlift. Moments about the shoulder would be minimal when using this technique but greater back and/or leg strength would be required. Such a strategy, however, was not observed, and instead postures were characterized by minimal torso flexion.

Higher shoulder moments during thigh-height push/pull exertions also support the hypothesis that upright torso postures are preferred in that participants were willing to tolerate larger moments about the shoulder to avoid forward flexion of the torso. Higher moments during one-hand thigh-height push exertions could have resulted from an

inability to correctly identify and exclude internally braced trials from the analysis. Such an error in tactic identification, however, would not explain the higher moments observed during two-hand thigh-height pushes, or in one and two-hand thigh-height pulls, since bracing was only utilized during one-hand pushes and upward exertions.

Torso flexion is associated with increased loading of the low-back resulting from the moment required to support the weight of the torso and increased levels of co-contraction occurring with torso flexion (Granata et al., 2005). Thus a preference towards an erect torso is consistent with a desire to reduce low-back flexion/extension moments. Alternatively, successful completion of the task required participants to monitor the forces exerted on the handle via a force-feedback display mounted near the force handle, and this visual constraint on the task may have resulted in more upright torso postures. However, the location and orientation of the display was adjusted for each trial condition to minimize the effects of the visual requirement on the task posture.

Pelvis Location and Orientation

Data are consistent with the hypothesis that rotational moments about the low-back are minimized by decreasing the moment arm through a lateral shift in pelvis location towards the hand-force plane and/or axial rotation of the trunk. The effect was strongest for one-hand pull exertions, and trunk rotation was not found to be significant during one-hand push exertions. Data suggest that a lateral shift in pelvis location may be the primary mechanisms for reducing low-back rotational moments during one-hand push exertions; however, changes in trunk rotation may have been masked by the presence of two different strategy (open and closed torso postures), and the inability to accurately and consistently identify each strategy for small changes in torso orientation.

Base-of-Support

The center-of-pressure (COP) was hypothesized to lie at the active edge of the BOS and the fore-aft offset from the active edge of the BOS to the pelvis was hypothesized to be only as large as required for the moment generated by body weight to counter the moment due to the applied hand force. This is consistent with the work of Holbein et al. (1997) that showed when lifting loads, people were willing to shift their COP to the edge of the BOS. A strong relationship was found between this fore-aft offset

from the pelvis to edge of BOS and hand force, and supports the hypothesis that body weight is recruited during push/pull exertions to generate the required hand forces. The offset computed from balance requirements, however, was found to underestimate the actual offset quantified from data. The assumption that the COP lies at the edge of the BOS implies that only the active foot is loaded. This assumption is valid for a subset of high-force trials (e.g. when pushing people were observed to lift their front foot, utilizing the weight of the unloaded extremity to increase the moment due to body weight), but underestimation of the offset overall indicates that the passive foot is loaded during most exertions. A small BOS during low-force exertions and a lengthening of the BOS with increasing horizontal force suggests that the COP is located near the center of the BOS during low-force exertions and moves towards the edge of the BOS as the level of force increases.

Other possible explanations for the underestimation in fore-aft offset include: (1) approximation of the whole-body center-of-mass (COM) location by torso COM location, (2) errors in estimating subject-specific distribution of mass across segments, (3) a “cost” associated with repositioning the feet. This last point refers to the idea that people choose foot placements that they know from experience are adequate and then, if possible, use other means, such as modifying elbow angle to adjust their posture as necessary. Placing their feet such that the COP lies just at the edge of the BOS requires greater precision and is risky in the sense that if people underestimate how large an offset they need then they have to either incline their torso further to generate more moment from body weight, or move their feet. This concept of setting the feet and then essentially using elbow angle to adjust the offset is consistent with the large variability found in elbow angles, and is supported by the work of Okunribido and Haslegrave (2008) who described arm posture as an “active aspect of whole body force exertion”. Their work on two-hand push exertions indicates that arm postures act to enhance hand force capability and/or allow for modulation of hand forces.

The interaction between torso inclination and the fore-aft offset must also be considered. This interaction results from the fact that people can shift their COM with respect to the COP by changing the torso inclination angle and/or moving the feet, or altering the distribution of load between the feet to change the offset between the COP

and pelvis. Kinematic constraints imposed by a low-handle height resulted in more forward torso inclination during thigh-height pulls, and a larger offset between the edge of the BOS and pelvis, as compared to pulls at elbow-height and overhead. However, the fore-aft distance from the edge of the BOS to the COM was not found to differ significantly across handle heights, indicating that the forward shift in COM associated with torso inclination is countered by the shift in COM that accompanies the rearward shift in pelvis during thigh-height pulls.

4. Develop models from laboratory data to predict key postural metrics not explained by hypothesized biomechanical principles.

A laboratory study was designed and conducted to collect postural and force data for one- and two-hand exertions under a large number of test conditions. The scope of the experiment and minimal constraints on posture resulted in a large and complex data set. Participants were free to choose their posture, and for a given task condition different postural tactics were observed which required that the data be segregated by tactic for analysis. Models that span tactics were preferred, but when behaviors within tactics were found to be fundamentally different a separate model was required for each tactic. Creating models that accurately predict postural metrics across tactics is difficult as evident by the poor predictions for up/down exertions.

Posture-prediction models applicable to ergonomics analysis typically define a posture by predicting Euler or Cardan rotation sequences at joints. This approach is problematic in that joint-angle conventions differ between digital human modeling packages. Differences in joint-angle definitions hinder implementation of such algorithms and are one reason why the current model instead predicts global postural metrics. Furthermore, the chosen postural metrics are considered to be biomechanically critical, meaning that ergonomic analyses are dependent on the accuracy of these aspects of posture. One key aspect of posture is the location of the shoulder(s) with respect to the point of force application since it is a determinant of shoulder loading.

In this study, shoulder location is predicted by satisfying a shoulder moment threshold of 20 Nm. This threshold is based on the observation that 90% of trials were characterized by shoulder flexion/extension moments less than or equal to 37 Nm. Linear statistical models were developed in Chapter 4 and Chapter 5 to predict a shoulder

flexion/extension target value for a given task condition, but yielded poor model performance. The poor performance is attributable to an absence of data at intermediate handle heights, and the small moments and change in sign that occur as the model crosses through zero. A shoulder moment threshold was found to yield better model performance but also has limitations. The threshold is currently independent of strength capability since isolated shoulder strength measures were not found to be a significant predictor of posture; however, given a larger and more diverse population the threshold would likely depend on individual shoulder strength. Also, if task constraints prevented people from reducing moments at the shoulder via one of the three mechanisms described earlier (redirecting the hand force vector, altering shoulder location, internal bracing) then a moment threshold would likely not produce accurate postures across a population with varying strength capability. Under these conditions, it is expected that postures would be more dependent on individual shoulder strength.

5. Develop and validate a three-dimensional posture prediction algorithm that combines kinematics, basic mechanics, and biomechanical principles in a hierarchical structure to predict whole-body postures for standing hand-force exertions.

Current Approaches to Posture Prediction

Simulation of human postures and motion is an active area of research with significant modeling efforts in the areas of optimization, statistical modeling, inverse kinematics, artificial neural networks, and motion modification. Examples of each approach follow and additional review of the posture-prediction literature provided in Chapter 1.

Optimization-Based Posture Prediction

Many early optimization-based modeling efforts focused on sagittal-plane lifting. Dysart and Woldstad (1996) developed a posture prediction model for sagittal-plane lifting wherein different optimization criteria were used to select an “optimal” posture from the set of kinematically feasible postures. Different optimization criteria considered include: (1) minimal effort, where effort is defined as the total torque summed over all joints, (2) maximal percent strength (i.e. the posture that distributes torques most evenly across joints relative to the strength capability of each joint), and (3) maximal body

stability or balance, where the difference between torques at the heel and ball of foot served as a measure of the ability to resist falling. On average the minimal effort criteria was found to perform best across the range of conditions investigated; however, discrepancies between predicted and actual postures were large and not within an acceptable range. Prediction error was defined as the Euclidean distance between select postural features. The features used included planar hip location and forearm orientation. Dysart and Woldstad also noted the large differences in postures selected across individuals. Specifically, when lifting from a low height, some participants chose to squat while the majority choose a stoop posture. This observation indicates the need for models capable of producing the range of postural behaviors commonly observed across individuals.

Statistical Modeling and Data-Based Inverse Kinematics

Beck (1992), using data from Kilpatrick (1970) and Snyder (1972), developed a behavioral inverse kinematics algorithm that predicts segment positions based on hand location and orientation, and worker height and weight. This posture-prediction algorithm is currently implemented the University of Michigan's 3D Static Strength Prediction Program. Seidl (1994) developed a posture-prediction algorithm for use in RAMSIS that maximizes the likelihood of joint angles relative to a database of human postures for similar tasks. The reliance of Seidl's algorithm on a database of similar human postures highlights the dependence of statistical approaches on an underlying dataset. These methods provide validated accuracy for tasks similar to those in the underlying dataset, but accuracy degrades substantially for task conditions outside of the range of the underlying data.

Artificial Neural Networks

Artificial neural networks have been used by several researchers to develop posture prediction models. Human posture or motion data is used to train the networks and a separate set of data used to assess model performance. Jung and Park (1994) developed a model for predicting human reach and found no significant difference between actual and predicted (x, y, z) joint locations. Whole-body lifting postures, and the kinematics of lifting and lowering loads were predicted by Perez (2005). Two distinct networks were developed. The first network was developed and trained to predict three-

dimensional lifting postures for a given target location. A second network was developed to predict joint angles as a function of time for the actions of lifting and lowering loads. Model development and assessment focused on sagittal-plane symmetric lifts; however, the model is capable of predicting three-dimensional symmetric, and asymmetrical lifting postures. Differences in actual and predicted kinematics were quantified by RMSE in joint locations and angles. On average, the RMSE in joint angles was approximately 20 degrees with larger errors for participants not in the training set. While posture prediction using neural networks shows promise, there are several drawbacks to this approach. A database of motions is required to train the network. Furthermore, motions in the training set must be similar to those to be predicted for the model to perform well. Models also often rely on knowledge of an individual's strength and anthropometry. Lastly, Perez (2005) found the expansion of predictions from two to three-dimensions to be computationally costly.

Motion Modification

Park et al. (2004) has reported motion modification to be successful approach provided that a database of similar motions and postures is available. Motion modification is well suited for tasks such as vehicle ingress/egress, in which the span of variables affecting the motions is relatively small (Dufour et al., 2001). However, this approach does not provide a general solution to the prediction of postures in a variety of novel tasks.

Current Biomechanics-Based Posture-Prediction Model Formulation

As stated by Haslegrave (1992), “a simple biomechanical analysis will show, the posture adopted when exerting force is important for two reasons: it affects both the strength which a person is able to exert and the resultant loading on his/her body, since it determines the geometry and mechanical advantage of the muscles involved in the exertion, and equally importantly affects stability while performing the task”. Given the strong biomechanical relationships between hand force and posture a model which uses biomechanical principles to predict three-dimensional whole-body postures for standing hand-force exertions was proposed. Postures and postural changes measured in the laboratory were found to be consistent with the following primary biomechanical hypotheses:

- (i) Standing hand forces are performed in a manner that reduces moments about the shoulder by: (a) directing the hand force vector towards the glenohumeral joint and/or (b) decreasing the shoulder moment arm.
- (ii) Within the constraints of kinematics, only the minimal amount of torso inclination necessary to generate the required hand forces is used, except as necessary to reduce shoulder loading.
- (iii) One-hand force application postures are consistent with reducing the rotational moment about the inferior-superior axis of the lower back.
- (iv) Standing balance requirements can be used to set foot placements with respect to whole-body center of mass.

These hypotheses were used to structure a biomechanics-based posture-prediction model and the empirical results supporting each hypothesis used to predict postural features not determined by mechanics. The model performed well with correlation coefficients ranging from 0.531 to 0.847; however, model predictions for push/pull exertions are driving the high correlations. Model performance was much poorer for vertical up/down exertions. In response, suggestions for improving model performance through reformulation of certain aspects of the model are discussed in the following section.

While not without limitations, the current modeling structure has several strengths worth noting. The simplicity of the model makes it easy to publish, in complete form, with all the necessary information for it to be readily implemented. Most other approaches are joint-angle-convention dependent and require special code and algorithms (e.g. Sequential quadratic programming, a standard technique for solving nonlinear optimization problems) and cannot be implemented from published information. Thus, while it is possible that another modeling approach might be more effective, the current model structure, although simple, performs well, especially for push and pull type exertions. Ease of implementation and computational efficiency increase the likelihood of such a model being implemented into existing DHMs.

Opportunities to Improve Model Performance

Although the model described in Chapter 6 performed well for a variety of task conditions, poor correlations between predicted and observed values were noted for certain types of exertions, such as upward and downward trials at elbow height. These

discrepancies result in part from the overly simplified approach that the model uses to maintain shoulder moment within a limit. If the initially calculated moment exceeds the maximum permitted value, the model lowers the shoulder while maintaining elbow angle. This approach works well for horizontal pushes and pulls at elbow and thigh heights, where it captures the typical behavior well, but upward and downward exertions were characterized by a wider range of tactics. For upward exertions, some subjects pulled upward with nearly straight elbows and moved their shoulders directly above the handle. This behavior is consistent with the proposed goal of maintaining shoulder moment below a criterion value (the vertical force vector passes close to the glenohumeral joint) but the behavior (raising the shoulder and moving it forward) is not captured by the model. Conversely, some participants flexed their elbows maximally and located their shoulders very close to the hand, effectively bracing their forearms against their arms to obtain a large force with a relatively small shoulder moment.

The results suggest an alternative approach to computing shoulder location and torso inclination, namely a weighted optimization process. In brief, a cost function representing a weighted sum of the shoulder moment in excess of the criterion and the torso deviation from neutral (angle with respect to vertical) could be minimized. The weights could be chosen empirically to match the observed behavior. This approach, of minimizing the deviation from multiple empirically-determined target values, has been effective for predicting automobile driving postures (Reed et al. 2000).

An intriguing aspect of this approach is that it may be able to predict the variations in tactics that are observed in upward and downward exertions, merely by starting the optimization with different initial conditions. Consider an elbow-height upward exertion: starting the shoulder above and relatively close to the handle in the fore-aft direction, with an upright torso, would be likely to converge to an extended-elbow posture “pulling up” with an upright torso. In contrast, starting the optimization with a more-flexed elbow and the shoulder lower than the handle would tend to converge to a flexed-elbow, “push up” posture. The potential for this type of simple optimization approach to generate more robust predictions should be explored in future work. Note that the correct weighting of the elbow, shoulder-moment, and torso inclination values

can be determined by an optimization problem that determines the weights (or weighting functions) that best fit the data.

Another aspect of model performance that should be improved is the prediction of the base of support location. As noted in Chapter 6, the typical location of the active boundary was more extreme than that predicted by the model, which identifies the minimal deviation from neutral that is required to generate the required moment. Examination of the videos from the testing showed that the subjects were often conservative when locating their feet prior to the exertion. That is, they chose a more extreme base of support than strictly necessary, which allowed them to shift their center of pressure within the expanded BOS (primarily by moving the pelvis fore-aft) and thereby fine-tune their force magnitude, as required by the task. This behavior has been noted recently by Okunribido and Haslegrave (2008), who described the elbow-angle transitions that accompany the development of push force with fixed foot placements. One promising approach to representing this behavior in the model would be to predict foot placements empirically, similar to the methodology described by Wagner et al. (2006), followed by computation of the fore-aft pelvis location based on center-of-pressure requirements for balance. This approach could be validated both through posture data analysis and by reference to force-plate data obtained during some trials in the current study.

7.3. Limitations

Laboratory Study

The laboratory study was conducted to elicit the range of postural behaviors used in industry when performing standing hand force exertions, and to quantify the effects of hand force on posture. This study was motivated by the need for improved posture prediction capability within DHMs for the purpose of ergonomic assessments, however the applicability of this work to the industry setting is limited in several ways by the experimental design.

- Nineteen subjects (9 men and 10 women) participated in the study, all of whom were young (college age), thin (average BMI < 30) individuals with no manual materials handling experience. The demographics of the laboratory participants may not be representative of industry workers and

postures adopted by participants in the laboratory may not be consistent with postures of an experienced worker. However, at the onset of the experiment participants practiced the exertions under the various test conditions and were encouraged to practice each trial until they had identified their preferred posture and felt comfortable with the trials. Furthermore, behaviors observed in the laboratory were qualitatively consistent with those observed in automotive plants.

- An attempt was made to recruit participants with a wide range of body dimensions and strength capabilities. However, when subject strength values were compared to strength values from the literature most participants were found to be relatively weak compared to the population.
- The study was conducted in a laboratory environment that is not representative of the industrial setting in which the types of jobs to be analyzed are performed. Unnatural postures may have resulted from the retro-reflective markers affixed to the subjects skin and clothing, especially since the markers on the back of the hand sometimes interfered with their ability to easily grip the force handle. Visual feedback provided on hand force may have resulted in unnatural neck postures. Force plates recessed in the floor were used to capture reaction forces. Participants' attention was not directed towards the force plates, however over the course of the experiment some participants became aware of their purpose and as a result may have altered their foot placements.
- Literature values were used to define mid-thigh and elbow-height handle locations as a percent of stature. Due to differences in body-proportions across individuals the percentages used may not have been equivalent to mid-thigh and elbow-height for all subjects.
- Exertions were performed on a raised platform with a painted surface and participants wore their own shoes during the experiment. During high force exertions some participants slipped and in response altered their posture in an attempt to achieve better footing. The insufficient friction at the shoe-floor interface for a subset of participants may have resulted in

significantly different postures. However, analysis of postural data found postures to be consistent across all subjects suggesting that frictional limitations did not result in significantly different postures.

- Many industry jobs involving force exertion involve the manipulation of manual materials handling devices. In the laboratory study participants exerted force on a fixed handle. Postural strategies may have been different if the handle were expected to move.
- Participants exerted force on a smoothly contoured cylindrical handle with a high-friction rubber coating. The diameter of the handle was selected to be within the range of preferred handle diameters published in the literature. Had subjects been required to exert force on a handle that was more difficult and/or less comfortable to grasp different behaviors may have resulted. Furthermore, participants were restricted to an overhand or underhand power grip whereas workers are free, within the constraints of the job, to choose how they grip a part or tool when performing a job.
- Only right-handed participants were recruited for the study and it was assumed that left-handed workers would exhibit the same behaviors.
- Given the duration and nature of the study participants may have become fatigued over the course of the study, which could have affected the observed behaviors. However, strength measures were obtained before and after the study and a significant decrease in strength, indicative of fatigue, was not observed.

Posture Prediction Model

The model predicts a whole-body posture for single- and two-handed force exertions based on biomechanical hypotheses, behavior based inverse kinematics, and empirical relationships derived from the laboratory study. As discussed in Chapter 6, the model is limited by the underlying data and by the design choices made in the formulation of the model. People knowledgeable about other modeling approaches that have been applied to whole-body posture prediction, such as artificial neural networks (Perez, 2005) and strength optimization based on joint angles (Seitz et al. 2005) might be optimistic that a more complex model formulation could produce better results. However,

the statistical analyses in Chapters 4 and 5 suggest caution. For example, strength was not found to be an important predictor of posture. Moreover, methods that employ a more holistic approach are unlikely to do a better job of predicting the critical degrees of freedom, such as torso inclination, than a model built directly on data, as in the current approach. Improvements to the current model are more likely to come from changes to the individual parameter models rather than from a wholly different approach.

Importantly, the data show a large amount of intersubject variation in posture that is unrelated to subject descriptors, such as stature, body weight, and strength. Although this is unsatisfying when trying to create a model of human behavior, it reflects a bound on what a posture-prediction model can be expected to accomplish. The current model formulation was chosen in part because it offers the potential for stochastic simulation by randomly varying key variables, such as torso angle, according to the distributions of residual variance in the regression models. This approach could be pursued as a means of improving the utility of ergonomic analyses with human figure models for identifying potentially hazardous jobs.

7.4. Future Research

The findings of this research, along with its limitations, identify several areas for future work.

- Data from a more diverse population are needed. The laboratory study focused on generality with respect to force direction, task location, and force magnitude, but did not sample people with a wide range of age, body mass index, or industry experience. The selection of the laboratory population was justified, since for this first comprehensive study of these postures an emphasis on subject fitness and ease of capturing postures was needed. However, the applicability of the model to simulating industrial workers would benefit from using data from a more diverse subject pool. In addition to differences in anthropometry and strength capability, experienced workers may exhibit different tactics.
- More research is needed on tactic selection for hand-force exertions, particularly work to understand how worker characteristics affect tactic selection. Such a study might have a substantial field component,

examining postures in industry in relation to the postures observed in the laboratory. Also, replicating the current study with a more diverse subject pool, specifically industrial workers, would allow tactics used by experienced workers to be identified and compared with tactics of the current inexperienced subjects.

- During two-hand exertions hand forces were assumed to be equally distributed between the right and left hand. Okunribido and Haslegrave (2008) reported significant differences in vertical force magnitude between the right and left hand during two-hand pushes indicating that this assumption may not be valid. They also observed that lateral forces measured at the right and left hand acted in opposite directions which could explain why lateral off-axis forces were not found in the present work to be significant during two-hand exertions. In addition to force, the moments exerted on the handle also were quantified and should be used along with the location of the right and left hand to estimate the actual distribution of forces between the hands. This research may also benefit from repeating this work or a subset of the study presented in this dissertation with individual instrumented handles for each hand.
- The model performance limitations described in Chapter 6 should be addressed by additional analyses of the currently available data and, if necessary, reformulation of the regression equations. In particular, the relatively poor performance of the model for vertical exertions should be addressed, and an appropriate BOS margin for the active boundary should be implemented.
- Future studies should include consideration of postural constraints, such as objects in the environment. By design, the current study minimally restricted task postures, but industrial tasks are often performed in environments with substantial constraints. As a first step, studies should examine the effects of a horizontal restriction on fore-aft foot and pelvis position, such as that posed by the edge of a parts bin or the fender of a car.

- Several interesting postural behaviors (e.g. axial rotation of the trunk and hyperextension or toggling of the lumbar spine) were observed which suggest that the meaning of low-back moments and compression force needs to be explored further in terms of posture selection. Rotational moments about the lumbar spine were quantified and found to be less than 21 Nm in 90% of all trials which is significantly less than the maximum twisting moments of 50 to 60 Nm reported by Marras et al. (1998). Low-back compression forces were estimated by a third-order polynomial in low-back moments developed by McGill et al. (1996) and found to be less than or equal to 1,756 N for 90% of all trials which is approximately half the NIOSH compression action limit. Lett and McGill (2006) reported peak compression forces of approximately 2,000 to 4,000 N during push/pull exertions of 45.5 N (10 lbs) to 400.5 N (90 lbs) at waist and shoulder height. In the current study, push/pull forces spanned a similar range and yet low-back compression forces, on average, were less than those reported by Lett and McGill (2006). The relatively low rotational moments and compression forces suggest that people may be sensitive to low-back loading and thus adopt postures to reduce these loads; however, this hypothesis is contrary to the work of Thompson (1993) who found no relationship between rating of perceived exertion on the back and L5/S1 compression forces.
- In the current study, internal bracing was observed as a strategy to generate increased hand force while circumventing the strength limitations of the shoulder. This strategy was most prevalent during one-hand forward (push) and upward exertions at thigh and elbow-height. Internal bracing is difficult to identify; however, review of the trial videos suggests that internal bracing was used in approximately 15% of elbow-height forward exertions and 8% of elbow-height upward exertions. The strategy is even more prevalent for thigh-height forward exertions with approximately 56% of these trials being characterized by internal bracing. Internal bracing is likely to be important for some tasks in industry, so more work

should be done to understand the situations in which internal bracing is likely and the consequences of this tactic for musculoskeletal loading.

- External bracing, in which the non-task hand rests on or grips an object in the environment, is common for one-hand industrial tasks. Behaviors that include this tactic should be studied to predict when people use contralateral hand bracing and the effects of that tactic on posture and joint loading.
- The effects of object orientation, object type, hand-object coupling, and grasp on posture should be investigated. When pushing on fixed cylindrical handles Okunribido and Haslegrave (2008) found handle orientation to have a significant effect on wrist and forearm postures suggesting that the upper-extremity postures quantified in this dissertation may be specific to the chosen handle orientations. Given the kinematics of the human body, differences in upper-extremity postures associated with a change in handle orientation may result other whole-body postural differences; however, the work of Okunribido and Haslegrave (2008) only examined arm postures. Further research is needed to understand the effects of handle, and more generally, object orientation on whole-body force exertion postures. In addition, object type, the available friction at the hand-object interface, and grasp posture are likely to effect force-exertion postures and should be investigated in future studies.
- The dynamics of hand-force exertions should be explored to determine if model predictions hold for dynamic exertions. Thompson (1993), in her analysis of the perception of shoulder loading, found participants to be sensitive to whether an exertion was dynamic or isometric, with participants being more sensitive to the dynamic exertions. This finding suggests that people's response to shoulder moments may differ between isometric and dynamic exertions indicating that different models may be required to accurately predict shoulder locations during isometric and dynamic exertions.

7.5. References

- Beck, D. (1992). Human factors of posture entry into ergonomics analysis systems. PhD thesis, The University of Michigan, Ann Arbor, MI.
- de Looze, M. P., van Greuningen, K., Rebel, J., Kingma, I., and Kuijer, P. P. (2000). Force direction and physical load in dynamic pushing and pulling. *Ergonomics*, 43(3):377–390.
- Dickerson, C. (2005). A biomechanical analysis of shoulder loading and effort during load transfer tasks. PhD thesis, The University of Michigan, Ann Arbor, MI.
- Dufour, F., Lino, F., and Le Coz, J.-Y. (2001). Vehicle accessibility. Technical Report 2001-01-3431, SAE International, Warrendale, PA.
- Dysart, M. J. and Woldstad, J. C. (1996). Posture prediction for static sagittal- plane lifting. *J Biomech*, 29(10):1393–1397.
- Gil Coury, H., Kumar, S., Rodgher, S., and Narayan, Y. (1998). Measurements of shoulder adduction strength in different postures. *International Journal of Industrial Ergonomics*, 22:195–206.
- Granata, K. R. and Bennett, B. C. (2005). Low-back biomechanics and static stability during isometric pushing. *Human Factors*, 47(3):536–549.
- Granata, K. P., Lee, P. E., and Franklin, T. C. (2005). Co-contraction recruitment and spinal load during isometric trunk flexion and extension. *Clin Biomech (Bristol, Avon)*, 20(10):1029–1037.
- Haslegrave, C. M. (1992). Predicting postures adopted for force exertion: Thesis summary. *Clinical Biomechanics*, 7:249–250.
- Holbein, M. and Redfern, M. (1997). Functional stability limits while holding loads in various positions. *International Journal of Industrial Ergonomics*, 19(5):387–395.
- Hoozemans, M. J. M., et al. (2004). Mechanical loading of the low back and shoulders during pushing and pulling activities. *Ergonomics*, 47(1):1–18.
- Jung, E. and Park, S. (1994). Prediction of human reach posture using a neural network for ergonomic man models. *Computers Ind. Engineering*, 27(1-4):369–372.
- Kerk, C. (1992). Development and evaluation of a static hand force exertion capability model using strength, stability, and coefficient of friction. PhD thesis, The University of Michigan, Ann Arbor, MI.
- Kilpatrick, K. (1970). A Model for the design of manual workstations. PhD thesis, The University of Michigan, Ann Arbor, MI.

- Lett, K. K. and McGill, S. M. (2006). Pushing and pulling: personal mechanics influence spine loads. *Ergonomics*, 49(9):895–908.
- Marras, W. S., Davis, K. G., and Granata, K. P. (1998). Trunk muscle activities during asymmetric twisting motions. *J Electromyogr Kinesiol*, 8(4):247–256.
- Okunribido, O. and Haslegrave, C. (2008). Ready steady push - a study of the role of arm posture in manual exertions. *Ergonomics*, 51(2):192–216.
- Park, W., Chaffin, D., and Martin, B. (2004). Toward memory-based human motion simulation: Development and validation of a motion modification algorithm. *IEEE Transactions on systems man and cybernetics, Part A: systems and humans*, 34(3):376–386.
- Park, W., Martin, B. J., Choe, S., Chaffin, D. B., and Reed, M. P. (2005). Representing and identifying alternative movement techniques for goal-directed manual tasks. *J Biomech*, 38(3):519–527.
- Perez, M. A. (2005). Prediction of whole-body lifting kinematics using artificial neural networks. PhD thesis, Virginia Polytechnic Institute and State University.
- Reed, M., Manary, M., CAC, F., and Schneider, L. (2000). Comparison of methods for predicting automobile driver posture. In *SAE Transactions: Journal of Passenger Cars - Mechanical Systems*, volume 109, pages 2279–2290.
- Reynolds, L. (1999). Zeroing in on ergonomics costs and solutions. *HR Today*, 7.
- Schibye, B., Sogaard, K., Martinsen, D., and Klausen, K. (2001). Mechanical load on the low back and shoulders during pushing and pulling of two-wheeled waste containers compared with lifting and carrying of bags and bins. *Clin Biomech (Bristol, Avon)*, 16(7):549–559.
- Seidl, A. (1994). *Das Menschmodell I Ramsis: Analyse, Synthese, und Simulation dreidimensionaler Körperhaltungen des Menschen [The man-model RAMSIS: Analysis, Synthesis, and simulation of three-dimensional human body postures.]*. PhD thesis, Technical University of Munich.
- Seitz, T., Recluta, D., Zimmermann, D., and Wirsching, H.-J. (2005). Focopp - an approach for a human posture prediction model using internal / external forces and discomfort. Technical Report 2005-01-2694, SAE International, Warrendale, PA.
- Snyder, R., Chaffin, D., and Schultz, R. (1972). Link system of the human torso. HSRI Report 71-112, Highway Safety Research Institute, and The University of Michigan, Ann Arbor, MI. and AMRL-TR-71-88, Aerospace Medical Research Laboratories, Ohio.

- Soderberg, G. and Blaschak, M. (1987). Shoulder internal and external rotation peak torque production through a velocity spectrum in differing positions. *The Journal of Orthopaedic and Sports Physical Therapy*, 8(11):518–524.
- Sommerich, C. and Hughes, R. (2006). Aetiology of work-related disorders of the rotator cuff tendons: Research and theory. *Theoretical Issues in Ergonomics Science*, 7(1):19–38.
- Sommerich, C., McGlothlin, J., and Marras, W. (1993). Occupational risk factors associated with soft tissue disorders of the shoulder: a review of recent investigations into the literature. *Ergonomics*, 36(6):697–717.
- Thompson, D. (1993). The perception of physical stress as a measure of biomechanical tolerance. PhD thesis, The University of Michigan, Ann Arbor, MI.
- Wagner, D., Reed, M., and Chaffin, D. (2005). Predicting foot positions for manual materials handling tasks. Technical Report 2005-01-2681, SAE International, Warrendale, PA.
- Wagner, D., Reed, M., and Chaffin, D. (2006). A task-based stepping behavior model for digital human models. In *SAE Transactions: Journal of Passenger Cars - Electronic and Electrical Systems*, volume 115, Warrendale, PA.